Daily Climate Change Data Generation and Dissemination

Gohe Amhayesus Metaferia

Thesis submitted under the supervision of

Dr. Ousmane Seidou

To the Faculty of Graduate and Postdoctoral Studies

In Partial Fulfillment of the Requirements for the Degree of

Master of Applied Science in Civil Engineering

Under the auspices of the Ottawa-Carleton Institute for Civil Engineering

uOttawa

Civil Engineering, Department of

University of Ottawa

Ottawa, Ontario, Canada

ABSTRACT

The worldwide challenges to achieve cost effective protection against global warming impacts and to acquire reliable decision making tools continually force new developments in the area of climate change research. Climate change impacts projections involve several steps: emission scenarios generation, Global Circulation Models and Regional Climate Models (GCM/RCM) runs, downscaling, impact model running, analysis of results and decision making. Each task is done by people with different expertise who rely on the work of previous analysts. Impact modelers start from GCM/RCMs outputs and turn them into biophysical impacts. Unfortunately, GCM/RCMs outputs are often biased and need to be processed before being fed into impact models. This thesis describes the effort carried out to alleviate the burden of downscaling coarse hydro-climatology data outputs from GCM/RCM and making results readily available for climate change impact analysis for specific regions, particularly in the African continent.

GCM/RCM outputs are highly unreliable at the sub-grid scale to be used for region specific impact analysis (Wilby, Hay, & Leavesly, 1999). Furthermore, raw GCM/RCM outputs are often downscaled under the premises that the latter offer very coarse spatial resolution.

The Internet is a common resource for users of climate change data to access relevant information. Web-based interfaces offer users the capability to retrieve such data. This thesis involves the development of a new web-portal, which addresses the demand for climate change data at the daily scale. It is a user-friendly interactive web-based interface with multiple functionalities including: capacity to process information, capacity to search, sort,

retrieve and filter data and download features. Six climate variables are considered in this project: precipitation, maximum temperature, minimum temperature, wind speed, relative humidity and solar radiation. The aforementioned climate variables have been downscaled to specific geographical locations and results have been made available at a fine temporal resolution – the daily scale. The data portal currently hosts climate change data for nine stations in western Africa: Agadez, Brini N'Konni, Gaya, Maine Soroa, Maradi Airport, Niamey Airport, Tahoua, Tillabery and Zinder Airport. The above mentioned climate stations are all located in Niger. Nonetheless, the project aims to expand and cover further ground in Africa.

Quantile - Quantile downscaling, also known as Quantile-Quantile mapping, matching or transformation is a statistical procedure used in this project to downscale raw GCM/RCM outputs. GCM/RCM outputs from the AMMA-Ensemble sets under the SRES A1B scenario were used as raw data.

Keywords: Climate Change, Impact Assessment, Daily Climate Data, Web Portal, Downscaling, Quantile-Quantile method.

ACKNOWLEDGMENTS

I would like to express my warmest gratitude to my advisor Dr. Ousmane Seidou for the wealth of knowledge he shared and guidance offered through out this valuable learning experience. I would also like to thank him for his patience and continued support as a valued mentor. Furthermore, I would like to acknowledge generous financial and logistic support received from the University of Ottawa and the FACE project (funded by the International Development Research Centre). I would also like to thank faculty members, fellow students and everyone who contributed to the completion of this work.

A special thanks to my family. I will forever be grateful to my parents, my brother and my sister who never ceased to encourage and support me. Finally, I would like to express my appreciation to my beloved Abeba who cheered me through many sleepless nights writing this thesis and offered her always-refreshing perspective.

TABLE OF CONTENTS

LIST OF TABLES

LIST OF FIGURES

LIST OF ABBREVIATIONS

Acronym	Definition
AGRHYMET	Centre Regional de Formation et d'Application en Agrométéorologie et Hydrologie Opérationnelle
AMMA	African Monsoon Multidisciplinary Analysis
CCAFS	Climate Change, Agriculture and Food Security
CDD	Maximum length of dry spell
CDF	Cumulative Distribution Function
CMIP	Coupled Model Intercomparison Project
CO_2	Carbon Dioxide
CORR	Corrected
CWD	Maximum length of wet spell
EPA	Environmental Protection Act
ETCCDI	Expert Team on Climate Change Detection and Indices
FACE	Fair face Aux Changement climatiques Ensemble
GCM	Global Circulation Model
GHG	Green House Gas
IPCC	Intergovernmental Panel on Climate Change
Km	kilometer
Km^2	kilometer square
KS	Kolmogorov – Smirnov
m/s	Meter per second
mm	Millimeter
NASA	National Aeronautics and Space Administration
NCEP	National Center for Environmental Prediction
NOAA	National Oceanic and Atmospheric Administration
OBS	Observed
^oC	Degree Celsius
PCP	Precipitation
PCPTOT	Annual total precipitation in wet days
QQ	Quantile - Quantile
R01mm	Annual count of wet days (over 1mm)
R10mm	Annual count of heavy precipitation days (over 10mm)
R20mm	Annual count of very heavy precipitation days (over 20mm)
R95pTOT	Annual total precipitation when daily precipitation is over the 95th percentile of daily precipitation during 1961-1990
R99pTOT	Annual total precipitation when daily precipitation is over the 99th percentile of daily precipitation during 1961-1990
RCM	Regional Climate Model
Rx1day	Monthly maximum 1-day precipitation
Rx5day	Monthly maximum consecutive 5-day precipitation
SDII	Simple precipitation intensity index
SIM-FUT	Simulated Future
SRES	Special Report on Emission Scenarios
UN	United Nations
UNFCCC	United Nations Framework Convention on Climate Change
USA	United States of America
USGS	United States Geological Survey
W/m^2	Watts per meter square

Chapter 1. INTRODUCTION

1.1 Motivation

"Warming of the climate system is unequivocal, as is now evident from observations of increases in global average air and ocean temperatures, widespread melting of snow and ice, and rising global average sea level." (Intergovernmental Panel on Climate Change, 2007)

"The scientific evidence is clear: global climate change caused by human activities is occurring now, and it is a growing threat to society." (American Association for the Advancement of Science, 2006)

The current course of climate change and the limited actions taken thus far to reduce the risks associated with its impact can lead to sever implications on human and natural systems (IPCC - Climate change Synthesis Report, 2014). Researchers and policy makers have expended tremendous effort in devising an intervention to this pressing issue. Two main channels of action have been adopted in an attempt to curb and mitigate the risks associated with climate change impact hazards. The most widely discussed and engaged undertakings are the efforts to reduce the concentration of greenhouse gases (GHGs) in the atmosphere by reducing the emission levels of GHGs. Embracing offensive strategies to tackle climate change at its source by limiting the very agents that fuel its vigor is fundamental. Several campaign initiatives have seen the light of day in the past three decades with a common goal to reduce GHG emission levels. The 1992 Kyoto treat has been the prime example of international collaborative efforts to tackle climate change at its source. The newest form of such international protocols is expected to be presented at the December 2015 UN Framework Convention on Climate Change (UNFCCC) in Paris. The

new protocol will encompass reduction of GHG emission levels for every nation member of the UN. The agreed upon measures are anticipated to go into effect by the year 2020. Moreover, several scale of government as well as Non-Governmental Organizations (NGOs) have put forth and implemented similar initiatives. Likewise, we have witnessed a rise in private corporations sense of environmental responsibility. A considerable number of large to small-scale corporation have nowadays environmentally sustainable practices incorporated into their mandates.

We believe nonetheless, that mitigation and adaption strategies are complementary and equally necessary. It is perhaps important today more than ever to plan a future with climate change given the already observed consequences (Onur & Tezer, 2015). Adaptation planning requires reliable climate change impact predictions for various sectors. Acquiring such information can prove to be a challenging task for non-climate change experts. Data on different variables of our climate that are indicative of change is required in order to assess the risks associated with climate change impacts and ultimately devise adaptation plans. Precipitation volume, minimum and maximum temperatures, relative humidity, wind speed and solar radiation are the top contenders amongst variables studied in the scope of climate change. Amongst which, precipitation and temperature are the most widely used gauges of climate change across all sectors. Changes in patterns, trend, frequency and intensity of climate variable are aspect studied to monitor and predict change in our climate.

1.2 Research Objectives and Contributions

Although, monthly downscaled data are available to the general public (Tabor & Williams, 2010), a challenge remains in providing access to daily climate data. National and international climate research institutes play a significant role in the effort to make climate simulation data available at the daily and sub daily scales. While daily climate data outputs from GCMs and

RCMs are a valuable asset in impact assessment for several sectors, scholars agree that most models require finer spatial resolution than what is currently available. Moreover GCM/RCM outputs are highly unreliable at the sub-grid scale to be used for region specific impact analysis (Wilby, Hay, & Leavesly, 1999). Consequently, downscaling techniques are consistently applied to achieve finer resolution. Leaving the downscaling process to end-users in various sectors – who are often non-experts in the science of climate data – can lead to unreliable outcomes and more importantly to ineffective solutions for climate change adaptation.

This Thesis proposes a digital dissemination method of reliable daily climate change data downscaled to specific stations. A web-based user interface has been implemented along with access to a database hosting the climate change data. Furthermore, climate change impact analysis tools such as extreme event computation as well as temporal distribution analysis of climate variables is offered. The objectives of the present Thesis are as follows:

i. Document the necessity for sectorial impact assessment of climate change and the need for finer resolution climate change data;
ii. Examine the performance of the proposed downscaling approach – i.e. the Quantile-Quantile mapping;
iii. Produce data storage and maintenance system to manage and disseminate downscaled climate change data;
iv. Validate the usability of the corrected climate change data by examining the predicted evolution of climate variables: Illustrate how the new web portal can be used to investigate changes in trend, frequency and intensity of precipitation and temperature for nine regional climate models of the AMMA-ENSEMBLE collection at the Niamey airport in Niger.

1.3 Thesis Outline

The present Thesis is divided into eight chapters.

- Chapter 1 describes the motivation behind the work. It also introduces the thesis hypothesis and contributions.
- Chapter 2 offers a background on climate change, the works undertaken to mitigate and adapt to it and the challenges within.
- Chapter 3 explores the various climate change data currently available to the general public as well as the different methods of downscaling GCM/RCM outputs.
- Chapter 4 investigates existing systems that allow access to downscaled climate data.
- Chapter 5 covers the approach used to downscale outputs from global and regional climate models.
- Chapter 6 is a validation of the Quantile-Quantile downscaling approach through a case study.
- Chapter 7 showcases the *Daily Climate Change Data Portal*
- At last, chapter 8 summarizes the main conclusions of this Thesis and presents an outlook for future work.

Chapter 2. LITERATURE REVIEW

2.1 Climate Change

The fluctuations of atmospheric temperature and its impact on our climate have been a point of discourse amongst policy makers, scientists and concerned citizens. Earth's natural greenhouse effect ensures that temperatures are kept at optimal levels to sustain life. However, in the past half of a century, the level of GHGs emitted has not been consistent with the level of GHGs removed from the atmosphere. The National Oceanic and Atmospheric Administration (NOAA) has indirectly measured historical carbon dioxide (CO_2) concentrations in the atmosphere by analyzing core samples collected from ice glaciers. Figure 1 below is a plot of computed atmospheric concentration of CO_2 since over four hundred thousand years ago.

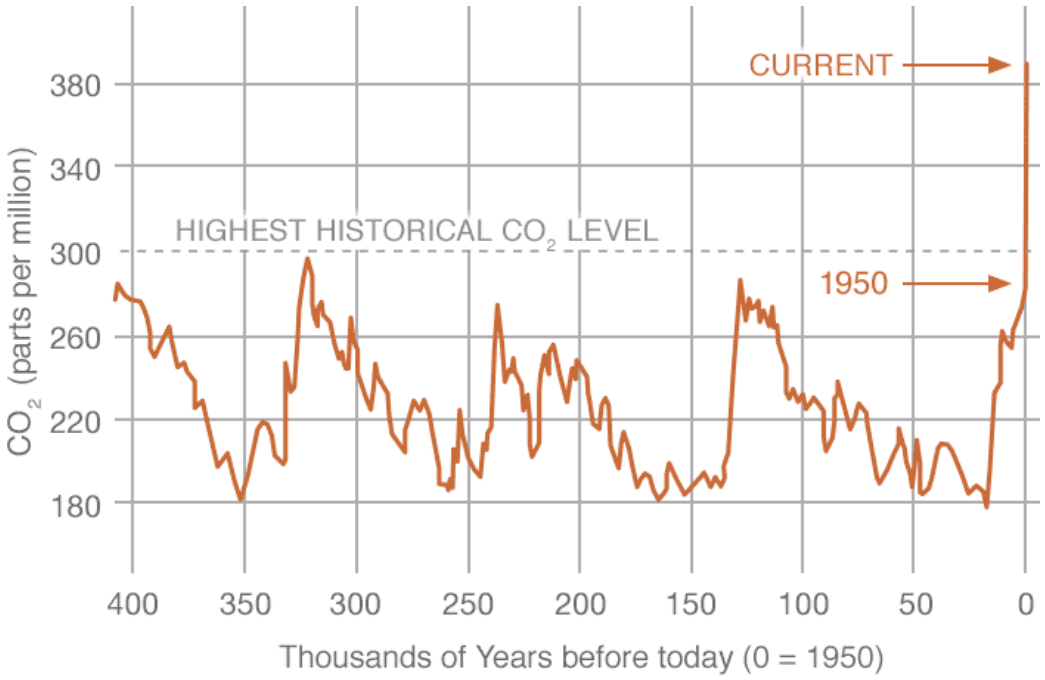

Figure 1 - Atmospheric concentration of Carbon dioxide reconstructed from ice cores by the NOAA – Global Climate Change. Vital Signs of the Planet

This exuberant increase in CO_2 atmospheric concentrations in turn, has resulted in the increase of Earth's atmospheric temperature by approximately 1 °C (Serreze, 2009). This seemingly minor transformation in temperature has resulted in considerable changes in our climates' cycles. Therefore it is imperative to explore the factors that have contributed to the increased levels of GHGs into the atmosphere and to assess the impact of climate change. The graphical illustrations compiled by the National Aeronautics and Space Administration (NASA) in Figure 2, Figure 3 and Figure 4 below are testament to the disconcerting increase in surface temperature over the years.

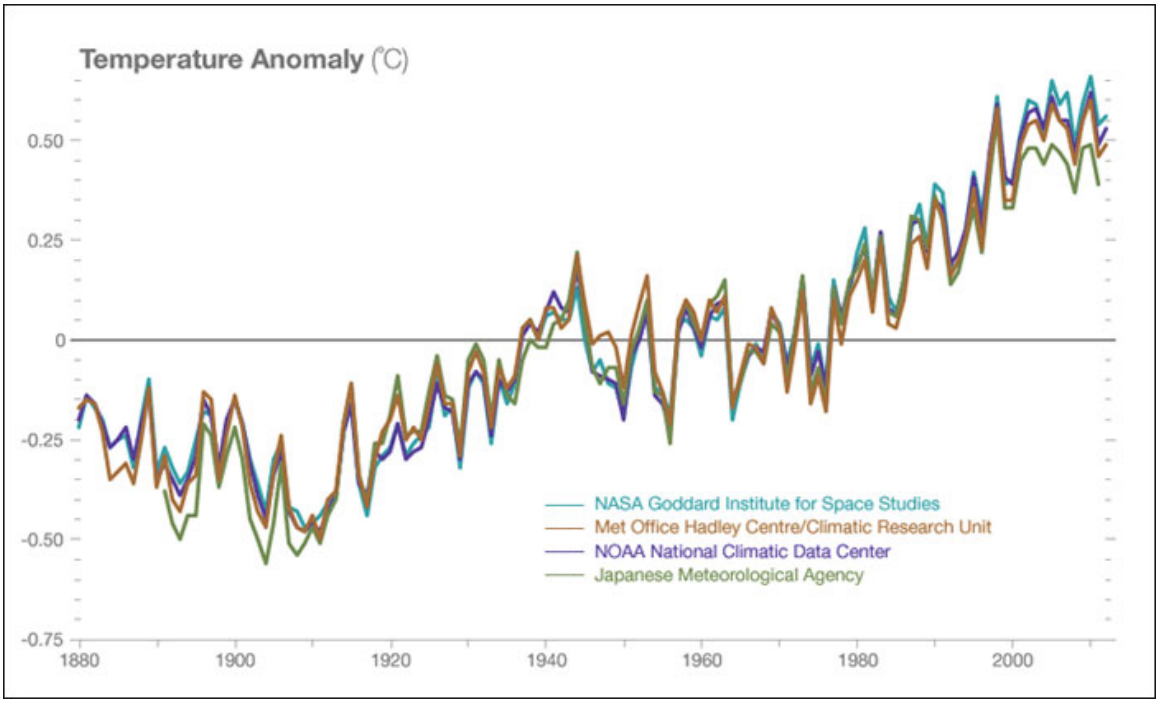

Figure 2 - Global temperature reported by the NASA

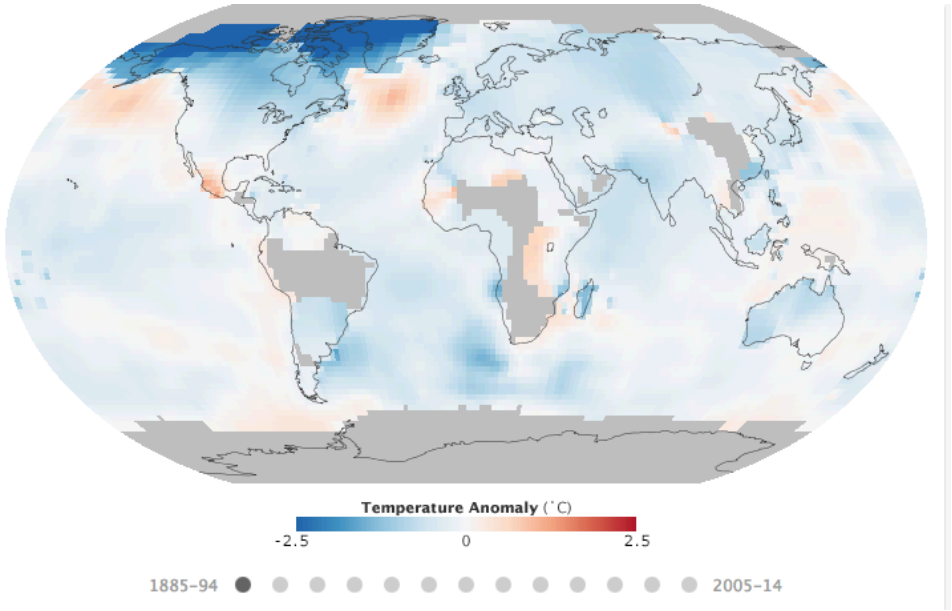

Figure 3 - Global temperature reported by the NASA (1885-94)

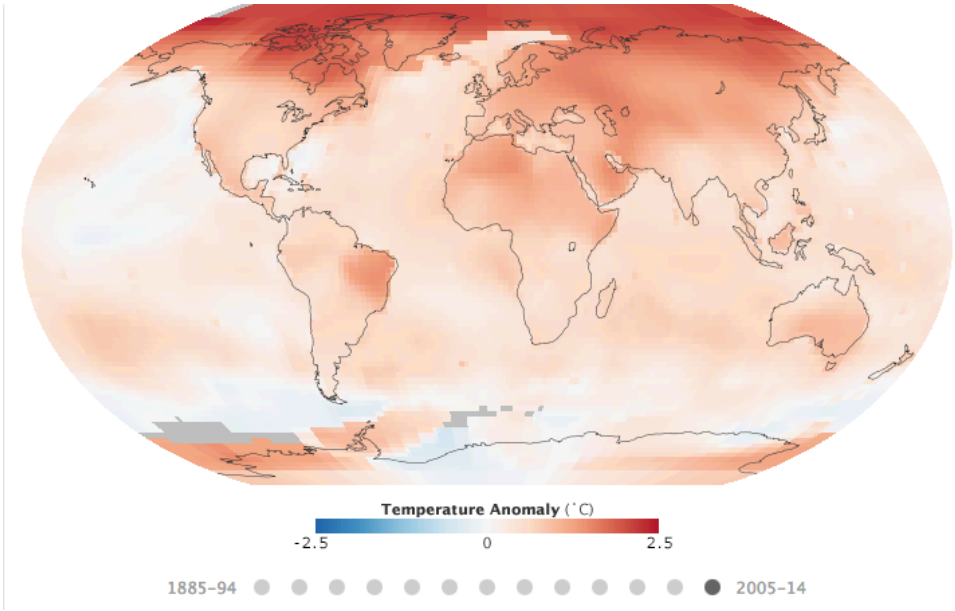

Figure 4 - Global temperature reported by the NASA (2005-14)

Researchers have identified several factors that have contributed to the increased levels of GHGs into the atmosphere. While some of these factors are naturally induced such as GHGs released from volcanic eruptions, plate tectonics, and biotic processes, others are man-made (Froster & Ramasamy, 2007). Human activities of powering heavy machinery in factories and treatment

plants, as well as the use of automobiles and airplanes have all caused the emission of large volumes of carbon dioxide, methane and halo carbon gases into the atmosphere. Data gathered and compiled by the Environmental Protection Act (EPA) of the United States of America (USA) indicated that the production and consumption of energy is the largest contributor to GHG emissions globally.

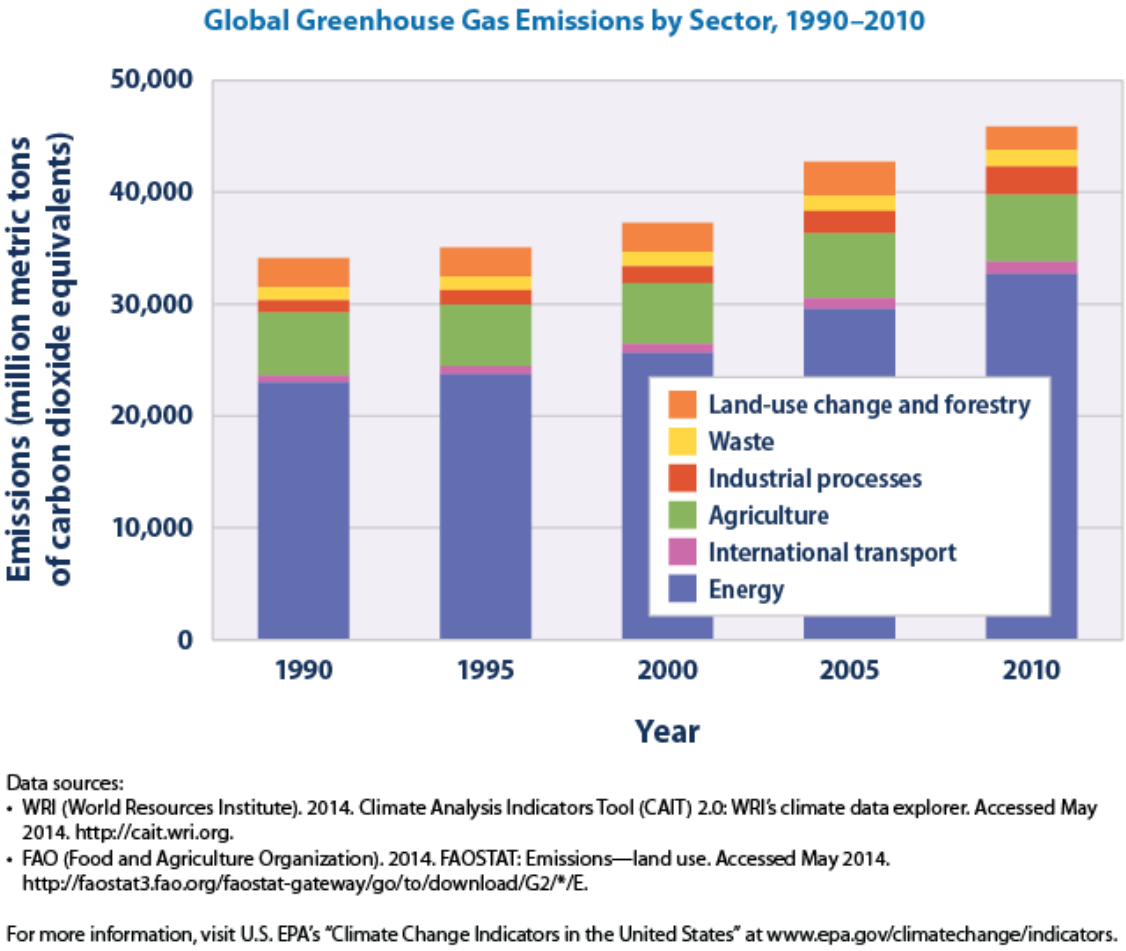

Figure 5 - Global GHG Emissions by Sector (1990 - 2010)

This is further exasperated by clearing out massive lands of vegetation, which are instrumental in removing GHGs from the atmosphere (Froster & Ramasamy, 2007). Therefore, researchers and policy makers have placed significant emphasis to mitigating human activities that continue to

fuel the emission of GHGs into the atmosphere. There is global consensus that irrevocable changes are already underway. The introduction of altering climate processes such as precipitation and temperature trends, frequencies and intensities has exposed the environment, socio-economic dynamics, and population health to vulnerabilities. It is hence perhaps important today more than ever to plan a future with climate change given the already observed consequences (Onur & Tezer, 2015)

2.2 Adapting To Climate Change: Impact Assessment Across All Sectors

2.2.1 Adapting to climate change

Climate changes resulting from increased atmospheric temperature can have many adverse effects on the fauna, the flora, public health, precipitation levels, water resources as well as energy sources. Consequently, researchers in multiple sectors and policy makers alike are left with the burden to analyze climate change impacts and devise adaptation plans.

The UNFCCC identifies five general components that constitute adaptation efforts. The list includes:

- Monitoring evolution of all aspects affected by climate change such as climate variables, socio-economic indicators and environmental gauges;
- Assessing of climate impacts and vulnerabilities across all sectors;
- Devising adaptation plans followed by their implementation;
- And monitoring and evaluating adaptation actions.

The present Thesis places the University of Ottawa's climate research group and others like it in the center of the aforementioned process of combating climate change. Figure 6 below is a graphic illustration underling the contributions of the work discussed in the present Thesis.

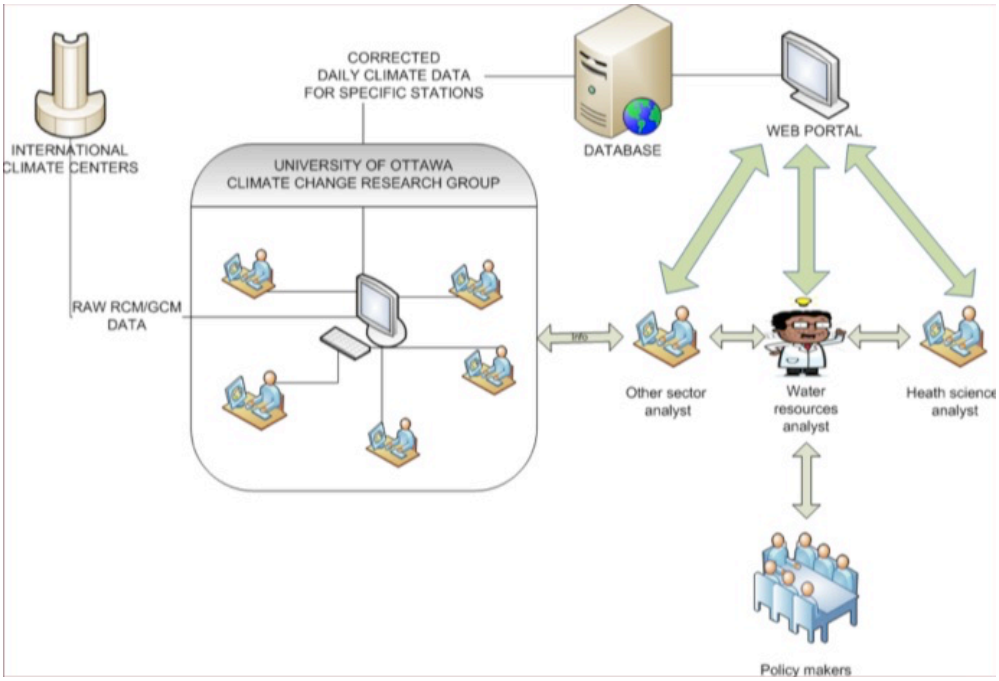

Figure 6 - Adapting to climate change

2.2.2 Climate change impacts

It is important to appreciate the spectrum that climate change impacts can extend to: all aspects of the environment (i.e. fauna and flora) as well as socio-economic dynamics. As such, professionals in all sectors are working tirelessly to combat climate change.

Climate change can place tremendous stress on the habitat in which animals dwell. For example, it can significantly alter the ecosystem of freshwater through changes in water temperature, accumulation of polluted precipitations, and decreasing oxygen levels as a result of over blooming allege population (Hansen, 2007). This not only compromises the aquatic population but also communities whose economies and survival rely heavily on fish trade (Hansen, 2007). The effects of climate change on animals are not limited to aquatic population; it can also apply to terrestrial and aerial animals. Therefore, it is crucial to find solutions to mitigate its effects.

There is a strong relationship that exists between agriculture and climate. Any change in climate cycles will therefore have repercussions on the survival of crops and the population it serves

(Sultan, 2012). Developing countries, whose economies are highly dependent on agriculture, are extremely susceptible to the adverse effects of climate change. Prolonged drought sessions in regions such as the sub-Saharan Africa, where food shortage is common, can expect to witness devastating strains on their food sustenance which will in turn impact the lives of millions of inhabitants (Sultan, 2012).

Researchers have also explored the potential implication climate change can have on public health. In their research, Kjellstrom, T., et al (2007) indicate how the rise in atmospheric temperature induced by GHGs can enhance incidents of heat-associated medical concerns such as heat stroke. Meanwhile, notable changes in precipitation levels can result in vector-borne disease including malaria and dengue. This in turn will cause those populations with inadequate public healthcare systems to suffer. Moreover, extreme weather conditions and the affiliated stress it places on communities, will inadvertently impact the mental health of communities worldwide (Kjellsrtrom, Butler, Lucas, & Bonita, 2010).

The adverse effects of climate change briefly discussed above, merely offer a glimpse into the magnitude of damage it can render, if left unattended. It is therefore imperative that policy makers and researchers in many sectors utilize their resources efficiently to tackle the obstacle of the emission of high level of GHGs into the atmosphere.

2.3 Issue: lack of access to data

The Internet has revolutionized the way information is stored and transmitted globally. It has been utilized to report up to date information on social, economical, political and geographical developments. This information is then used to research and enact policies, which mitigate issues such as poverty and/or severe drought episodes (Hinson & Adjasi, 2009). The Internet is a common resource for users of climate change data to access relevant information. For the

purpose of this thesis, lack of Internet access is defined as inadequate infrastructure. This can be characterized by low Internet speed, equipment scarcity such as access to computers and insufficient personnel training.

While Internet access has been growing rapidly worldwide, some regions are still lagging behind. A primary example is the continent of Africa, where in 2008 only 5% of its residents were reportedly connected to the Internet (McKague, Zurubchen, Donjakowski, Ervin, Heckathorn, & Morgan, 2009). The study contrasts these figures with North America where roughly 74% of the population accesses the Internet (McKague, Zurubchen, Donjakowski, Ervin, Heckathorn, & Morgan, 2009). It is important to note however, this digital divide is not limited between developing and developed countries. Digital divide is evident within Africa as well. Most Internet activity and infrastructure is concentrated in few countries such as South Africa, Botswana and Kenya (Stork, Clandro, & Gamage, 2014). Figures for countries like Ethiopia and Tanzania show that in 2011/2012 the Internet usage of people age 15 years old and above was estimated to be about 3%. The study further reveals that 67% of Ethiopians who had access to Internet were first introduced to it through their mobile phones (Stork, Clandro, & Gamage, 2014). This suggests institutionalized use of Internet in these developing countries is still at its primary stage.

Climate data manipulations, which aim to better predict climate changes, depend highly on strong infrastructure in order to be optimally efficient. One of the leading objectives of this thesis is to alleviate the burden to search or produce reliable station scale daily climate change data.

The challenge of inadequate Internet infrastructure in certain parts of the world is one that needs further attention. Nonetheless, this thesis suggests an improvement to the current system by

offering an easy and fast means of acquiring reliable daily climate change data for end-users in all sectors with limited resources.

The issue of insufficient data and the use of unreliable data can be hindering to the efforts to battle the impacts of climate change. The use of poor data can render unreliable research outcomes and consequently incoherent solutions across different sectors. The obtained corrupt information may lead to poor decisions and planning. Moreover, this imposes undue burden on the shoulders of sectorial analysts to obtain reliable climate change information. This is problematic because most end-users are not climate data experts.

Although, monthly downscaled data are available to the general public, a challenge remains in providing access to daily climate data (Tabor & Williams, 2010). National and international climate research institutes play a significant role in the effort to make climate data available at the daily and sub daily scales. They offer daily climate data in grid formats obtained from Global Circulation Model and Regional Climate Model (GCM/RCM) outputs. While daily climate data outputs from GCMs and RCMs are a valuable asset in impact assessment for several sectors, scholars agree that most models require finer spatial resolution than what is currently available. Wilby, R.L. and Wigley, T.M.L., (1997) explain how hydrological models for instance are focused on local processes that occur at much smaller scales than that of the GCM and RCM output grids. These scale mismatches are of concern due to the uncertainties they entail.

The change from coarse scale point format grids to sub grid coordinates fails to incorporate local climate gradients. Uncertainties in the information contained in GCM/RCM model outputs are manifested with strong biases, erroneous probability distributions, and inaccurate temporal distributions (Noguer, Jones, & Murphy, 1998; Pan et al., 2001; Sharma, Coulibaly, & Dibike, 2011). Furthermore, coarse grid data sets ignore region specific factors governing local climate

gradients (Mahe et al., 2013). Local factors may include physical barriers such as a mountain that is able to alter the process cycle of atmospheric convection cells. Another aspect of local climate that is often misrepresented in GCMs and RCMs is the highly variable population density. Population density is a known indicator of various factors impacting climate such as urbanization and land use to name a few. Moreover, GCMs are unable to simulate processes leading to extreme events (Maraun, et al., 2010).

The application of bias correction in different models in various studies is set to provide consistency of data (Christensen et al., 2008; Hashino, Bradley, & Schwartz, 2006). Downscaling techniques have emerged as a result of the need to correct uncertainties arising from the scale mismatch between available climate data and impact analysis requirements.

Chapter 3. CLIMATE DATA DOWNSCALING

3.1 Global Circulation Models

R. L. Wilby et al. (2011) define climate data downscaling as a set of techniques used to harvest local scale data sets – i.e. less than 100 kilometers – from global or regional data sets with coarser resolutions. Climate data downscaling can be a tedious and repetitive task. Moreover, it requires expert knowledge and knowhow to obtain reliable results. It has been thus far imposed that such tremendous efforts are essential to provide decision makers with much needed high-resolution climate data (R. L. Wilby et al., 2011). The first downscaling attempts trace back to the 1950s where meteorologist established statistical correlation between observed data and numerical weather predictions to forecast short term estimates for variables such as surface wind direction and magnitude, precipitation characteristics such as type and volume, minimum and maximum temperatures, cloud cover as well as visibility (R. L. Wilby et al., 2011).

The efforts discussed in this thesis pertain to downscaling data outputs from GCM and RCM simulations.

Stone, P.H. and Risbey, J.S. (1990) interpret GCMs as computational models that infer 'dynamical and thermo-dynamical processes' from primary physics principles in order to establish a comprehensive representation of the earth's climatic phenomena at global scales. Moreover GCM parameterizations are tuned to be sensitive to contributing and/or resulting processes such as glacier activity and ocean processes for instance. Data outputs from GCMs are presented in a grid point format. The resolution of such grids often towers over 100 kilometers (R. L. Wilby et al., 2011). GCMs simulations are run based on various scenarios postulated by

climate change research organizations such as the Intergovernmental Panel on Climate Change (IPCC).

3.2 Dynamical downscaling – Regional Climate Models

Chen, J. et al. (2012) explain that dynamical downscaling is a complex process that involves running climate model simulations at finer spatial resolution resulting in regional climate models (RCM). RCMs inherit their initial and time-dependent boundaries from the GCM they are based up on. In addition, they take into account local convection cells and other local climate forcing agents in their parameterization and formulation to allow for an improved representation of the region's climatic characteristics. Maraun, D. et al. 2010 agree that RCMs tend to better simulate the spatio-temporal characteristics of climate variable at higher resolution than GCM are able to. Furthermore, the improvement witnessed over GCM outputs can be attributed to comprehensive representation of the local topography and fine‐scale dynamical and physical processes.

Nevertheless, RCMs only yield reliable climate extremes at the grid cell scale. As such, a typical RCM model of 25 to 50km square resolution is only reliable at a scale of about 100 km square. Moreover, dynamical downscaling requires considerable computational power (Chen, J. et al., 2012). As a result, fine resolution RCM outputs from multiple models are hard to come by, particularly for the same region. As such, climate change data users are often left with a singular climate change scenario and are unable to draw conclusion by comparing different possibilities.

3.3 Regression Based Downscaling Technique

Though in most cases out of lack of options for alternatives, some studies choose to directly apply climate model outputs in their climate change impact analysis despite the uncertainties and strong biases associated with them. Chen, J. et al. (2011) examined the performance of several

climate data downscaling methods including the direct use of climate model outputs without any bias corrections. Compared to Global circulation models, regional climate models are expected to offer improved spatial resolution for a restricted target region. Chen, J. et al. (2011) state that in instances where the study area is less than that of the RCM used, it may be acceptable to directly use climate data outputs from RCMs and assume that the biases are weak enough to be ignored. Nonetheless, the same study concluded that the direct use of climate model outputs still present higher biases than other downscaling methods and could also be incoherent with the observed historical data.

In an effort to correct uncertainties in GCM/RCM outputs, many climate change data users apply a technique commonly known as the delta change approach (Themebl & Gobiet, 2011). Using this approach, a climate change offset is applied to the observed historical data. The climate change offset is obtained by computing the mean differences between GCM/RCM future values and historical period values at either the annual or monthly scales. While it is possible to deduct how monthly or annual means of climate variables evolve with the delta change method, it is virtually impossible to determine frequency and amplitude variability with time of extreme climate events.

Another basic approach to achieve higher spatial resolution is to undertake the primal task of linear interpolation between neighboring grid points from the GCM/RCM output data sets. R. L. Wilby et al. (2011) emphasize on the minute efforts required and the speed at which the aforementioned technique can deliver higher spatial resolution. Meanwhile, the scholars also remind us that the method gives no regards to physical stimuli that stem from the local geography such as topography or vegetation, climatic history or any factors affecting the climate. The method is only certain in cases where acceptable uniformity is witnessed and no climate

variability is expected. Consequently, simple interpolations struggle to earn the trust of decision makers as they fail to appreciate the subtle location climatic gradients.

3.4 Statistical Downscaling

Statistical downscaling is the method of choice for many because of the minimal computational cost requirements and simpler mathematical concepts involved (Seidou, O. et al., 2011). Perhaps the most appealing advantage of statistical downscaling is their ability to yield location specific climate data at a point-scale (Fowler, H.J., et al., 2007). Statistical downscaling techniques can be classified into three families: transfer functions, weather typing and stochastic weather generator (Chen, J. et al., 2012). Nonetheless, many studies combine several aspects of the three identified categories. The focus of the present Thesis is kept on transfer function based statistical downscaling.

Transfer functions attempt to draw and exploit the relationship between observed local historical climate data and coarse grid climate outputs from GCMs and RCMs. However, one should always carefully examine the relationship. Studies have shown that seasonal climate cycle may vary annually (Wilby, R.L. and Wigley, T.M.L., 1997)). The appeal of transfer functions stems from their relative ease of application. Moreover, once a process is established, the transfer function based downscaling method can be applicable to entirely diverse regions with little or no alteration required to the process (Fowler, H.J., et al., 2007). Generally, the objective of transfer function based statistical downscaling methods is determine the function $F(X)$ that is able to correct a modeled variable $X_{RCM/GCM}$ in an attempt to match its probability distribution to that of the observed historical variable X_{OBS} (Gudmundsson, L. et al. 2012).

Chapter 4. CLIMATE DATA PORTALS

In the course of this research, two main categories of climate data distribution avenues that currently exist on the Internet have been identified. The leading factor that distinguishes the two families of climate change data distribution from one another is the target audience they address. Dissemination of climate change data as such has had two very distinct objectives:

- Sharing climate change research outputs with fellow experts of the domain in hopes of advancing our collective understanding of the issue at hand.
- Spreading awareness to the general public on the issue of climate change.

4.1 Dissemination of specialized climate change data

This realm of climate change data circulation is inherently narrow due to the level of expertise required to secure membership. Participants are often large-scale international institutions such as the IPCC, regional projects, amply funded national establishments such as the NOAA or academic research initiatives in higher education levels.

Major national and international institutions such as the NOAA and IPCC offer global scale GCM simulation outputs. GCM outputs are usually presented in a point grid format. The IPCC and other organizations alike offer data for a variety of specific climate variables ranging from surface climate indicators to atmospheric as well as hydrospheric climate metrics. Surface climate variables are the most frequently used to monitor and evaluate changes in climate trends. Commonly used surface climate variables include precipitation, temperature, humidity, wind and solar radiation. Data for the later is often available at different temporal scales ranging from daily

to annual. While the available temporal spectrum is vast, GCM outputs are often constrained to coarse spatial scales in the order of 100 square kilometers (R. L. Wilby et al., 2011).

Climate change data circulating amongst experts of the field is often cryptic and requires data manipulation and management skills from the user. Research outputs offered by the aforementioned institutions are often accompanied by metadata with minimal instructions to gain access or extract subsets of data. These sets of data are often comprised of large volume of numerical figures with minimal to no interpretations, scientific or otherwise. Moreover, they are available in archival data formats such as NetCDF or OPenDAP. The latter are software libraries and communication protocols designed and conceived for the sole purpose of scientific data storage and distribution. These data management tools introduce yet again an added requirement to share climate data with the elites of the industry. The user is not only required to be well versed in the practices of climate data but is also expected to possess the skills and training to work with specialized software and protocols. Furthermore, the volume and variety of data offered by the aforementioned international organizations are immense and overwhelming for the average end user. IPCC initiatives such as the CMIP for example are putting forth close to two petabytes of GCM data each.

In parallel to the GCM outputs, regional collaborations are able to produce and offer outputs from climate model simulations at the regional scale. Although users of RCM outputs benefit from refined spatial resolution, they are faced with the same challenges: expert knowledge and skills are required to manipulate and hence use of climate change data from RCM outputs remains constrained to the elite few.

4.2 Dissemination of climate change data for general public awareness

On the other hand, a large number of online as well as printed outlets offer simplified analytics of climate change. Often climate change is presented as a singular figure representing either an increase in mean annual temperature or increase in sea levels. Perhaps the most frequently encountered form of information in regards to climate change is simply a narrative with very limited scientific presentation of research outcomes: a dominant portion of the available data is merely presented as possibilities of drought and flood misfortunes. The one-dimensional nature of the information serves its purpose and is well intended to the target audience – i.e. the general public.

4.3 Dissemination of downscaled climate change data for impact assessment

The aim of this Thesis is not to discredit the numerous research initiatives that have yield very valuable publications. This Thesis merely seeks to underline the lack of appropriate data dissemination for climate change impact assessment. As stated earlier, the ripples of climate change impact reach far beyond weather and climate. Various sectors are impacted, directly or indirectly. The professionals working across these sectors are left with the burden of planning a future with changing climate conditions. To do so, sectorial analysts require reliable climate change information pertinent to their specific location of study. This is problematic because, first of all, most end-users are not climate data experts. Secondly, the remainder of climate change information intended for the general public is too simplistic and of no value for impact assessment. As such, sectorial analysts often revert to unfitting practices using climate change data intended for experts. Primal linear downscaling is often applied to GCM and RCM outputs. Perhaps the most inappropriate use of GCM/RCM outputs for impact assessment is the direct application without any bias correction. The issue of insufficient data and the use of unreliable

data can be hindering to the efforts to battle the impacts of climate change. The use of poor data can render unreliable research outcomes and ultimately incoherent solutions across different sectors.

The climate change data dissemination proposed in the present Thesis is part of an emerging trend. Efforts are being made in this domain to downscale climate change data and offer reliable information for sectorial analyst to perform meaningful impact assessment. The main intent is to fill the gap currently existing and alleviate undue burden on end users of the data that are not experts. To name a few, the following is a list of some such portals for downscaled climate change data dissemination:

- "Climate Change Knowledge Portal" by the World Bank group
- "CCAFS GCM Data Portal" by the Center for Tropical Agriculture
- "Regional and Global Climate Data" by the United States Geological Survey

The above mentioned data portals and others alike, focus mostly on the North American and European continents. It appears that the African continent in particular is the subject of much lesser attention. This perhaps is fostered by the obvious financial constrains that African nations experience. Moreover, the downscaling technique applied in the course of the formulation of the present Thesis exhibits advantages over the ones applied in other data portals – i.e. variations of the delta method and linear regressions.

Chapter 5. THE QUANTILE-QUANTILE DOWNSCALING APPROACH

5.1 Climate models used: AMMA-Ensemble, A1B scenarios

Global Circulation Models are representations of the phenomena and cycles within the globe affecting the evolution of its climate. The leading international body in the assessment of climate change – The Intergovernmental Panel on Climate Change (IPCC) – has defined several families of plausible scenarios in which dynamic systems such as demographics, socio-economic development and technological advances determine emission levels of GHGs. The different scenarios pause alternative hypotheses resulting in various GHG emission levels and in turn determine how the representation of the earth's climatic unfolds at global scales. Each scenario entails specific postulations in terms of demographic, socio-economic, technological, and environmental developments. The AMMA-Ensembles models used in the scope of this project are based on A1B scenarios. The A1 family of scenarios is officially defined by the IPCC SERS (Special Report on Emission Scenarios) as one that "describes a future world of very rapid economic growth, global population that peaks in mid-century and declines thereafter, and the rapid introduction of new and more efficient technologies." The A1B sub-category of scenarios are driven by the assumption that future technological advances will be balanced across different energy sources and that several energy sources will be used evenly.

While it is obvious future uncertainties are inherent, the SERS scenarios are essential tools for impact assessment and policy makers. As such, GCM simulations and outputs are indispensable in the assessment of climate change. However, the spatial resolution at which the latter outputs are available is often of concern given their coarse nature.

The African Monsoon Multidisciplinary Analysis (AMMA) is a project that aims to explain the impacts of climate change on the African continent. It particularly focuses on the interaction between different cycles ranging from convective cells to global hydrospheric and atmospheric circulations on an array of different time scales. In collaboration with the Ensembles initiative, a set of AMMA-Ensembles Regional Climate Models have been made available in an effort to offer finer spatial resolution (50 x 50 km) than that available from GCM outputs which are usually in the range of 100 x 100 km to 300 x 300 km. Although RCM outputs provide greater spatial resolution for climate data, the needs for climate change impact analysis are far from being met. Impact assessment requires region specific data that incorporate local climate agents to yield reliable conclusions. Table 1 below lists the AMMA-Ensemble regional climate models used in this project.

Table 1 - The AMMA-Ensembles Experiment

Institution	IPCC SERS Scenario	RCM	Resolution	Span	Identifier
KNMI	A1B	RACMO	50 km	1970-2050	KNMI-RACMO2
DMI	A1B	HIRHAM	50 km	1989-2050	DMI-HIRHAM5
ICTP	A1B	RegCM	50 km	1980-2100	ICTP-REGCM3
METNO	A1B	HIRHAM	50 km	1990-2050	METNOHIRHAM
HC	A1B	HadRM3p	50 km	2951-2100	METO-HC_HadRM3.0
GKSS	A1B	CLM	50 km	1961-2050	GKSS-CCLM4.8
INM	A1B	RCA	50 km	2951-2100	INMRCA3
MPI	A1B	REMO	50 km	1951-2050	MPI-M-REMO
CHMI	A1B	Aladin	50 km	1991-2050	CHMIALADIN

5.2 Observed data

Data sets of daily values of precipitations, maximum as well as minimum temperatures, relative humidity, wind speed and solar radiation gathered at given climate recording stations are used for the purpose of this study. Note however, that the historical climate data may present several data points with missing or inacceptable values. Consequently, missing observed data points and data sets were substituted with National Center for Environmental Prediction (NCEP) reanalysis data.

5.3 The Quantile-Quantile method

The Quantile-Quantile downscaling method is a statistical approach that aims to apply an empirical cumulative probability function (CDF) from a set of control data to that of a target data (Gudmundsson, L. et al. 2012). In the case of climate data downscaling, the control data set is historical observation. Measured data is regarded as the benchmark for any modeling work attempting to simulate the physical quantity in question. If we denote $F_{GCM/RCM}$ as the CDF of the modeled variable $X_{RCM/GCM}$ and F_{OBS}^{-1} as the inverse CDF of the observed historical variable X_{OBS}, the Quantile-Quantile transformation can be expressed as follows.

$$X_{CORR} = F_{OBS}^{-1}\left(F_{GCM/RCM}\left(X_{RCM/GCM}\right)\right)$$

Where X_{CORR} is the corrected GCM/RCM output data set.

The empirical CDF applied in the case of Quantile-Quantile approach is a step function that estimates the true exceedance probability of the data points in a given sample. For illustration purposes, daily minimum temperature in the month of August at the Niamey Airport climate

station is used. As illustrated in Figure 7 below, a binary mapping is established to correct the distribution of the modeled quantity based on observed historical measurements.

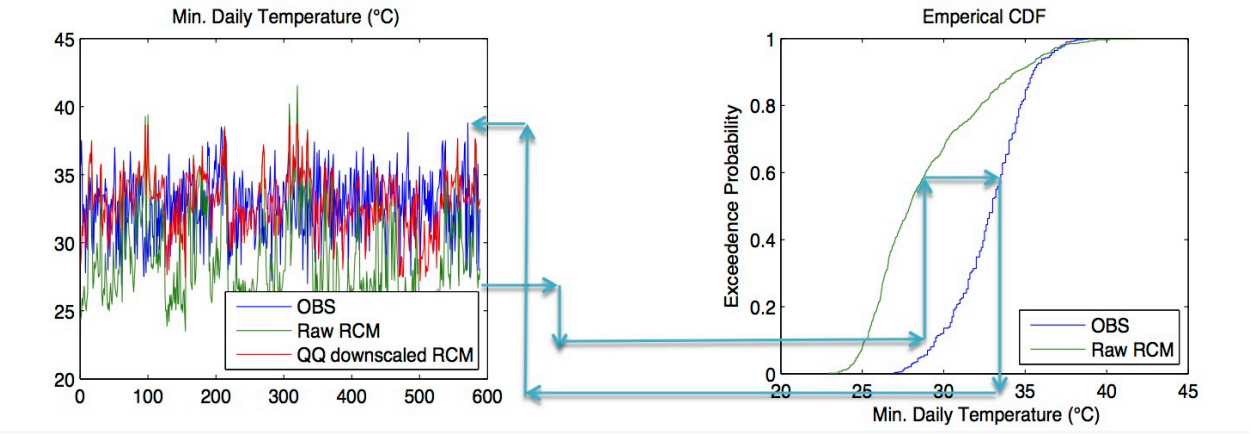

Figure 7 - Graphical illustration of Quantile-Quantile Mapping

5.4 Impact assessment tools and Performance evaluation

An essential aspect of climate data downscaling is to be able to evaluate and quantify its performance. Moreover, it is crucial to yield tangible tools to advance global efforts to adapt to climate change. In this section, we will review techniques applied to validate the downscaling skill of the Quantile-Quantile approach. Although evaluation metrics vary depending on the end user's needs, climate downscaling methods are expected to satisfy a number of checks. We are particularly interested in the ability of the method to replicate characteristics the observed historical data. Consequently, any validation method is at the mercy of the quality as well as quantity of the observed historical data.

While we subject the downscaling approach to a minimum standard of being able to reproduce different observed variables, it is equally important to evaluate the downscaling method's skill to reproduce various characteristics of the same climate variable such as precipitation indices for

instance. We will discuss further in this thesis extreme climate indices established by the Expert Team on Climate Change Detection and Indices (ETCCDI).

The needs of climate data end-users vary vastly. Contingent on socio-economic demands, geo-political pressure, demographic needs and sector of study, climate change data may be subject to diverse seasonal assessments (Maraun, D. et al., 2010). Hence, depending on the end user, additional information may be required for a specific season. Monsoonal climates such as in West Africa require accurate prediction of precipitation occurrence and intensity given that the region relies heavily on seasonal rainfall for its agriculture and food sustenance.

5.4.1 Probability distributions

While absolute error between model outputs and historical benchmark is an acceptable evaluation of downscaling methods, it is fundamental to study probability distribution of the downscaled outputs. The commonly agreed upon rule in climate modeling is that simulated variables should exhibit similar probability distributions to that of the observed historical data. It is believed that probability scoring performance measures are better suited to gain meaningful perception for continuous climate events such as precipitation (Maraun, D. et al., 2010).

Furthermore, all evaluations of climate modeling performance are expected to be carried out in a two-step process on independent portions of the data set, i.e. a calibration or training period and a validation period. As such, monthly probability distribution analysis has been incorporated in this project to offer reliable means of evaluating the downscaling method applied. The monthly probability distributions offer comparison between observed data, raw RCM outputs and downscaled RCM outputs. The comparisons are available over several time period including the calibration period and validation period.

5.4.2 Binary scoring

In addition to the monthly probability visualization available for each climate variable, binary occurrence probability scoring has also been incorporated. Similar to the probability distributions, the binary probability scoring is done over different time periods to maintain the integrity of the performance evaluation process. The binary scoring is a useful tool to reliably predict the likelihood of daily precipitation occurrence in a given month during a specific time span into the simulated future.

5.4.3 Kolmogorov – Smirnov

While visual inspection of graphical representation of the probability density functions is a reasonable approach of evaluating if two samples follow indeed comparable probability distributions, the Kolmogorov – Smirnov (KS) test offers more meaningful and tangible assessment. There are several variations of the KS test. The present Thesis will however, only discuss and apply the two-sample-KS-test.

The KS test is a nonparametric statistical measure, which means it does not require any assumptions as to the probability distributions of the samples being evaluated. This characteristic makes the KS test very attractive particularly in climate change studies given that climate variables have proven to exhibit metamorphic distributions under certain scenarios. Hence, the test can be performed on observed as well as simulated samples without the need to fit a distribution.

Test results from the KS test are binary with the null hypothesis stating that the two samples follow the same continuous probability distribution. The alternative hypothesis states the contrary – the two samples do not follow the same continuous probability distribution. Distance

between the empirical cumulative density functions of the two samples as follows is used to perform the test:

$$D = \sup_x \left(|F_1(x)| - F_2(x)|\right)$$

Where F_1 and F_2 are the empirical distribution functions of the two samples, and sup is the supreme function. The null hypothesis is confirmed for specified values of tolerance p.

5.4.4 Extreme event indices

Extreme climate event predictions have a vast array of applications particularly in hydraulic planning. Maraun, D. et al. 2010 underline the importance of accurately predicting precipitation intensity given that it is an essential input in to the design of urban drainage networks. The historic accounts of flood instances in Boscastle, Southwest England and Hampshire, South England in 2004 and 2001, respectively are perfect anecdotal proof of the importance of climate extremes. While both events are hydrological extremes of high run-off, the events leading to the floods are far from alike. The August 2004 flood was caused by 181 mm of rainfall, which occurred in only five hours. In comparison, the 2001 flood was caused by a record high 8-month total precipitation leading to groundwater overflow.

In light of the importance of climate extremes, extreme climate change indices have been studied and incorporated in this project.

Table 2 below lists a selected number of climate change indices that have been chosen for this end.

Table 2 – ETCCDI Climate change indices

Indices identifier	**Indices name**	**Definition of indices provided by the ETCCDI**
PCPTOT	Annual total precipitation in wet days	Let RR_{ij} be the daily precipitation amount on day *i* in period *j*. If *I* represents the number of days in *j*, then $\mathrm{PCPTOT} = \sum_{i=1}^{I} RR_{ij}$
R99pTOT	Annual total precipitation when daily precipitation is over the 99th percentile of daily precipitation during 1961-1990	Let RR_{wj} be the daily precipitation amount on a wet day *w* (RR ≥ 1.0mm) in period *i* and let RR_{wn99} be the 99th percentile of precipitation on wet days in the 1961-1990 period. If *W* represents the number of wet days in the period $\mathrm{R99pTOT} = \sum_{w=1}^{W} RR_{wj}$ for $RR_{wj} > RR_{wn99}$
R95pTOT	Annual total precipitation when daily precipitation is over the 95th percentile of daily precipitation during 1961-1990	Let RR_{wj} be the daily precipitation amount on a wet day *w* (RR ≥ 1.0mm) in period *i* and let RR_{wn95} be the 95th percentile of precipitation on wet days in the 1961-1990 period. If *W* represents the number of wet days in the period $\mathrm{R95pTOT} = \sum_{w=1}^{W} RR_{wj}$ for $RR_{wj} > RR_{wn95}$
CWD	Maximum length of wet spell	Maximum number of consecutive days with RR ≥ 1mm
CDD	Maximum length of dry spell	Maximum number of consecutive days with RR < 1mm
R20mm	Annual count of very heavy precipitation days (over 20mm)	
R10mm	Annual count of heavy precipitation days (over 10mm)	
R01mm	Annual count of wet days (over 1mm)	
SDII	Simple precipitation intensity index	Let *RRwj* be the daily precipitation amount on wet days, w (RR ≥ 1mm) in period *j*. If *W* represents number of wet days in *j* $\mathrm{SDII_j} = \frac{\sum_{w=1}^{W} \mathrm{RR_{wj}}}{W}$
Rx5day	Monthly maximum consecutive 5-day precipitation	
Rx1day	Monthly maximum 1-day precipitation	

5.4.5 Return period

The interval at which process of interest is likely to reoccur is known as the return period. Serinaldi, F. (2014) claims that the concept of return period is perhaps the most widely used tool in evaluating the risk associated to reoccurring hazards. It is also the single most used design parameter for hydraulic structures (Salas, J.D. and Obeysekera, J., 2014). The return period (T) is defined as the mean span of time lapse at which a process is expected to repeat with equal or greater magnitude. As such, the return period is inversely proportional to the likelihood of occurrence of the event it is associated to. The probability distribution is commonly computed based on empirical or historical observations of the process as follows

$$T = \frac{\mu}{p} = \frac{\mu}{\mathbb{P}|X > x|} = \frac{\mu}{1 - F(x)}$$

Where:

- X is a random variable describing the process of interest;
- μ denotes the average inter-arrival time between two realizations of the process
- p is the probability to observe realizations exceeding a specific value x
- $F(x)$ indicates the distribution function of X

Though return period is widely applied across a vast array of fields, its definition is often misunderstood and more importantly unrealistic conclusions are drawn from its analysis (Serinaldi, F., 2014). The most common flawed application of the return period stems from the fact that users forget that it is actually a statistical tool. Consequently, misconstrued statements are often made asserting that a certain extreme weather event of a given magnitude occurs only at specific time intervals. Nonetheless, it remains one of the least computationally demanding risk assessment tools provided proper understanding of its concept. Return period is commonly

expressed in years when applied in the field hydrology and climate change. Five return periods are traditionally used to evaluate the risk associated to hydrological and climate cycles. As such the same five periods – 5, 10, 20, 50 and 100 years – are used for the purpose of this Thesis to evaluate the outputs from Quantile-Quantile downscaling.

5.5 Limitations

As any scientific endeavor, the statistical downscaling approaches are based on a set of leading assumptions. The most significant assumption being that local statistical features are maintained in the future and thus are accepted to formulate meaningful evaluation of the processes' performance. Moreover, statistical downscaling and thus the Quantile-Quantile approach by association are inherently exceedingly sensitive to the quality and quantity of observed historical climate data. In the meantime, one of the strongest advantages of the Quantile-Quantile method is that it can be applied to any set of climate data that is reliably obtained. It is also worth noting the computational ease required as compared to dynamical downscaling techniques used to obtain RCM model outputs.

Chapter 6. VALIDATION OF THE QUANTILE-QUANTILE DOWNSCALING METHOD APPLIED TO A SET OF AMMA - ENSEMBLES REGIONAL CLIMATE MODELS AT THE NIAMEY AIRPORT

6.1 Study Area

The Niamey airport is located in the Southeastern outskirts of the Niger capital. The region rests on low altitude plateaus reaching approximately 200 meters. The Niamey airport climate station is located in the Niger River watershed. The Niger River is the principal river in Western Africa. Following the Nile River in Eastern Africa and The Congo River in Central Africa, the Niger River is the third largest in the continent at a length of 4,200 km.

As stated at several occasions throughout this thesis, the need for higher resolution climate data is reflected once more. The Niger River watershed, being as vast as it is, cannot be studied as a single entity with no appreciable climatic gradients. The river's catchment basin covers a total of 2.27 Million square kilometers, extending its resource to ten countries. Every country within the basin has unique geographic settings and characteristics as well as a wide range of available resources.

The region is known host to an annual rainy season lasting from three up to four months from June to September. The remainder of the year is mostly dry (Abrate, T. et al., 2013). Annual temperatures are known to fluctuate between 20 and 30 degrees Celsius.

6.2 Historical Observed Data

Available data sets of daily values of precipitation in millimeters, maximum as well as minimum temperatures in degree Celsius, relative humidity in percentage, wind speed in meters per second

and solar radiation in Watts per square meter at the Niamey Airport climate station were gathered for the purpose of this study from the AGRHYMET Center.

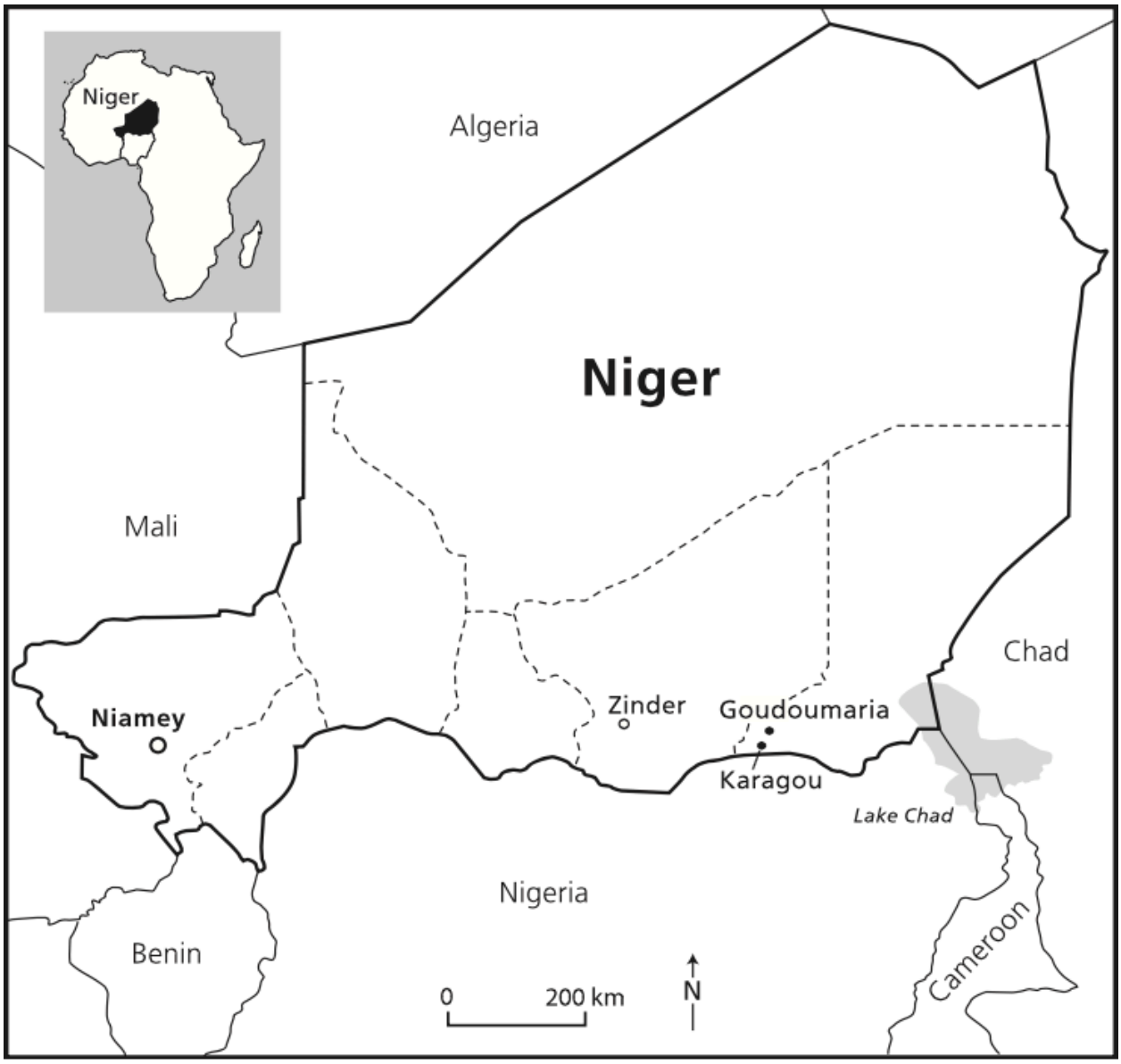

Figure 8 - Niamey, Niger (Reenberg, A. et al. 2013)

The historical climate data obtained span from January 1st, 1980 to December 31st, 2010. Note however, that several data points were missing values. Moreover, no observed data was obtained for the following three climate variables: relative humidity, wind speed and solar radiation.

Consequently, missing observed data points and data sets were substituted with NCEP reanalysis data.

6.3 NCEP Reanalysis Data

National Center for Environmental Prediction (NCEP) Reanalysis data are provided by the National Oceanic & Atmospheric Administration (NOAA). The climate reanalysis data are a result of data assimilation efforts by the Earth System Research Laboratory. The data sets are made available for public use in a standardized netCDF format. According to the NOAA, observed climate data used in the assimilations come from a variety of sources such as ground station recordings as well as satellite, radar and other remote sensing collections.

The NCEP Reanalysis "Surface Data" collection is offered in a grid point format of 2.5-degree latitude by 2.5-degree longitude spatial resolution. The "Surface Data" collection, which includes air temperature, precipitation, relative humidity and wind speed among others, is available at monthly, daily and sub - daily (6 hours) temporal scales. Likewise, solar radiation is offered at similar temporal scales as part of the "Other Flux" collection.

6.4 Results and Discussion

6.4.1 Daily time series

A set of time series plots at the daily scale for each AMMA-Ensemble regional climate model are shown in Figure 9 through Figure 32 below. The time series plots include observed, raw RCM outputs as well as Quantile-Quantile downscaled data for each climate variable. Although regional climate model outputs were extracted and downscaled for daily relative humidity, wind speed and solar radiation at the Niamey airport, the focus of the analysis and interpretations in this thesis is targeted on precipitation and daily maximum as well as minimum temperatures.

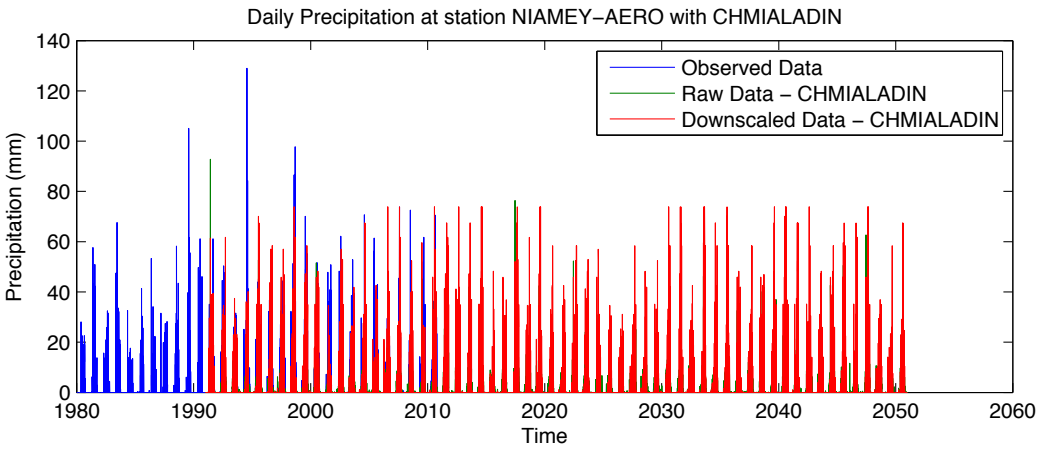

Figure 9 - Daily Precipitation at Niamey airport with CHMIALADIN

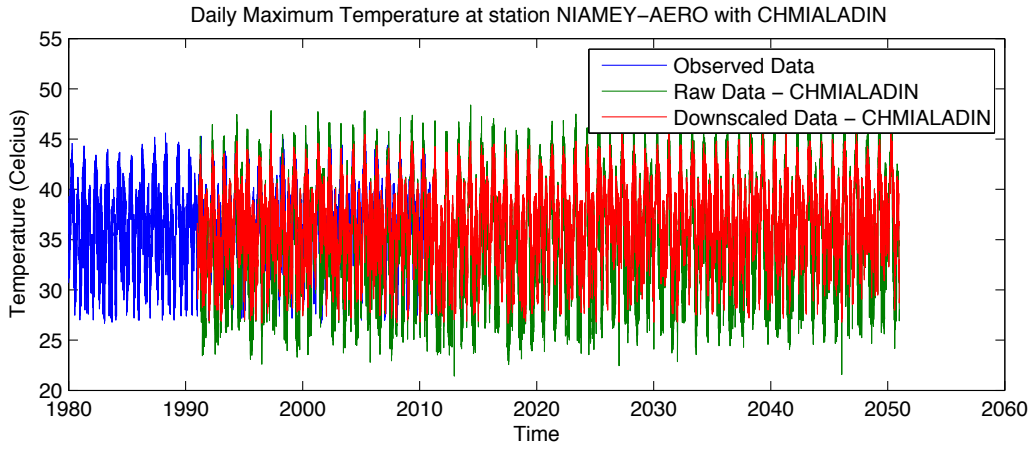

Figure 10 - Daily maximum temperature at Niamey airport with CHMIALADIN

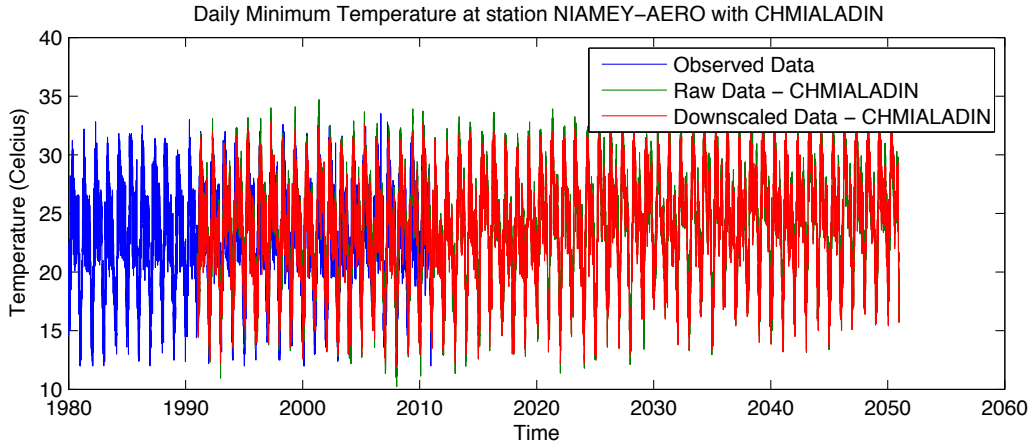

Figure 11 - Daily minimum temperature at Niamey airport with CHMIALADIN

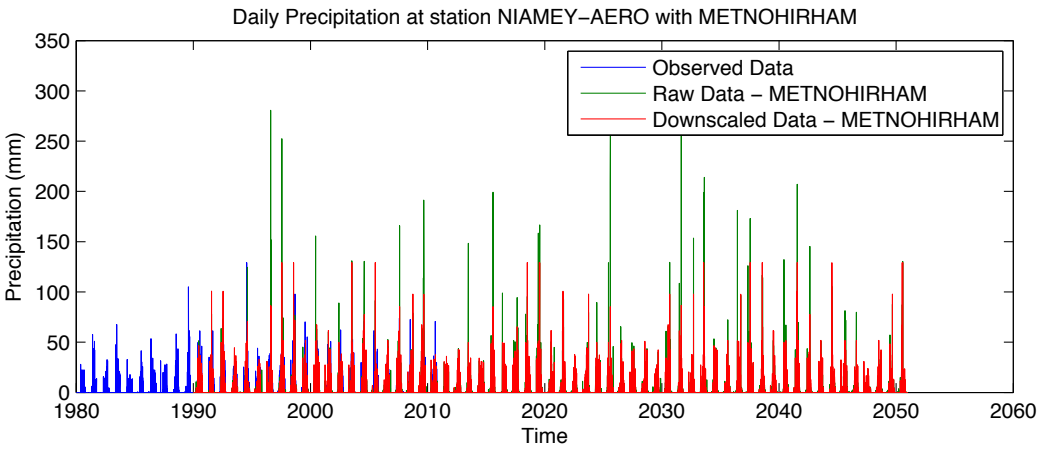

Figure 12 - Daily precipitation at Niamey airport with METNOHORHAM

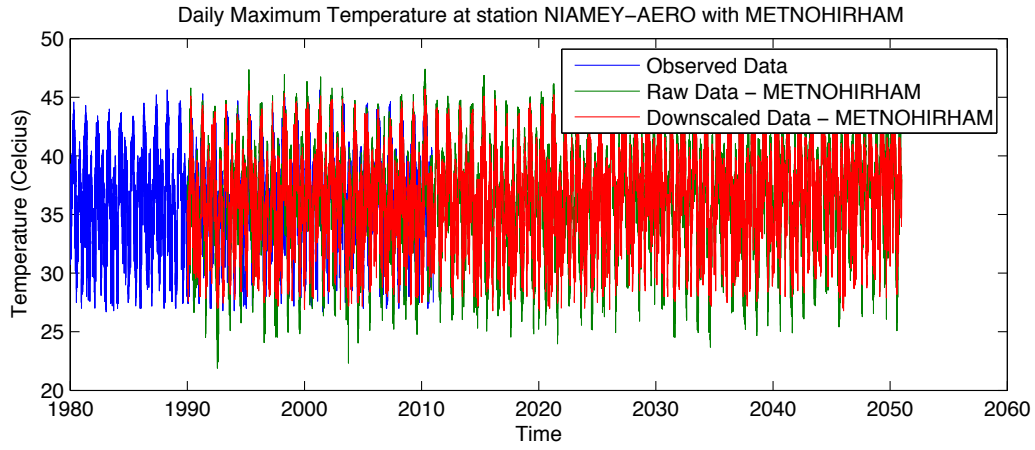

Figure 13 - Daily maximum temperature at Niamey airport with METNOHORHAM

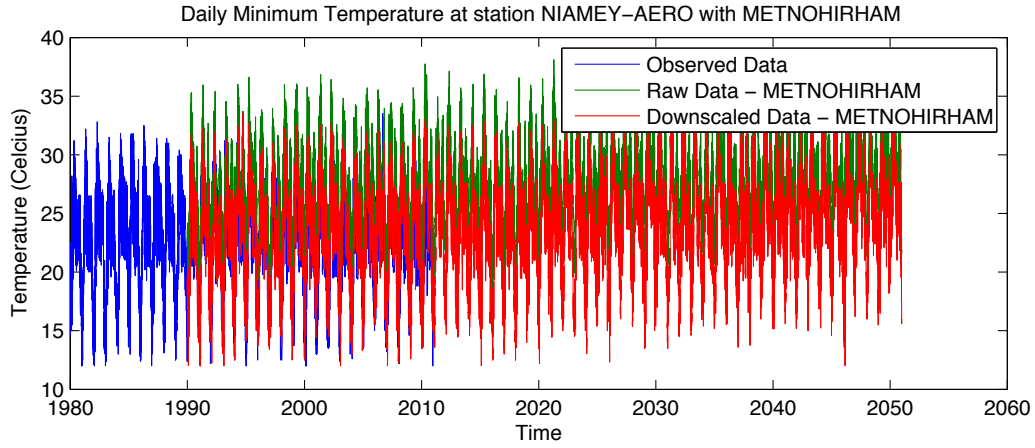

Figure 14 - Daily minimum temperature at Niamey airport with METNOHORHAM

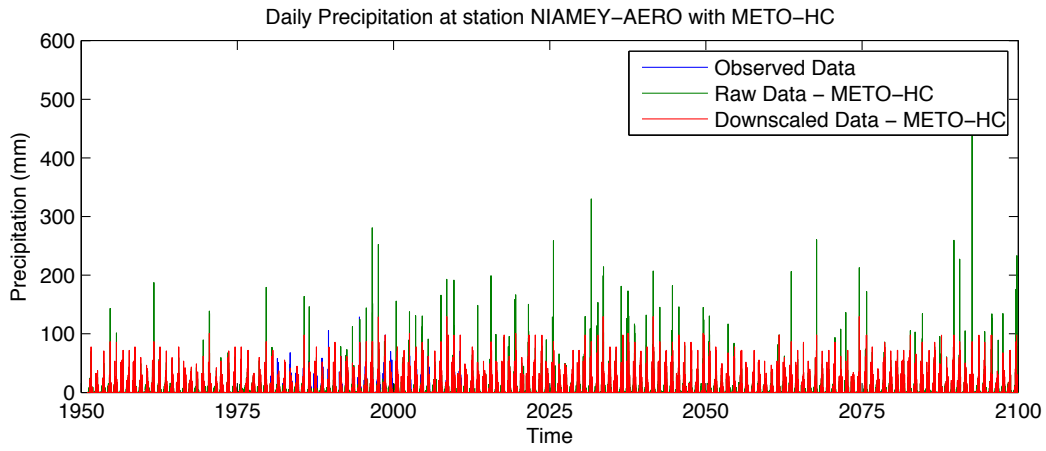

Figure 15 - Daily precipitation at Niamey airport with METO - HC

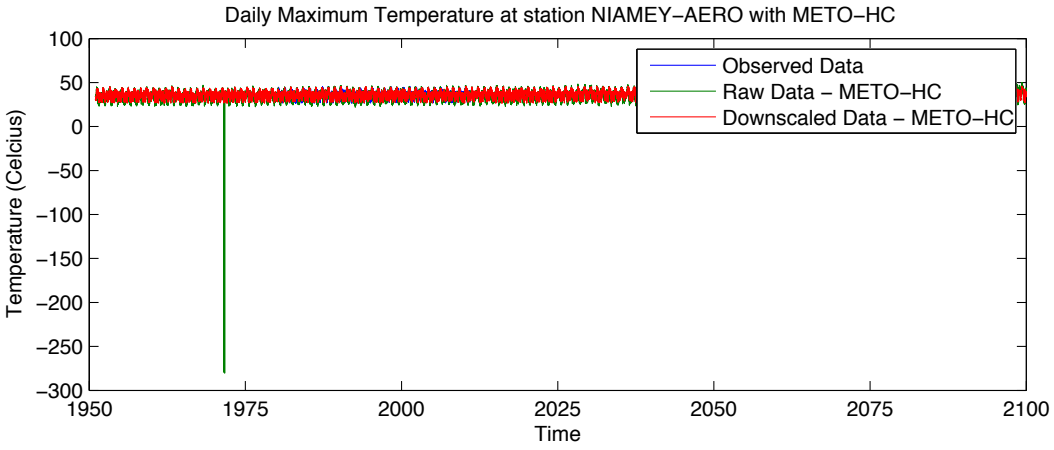

Figure 16 - Daily maximum temperature at Niamey airport with METO - HC

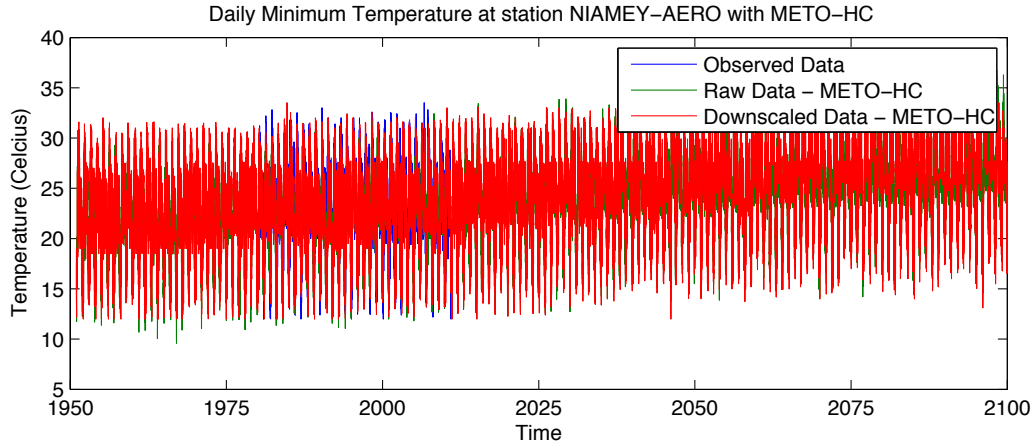

Figure 17 - Daily minimum temperature at Niamey airport with METO - HC

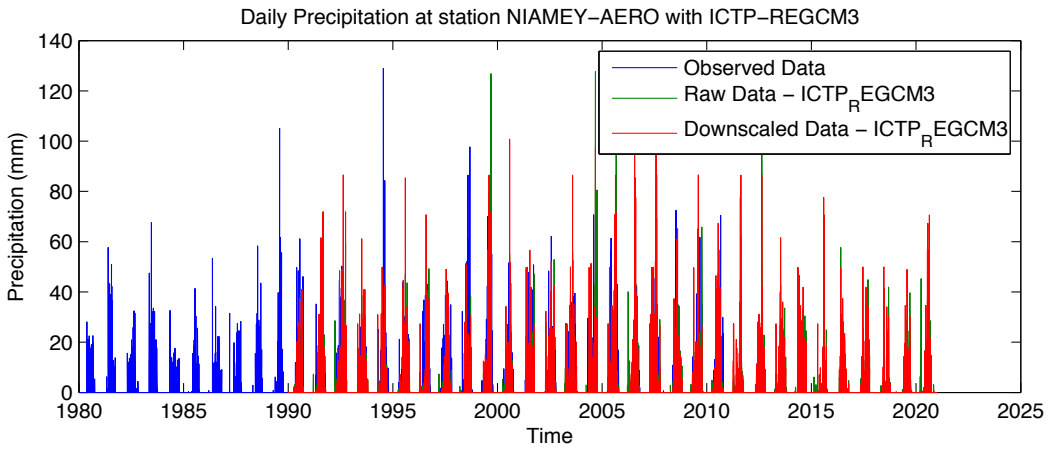

Figure 18 - Daily precipitation at Niamey airport with ICTP - REGCM 3

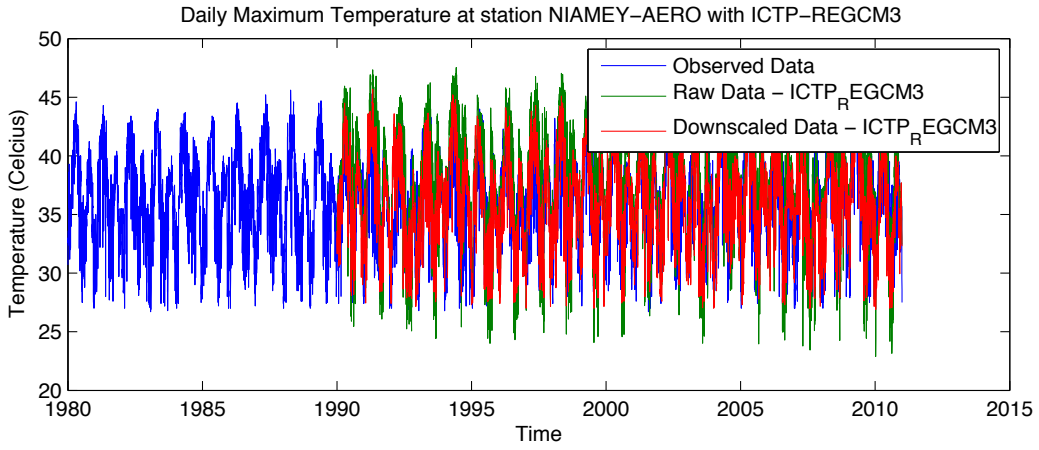

Figure 19 - Daily maximum temperature at Niamey airport with ICTP - REGCM 3

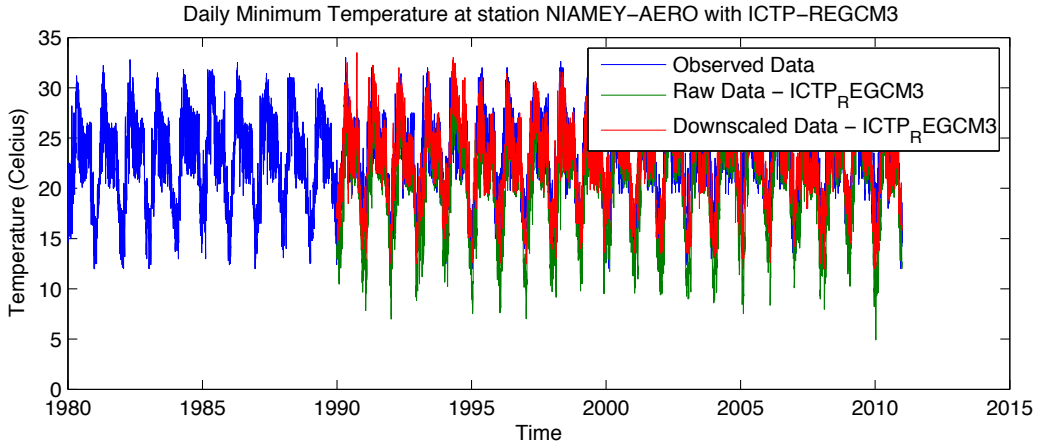

Figure 20 - Daily minimum temperature at Niamey airport with ICTP - REGCM 3

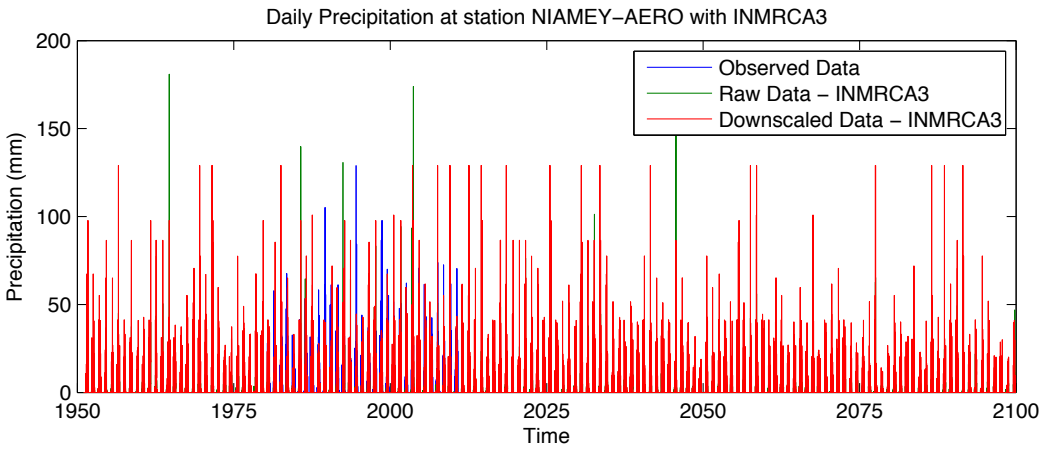

Figure 21 - Daily precipitation at Niamey airport with INMRCA 3

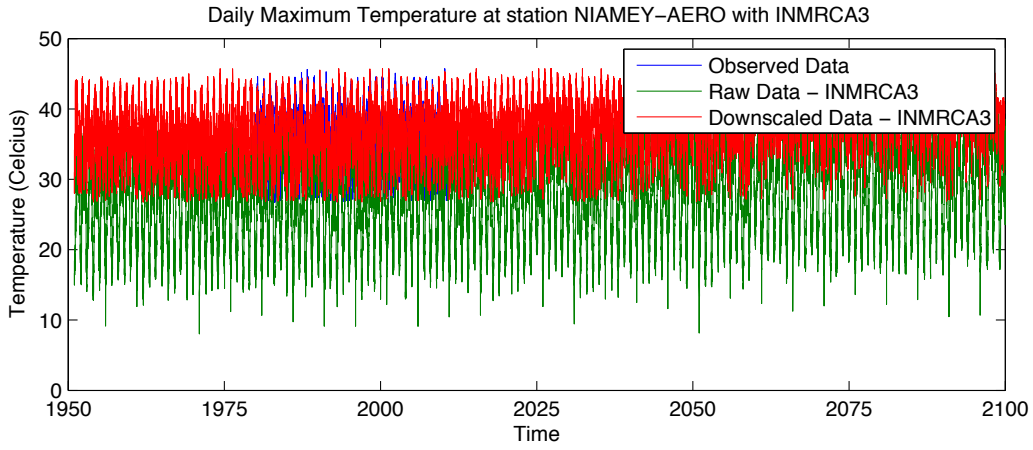

Figure 22 - Daily maximum temperature at Niamey airport with INMRCA 3

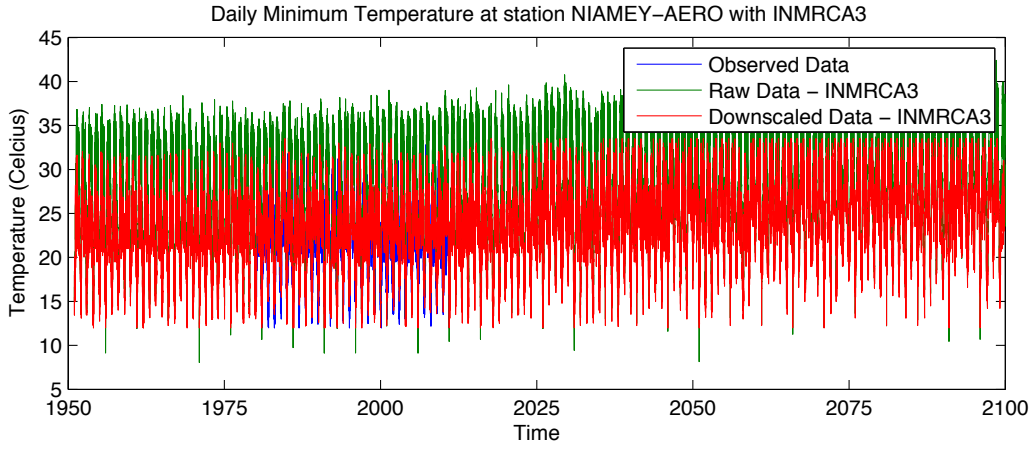

Figure 23 - Daily minimum temperature at Niamey airport with INMRCA 3

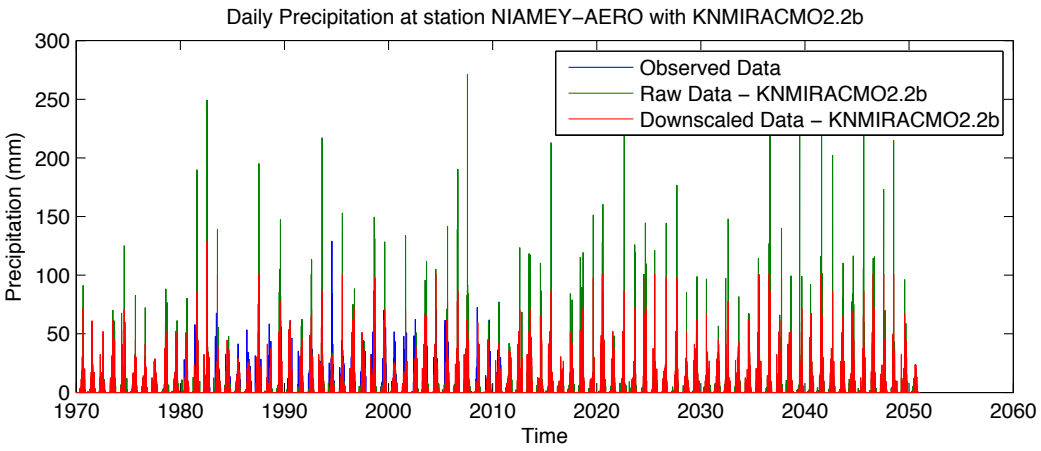

Figure 24 - Daily Precipitation at Niamey airport with KNMIRACM 02.2b

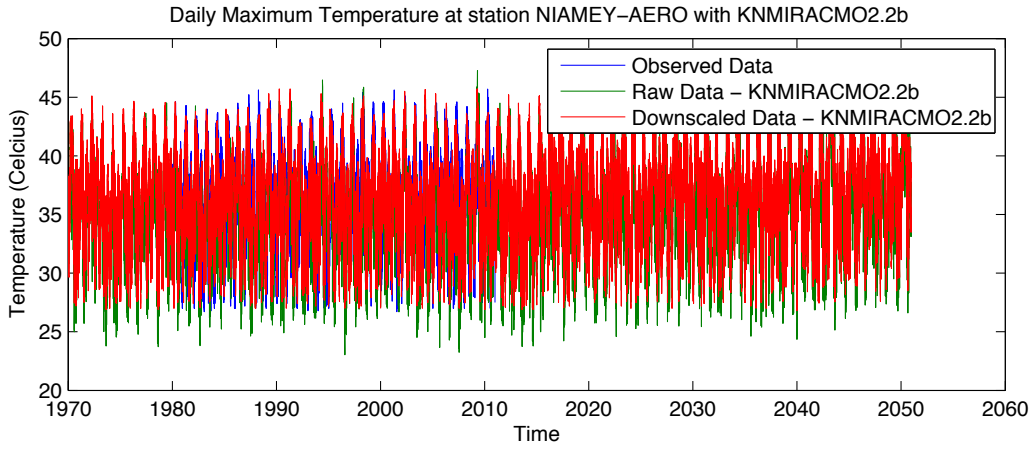

Figure 25 - Daily maximum temperature at Niamey airport with KNMIRACM 02.2b

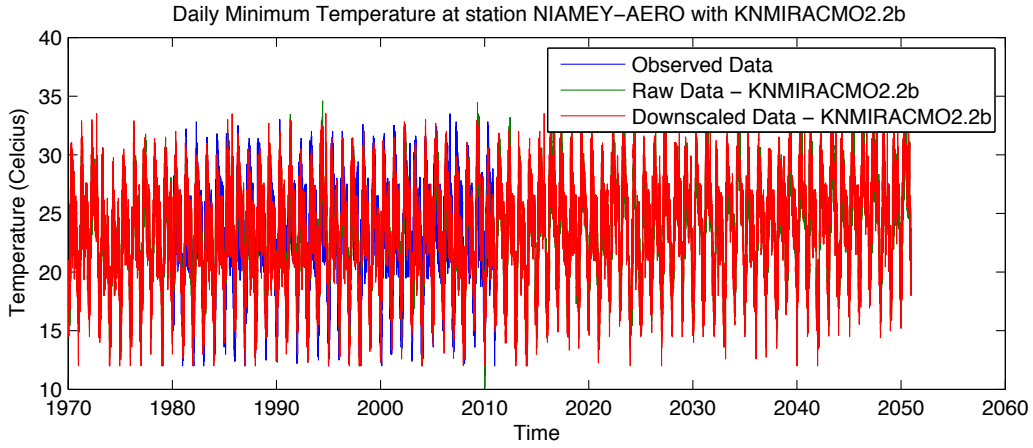

Figure 26 - Daily minimum temperature at Niamey airport with KNMIRACM 02.2b

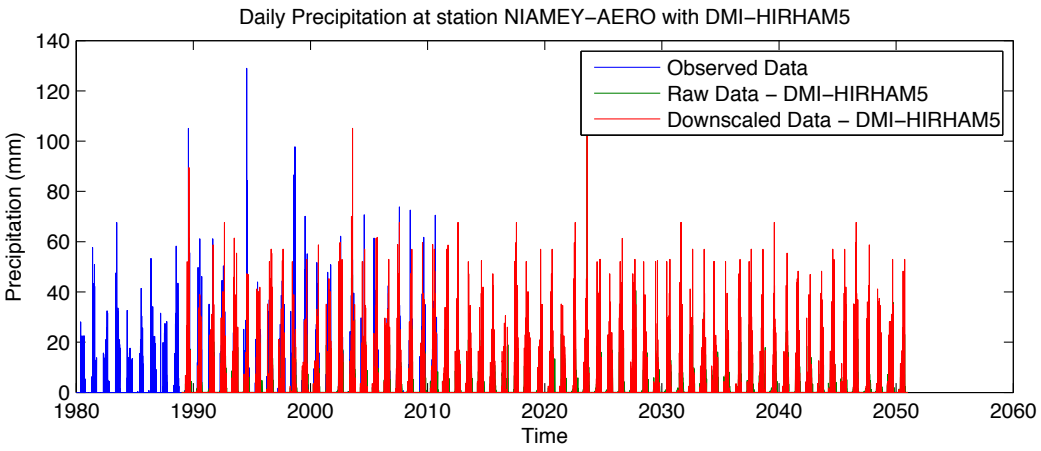

Figure 27 - Daily precipitation at Niamey airport with DMI - HIRHAM 5

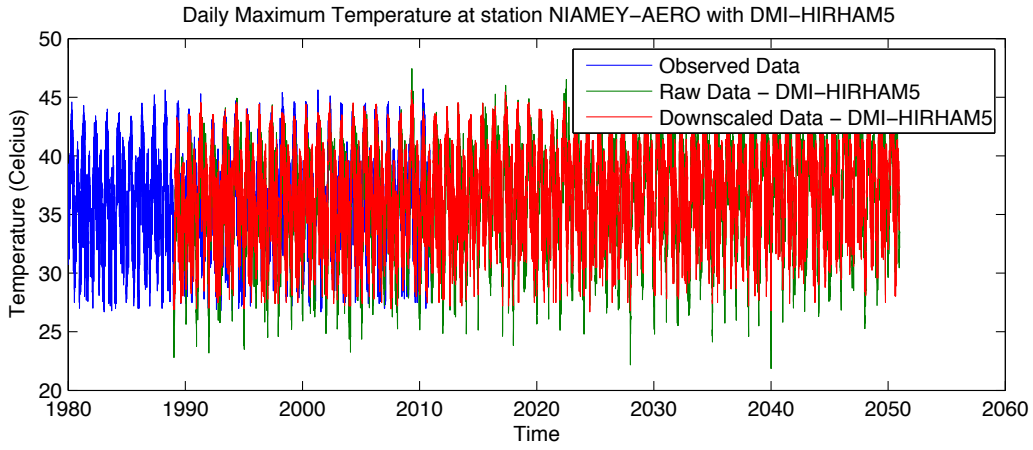

Figure 28 - Daily Maximum temperature at Niamey airport with DMI - HIRHAM 5

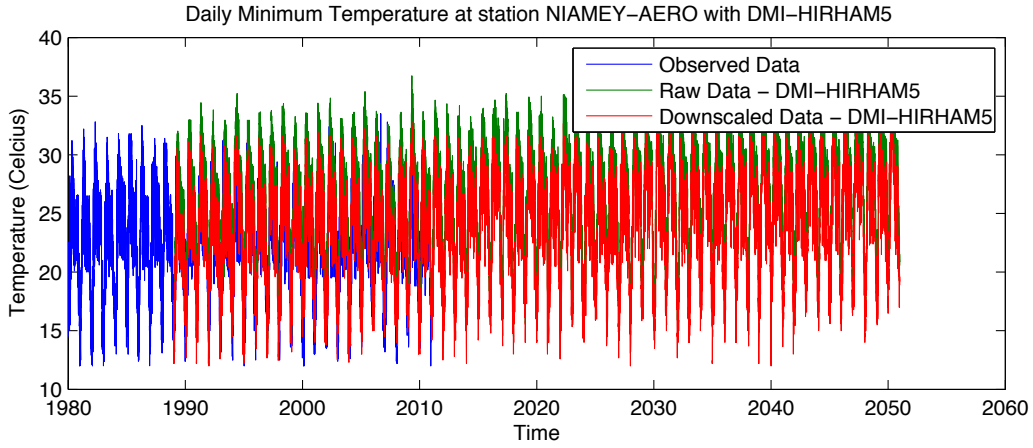

Figure 29 - Daily minimum temperature at Niamey airport with DMI - HIRHAM 5

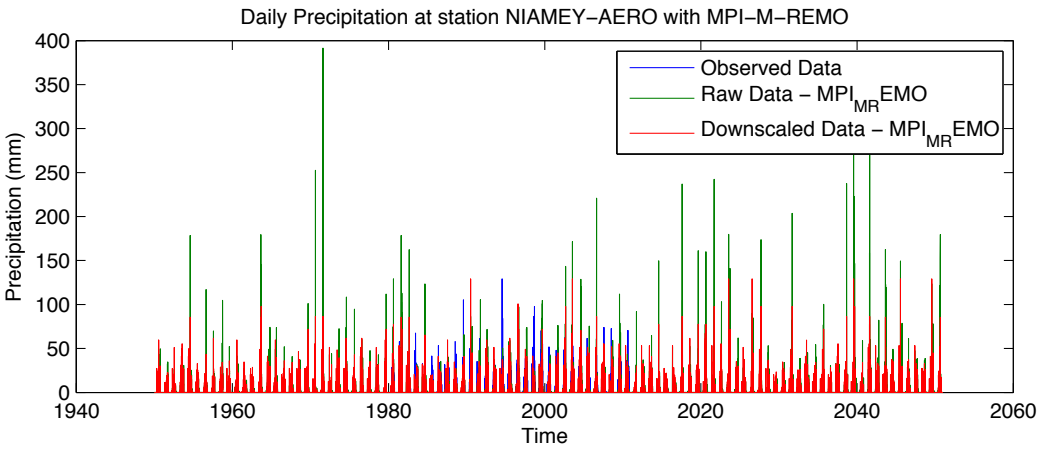

Figure 30 - Daily precipitation at Niamey airport with MPI - M - REMO

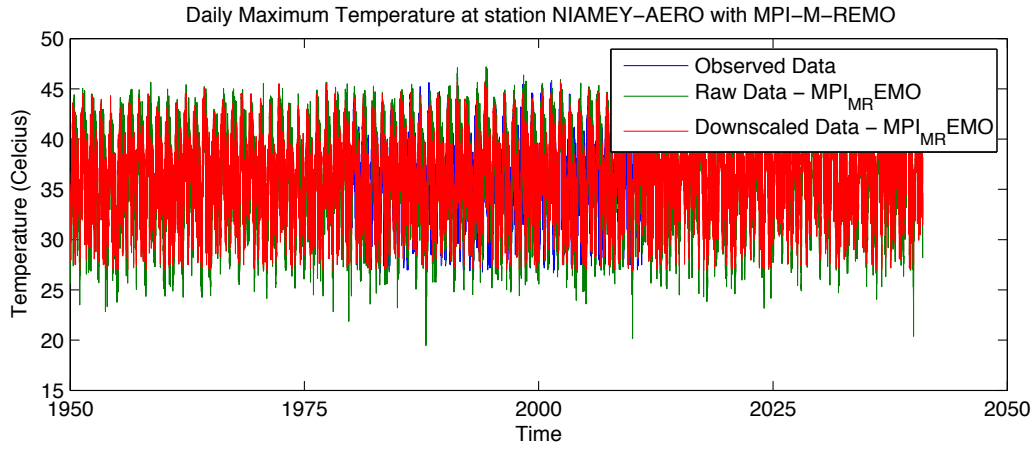

Figure 31 - Daily maximum temperature at Niamey airport with MPI - M - REMO

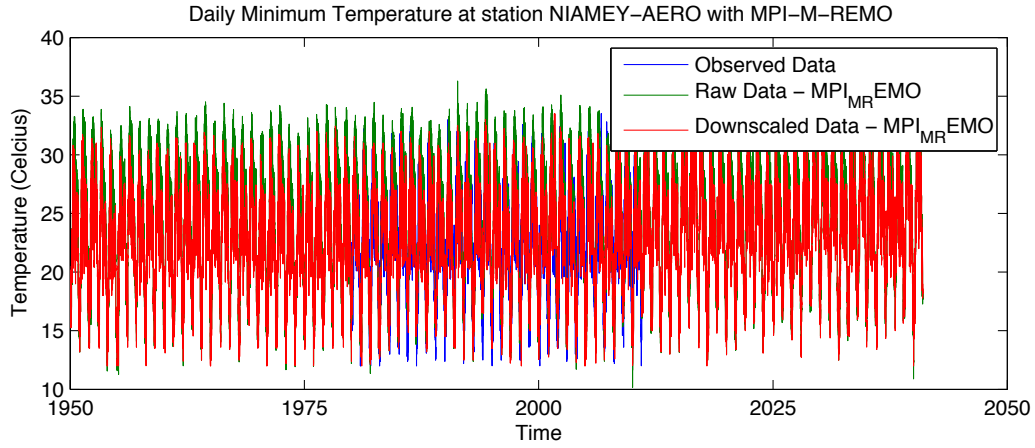

Figure 32 - Daily minimum temperature at Niamey airport with MPI - M - REMO

6.4.2 Monthly mean

In conjunction to daily scale plots, monthly means computed in several time brackets are also presented – i.e. from 2000 to 2050, from 2051 to 2075 and from 2076 to 2100. Note that, not all AMMA-Ensemble model outputs cover the full temporal spectrum herby examined. The analysis at the monthly scale is instrumental in providing insight as to the seasonal pattern of the climate variables studied. This allows the end user to investigate the seasonal evolution of climate variables over several time frames in the simulated future.

Moreover, in addition to the aforementioned temporal ranges, monthly mean plots allow comparison between observed and modeled data over the calibration and validation periods. While the plots are merely visual evaluations of the downscaling performance, the contrast between raw simulated GCM/RCM data (SIM) versus the downscaled climate data (CORR FUT) is flagrant. This supports to stipulation that the Quantile-Quantile downscaling approach is able to correct biases and restore seasonal patterns over the training period as well as the simulated future.

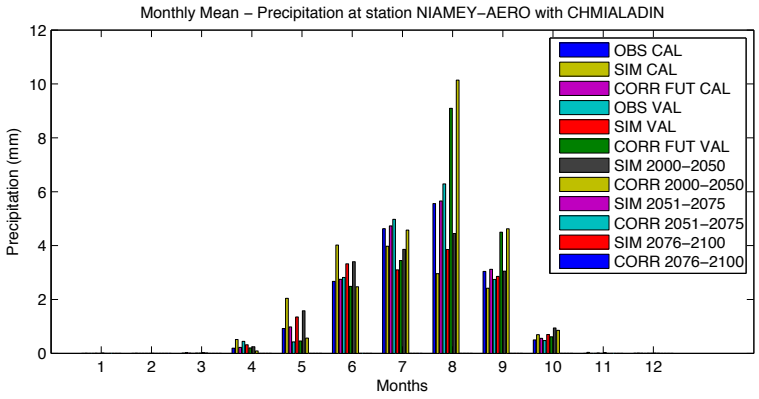

Figure 33 - Precipitation monthly mean at Niamey airport with CHMIALADIN

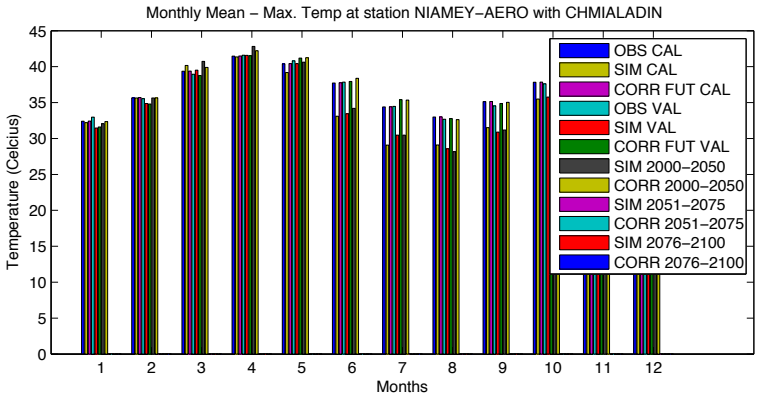

Figure 34 - Maximum temperature monthly mean at Niamey airport with CHMIALADIN

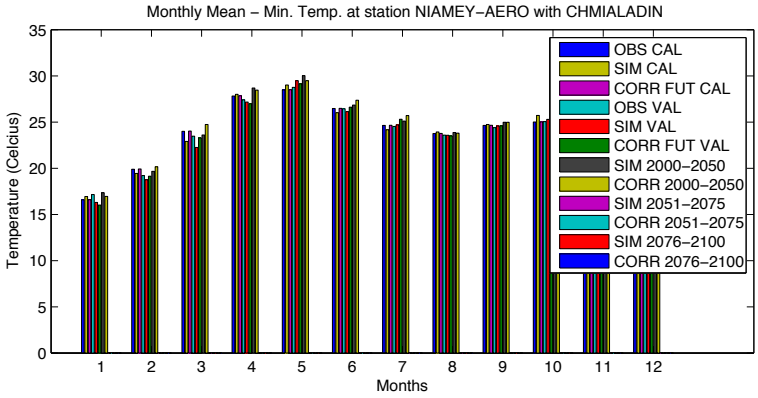

Figure 35 - Minimum temperature monthly mean at Niamey airport with CHMIALADIN

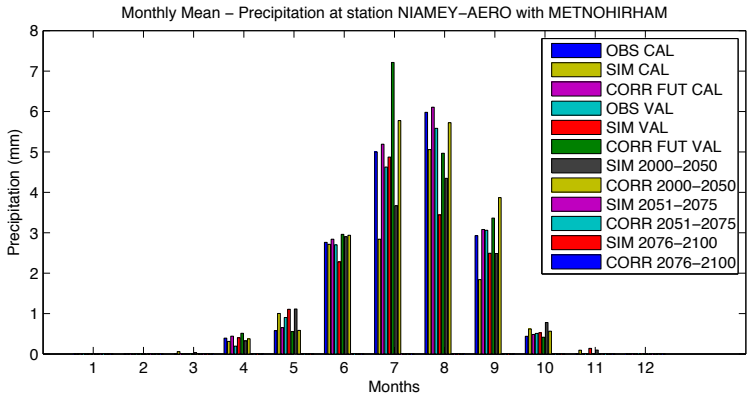

Figure 36 - Precipitation monthly mean at Niamey airport with METNOHORHAM

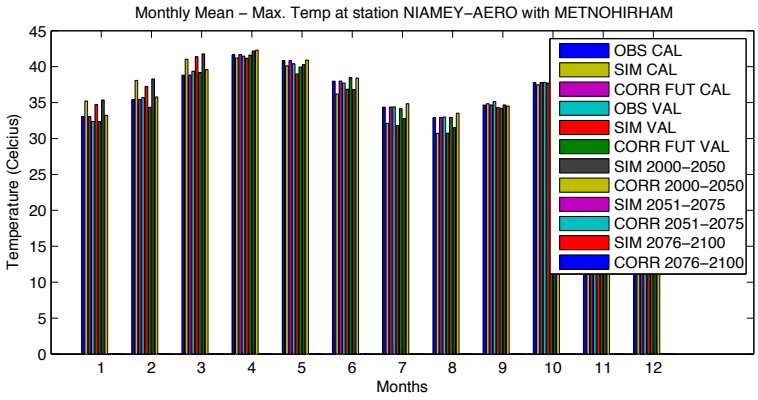

Figure 37 - Maximum temperature monthly mean at Niamey airport with METNOHORHAM

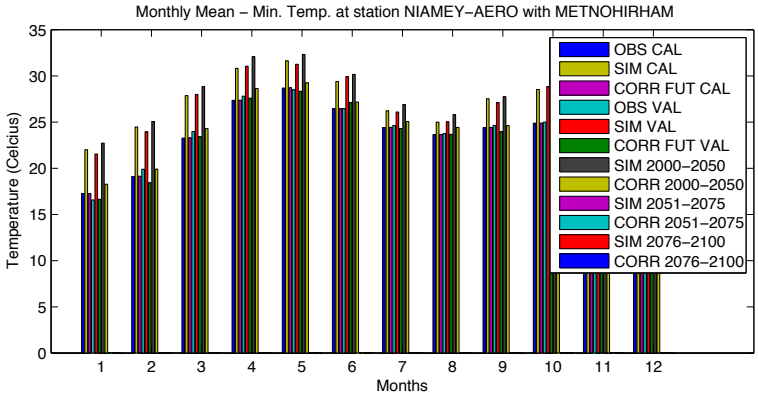

Figure 38 - Minimum temperature monthly mean at Niamey airport with METNOHORHAM

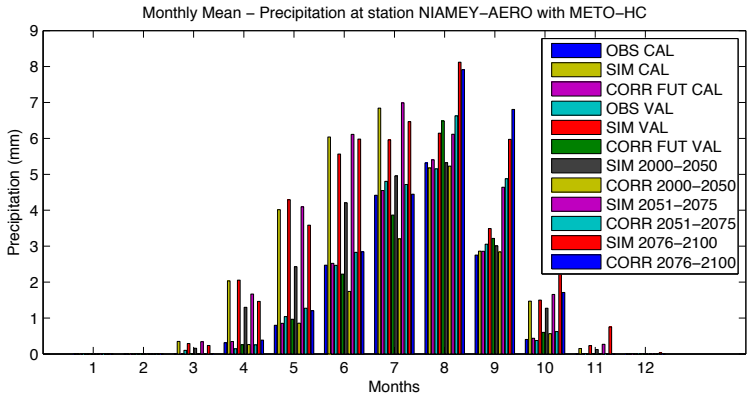

Figure 39 - Precipitation monthly mean at Niamey airport with METO - HC

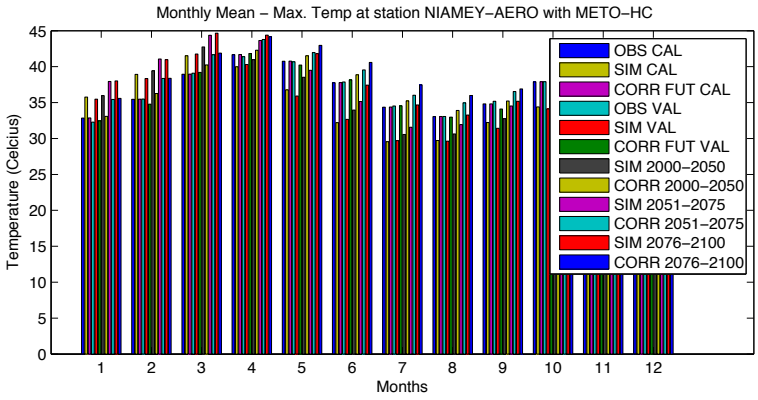

Figure 40 - Maximum temperature monthly mean at Niamey airport with METO - HC

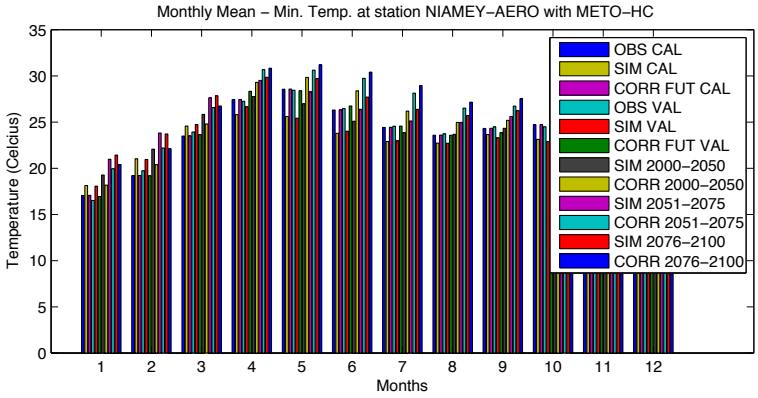

Figure 41 - Minimum temperature monthly mean at Niamey airport with METO - HC

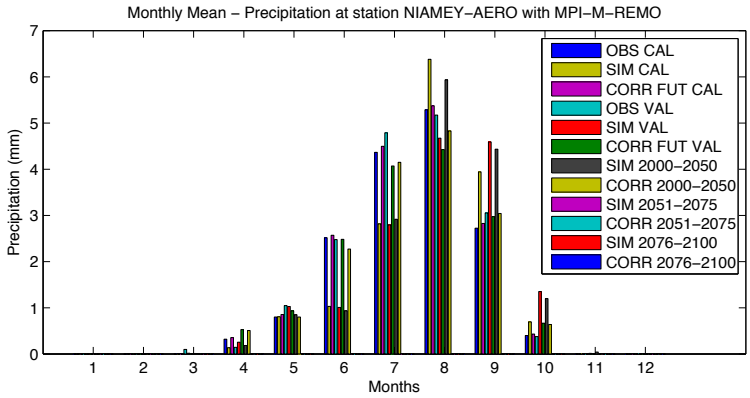

Figure 42 - Precipitation monthly mean at Niamey airport with MPI - M - REMO

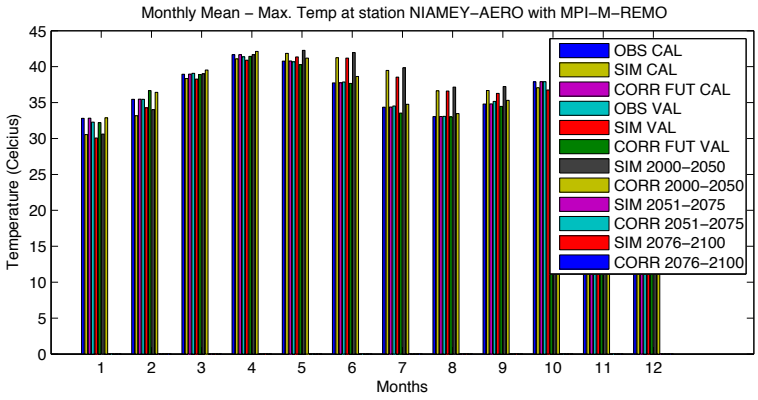

Figure 43 - Maximum temperature monthly mean at Niamey airport with MPI - M - REMO

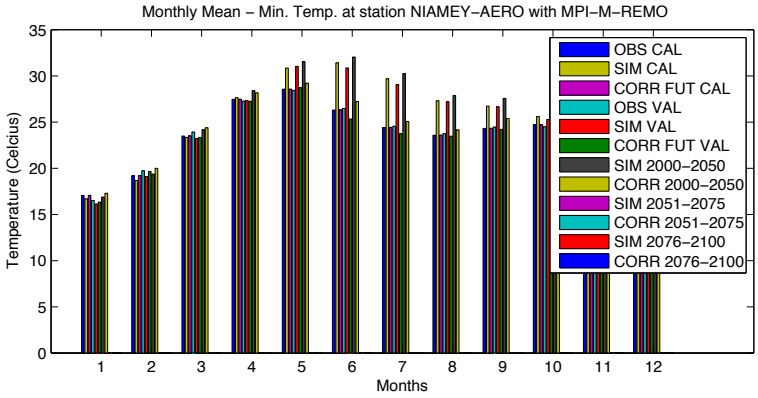

Figure 44 - Minimum temperature monthly mean at Niamey airport with MPI - M - REMO

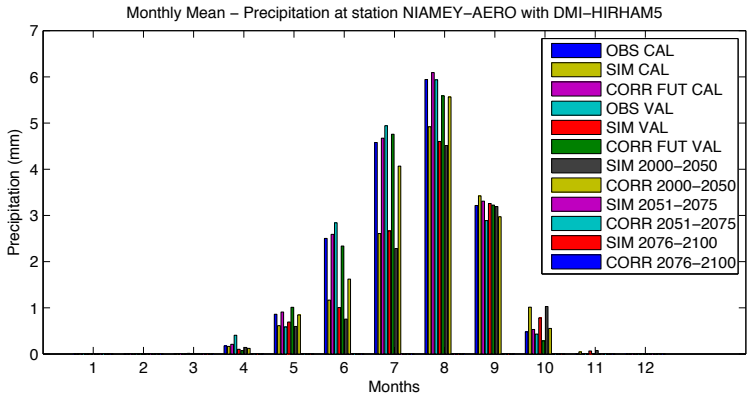

Figure 45 - Precipitation monthly mean at Niamey airport with DMI - HIRHAM 5

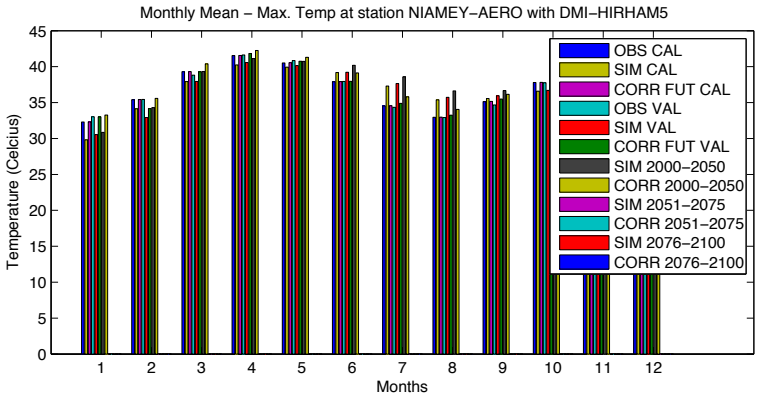

Figure 46 - Maximum temperature monthly mean at Niamey airport with DMI - HIRHAM 5

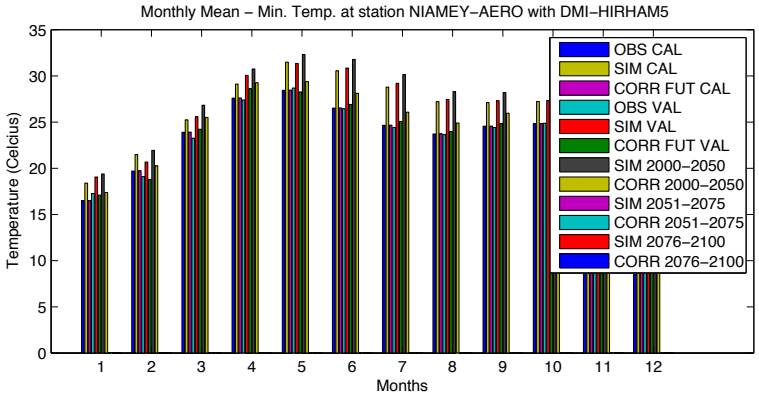

Figure 47 - Minimum temperature monthly mean at Niamey airport with DMI - HIRHAM 5

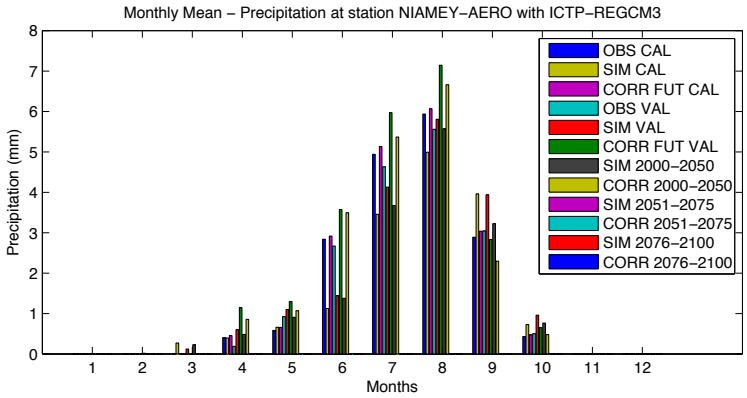

Figure 48 - Precipitation monthly mean at Niamey airport with ICTP - REGCM 3

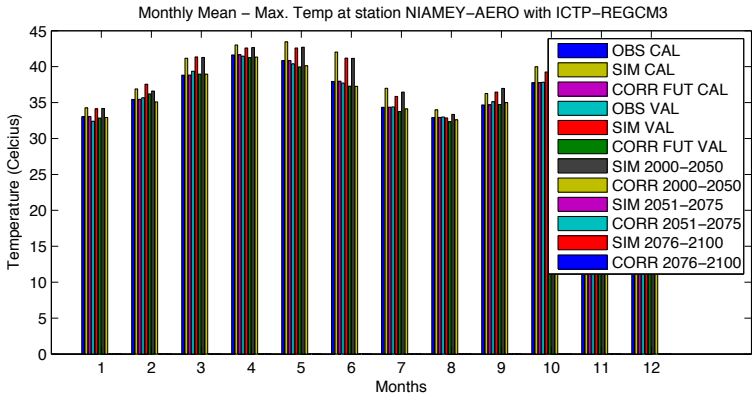

Figure 49 - Maximum temperature monthly mean at Niamey airport with ICTP - REGCM 3

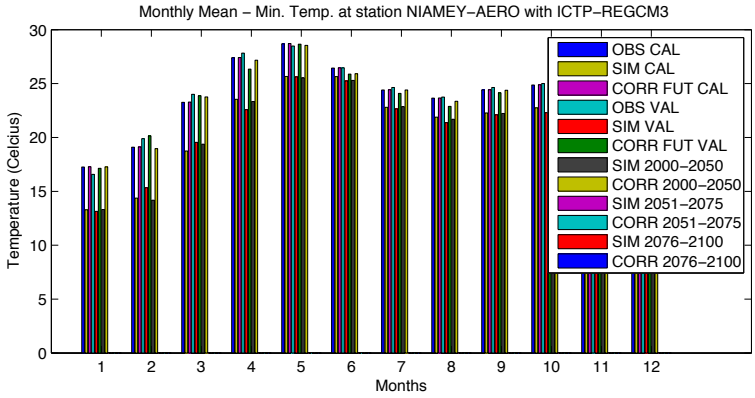

Figure 50 - Minimum temperature monthly mean at Niamey airport with ICTP - REGCM 3

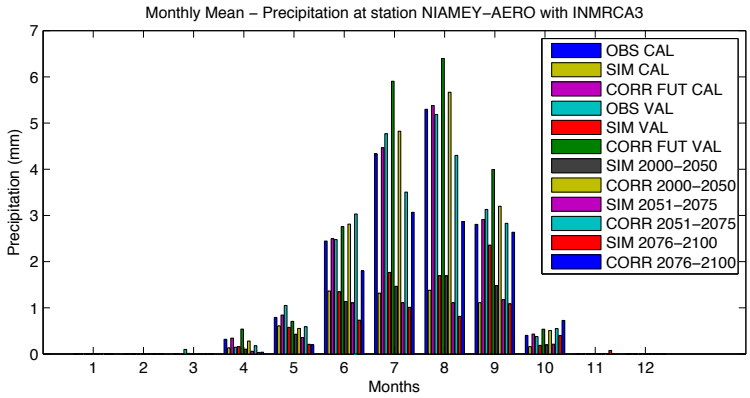

Figure 51 - Precipitation monthly mean at Niamey airport with INMRCA 3

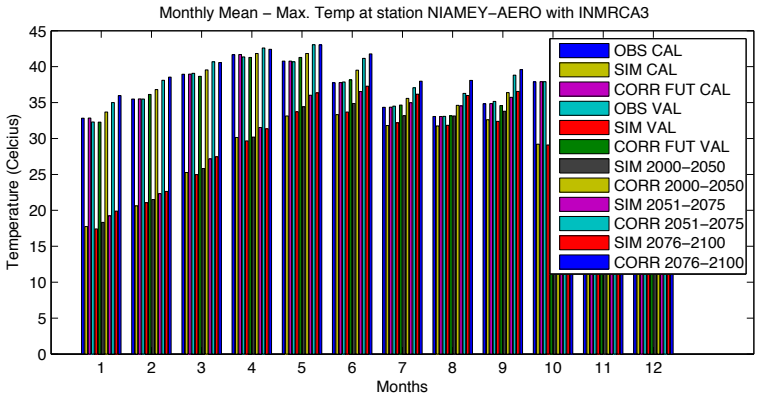

Figure 52 - Maximum temperature monthly mean at Niamey airport with INMRCA 3

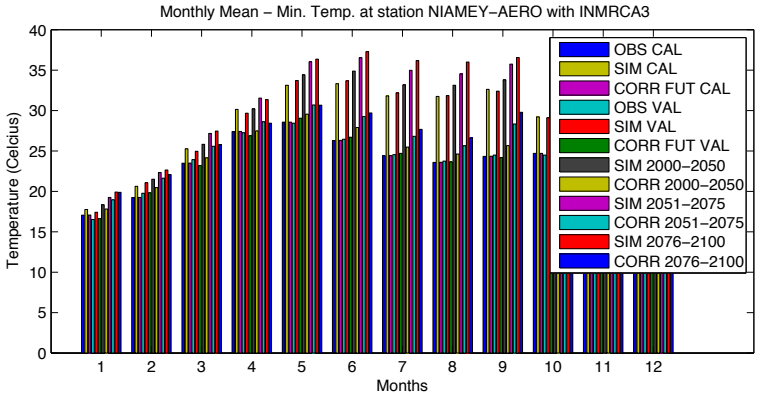

Figure 53 - Minimum temperature monthly mean at Niamey airport with INMRCA 3

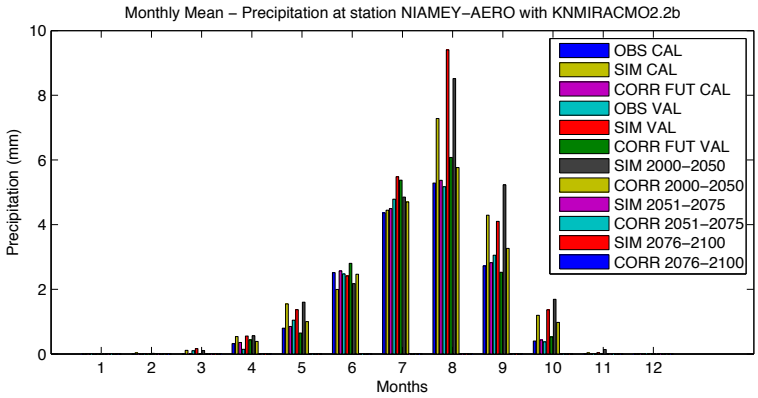

Figure 54 - Precipitation monthly mean at Niamey airport with KNMIRACM 02.2b

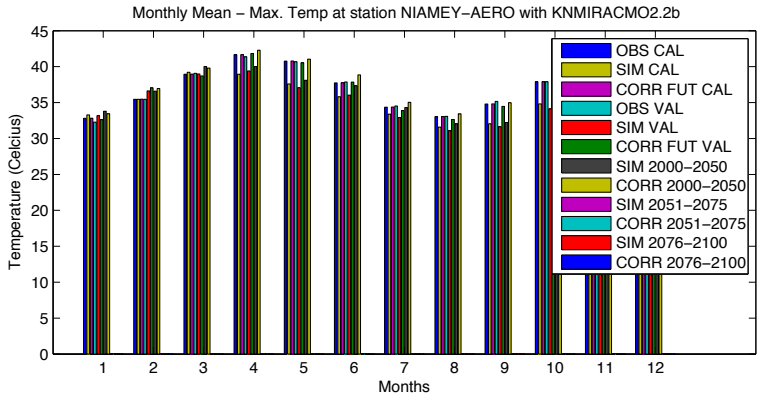

Figure 55 - Maximum temperature monthly mean at Niamey airport with KNMIRACM 02.2b

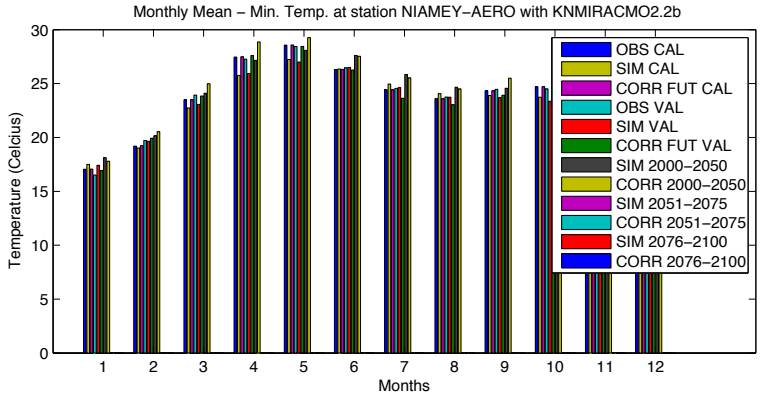

Figure 56 - Minimum temperature monthly mean at Niamey airport with KNMIRACM 02.2b

While the results from most of the climate models suggest little to no variations in monthly means of daily precipitation by 2050, it is interesting to note that CHMIALADIN predicts an increase from 5.5 to 10 mm in August and from 3 to 4.5 mm in September by the year 2050 as compared to the historical monthly mean leading up to 2010. Furthermore, the downscaled outputs of INMRCA3 predict a drop in monthly mean of daily precipitation during the rainy months of June through September by the year 2100. The predicted decrease is flagrant for the month of august at 2.5 mm.

Likewise, the downscaled AMMA-Ensemble outputs predict an increase of monthly average of daily minimum temperature by 0.5 to 2 degrees Celsius by the year 2050 and up to 5 degrees Celsius by 2100. Coincidently, daily maximum temperature is expected to rise by 0.5 to 1 degree Celsius by 2050 and up to 4 degrees Celsius by 2100. The most significant increases in temperature are expected in the months of August and September.

6.4.3 Annual mean

It was observed that annual mean of daily precipitation are not particularly useful in identifying changes patterns. Daily temperature predictions however, expect noticeable increase in daily temperature. Although the annual mean of daily maximum temperatures are only expected to increase by 1 degree Celsius by 2050 and 2 degrees by 2100 from 2010, we can expect the days to become warmer by more given that annual mean of daily minimum temperature is predicted to rise by up to 3 degrees by 2050 and up to 5 degrees by the year 2100.

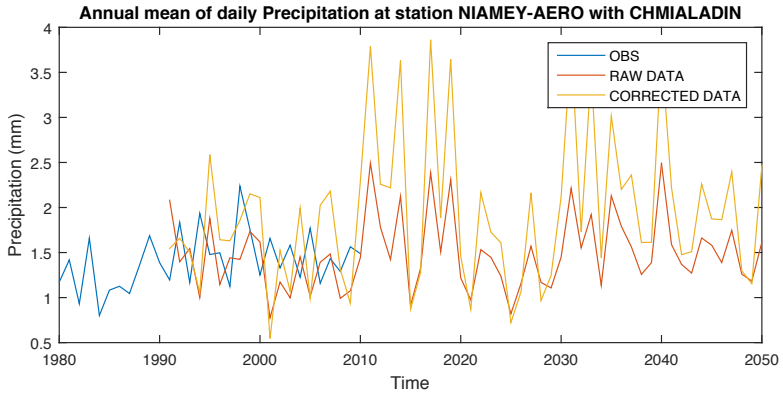

Figure 57 - Annual mean of daily precipitation at Niamey airport with CHMIALADIN

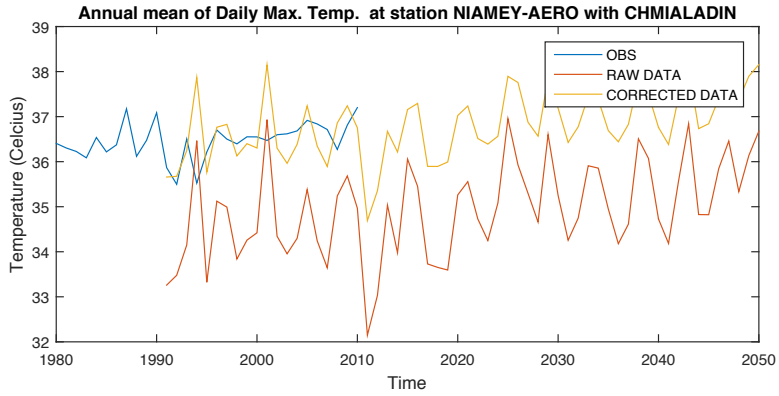

Figure 58 - Annual mean of daily maximum temperature at Niamey airport with CHMIALADIN

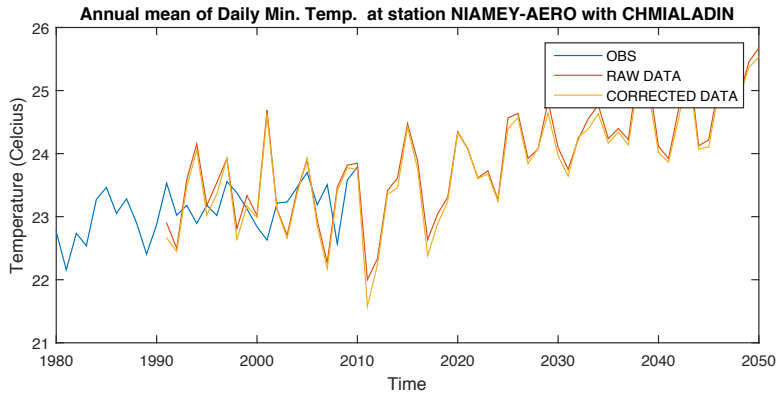

Figure 59 - Annual mean of daily minimum temperature at Niamey airport with CHMIALADIN

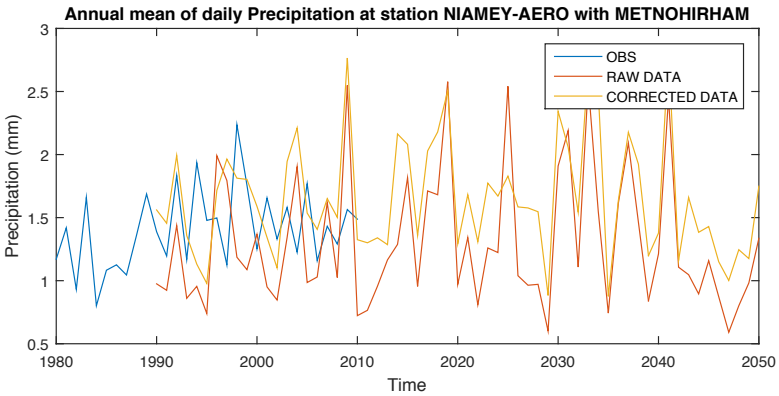

Figure 60 - Annual mean of daily precipitation at Niamey airport with METNOHORHAM

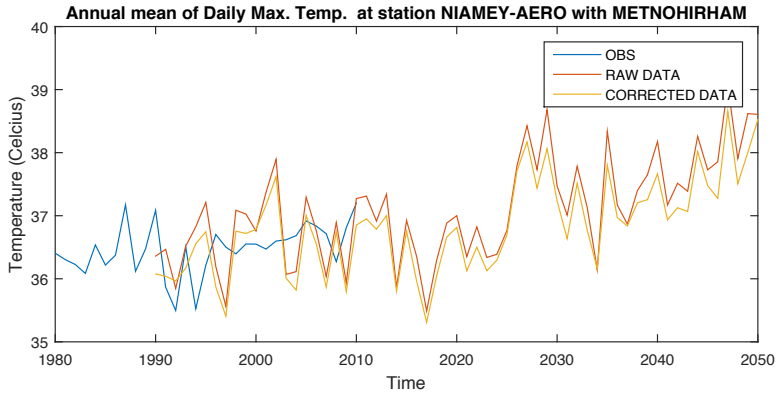

Figure 61 - Annual mean of daily maximum temperature at Niamey airport with METNOHORHAM

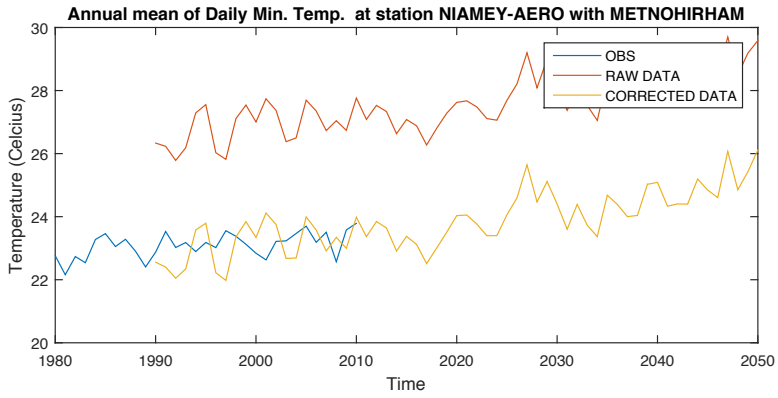

Figure 62 - Annual mean of daily minimum temperature at Niamey airport with METNOHORHAM

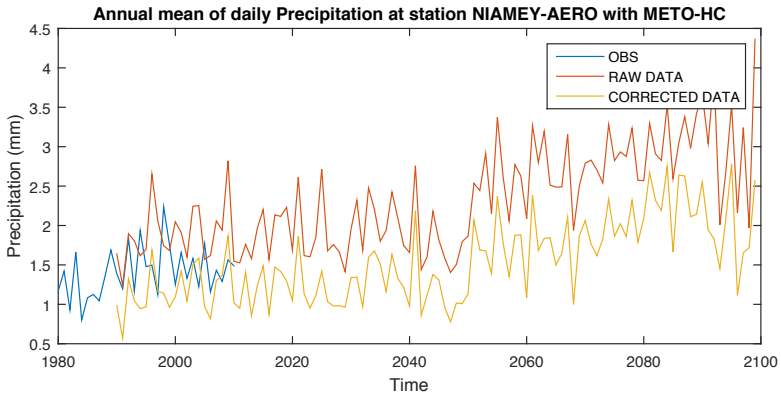

Figure 63 - Annual mean of daily precipitation at Niamey airport with METO - HC

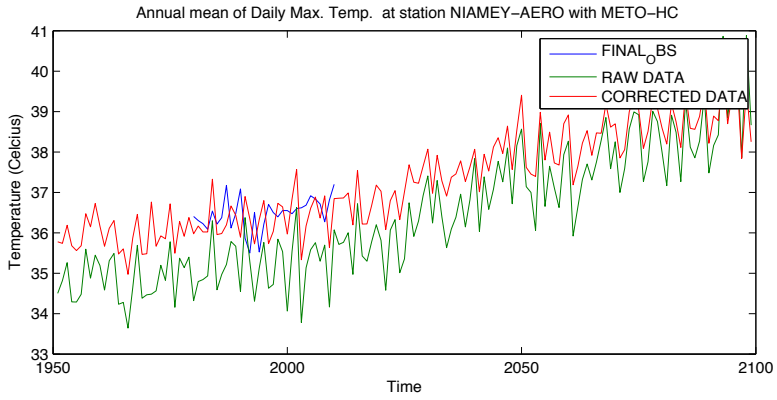

Figure 64 - Annual mean of daily maximum temperature at Niamey airport with METO - HC

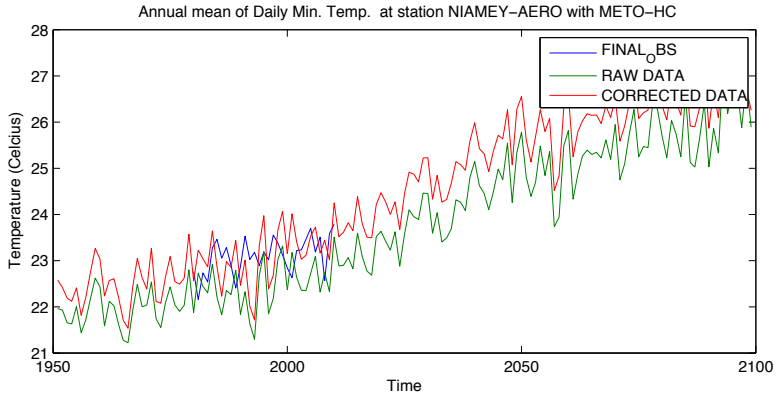

Figure 65 - Annual mean of daily minimum temperature at Niamey airport with METO - HC

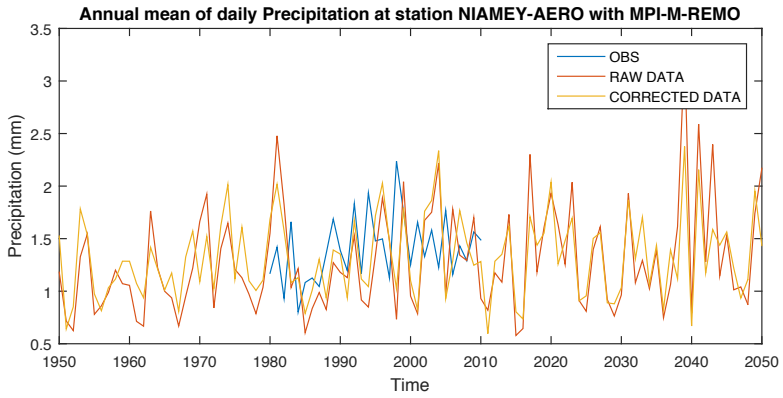

Figure 66 - Annual mean of daily precipitation at Niamey airport with MPI - M - REMO

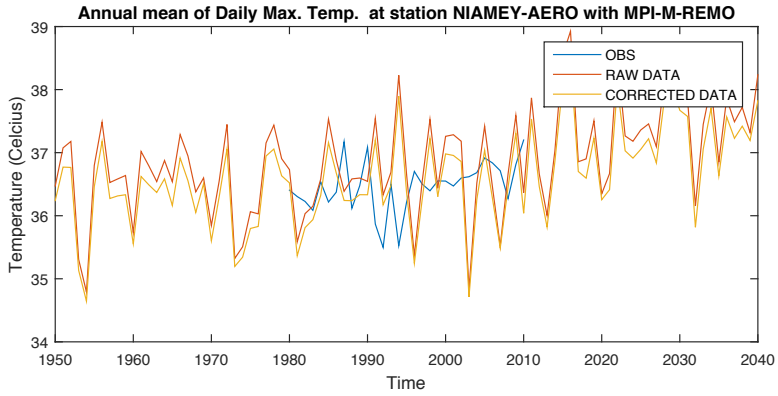

Figure 67 - annual mean of daily maximum temperature at Niamey airport with MPI - M – REMO

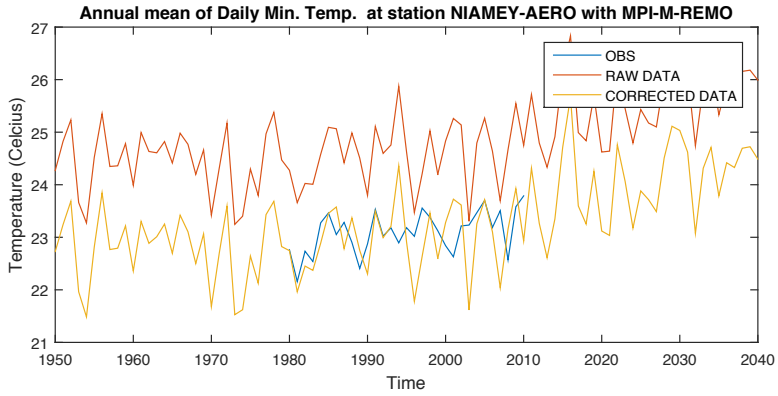

Figure 68 - Annual mean of daily minimum temperature at Niamey airport with MPI - M - REMO

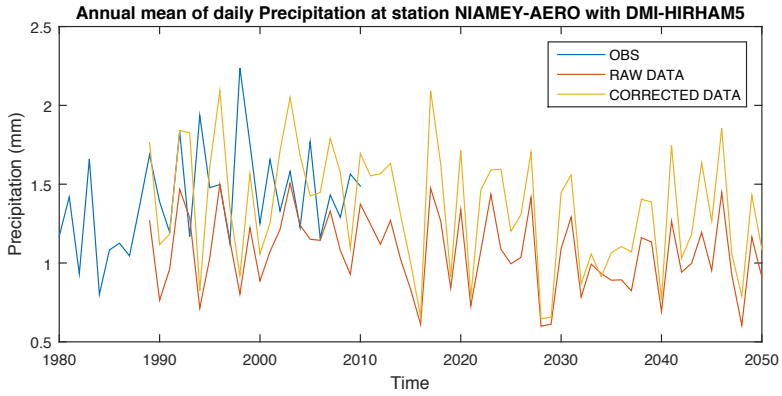

Figure 69 - Annual mean of daily precipitation at Niamey airport with DMI - HIRHAM 5

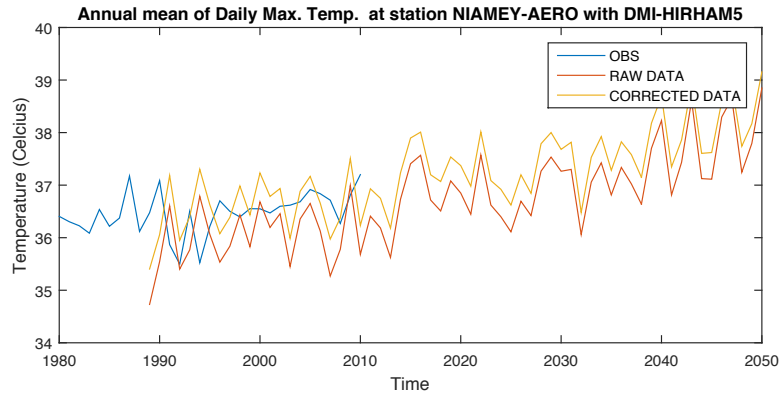

Figure 70 - Annual mean of daily maximum temperature at Niamey airport with DMI - HIRHAM 5

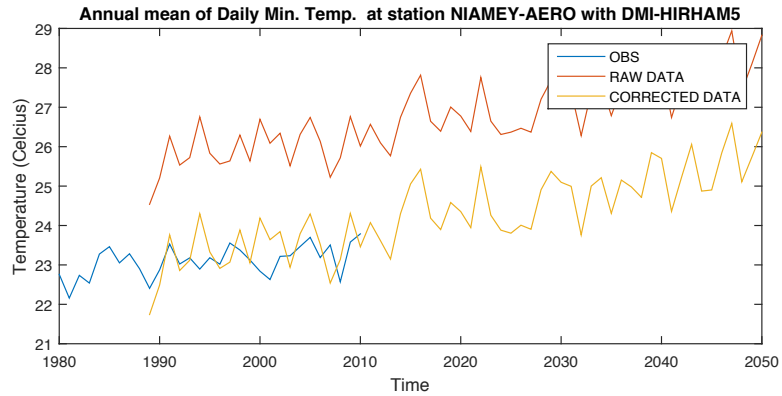

Figure 71 - Annual mean of mainly minimum temperature at Niamey airport with DMI - HIRHAM 5

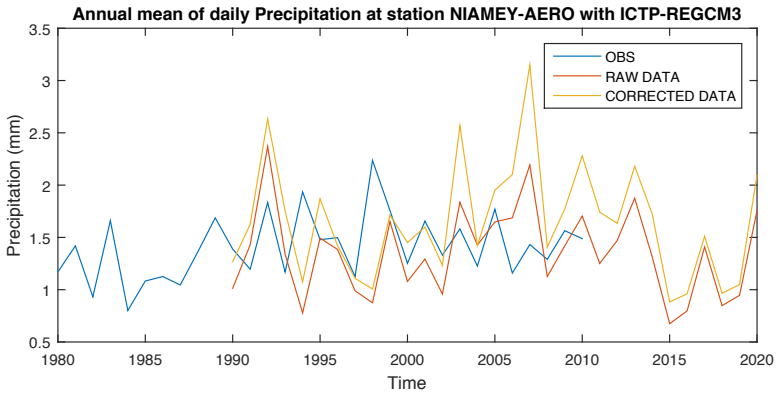

Figure 72 - Annual mean of daily precipitation at Niamey airport with ICTP - REGCM 3

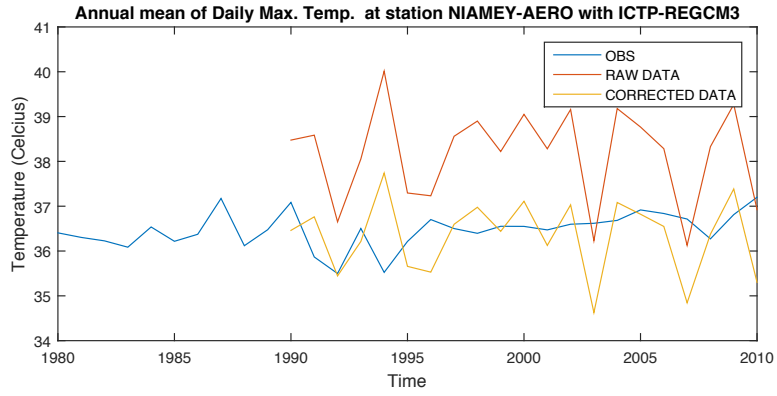

Figure 73 - Annual mean of daily maximum temperature at Niamey airport with ICTP - REGCM 3

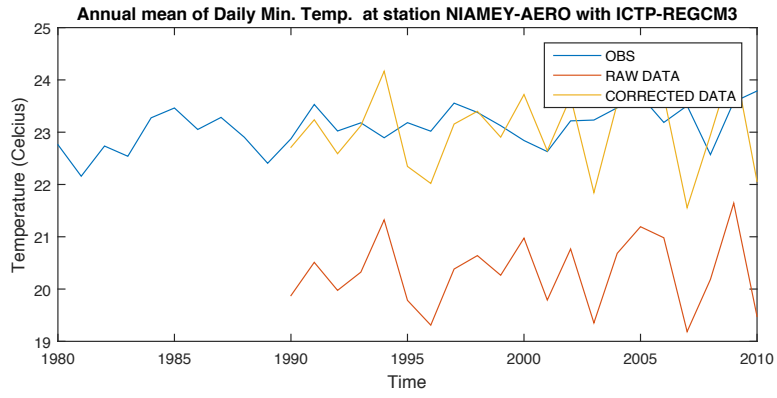

Figure 74 - Annual mean of daily minimum temperature at Niamey airport with ICTP - REGCM 3

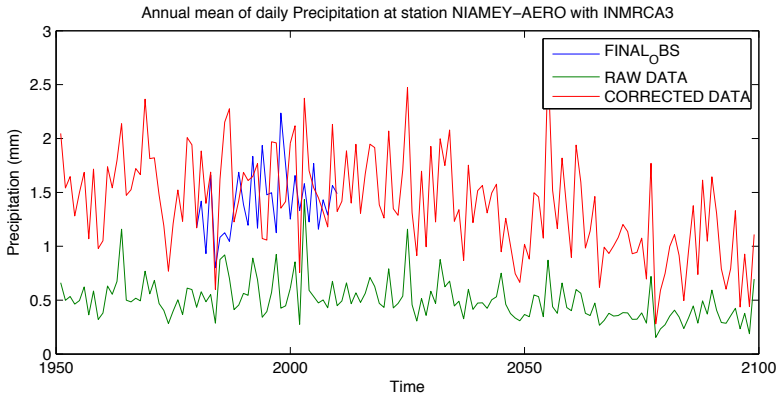

Figure 75 - Annual mean of daily precipitation at Niamey airport with INMRCA 3

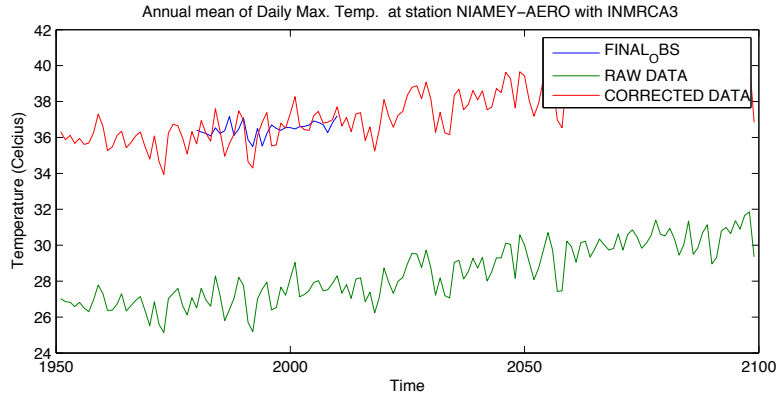

Figure 76 - Annual mean of daily maximum temperature at Niamey airport with INMRCA 3

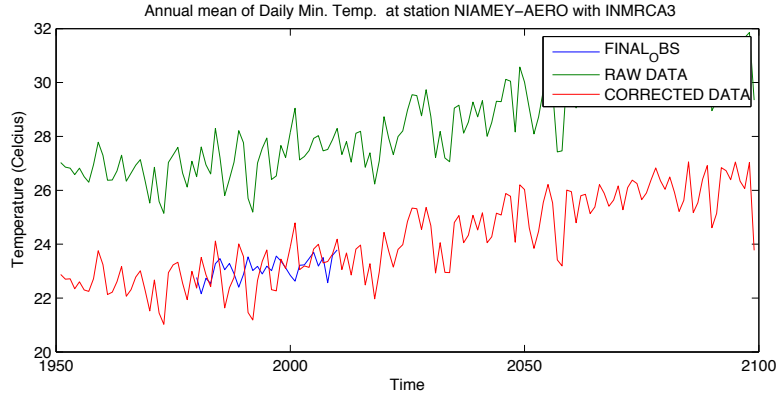

Figure 77 - Annual mean of daily minimum temperature at Niamey airport with INMRCA 3

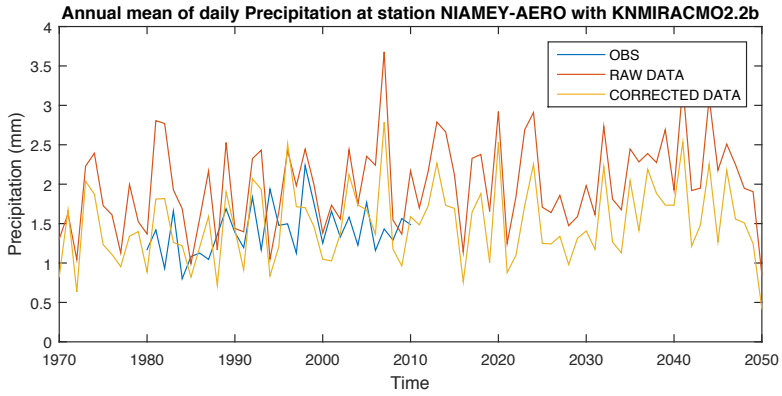

Figure 78 - Annual mean of daily precipitation at Niamey airport with KNMIRACM 02.2b

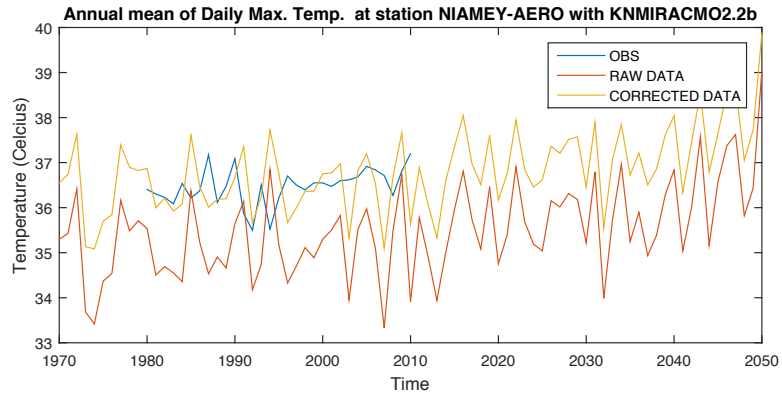

Figure 79 - Annual mean of daily maximum temperature at Niamey airport with KNMIRACM 02.2b

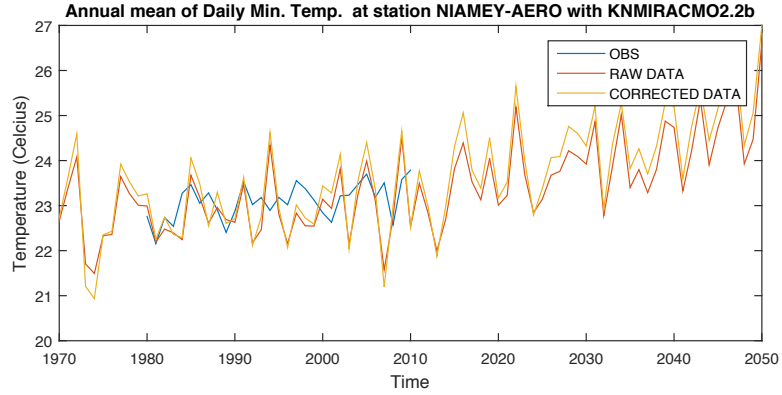

Figure 80 - Annual mean of daily minimum temperature at Niamey airport with KNMIRACM 02.2b

6.5 Quantile - Quantile Downscaling performance

One essential task in any modeling, or rather model output improvement like endeavors is to evaluate the performance and to quantify the competence of the effort by computing goodness - of - fit indicators. The Nash - Sutcliffe model efficiency coefficient is a commonly applied tool in evaluating model performance. The Nash - Sutcliffe coefficient can hence be deemed appropriate to evaluate and gain a general outlook on the performance of the Quantile - Quantile downscaling approach at the Niamey airport climate station. The model efficiency coefficient is computed as follows:

$$NS = 1 - \frac{\sum_t (Q_o - Q_m)^2}{\sum_t (Q_o - \overline{Q_o})^2}$$

Where NS is the Nash - Sutcliffe coefficient; Q_o and Q_m are the observed and modeled values at time t, respectively. And where $\overline{Q_o}$ is the mean observed value for the span of time studied. The Nash - Sutcliffe coefficient ranges in value from $-\infty$ to 1. A coefficient of 1 suggests absolute agreement between the observed historical data set and that of the model outputs.

In this study, the time span selected to evaluate the general performance of the Quantile - Quantile downscaling approached is the overlapping time lapse covered by both the observed historical data set and the model output data set.

As outlined in the below Table 3 - Nash - Sutcliffe Model Efficiency coefficients at Niamey Airport, virtually all cases of Quantile - Quantile downscaling efforts resulted in improved climate data.

The aforementioned improvements are quantified by the relative difference in Nash - Sutcliffe coefficients computed as follows:

$$improvement = \frac{NS_{RAW} - NS_{CORR}}{|NS_{RAW}|}$$

Where NS_{RAW} is the Nash - Sutcliffe model efficiency coefficient computed for the raw RCM model outputs. And where NS_{CORR} is Nash - Sutcliffe model efficiency coefficient computed for the RCM model outputs downscaled using the Quantile - Quantile approach.

Table 3 - Nash - Sutcliffe Model Efficiency coefficients at Niamey Airport

Climate Model	Climate Variable	Nash - Sutcliffe Model Efficiency Coefficient		Improvement
		Raw Model Outputs	Downscaled (Corrected) Model Outputs	
CHMIALADIN	Daily Precipitation	- 0.11	- 0.81	- 612.6%
	Max. Daily Temp.	- 0.58	0.23	140.3%
	Min. Daily Temp.	0.49	0.49	0.8%
DMI - HIRHAM5	Daily Precipitation	- 0.17	- 0.79	- 357.3%
	Max. Daily Temp.	- 0.10	0.17	280.8%
	Min. Daily Temp.	0.09	0.47	411.3%
GKSS - ECHAM5	Daily Precipitation	- 2.52	- 1.03	59.1%
	Max. Daily Temp.	- 0.34	0.22	162.6%
	Min. Daily Temp.	0.34	0.50	43.7%
ICTP_REGCM3	Daily Precipitation	- 0.64	- 1.12	- 74.4%
	Max. Daily Temp.	- 0.40	0.12	130.9%
	Min. Daily Temp.	- 0.05	0.45	993.3%
INMRCA3	Daily Precipitation	- 0.24	- 1.10	- 367.7%
	Max. Daily Temp.	- 7.42	0.17	102.3%
	Min. Daily Temp.	- 0.91	0.46	150.2%
KNMIRACMO2.2b	Daily Precipitation	- 1.85	- 1.02	44.9%
	Max. Daily Temp.	- 0.23	0.14	161.2%
	Min. Daily Temp.	0.50	0.44	- 11.0%
METNOHIRHAM	Daily Precipitation	- 1.46	- 1.06	27.0%
	Max. Daily Temp.	- 0.12	0.14	218.0%
	Min. Daily Temp.	- 0.30	0.47	253.8%
MPI_M_REMO	Daily Precipitation	- 1.27	- 0.88	30.6%
	Max. Daily Temp.	- 0.37	0.13	134.9%
	Min. Daily Temp.	0.18	0.46	156.4%

Although the Nash - Sutcliffe model efficiency coefficients indicate that the Quantile - Quantile downscaling approach yielded remarkable improvements over the raw RCM model outputs for daily maximum and minimum daily temperatures, it is worth noting that the coefficients also

suggest that the approach failed its purpose in the case of daily precipitation for the following regional climate models: CHMIALADIN, DMI_HIRHAM5, ICTP_REGCM3 and INMRCA3.

6.5.1 Monthly Probability Density Functions (PDFs)

While daily climate variable agreement between model outputs and observed historical data is a fair evaluation of the downscaling performance, it is important not to limit ones understanding of downscaling performance to simplistic evaluations. It is fundamental to incorporate an assessment of its ability to replicate probability distribution of historical data. It is believed that probability scoring performance measures are better suited to gain meaningful perception for continuous climate events such as precipitation (Maraun, D. et al., 2010).

Moreover, to ensure adequate results, a two-step evaluation is necessary on independent portions of the data set, i.e. a calibration or training period and a validation period. As such, you will find for each AMMA-Ensemble model a set of graphical representations illustrating probability density functions of both the calibration and validation periods for each climate variable. In addition, binary probability scoring is performed and offered in the form of bar plots indicating the probability of precipitation occurrence or not. Given that climate events are seasonal and continuous spanning over several days, the probability distribution analysis is carried out at the monthly scale.

6.5.2 Kolmogorov – Smirnov

Results from the Kolmogorov – Smirnov test confirm that the Quantile-Quantile downscaling method is able to improve probability distribution agreement of simulation outputs with the set benchmark – i.e. observed historical data – at every occasion without exception. Test results for the KS test are shown below. It is worth noting that while the QQ method is able corrects the probability distributions; the results in some cases are not in complete agreement with historical

data. While a quasi 100% agreement between observed and downscaled RCM outputs is expected, the KS test results over the validation periods confirm that the Quantile-Quantile method is indeed able to reproduce distribution – i.e. over 30% improvement has been noted in monthly distribution agreements. Table 4 below is a summary of the KS test results showing the number of successful downscaling attempts measured in months. Note that graphical representations of the PDF plots are enclosed in Appendix A for further visual evaluation of the QQ downscaling performance.

Table 4 - PDF agreements based on KS test

Models			PCP.	MAX. TEMP	MIN. TEMP.
CHMIALADIN	Calibration	Raw	5	1	4
		Corrected	12	12	12
	Validation	Raw	5	1	2
		Corrected	11	3	1
DMI-HIRHAM5	Calibration	Raw	6	0	0
		Corrected	12	12	12
	Validation	Raw	7	0	0
		Corrected	12	2	3
GKSS-ECHAM5	Calibration	Raw	7	0	0
		Corrected	12	12	12
	Validation	Raw	8	2	2
		Corrected	11	5	6
ICTP_REGCM3	Calibration	Raw	9	0	0
		Corrected	12	12	12
	Validation	Raw	8	2	2
		Corrected	11	5	6
INMRCA3	Calibration	Raw	7	0	0
		Corrected	12	12	12
	Validation	Raw	7	1	0
		Corrected	12	3	3
KNMIRACMO2.2b	Calibration	Raw	5	0	0
		Corrected	12	12	12
	Validation	Raw	5	0	0
		Corrected	12	1	3
METNOHIRHAM	Calibration	Raw	6	1	0
		Corrected	12	12	12
	Validation	Raw	5	0	0
		Corrected	11	5	2
METO-HC	Calibration	Raw	3	0	0
		Corrected	12	12	12
	Validation	Raw	3	0	0
		Corrected	11	3	4
MPI_M_REMO	Calibration	Raw	6	0	2
		Corrected	12	12	12
	Validation	Raw	6	0	1
		Corrected	12	4	2

Table 5 - KS Test results for Precipitation

Models	PCP	Months	1	2	3	4	5	6	7	8	9	10	11	12
CHMIALADIN	Calibration	Raw	100%	100%	100%	0%	0%	0%	0%	0%	0%	0%	50%	100%
		Corrected	100%	100%	100%	100%	100%	100%	100%	100%	100%	100%	100%	100%
	Validation	Raw	100%	100%	100%	0%	0%	0%	0%	0%	0%	0%	100%	100%
		Corrected	100%	100%	100%	100%	100%	100%	3%	15%	50%	100%	100%	100%
DMI-HIRHAM5	Calibration	Raw	100%	100%	100%	96%	0%	0%	0%	0%	0%	0%	100%	100%
		Corrected	100%	100%	100%	100%	100%	100%	100%	100%	100%	100%	100%	100%
	Validation	Raw	100%	100%	100%	50%	0%	7%	0%	0%	0%	0%	100%	100%
		Corrected	100%	100%	100%	100%	93%	34%	31%	19%	96%	96%	100%	100%
GKSS-ECHAM5	Calibration	Raw	100%	100%	100%	100%	0%	0%	0%	19%	0%	0%	100%	100%
		Corrected	100%	100%	100%	100%	100%	100%	100%	100%	100%	100%	100%	100%
	Validation	Raw	100%	100%	100%	100%	40%	0%	6%	0%	0%	0%	100%	100%
		Corrected	100%	100%	100%	100%	94%	89%	35%	4%	100%	100%	100%	100%
ICTP_REGCM3	Calibration	Raw	100%	100%	100%	12%	0%	8%	14%	3%	2%	100%	100%	100%
		Corrected	100%	100%	100%	100%	100%	100%	100%	100%	100%	100%	100%	100%
	Validation	Raw	100%	100%	100%	24%	0%	50%	0%	0%	0%	46%	100%	100%
		Corrected	100%	100%	100%	94%	94%	64%	4%	10%	100%	100%	100%	100%
INMRCA3	Calibration	Raw	100%	100%	100%	97%	0%	0%	0%	0%	0%	100%	100%	100%
		Corrected	100%	100%	100%	100%	100%	100%	100%	100%	100%	100%	100%	100%
	Validation	Raw	100%	100%	100%	51%	0%	0%	0%	0%	0%	31%	100%	100%
		Corrected	100%	100%	100%	100%	77%	76%	23%	16%	57%	87%	100%	100%
KNMIRACMO2.2b	Calibration	Raw	100%	100%	60%	0%	0%	0%	0%	0%	0%	0%	63%	100%
		Corrected	100%	100%	100%	100%	100%	100%	100%	100%	100%	100%	100%	100%
	Validation	Raw	100%	100%	18%	0%	0%	0%	0%	0%	0%	0%	100%	100%
		Corrected	100%	100%	100%	98%	82%	100%	97%	97%	96%	67%	100%	100%
METNOHIRHAM	Calibration	Raw	100%	100%	100%	14%	0%	0%	0%	0%	0%	0%	100%	100%
		Corrected	100%	100%	100%	100%	100%	100%	100%	100%	100%	100%	100%	100%
	Validation	Raw	100%	100%	100%	0%	0%	0%	0%	0%	0%	0%	100%	100%
		Corrected	100%	100%	100%	96%	65%	43%	0%	94%	93%	100%	100%	100%
METNOHIRHAM	Calibration	Raw	100%	100%	0%	0%	0%	0%	0%	0%	0%	0%	0%	100%
		Corrected	100%	100%	100%	100%	100%	100%	100%	100%	100%	100%	100%	100%
	Validation	Raw	100%	100%	0%	0%	0%	0%	0%	0%	0%	0%	0%	100%
		Corrected	100%	100%	100%	100%	100%	90%	77%	0%	14%	100%	100%	100%
METO-HC	Calibration	Raw	100%	100%	0%	0%	0%	0%	0%	0%	0%	0%	0%	100%
		Corrected	100%	100%	100%	100%	100%	100%	100%	100%	100%	100%	100%	100%
	Validation	Raw	100%	100%	0%	0%	0%	0%	0%	0%	0%	0%	0%	100%
		Corrected	100%	100%	100%	100%	100%	90%	77%	0%	14%	100%	100%	100%
MPI_M_REMO	Calibration	Raw	100%	100%	100%	100%	0%	0%	0%	0%	0%	0%	100%	100%
		Corrected	100%	100%	100%	100%	100%	100%	100%	100%	100%	100%	100%	100%
	Validation	Raw	100%	100%	100%	43%	0%	0%	0%	0%	0%	0%	100%	100%
		Corrected	100%	100%	100%	100%	100%	98%	45%	61%	70%	72%	100%	100%

Table 6 - KS Test results for Max. Temp.

Models	MAX	Months	1	2	3	4	5	6	7	8	9	10	11	12
CHMIALADIN	Calibration	Raw	100%	100%	100%	0%	0%	0%	0%	0%	0%	0%	50%	100%
		Corrected	100%	100%	100%	100%	100%	100%	100%	100%	100%	100%	100%	100%
	Validation	Raw	100%	100%	100%	0%	0%	0%	0%	0%	0%	0%	100%	100%
		Corrected	100%	100%	100%	100%	100%	100%	3%	15%	50%	100%	100%	100%
DMI-HIRHAM5	Calibration	Raw	100%	100%	100%	96%	0%	0%	0%	0%	0%	0%	100%	100%
		Corrected	100%	100%	100%	100%	100%	100%	100%	100%	100%	100%	100%	100%
	Validation	Raw	100%	100%	100%	50%	0%	7%	0%	0%	0%	0%	100%	100%
		Corrected	100%	100%	100%	100%	93%	34%	31%	19%	96%	96%	100%	100%
GKSS-ECHAM5	Calibration	Raw	100%	100%	100%	100%	0%	0%	0%	19%	0%	0%	100%	100%
		Corrected	100%	100%	100%	100%	100%	100%	100%	100%	100%	100%	100%	100%
	Validation	Raw	100%	100%	100%	100%	40%	0%	6%	0%	0%	0%	100%	100%
		Corrected	100%	100%	100%	100%	94%	89%	35%	4%	100%	100%	100%	100%
ICTP_REGCM3	Calibration	Raw	100%	100%	100%	12%	0%	8%	14%	3%	2%	100%	100%	100%
		Corrected	100%	100%	100%	100%	100%	100%	100%	100%	100%	100%	100%	100%
	Validation	Raw	100%	100%	100%	24%	0%	50%	0%	0%	0%	46%	100%	100%
		Corrected	100%	100%	100%	94%	94%	64%	4%	10%	100%	100%	100%	100%
INMRCA3	Calibration	Raw	100%	100%	100%	97%	0%	0%	0%	0%	0%	100%	100%	100%
		Corrected	100%	100%	100%	100%	100%	100%	100%	100%	100%	100%	100%	100%
	Validation	Raw	100%	100%	100%	51%	0%	0%	0%	0%	0%	31%	100%	100%
		Corrected	100%	100%	100%	100%	77%	76%	23%	16%	57%	87%	100%	100%
KNMIRACMO2.2b	Calibration	Raw	100%	100%	60%	0%	0%	0%	0%	0%	0%	0%	63%	100%
		Corrected	100%	100%	100%	100%	100%	100%	100%	100%	100%	100%	100%	100%
	Validation	Raw	100%	100%	18%	0%	0%	0%	0%	0%	0%	0%	100%	100%
		Corrected	100%	100%	100%	98%	82%	100%	97%	97%	96%	67%	100%	100%
METNOHIRHAM	Calibration	Raw	100%	100%	100%	14%	0%	0%	0%	0%	0%	0%	100%	100%
		Corrected	100%	100%	100%	100%	100%	100%	100%	100%	100%	100%	100%	100%
	Validation	Raw	100%	100%	100%	0%	0%	0%	0%	0%	0%	0%	100%	100%
		Corrected	100%	100%	100%	96%	65%	43%	0%	94%	93%	100%	100%	100%
METNOHIRHAM	Calibration	Raw	100%	100%	0%	0%	0%	0%	0%	0%	0%	0%	0%	100%
		Corrected	100%	100%	100%	100%	100%	100%	100%	100%	100%	100%	100%	100%
	Validation	Raw	100%	100%	0%	0%	0%	0%	0%	0%	0%	0%	0%	100%
		Corrected	100%	100%	100%	100%	100%	90%	77%	0%	14%	100%	100%	100%
METO-HC	Calibration	Raw	100%	100%	0%	0%	0%	0%	0%	0%	0%	0%	0%	100%
		Corrected	100%	100%	100%	100%	100%	100%	100%	100%	100%	100%	100%	100%
	Validation	Raw	100%	100%	0%	0%	0%	0%	0%	0%	0%	0%	0%	100%
		Corrected	100%	100%	100%	100%	100%	90%	77%	0%	14%	100%	100%	100%
MPI_M_REMO	Calibration	Raw	100%	100%	100%	100%	0%	0%	0%	0%	0%	0%	100%	100%
		Corrected	100%	100%	100%	100%	100%	100%	100%	100%	100%	100%	100%	100%
	Validation	Raw	100%	100%	100%	43%	0%	0%	0%	0%	0%	0%	100%	100%
		Corrected	100%	100%	100%	100%	100%	98%	45%	61%	70%	72%	100%	100%

Table 7 - KS Test results for Min. Temp.

Models	MIN	Months	1	2	3	4	5	6	7	8	9	10	11	12
CHMIALADIN	Calibration	Raw	100%	100%	100%	0%	0%	0%	0%	0%	0%	0%	50%	100%
		Corrected	100%	100%	100%	100%	100%	100%	100%	100%	100%	100%	100%	100%
	Validation	Raw	100%	100%	100%	0%	0%	0%	0%	0%	0%	0%	100%	100%
		Corrected	100%	100%	100%	100%	100%	100%	3%	15%	50%	100%	100%	100%
DMI-HIRHAM5	Calibration	Raw	100%	100%	100%	96%	0%	0%	0%	0%	0%	0%	100%	100%
		Corrected	100%	100%	100%	100%	100%	100%	100%	100%	100%	100%	100%	100%
	Validation	Raw	100%	100%	100%	50%	0%	7%	0%	0%	0%	0%	100%	100%
		Corrected	100%	100%	100%	100%	93%	34%	31%	19%	96%	96%	100%	100%
GKSS-ECHAM5	Calibration	Raw	100%	100%	100%	100%	0%	0%	0%	19%	0%	0%	100%	100%
		Corrected	100%	100%	100%	100%	100%	100%	100%	100%	100%	100%	100%	100%
	Validation	Raw	100%	100%	100%	100%	40%	0%	6%	0%	0%	0%	100%	100%
		Corrected	100%	100%	100%	100%	94%	89%	35%	4%	100%	100%	100%	100%
ICTP_REGCM3	Calibration	Raw	100%	100%	100%	12%	0%	8%	14%	3%	2%	100%	100%	100%
		Corrected	100%	100%	100%	100%	100%	100%	100%	100%	100%	100%	100%	100%
	Validation	Raw	100%	100%	100%	24%	0%	50%	0%	0%	0%	46%	100%	100%
		Corrected	100%	100%	100%	94%	94%	64%	4%	10%	100%	100%	100%	100%
INMRCA3	Calibration	Raw	100%	100%	100%	97%	0%	0%	0%	0%	0%	100%	100%	100%
		Corrected	100%	100%	100%	100%	100%	100%	100%	100%	100%	100%	100%	100%
	Validation	Raw	100%	100%	100%	51%	0%	0%	0%	0%	0%	31%	100%	100%
		Corrected	100%	100%	100%	100%	77%	76%	23%	16%	57%	87%	100%	100%
KNMIRACMO2.2b	Calibration	Raw	100%	100%	60%	0%	0%	0%	0%	0%	0%	0%	63%	100%
		Corrected	100%	100%	100%	100%	100%	100%	100%	100%	100%	100%	100%	100%
	Validation	Raw	100%	100%	18%	0%	0%	0%	0%	0%	0%	0%	100%	100%
		Corrected	100%	100%	100%	98%	82%	100%	97%	97%	96%	67%	100%	100%
METNOHIRHAM	Calibration	Raw	100%	100%	100%	14%	0%	0%	0%	0%	0%	0%	100%	100%
		Corrected	100%	100%	100%	100%	100%	100%	100%	100%	100%	100%	100%	100%
	Validation	Raw	100%	100%	100%	0%	0%	0%	0%	0%	0%	0%	100%	100%
		Corrected	100%	100%	100%	96%	65%	43%	0%	94%	93%	100%	100%	100%
METNOHIRHAM	Calibration	Raw	100%	100%	0%	0%	0%	0%	0%	0%	0%	0%	0%	100%
		Corrected	100%	100%	100%	100%	100%	100%	100%	100%	100%	100%	100%	100%
	Validation	Raw	100%	100%	0%	0%	0%	0%	0%	0%	0%	0%	0%	100%
		Corrected	100%	100%	100%	100%	100%	90%	77%	0%	14%	100%	100%	100%
METO-HC	Calibration	Raw	100%	100%	0%	0%	0%	0%	0%	0%	0%	0%	0%	100%
		Corrected	100%	100%	100%	100%	100%	100%	100%	100%	100%	100%	100%	100%
	Validation	Raw	100%	100%	0%	0%	0%	0%	0%	0%	0%	0%	0%	100%
		Corrected	100%	100%	100%	100%	100%	90%	77%	0%	14%	100%	100%	100%
MPI_M_REMO	Calibration	Raw	100%	100%	100%	100%	0%	0%	0%	0%	0%	0%	100%	100%
		Corrected	100%	100%	100%	100%	100%	100%	100%	100%	100%	100%	100%	100%
	Validation	Raw	100%	100%	100%	43%	0%	0%	0%	0%	0%	0%	100%	100%
		Corrected	100%	100%	100%	100%	100%	98%	45%	61%	70%	72%	100%	100%

6.5.3 Return periods

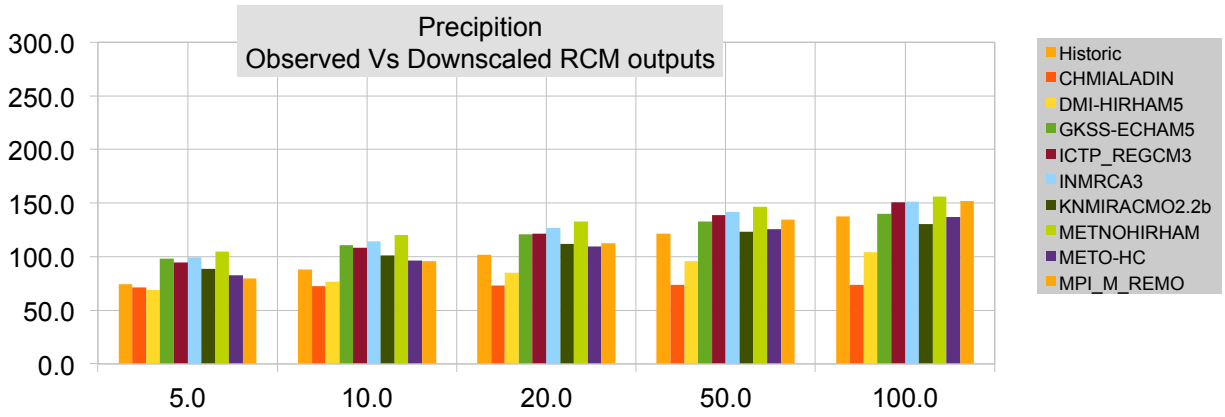

Figure 81 - Return Period - Precipitation - Obs. Vs. QQ-RCM

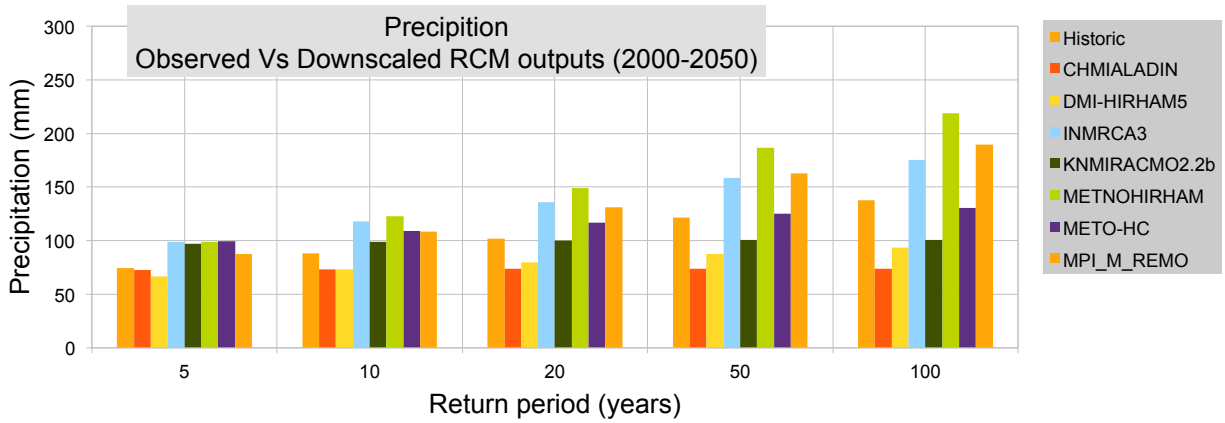

Figure 82 - Return Period - Precipitation - Obs. Vs. QQ-RCM (2000-2050)

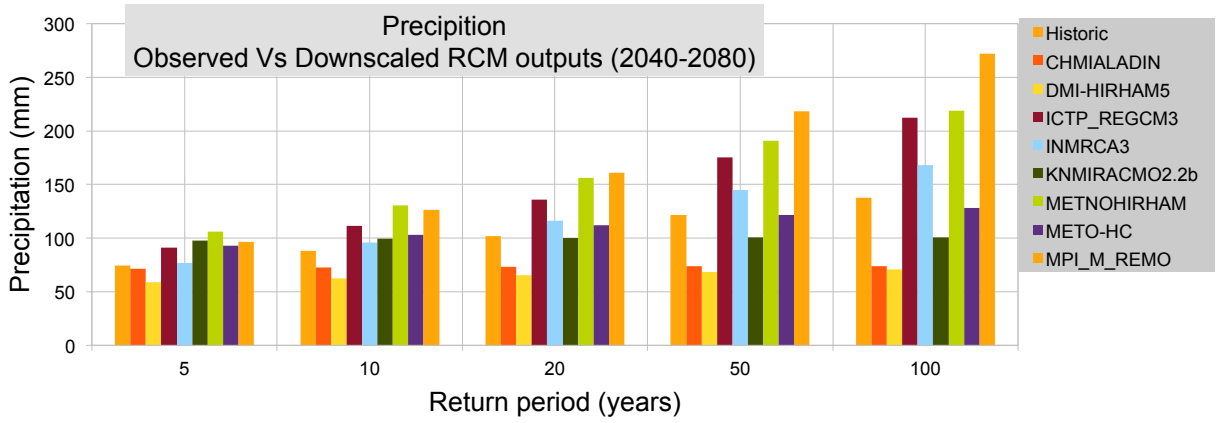

Figure 83 - Return Period - Precipitation - Obs. Vs. QQ-RCM (2040-2080)

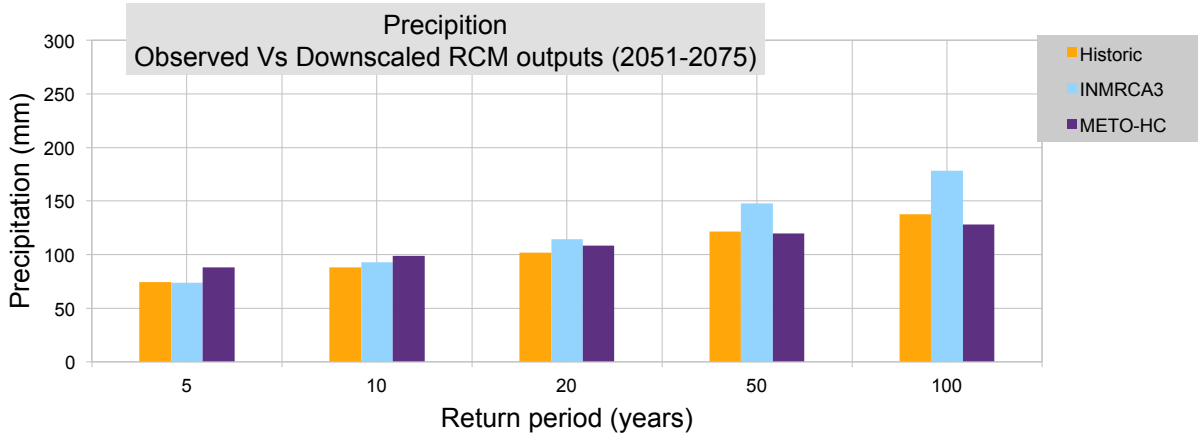

Figure 84 - Return Period - Precipitation - Obs. Vs. QQ-RCM (2051-2075)

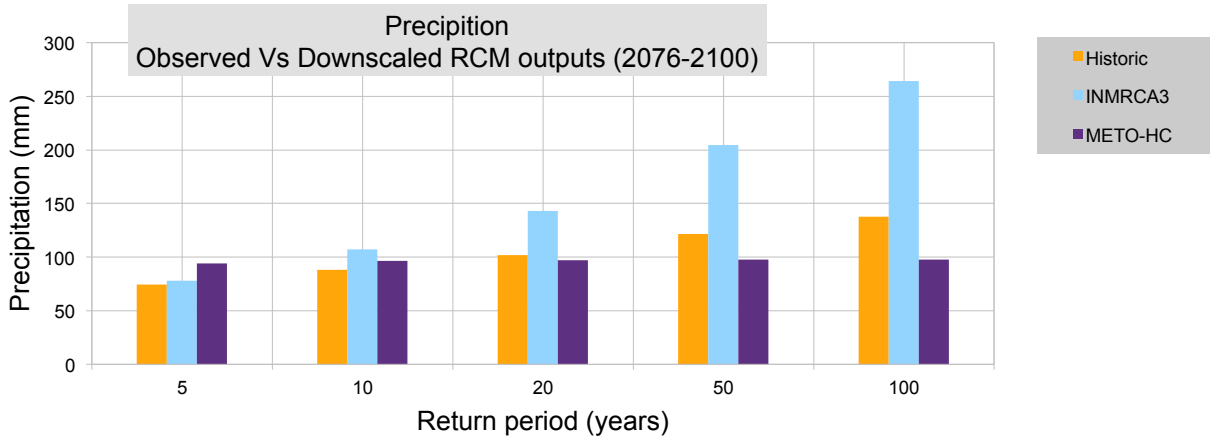

Figure 85 - Return Period - Precipitation - Obs. Vs. QQ-RCM (2076-2100)

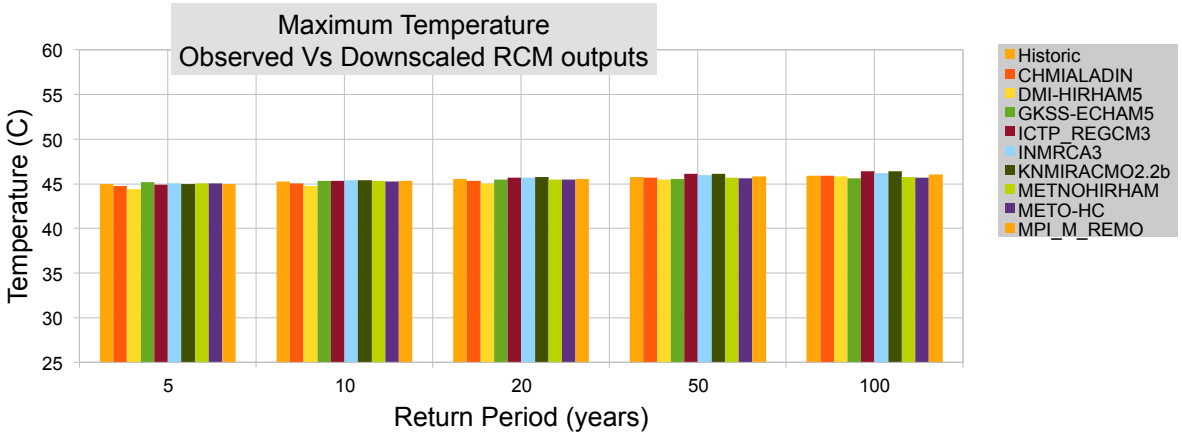

Figure 86 - Return Period – Max. Temp - Obs. Vs. QQ-RCM

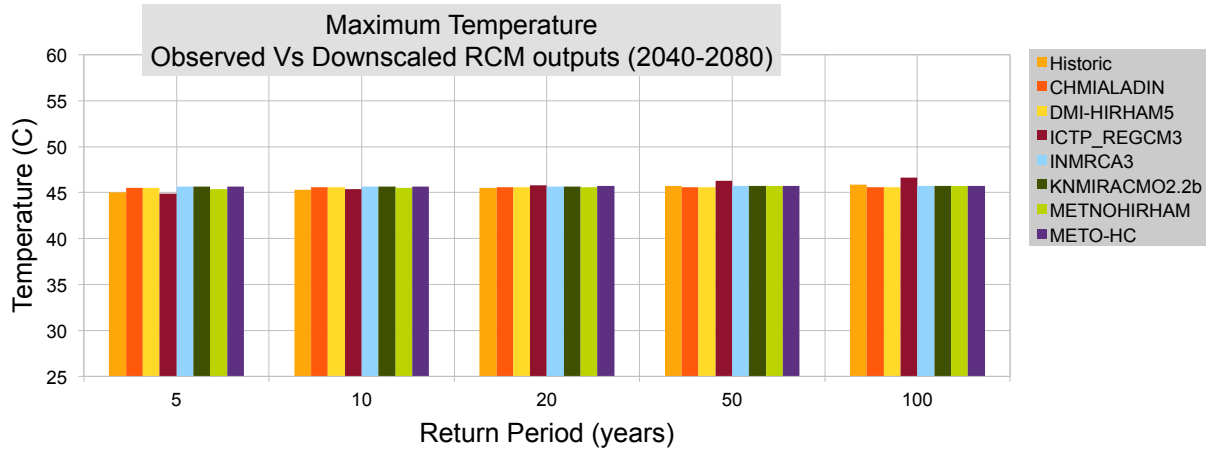

Figure 87 - Return Period – Max. Temp - Obs. Vs. QQ-RCM (2040 - 2080)

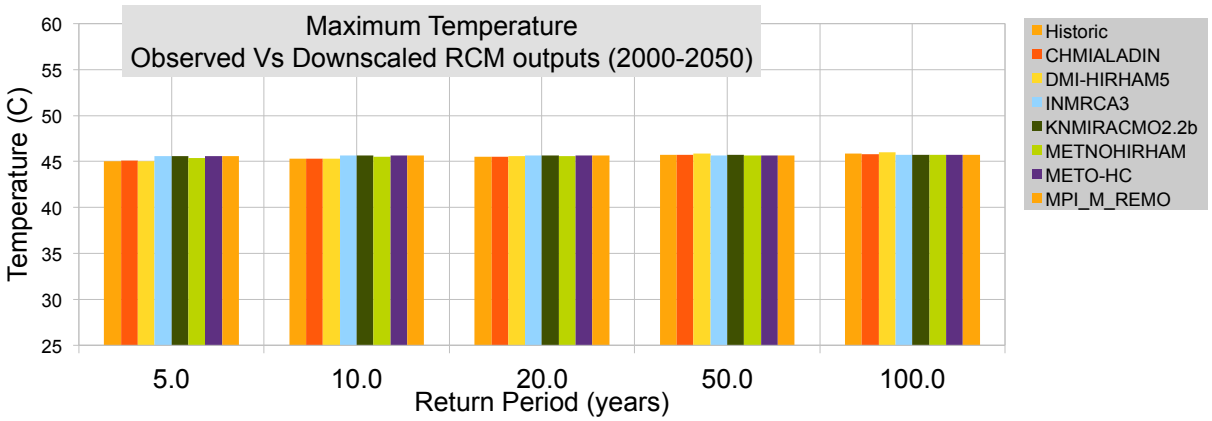

Figure 88 - Return Period – Max. Temp - Obs. Vs. QQ-RCM (2000 - 2050)

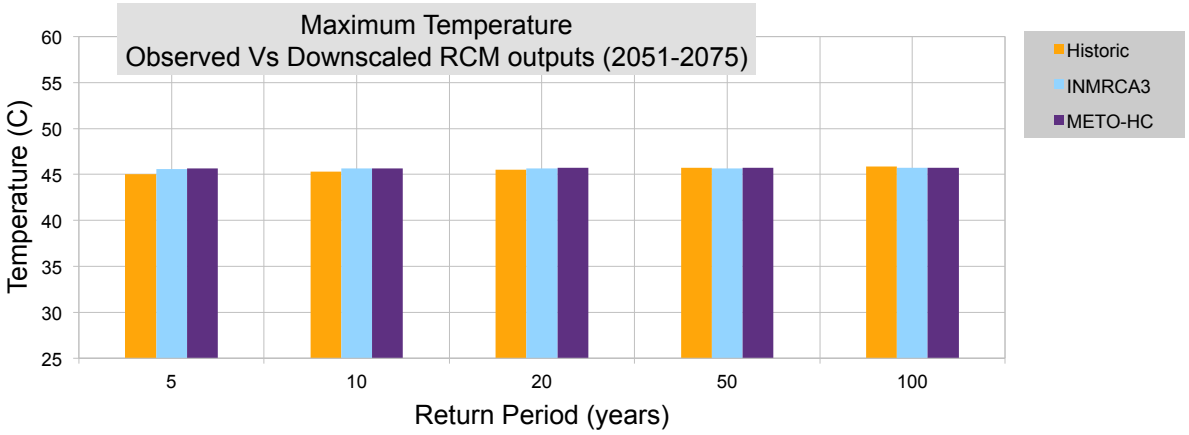

Figure 89 - Return Period – Max. Temp - Obs. Vs. QQ-RCM (2051 -2075)

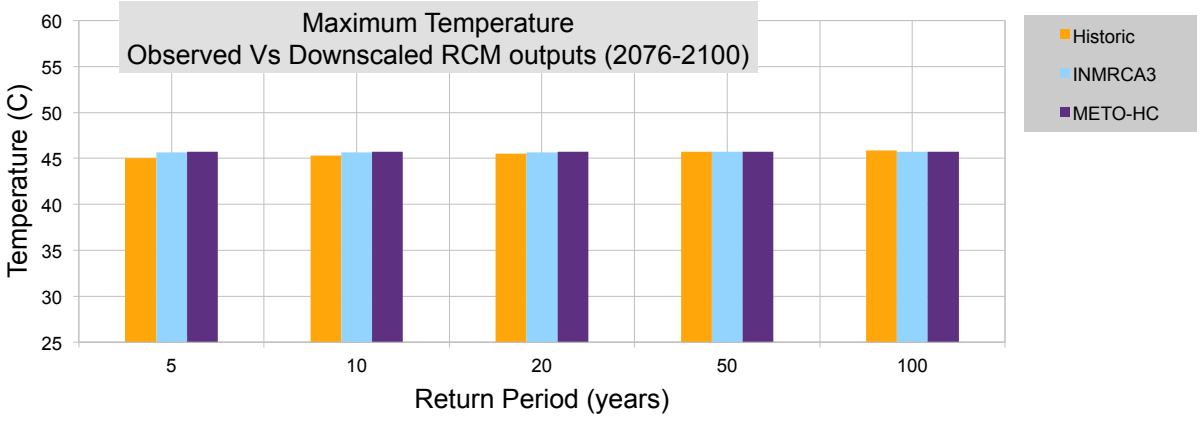

Figure 90 - Return Period – Max. Temp - Obs. Vs. QQ-RCM (2076 - 2100)

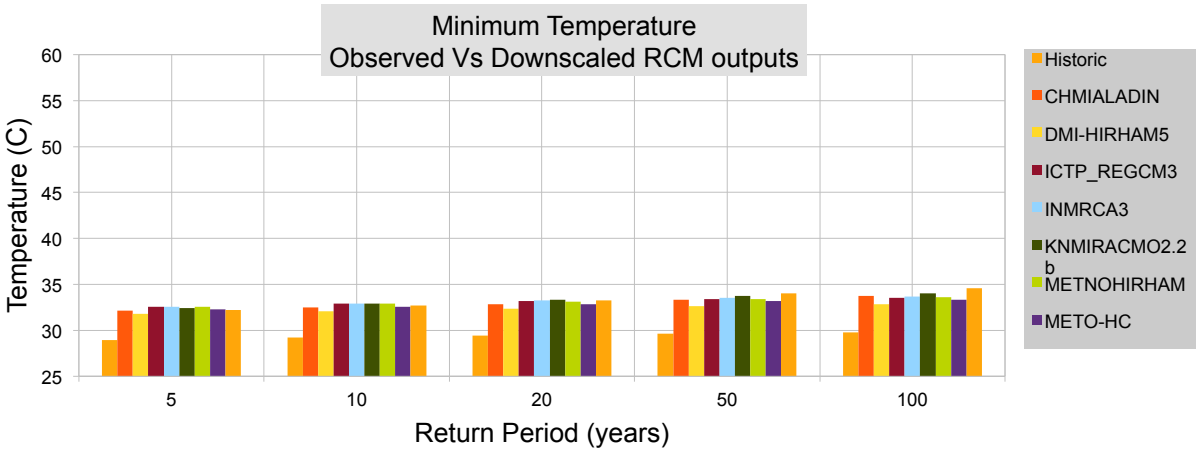

Figure 91 - Return Period – Min. Temp - Obs. Vs. QQ-RCM

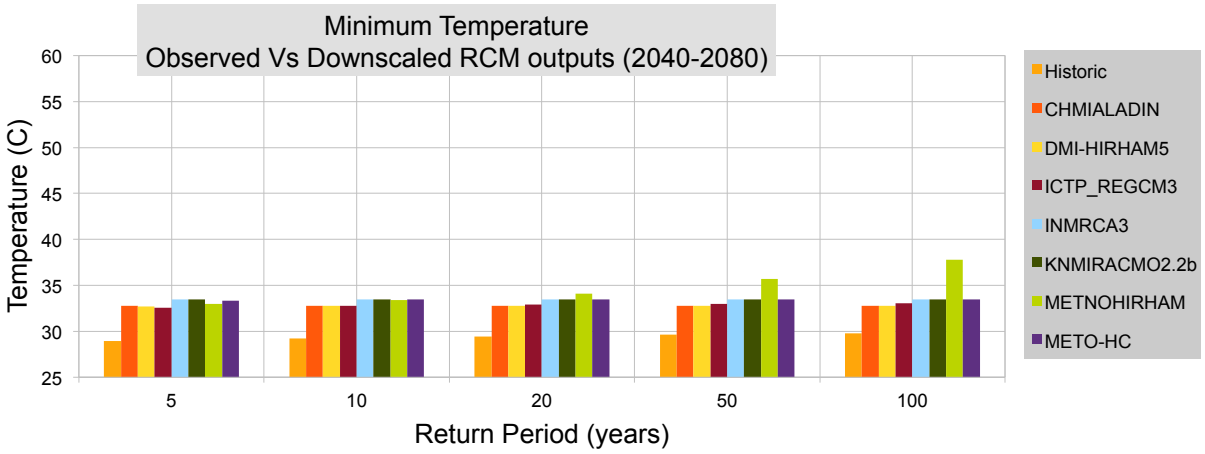

Figure 92 Return Period – Min. Temp - Obs. Vs. QQ-RCM (2040 - 2080)

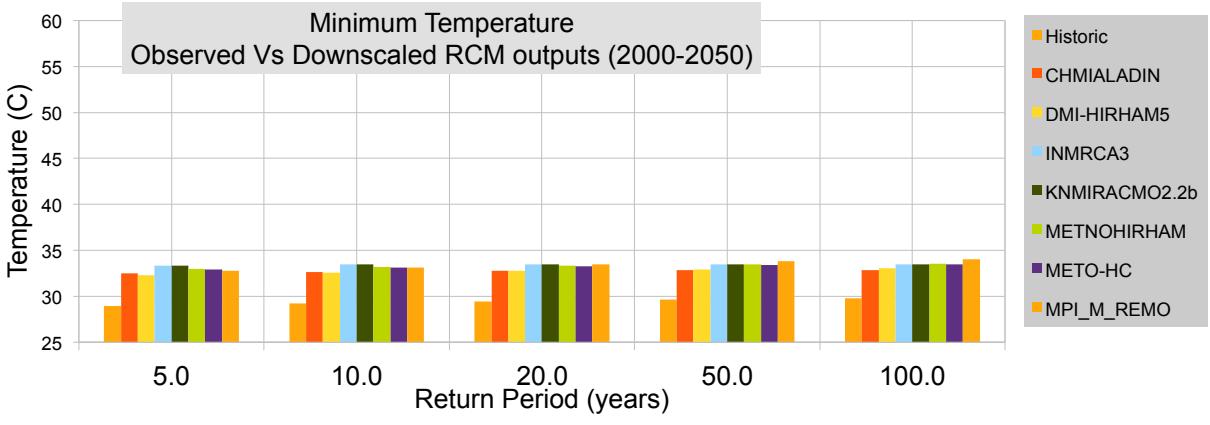

Figure 93 Return Period – Min. Temp - Obs. Vs. QQ-RCM (2000 – 2050)

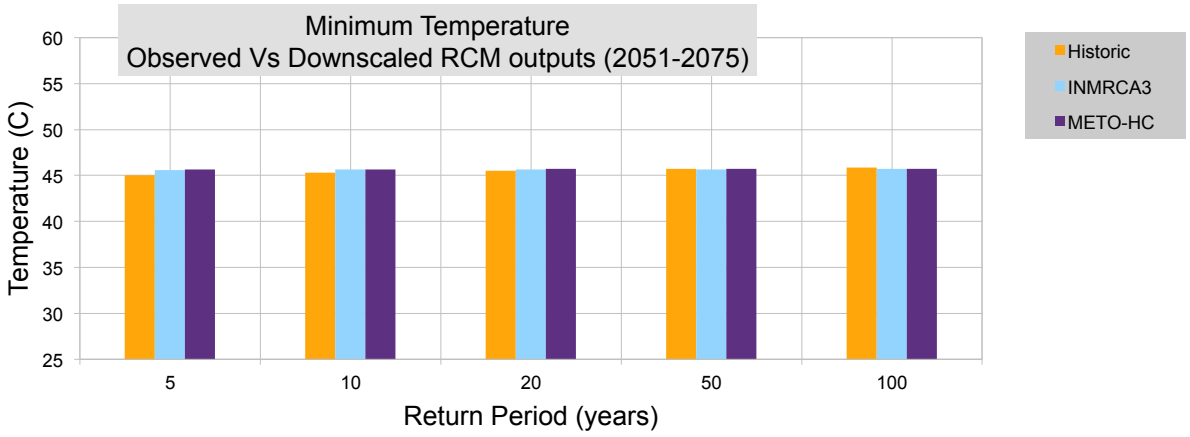

Figure 94 Return Period – Min. Temp - Obs. Vs. QQ-RCM (2051 – 2075)

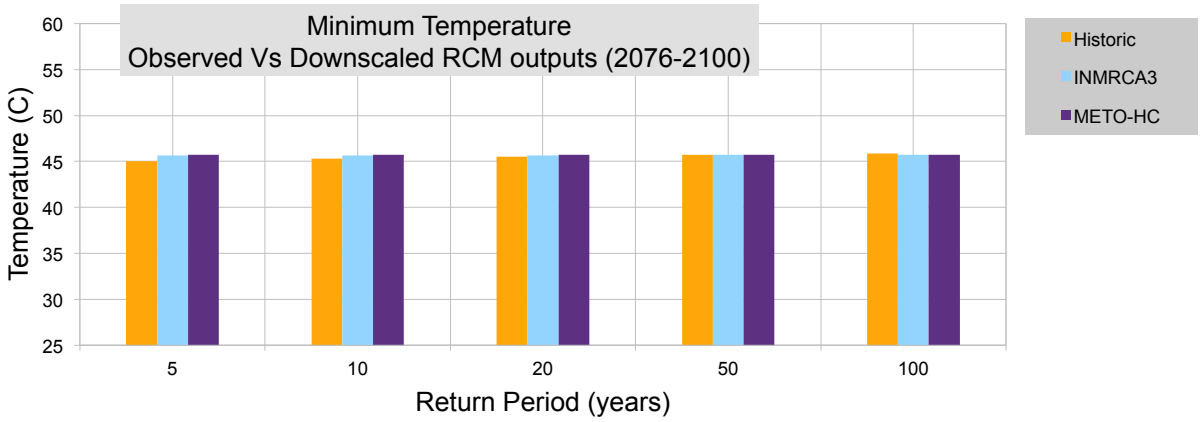

Figure 95 Return Period – Min. Temp - Obs. Vs. QQ-RCM (2076 – 2100)

6.5.4 Extreme event indices

In addition to offering valuable asset for climate change impact assessment, plots in figures below of extreme climate event indices are testament to the Quantile-Quantile downscaling method's performance. Figure 96 through Figure 167 below clearly illustrate the advantage gained by applying the Quantile-Quantile downscaling method: it is apparent that extreme event characteristics such as magnitude and frequency are replicated in the downscaled climate model outputs hence allowing realistic interpretation of the climate in the simulated future. Downscaled climate change simulation outputs exhibit agreement than with historic data over the observed

time frame. The witnessed agreements are systematically better than that between the observed historical data and raw climate simulation outputs from GCM/RCMs. It is however worth noting that the same conclusion may not be drawn for extreme precipitation volume indices such as the annual total volume of precipitation.

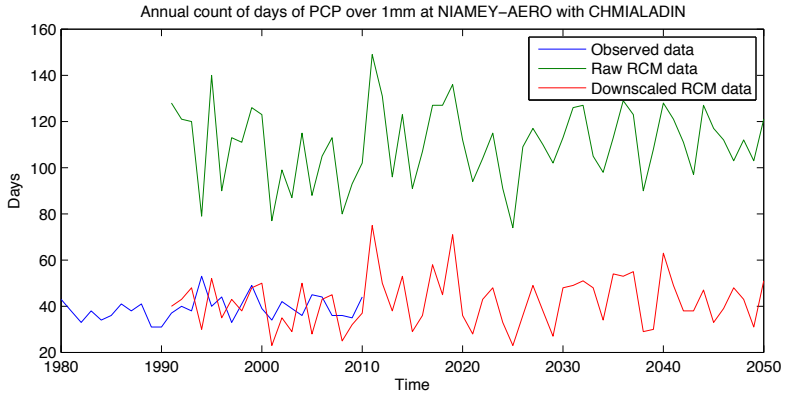

Figure 96 - Annual count of days of precipitation over 1mm at Niamey airport with CHMIALADIN

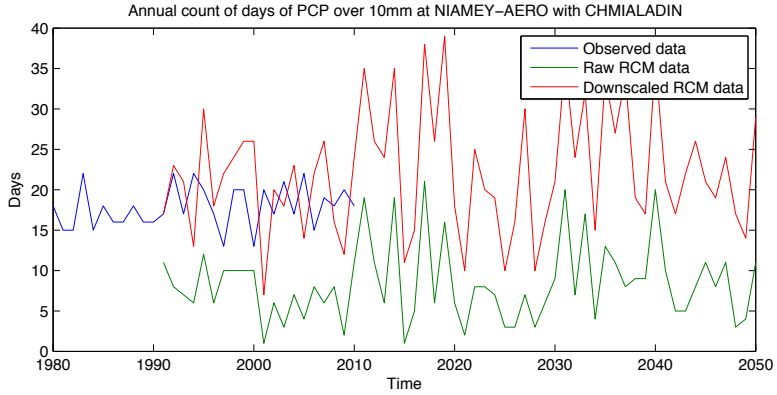

Figure 97 - Annual count of days of precipitation over 10mm at Niamey airport with CHMIALADIN

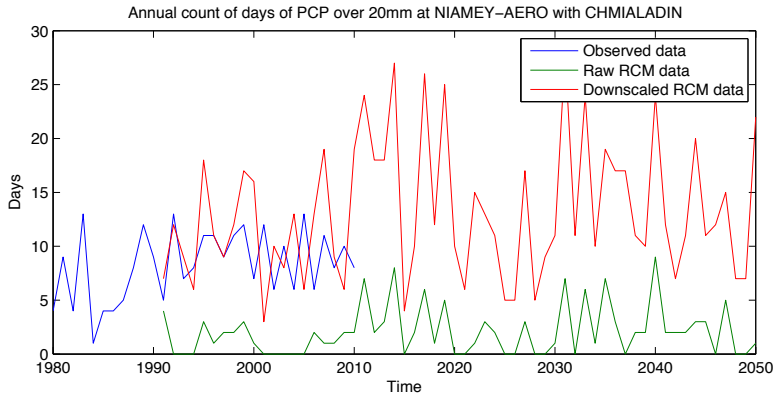

Figure 98 - Annual count of days of precipitation over 20mm at Niamey airport with CHMIALADIN

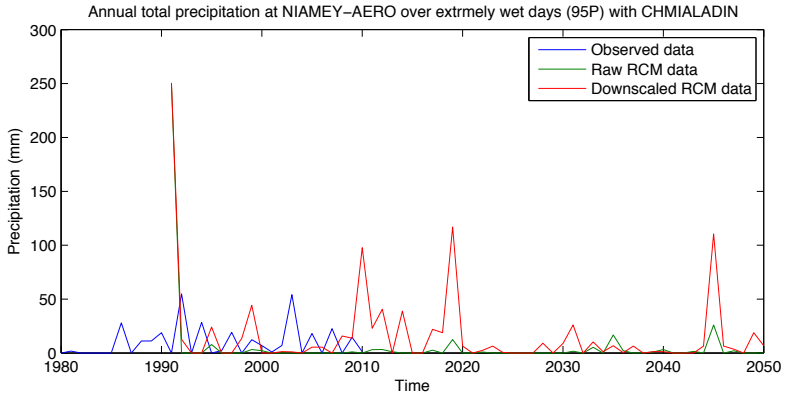

Figure 99 - Annual total precipitation over extremely wet days (95P) at Niamey airport with CHMIALADIN

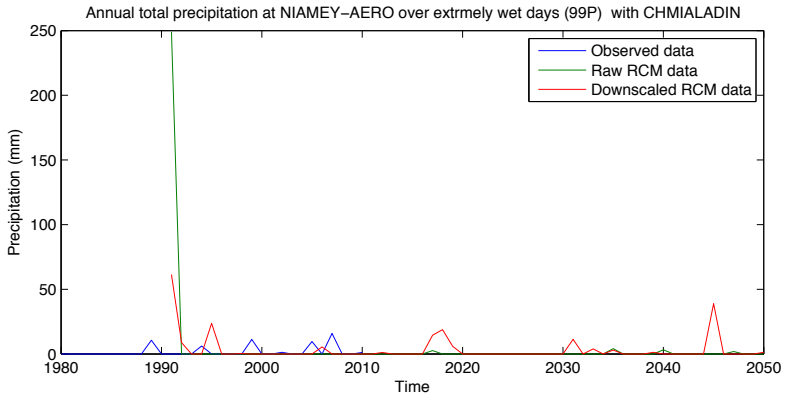

Figure 100 - Annual total precipitation over extremely wet days (99P) at Niamey airport with CHMIALADIN

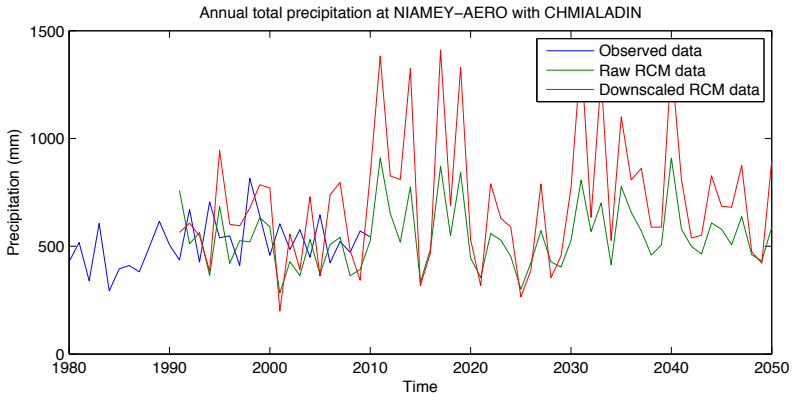

Figure 101 - Annual total precipitation at Niamey airport with CHMIALADIN

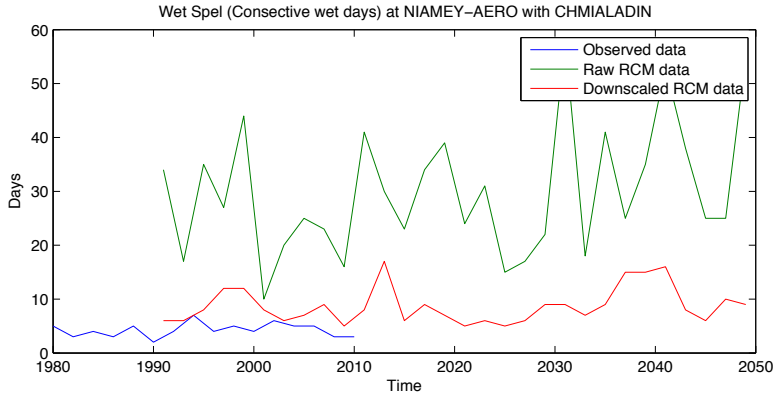

Figure 102 - Wet spell (consecutive wet days) at Niamey airport with CHMIALADIN

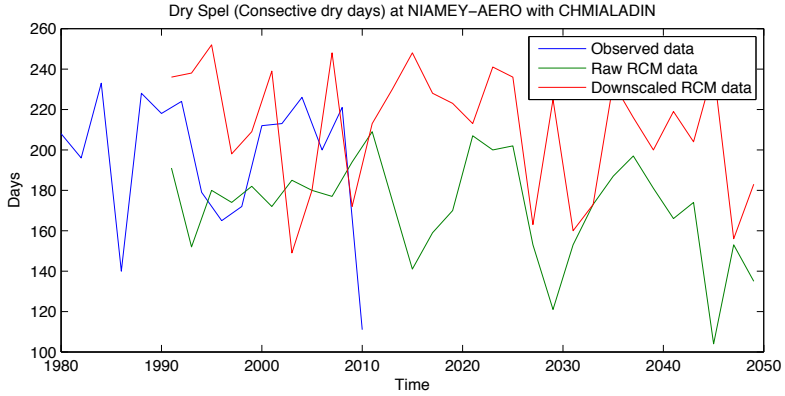

Figure 103 - Dry spell (consecutive dry days) at Niamey airport with CHMIALADIN

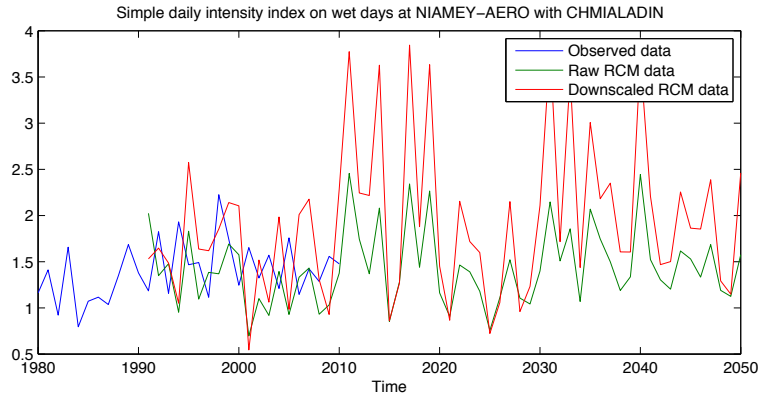

Figure 104 - Simple daily intensity index on wet days at Niamey airport with CHMIALADIN

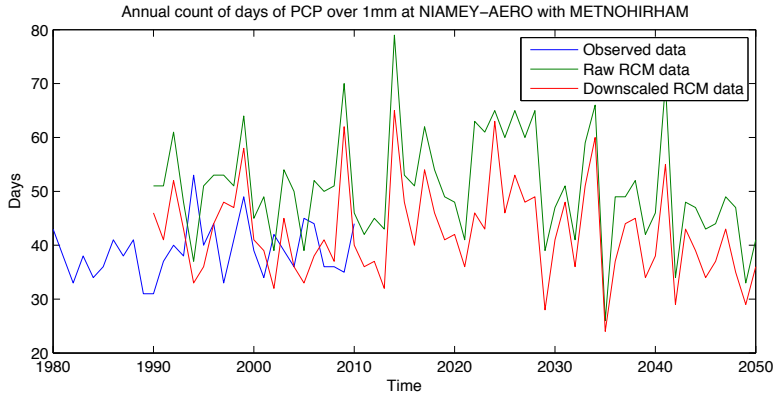

Figure 105 - Annual count of days of precipitation over 1mm at Niamey airport with METNOHORHAM

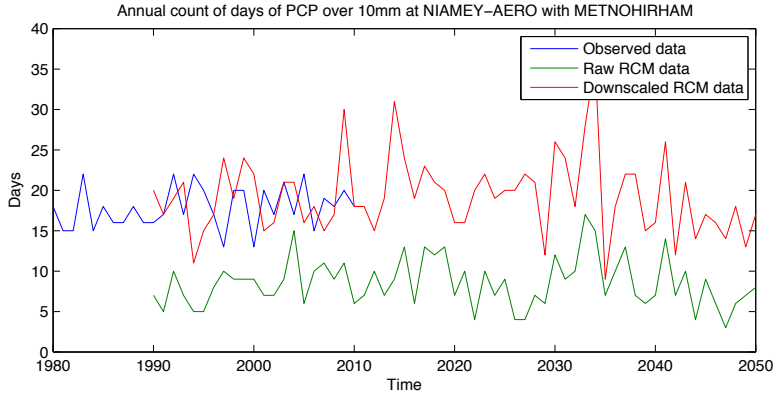

Figure 106 - Annual count of days of precipitation over 10mm at Niamey airport with METNOHORHAM

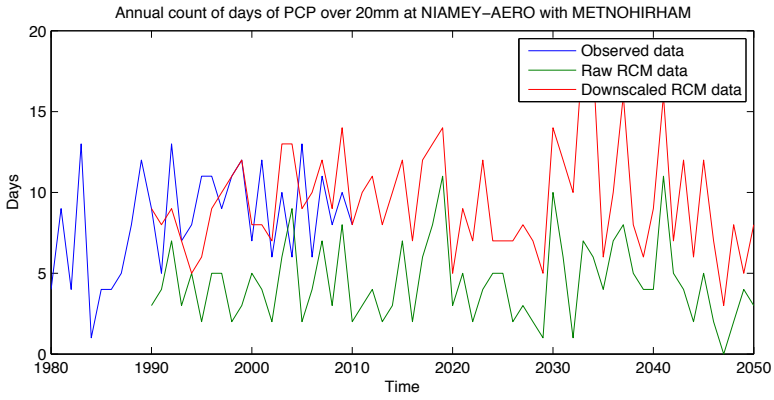

Figure 107 - Annual count of days of precipitation over 20mm at Niamey airport with METNOHORHAM

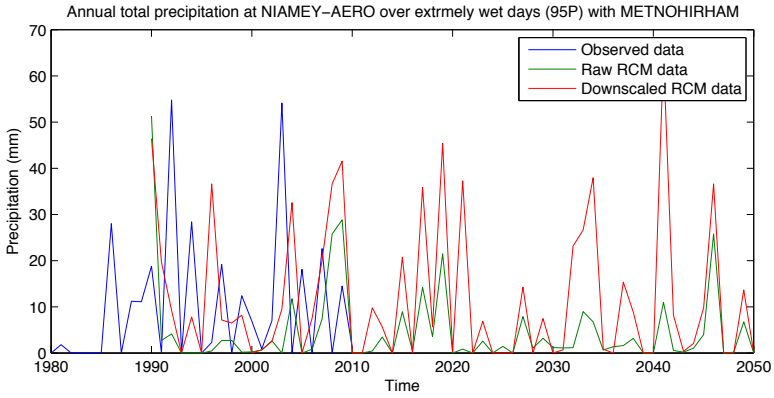

Figure 108 - Annual total precipitation over extremely wet days (95 P) at Niamey airport with METNOHORHAM

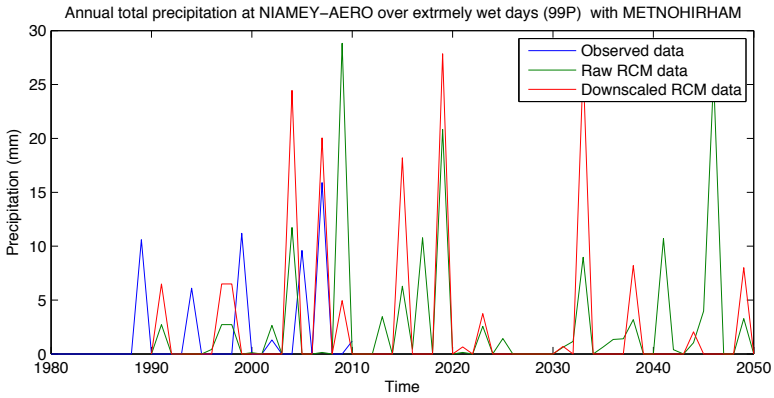

Figure 109 - Annual total precipitation over extremely wet days (99 P) at Niamey airport with METNOHORHAM

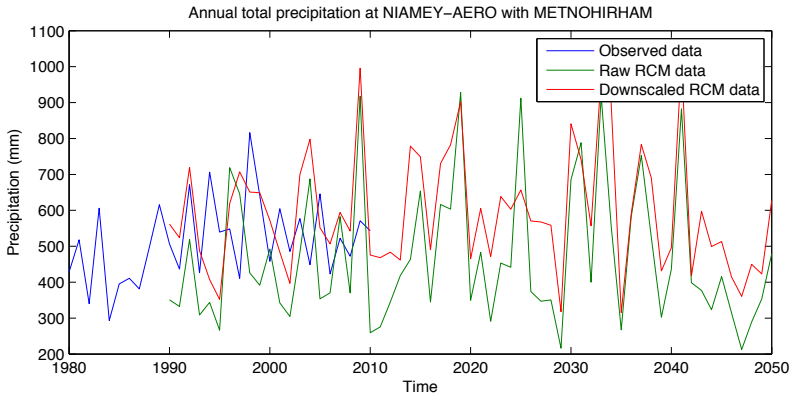

Figure 110 - Annual total precipitation at Niamey airport with METNOHORHAM

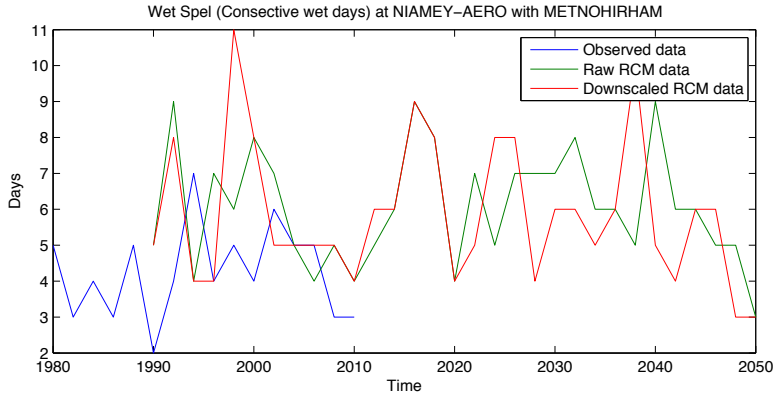

Figure 111 - Wet Spell (consecutive wet days) at Niamey airport with METNOHORHAM

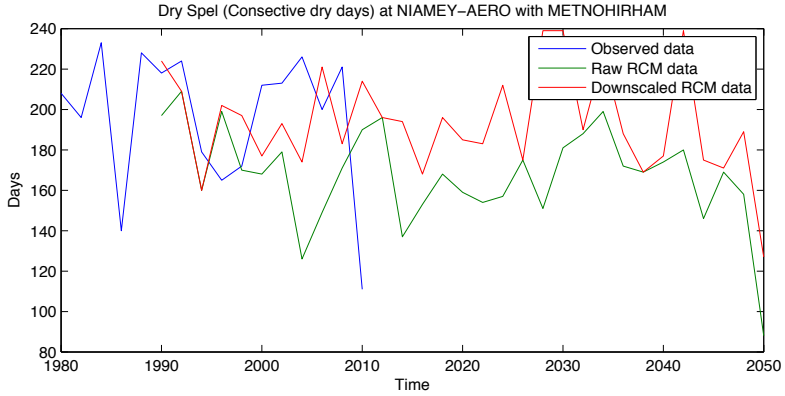

Figure 112 - Dry spell (consecutive dry days) at Niamey airport with METNOHORHAM

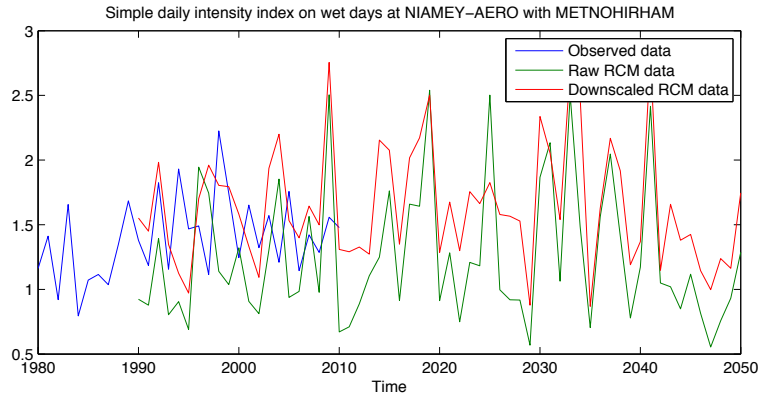

Figure 113 - Simple daily intensity index on wet days at Niamey airport with METNOHORHAM

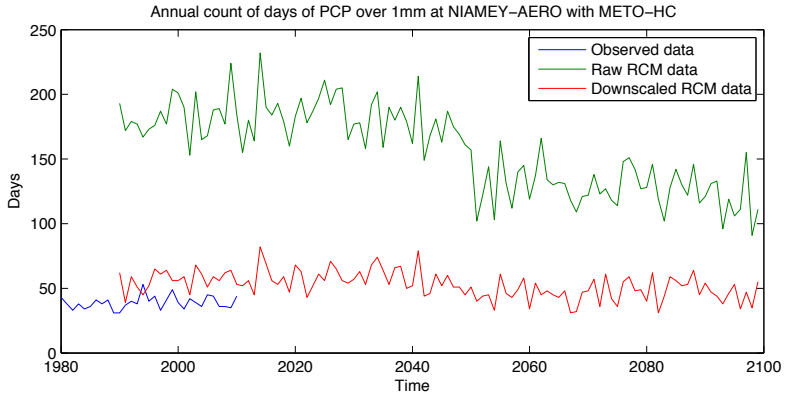

Figure 114 - Annual count of days of precipitation over 1mm at Niamey airport with METO - HC

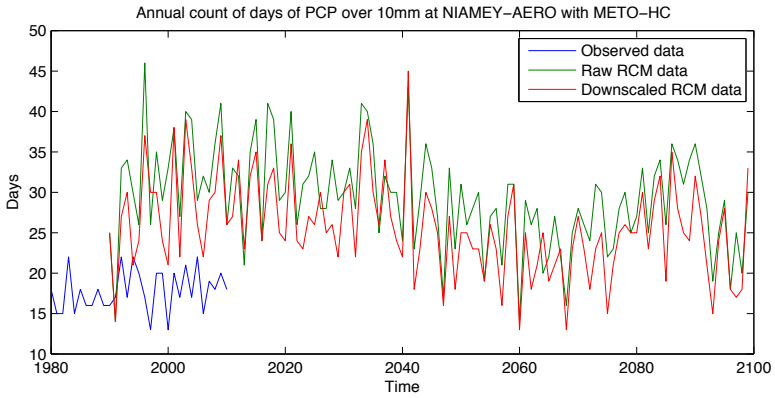

Figure 115 - Annual count of days of precipitation over 10mm at Niamey airport with METO - HC

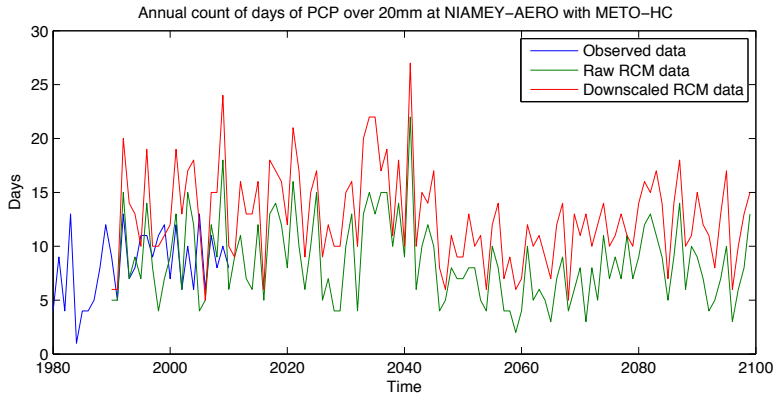

Figure 116 - Annual count of days of precipitation over 20mm at Niamey airport with METO - HC

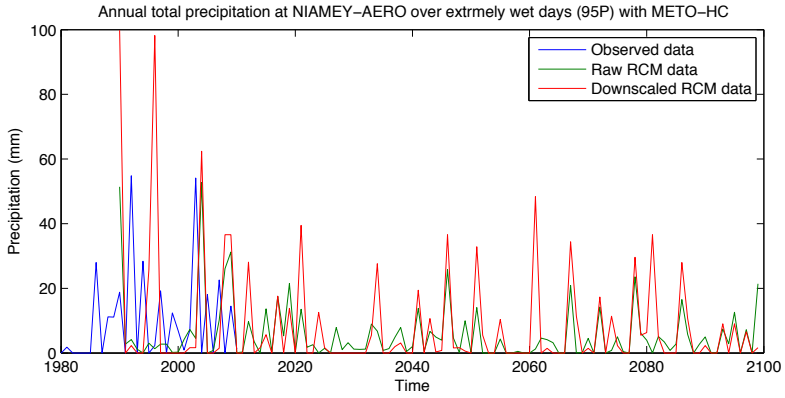

Figure 117 - Annual total precipitation over extremely wet days (95P) at Niamey airport with METO - HC

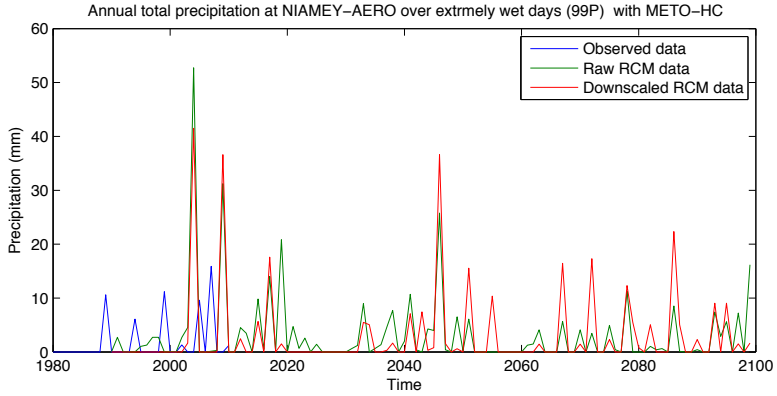

Figure 118 - Annual total precipitation over extremely wet days (99P) at Niamey airport with METO - HC

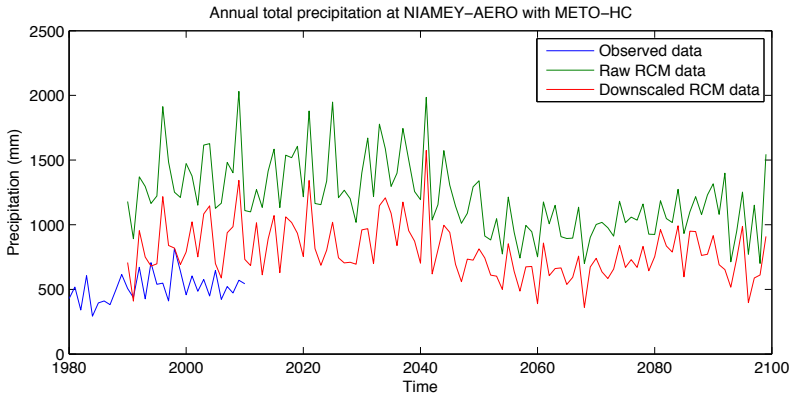

Figure 119 - Annual total precipitation at Niamey airport with METO - HC

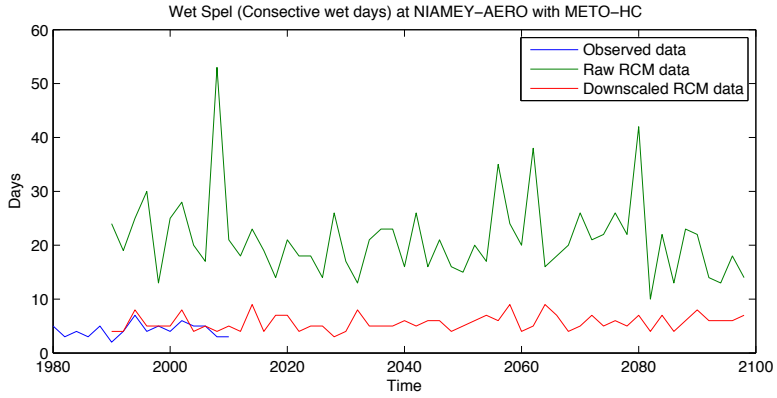

Figure 120 - Wet spell (consecutive wet days) at Niamey airport with METO - HC

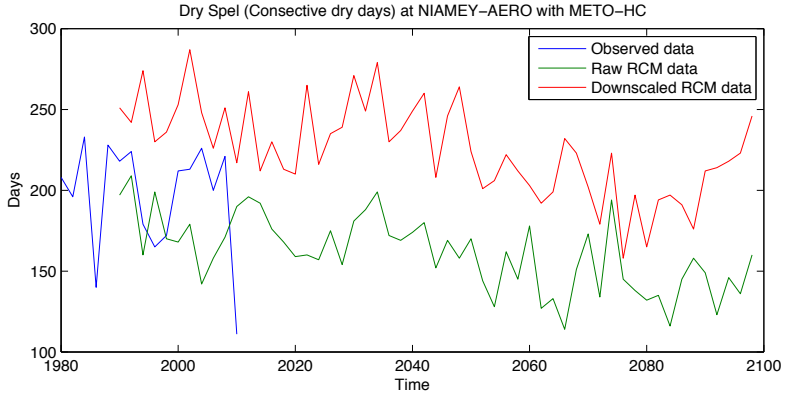

Figure 121 - Dry spell (consecutive dry days) at Niamey airport with METO - HC

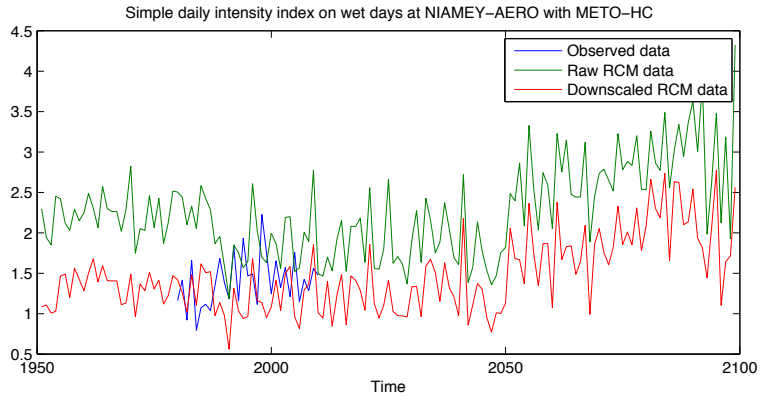

Figure 122 - Simple daily intensity index on wet days at Niamey airport with METO - HC

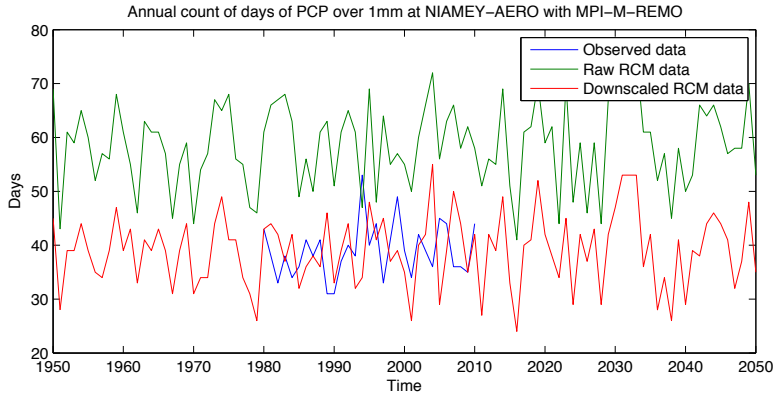

Figure 123 - Annual count of days of precipitation over 1mm at Niamey airport with MPI - M - REMO

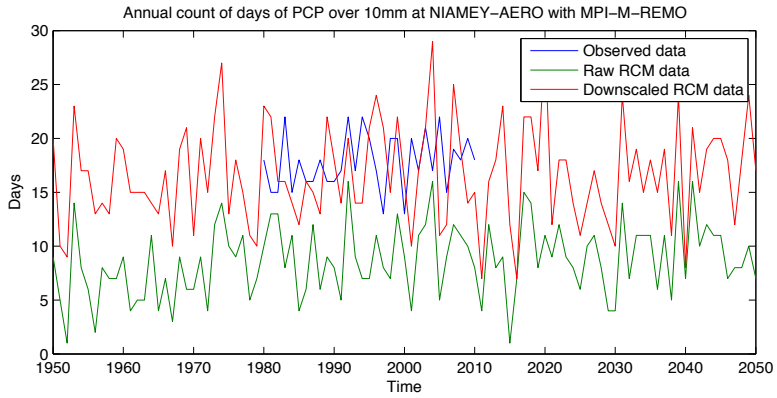

Figure 124 - Annual count of days of precipitation over 10mm at Niamey airport with MPI - M - REMO

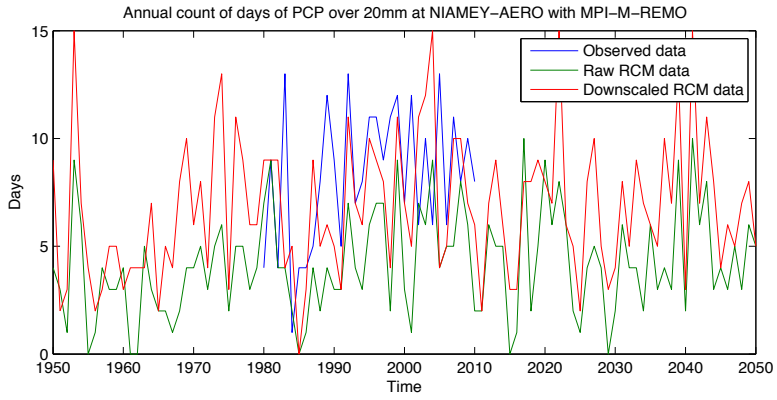

Figure 125 - Annual count of days of precipitation over 20mm at Niamey airport with MPI - M - REMO

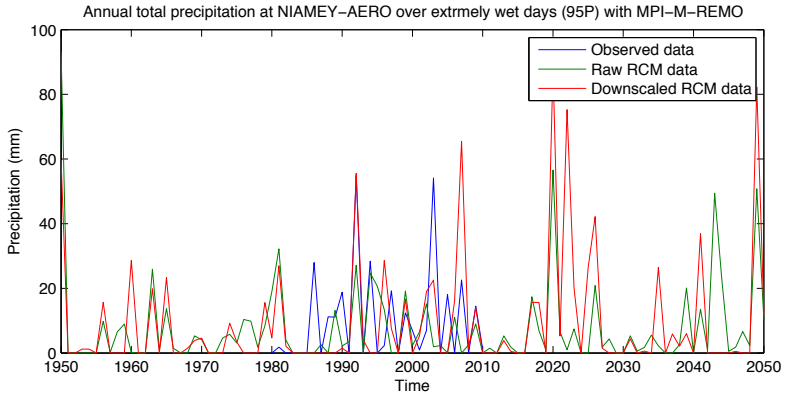

Figure 126 - Annual total precipitation over extremely wet days (95 P) at Niamey airport with MPI - M - REMO

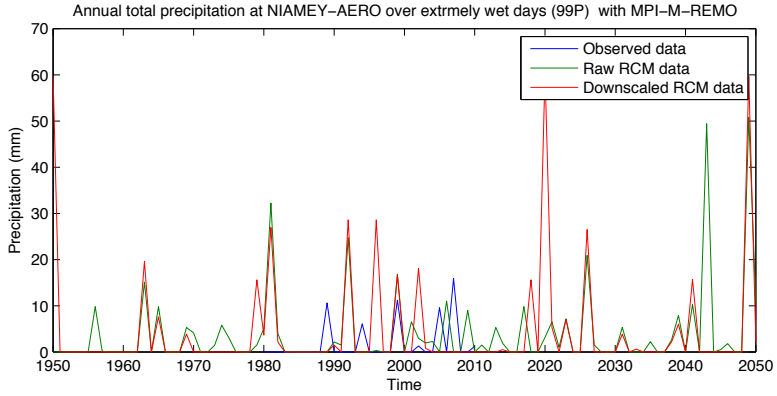

Figure 127 - Annual total precipitation over extremely wet days (99 P) at Niamey airport with MPI - M - REMO

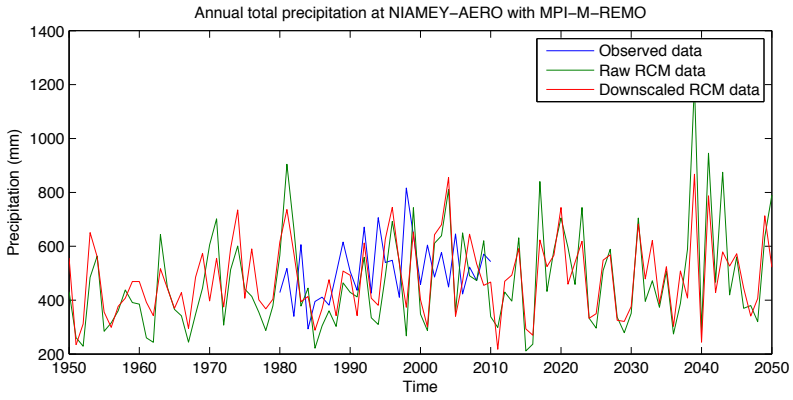

Figure 128 - Annual total precipitation at Niamey airport with MPI - M - REMO

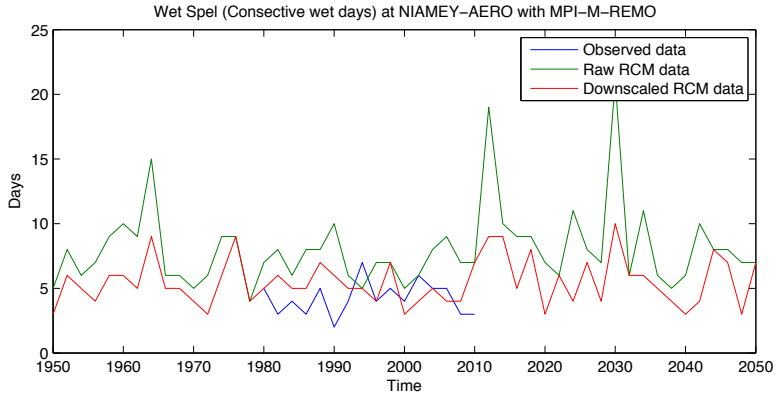

Figure 129 - Wet spell (consecutive wet days) at Niamey airport with MPI - M - REMO

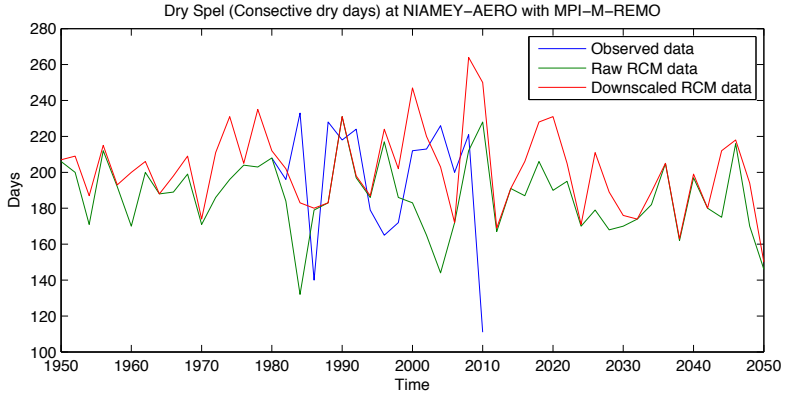

Figure 130 - Dry spell (consecutive dry days) at Niamey airport with MPI - M - REMO

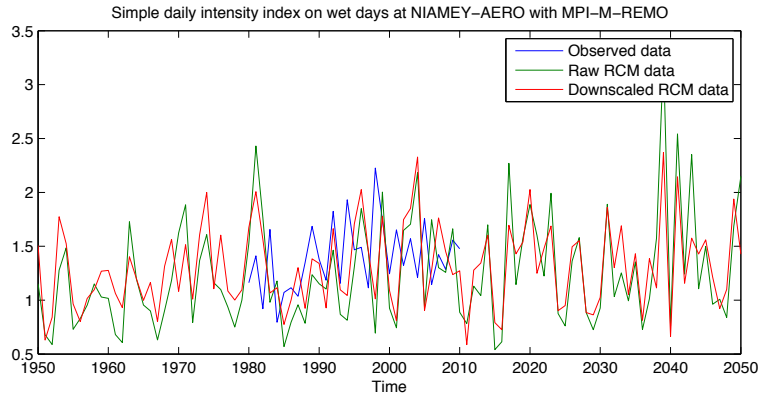

Figure 131 - Simple daily intensity index on wet days at Niamey airport with MPI - M - REMO

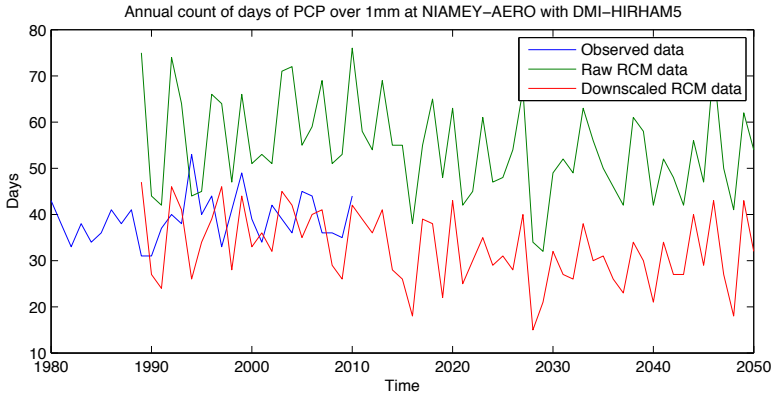

Figure 132 - Annual count of days of precipitation over 1mm at Niamey airport with DMI - HIRHAM 5

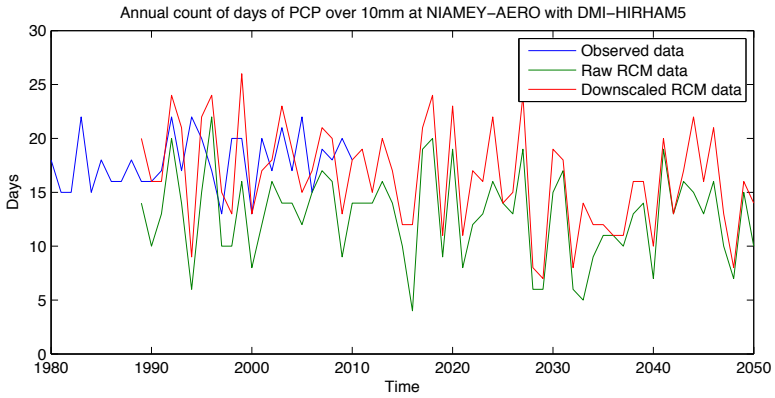

Figure 133 - Annual count of days of precipitation over 10mm at Niamey airport with DMI - HIRHAM 5

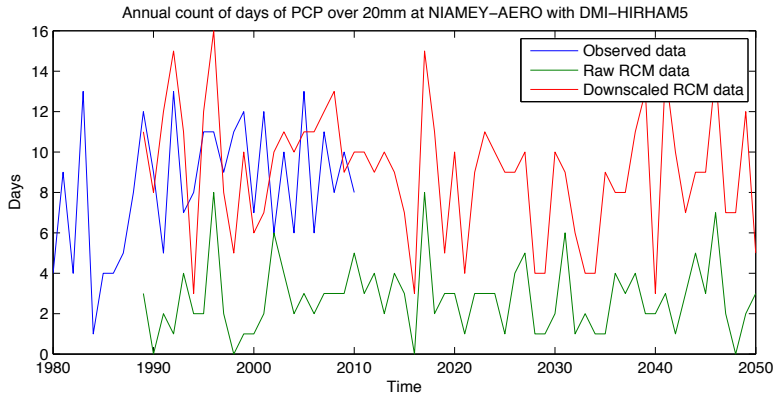

Figure 134 - Annual count of days of precipitation over 20mm at Niamey airport with DMI - HIRHAM 5

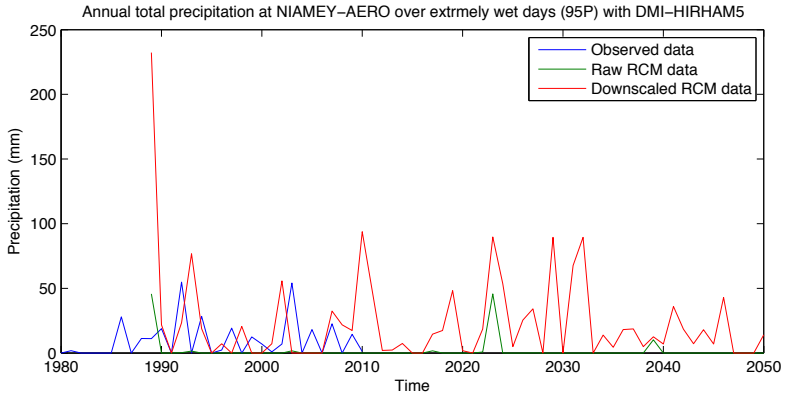

Figure 135 - Annual total precipitation over extremely wet days (95 P) at Niamey airport with DMI - HIRHAM 5

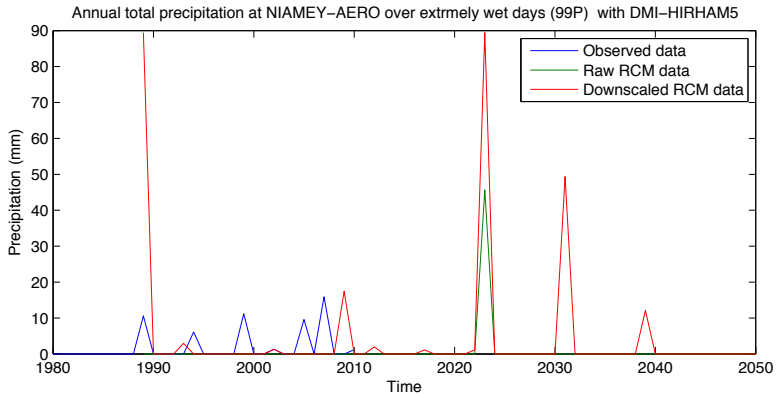

Figure 136 - Annual total precipitation over extremely wet days (99 P) at Niamey airport with DMI - HIRHAM 5

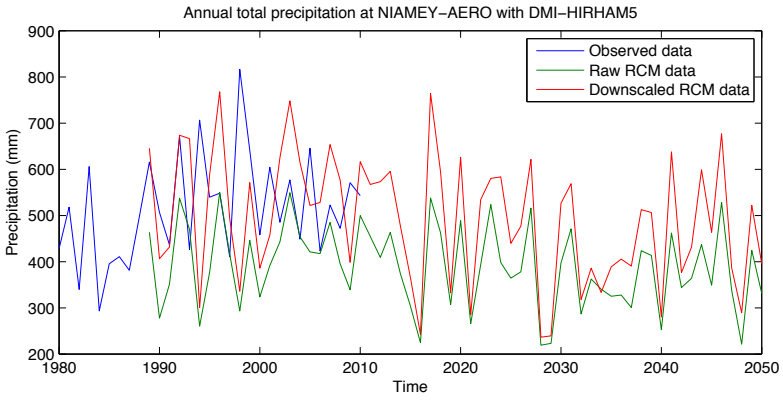

Figure 137 - Annual total precipitation at Niamey airport with DMI - HIRHAM 5

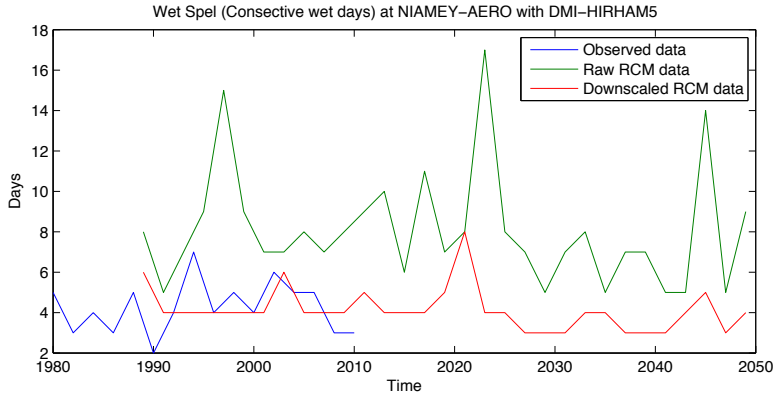

Figure 138 - Wet spell (consecutive wet days) at Niamey airport with DMI - HIRHAM 5

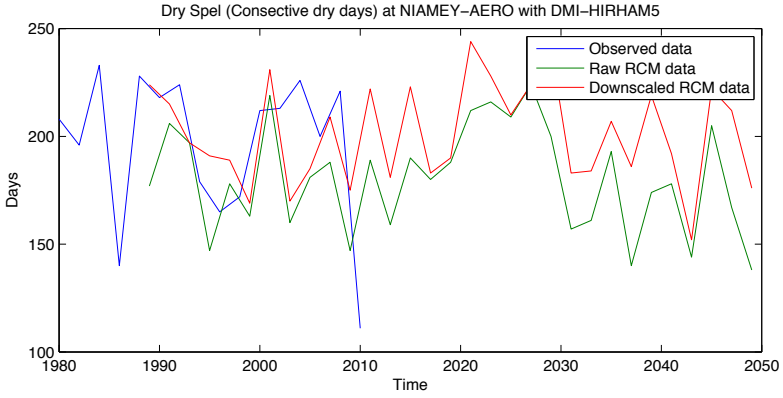

Figure 139 - Dry spell (consecutive dry days) at Niamey airport with DMI - HIRHAM 5

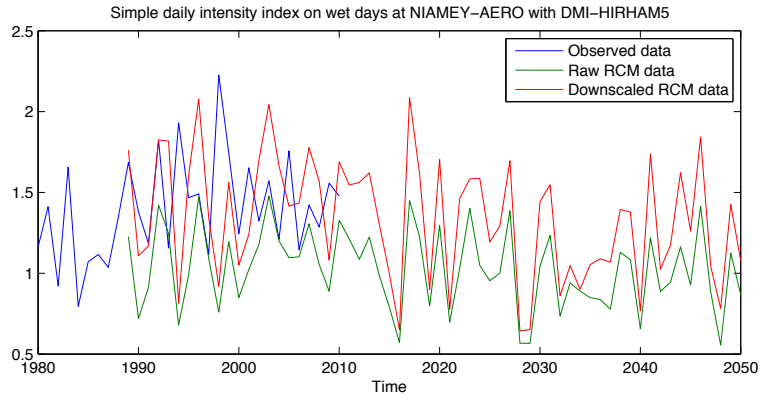

Figure 140 - Simple daily intensity index on wet days at Niamey airport with DMI - HIRHAM 5

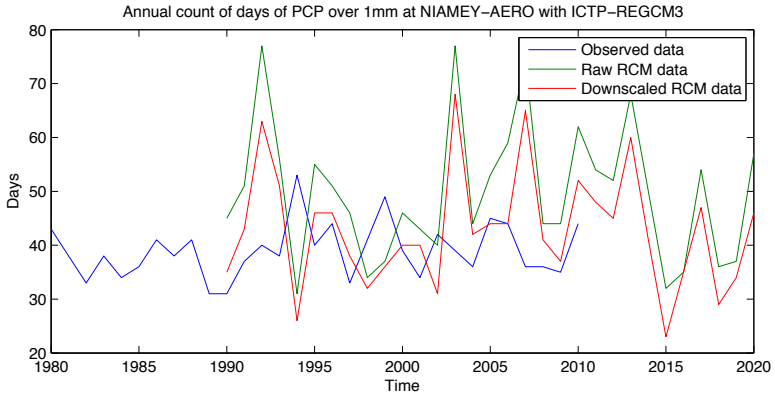

Figure 141 - Annual count of days of precipitation over 1mm at Niamey airport with ICTP - REGCM 3

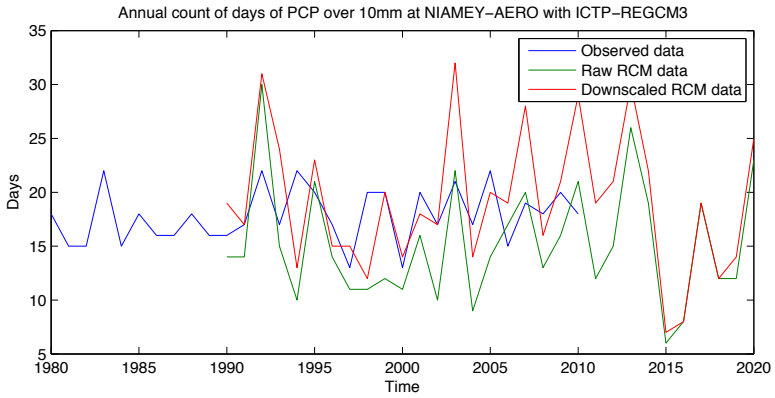

Figure 142 - Annual count of days of precipitation over 10mm at Niamey airport with ICTP - REGCM 3

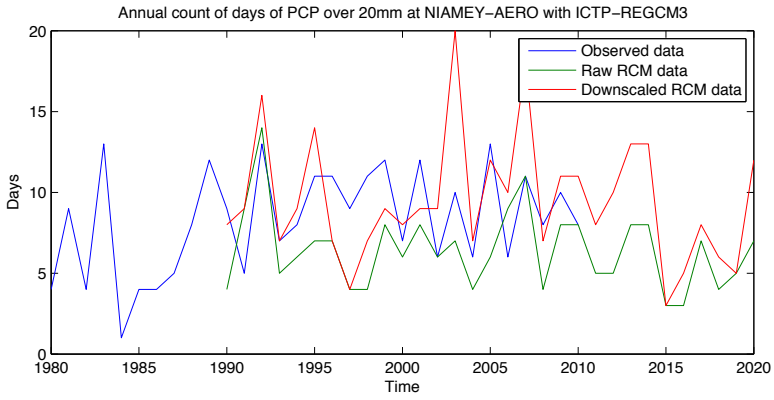

Figure 143 - Annual count of days of precipitation over 20mm at Niamey airport with ICTP - REGCM 3

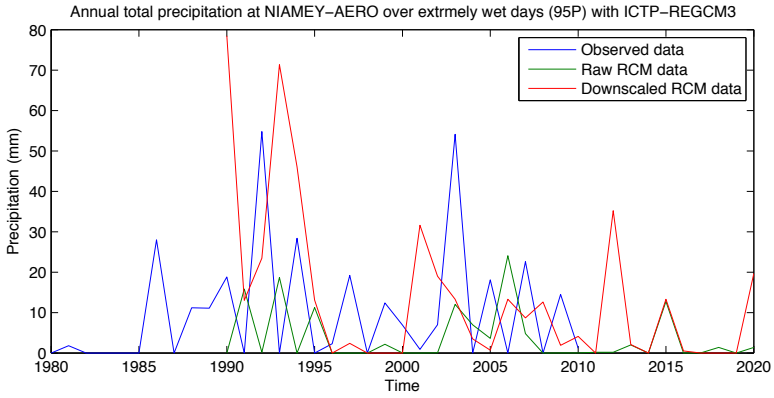

Figure 144 - Annual total precipitation over extremely wet days (95 P) at Niamey airport with ICTP - REGCM 3

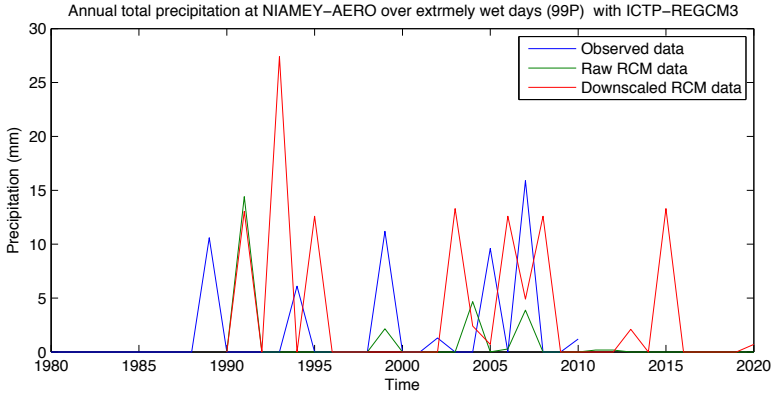

Figure 145 - Annual total precipitation over extremely wet days (99 P) at Niamey airport with ICTP - REGCM 3

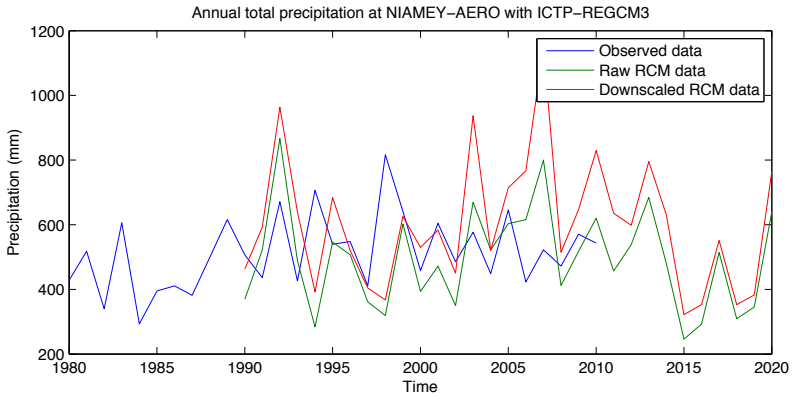

Figure 146 - Annual total precipitation at Niamey airport with ICTP - REGCM 3

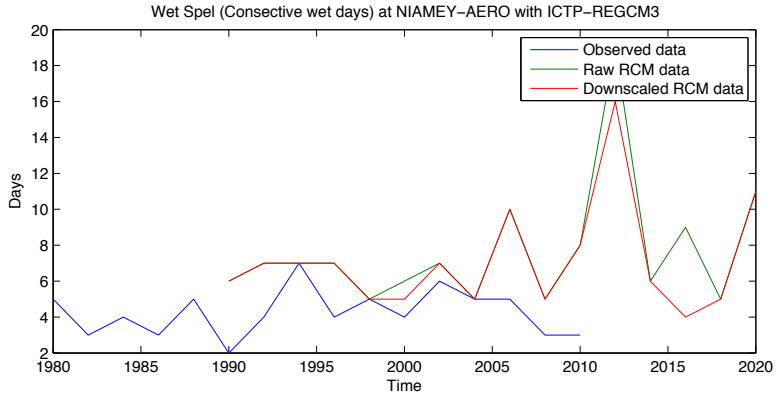

Figure 147 - Wet spell (consecutive wet days) at Niamey airport with ICTP - REGCM 3

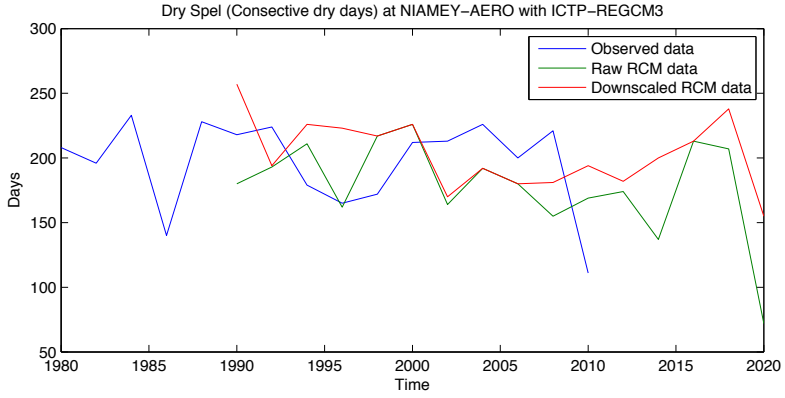

Figure 148 - Dry spell (consecutive dry days) at Niamey airport with ICTP - REGCM 3

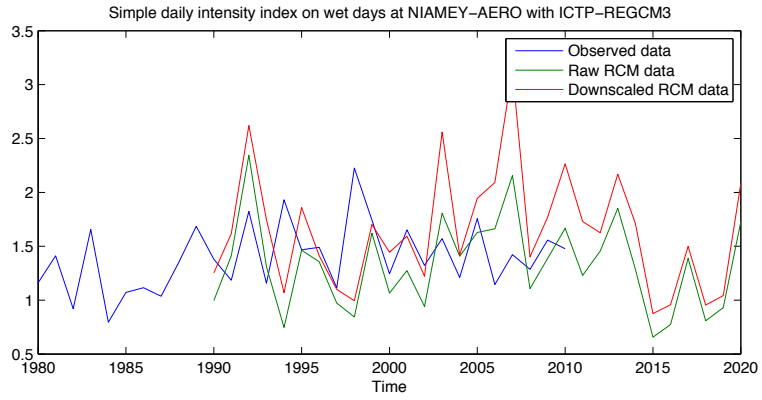

Figure 149 - Simple daily intensity index on wet days at Niamey airport with ICTP - REGCM 3

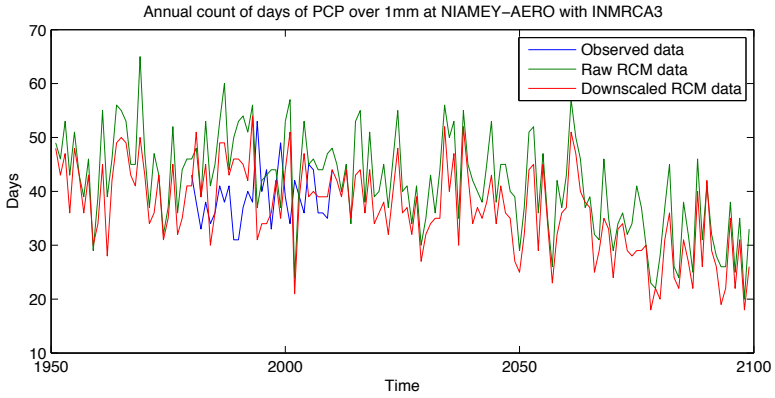

Figure 150 - Annual count of days of precipitation over 1mm at Niamey airport with INMRCA 3

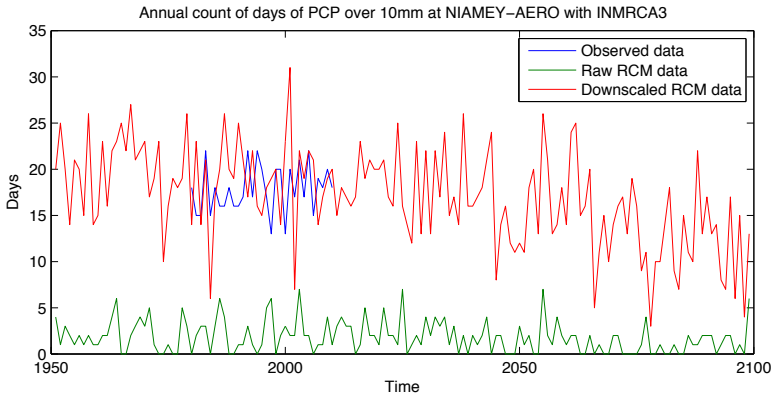

Figure 151 - Annual count of days of precipitation over 10mm at Niamey airport with INMRCA 3

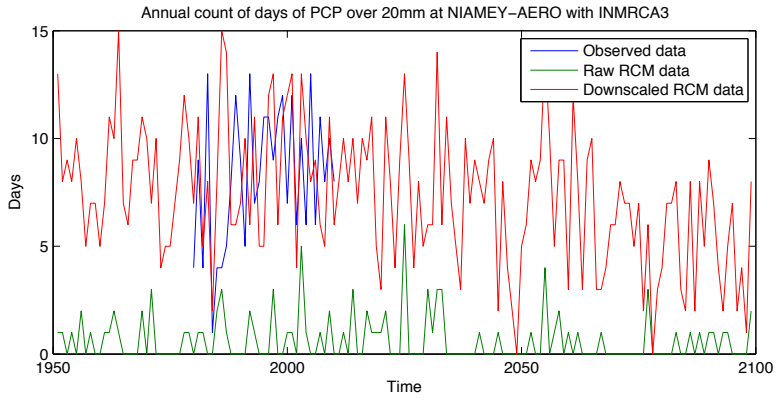

Figure 152 - Annual count of days of precipitation over 20mm at Niamey airport with INMRCA 3

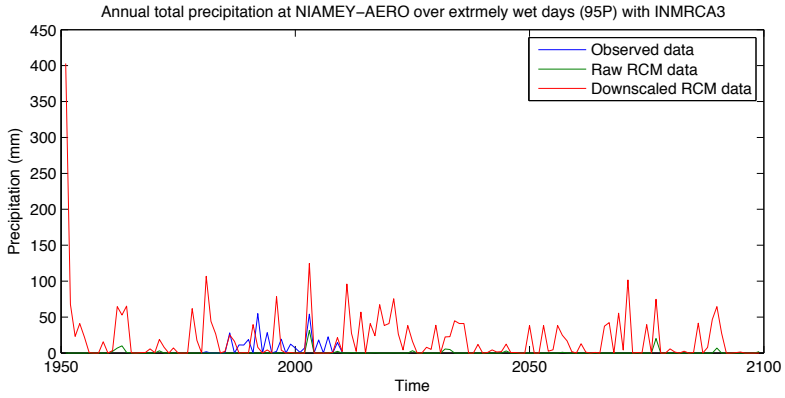

Figure 153 - Annual total precipitation over extremely wet days (95 P) at Niamey airport with INMRCA 3

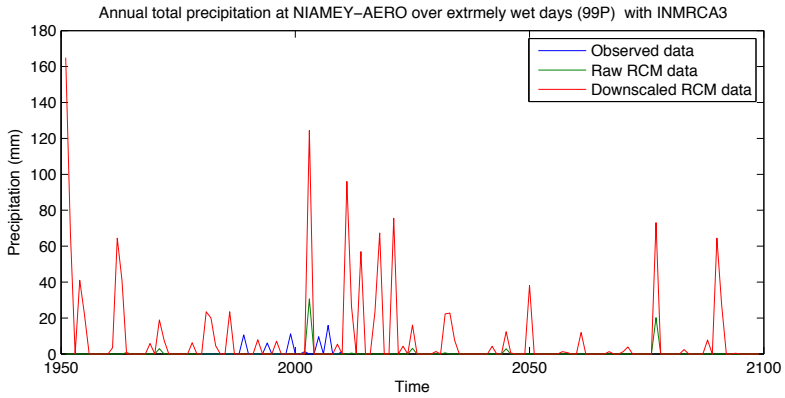

Figure 154 - Annual total precipitation over extremely days (99 P) at Niamey airport with INMRCA 3

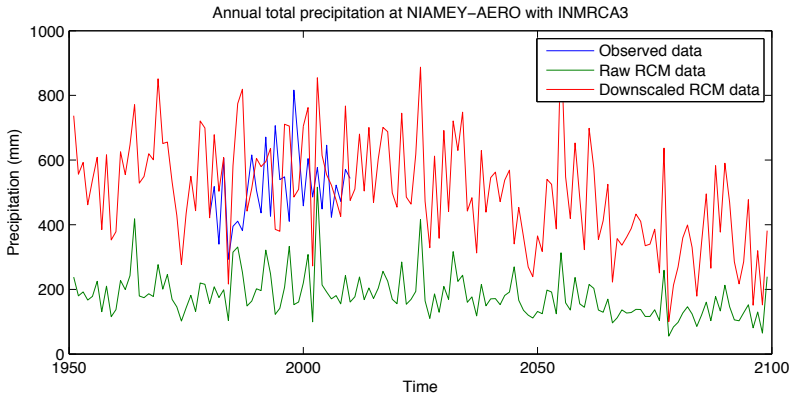

Figure 155 - Annual total precipitation at Niamey airport with INMRCA 3

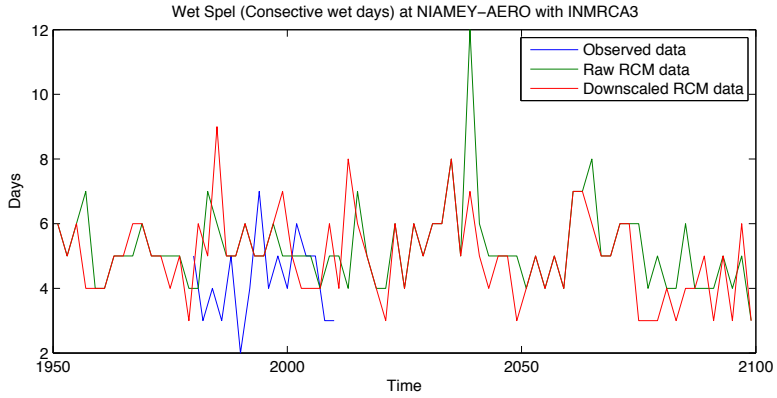

Figure 156 - Wet spell (consecutive wet days) at Niamey airport with INMRCA 3

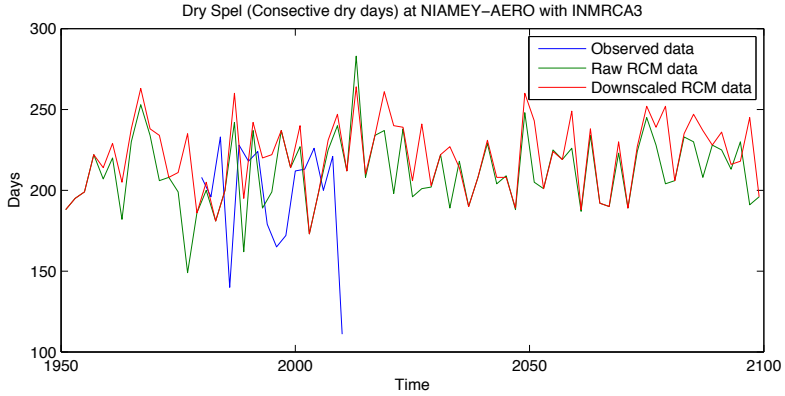

Figure 157 - Dry spell (consecutive dry days) at Niamey airport with INMRCA 3

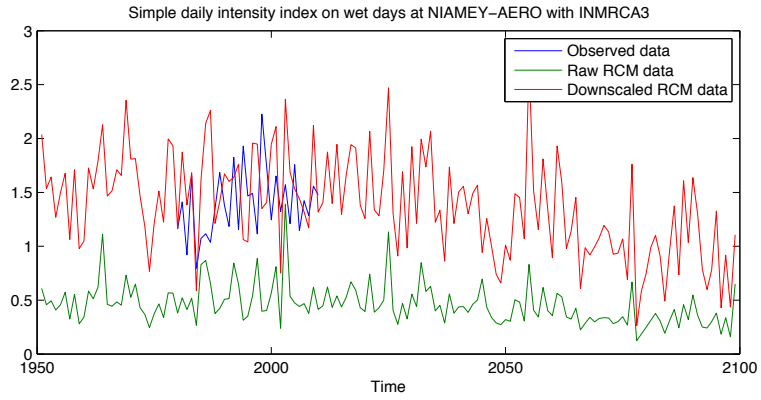

Figure 158 - Simple daily intensity index on wet days at Niamey airport with INMRCA 3

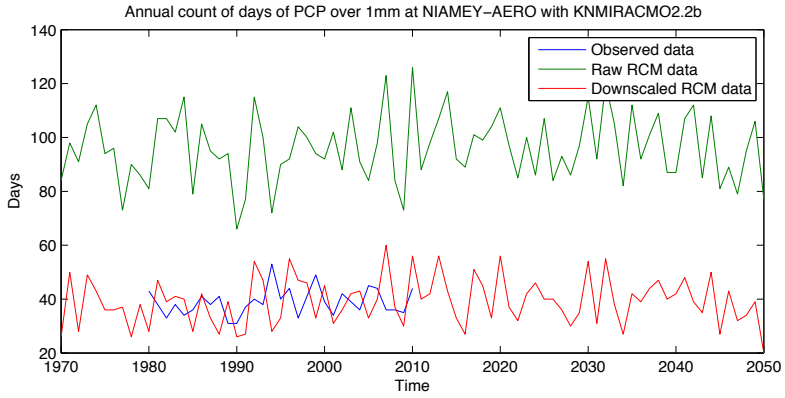

Figure 159 - Annual count of days of precipitation over 1mm at Niamey airport with KNMIRACM 02.2b

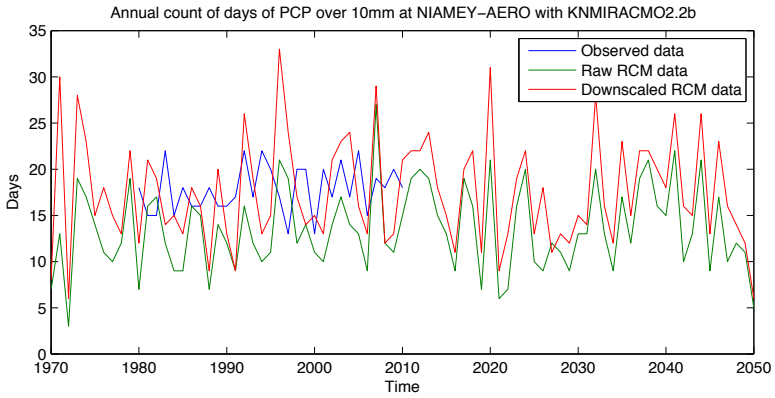

Figure 160 - Annual count of days of precipitation over 10mm at Niamey airport with KNMIRACM 02.2b

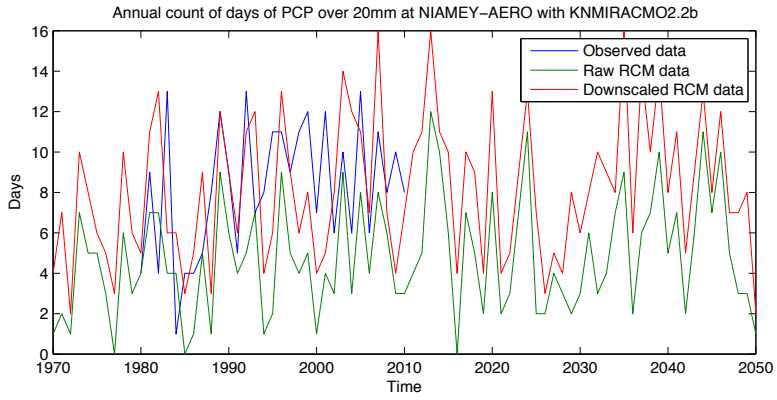

Figure 161 - Annual count of days of precipitation over 20mm at Niamey airport with KNMIRACM 02.2b

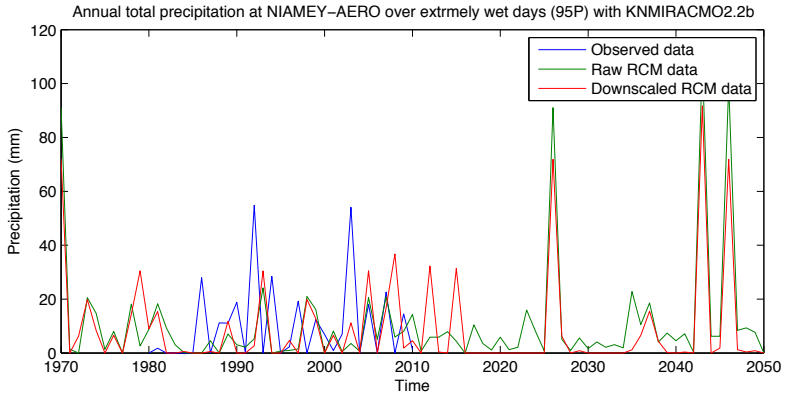

Figure 162 - Annual total precipitation over extremely wet days (95 P) at Niamey airport with KNMIRACM 02.2b

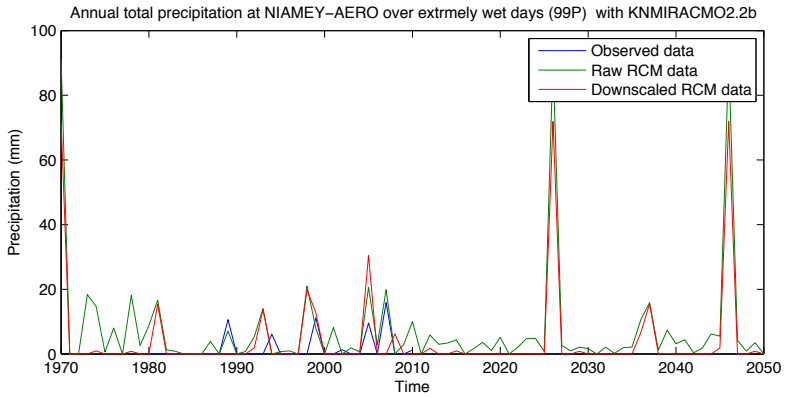

Figure 163 - Annual total precipitation over extremely wet days (99 P) at Niamey airport with KNMIRACM 02.2b

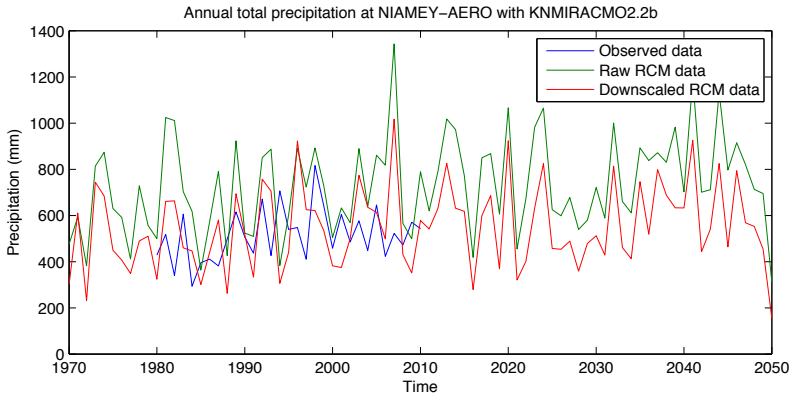

Figure 164 - Annual total precipitation at Niamey airport with KNMIRACM 02.2b

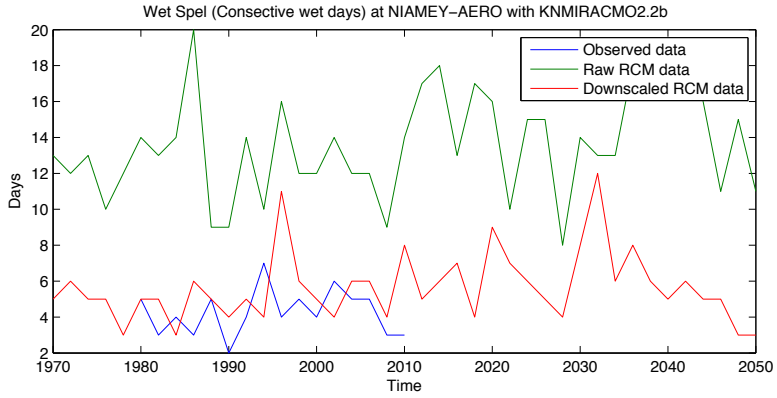

Figure 165 - Wet spell (consecutive wet days) at Niamey airport with KNMIRACM 02.2b

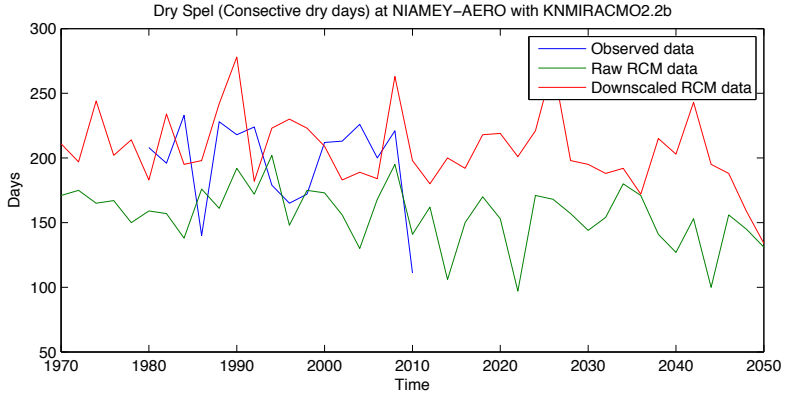

Figure 166 - Dry spell (consecutive dry days) at Niamey airport with KNMIRACM 02.2b

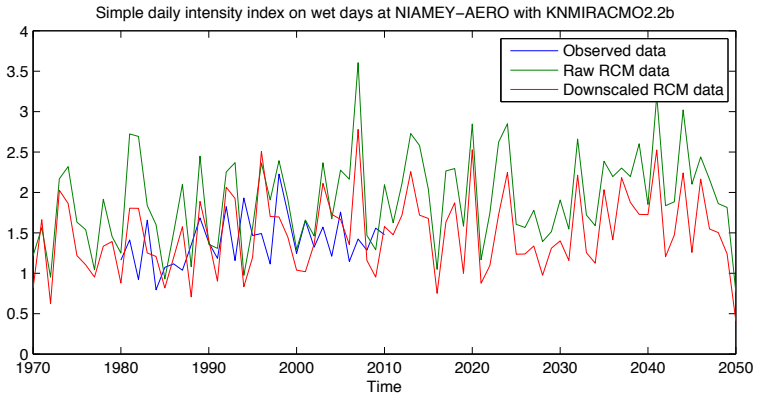

Figure 167 - Simple daily intensity index on wet days at Niamey airport with KNMIRACM 02.2b

6.5.5 Effects of calibration period selection approach on performance

As stated earlier, the Quantile-Quantile downscaling technique is sensitive to the quality and quantity of observed historical data used to calibrate. As such, emphasize is given here to the approach applied for calibration. There are essentially two major families of calibration techniques for statistical downscaling.

The first entails segregating two distinct time periods for calibration and validation. Consequently, the absence of chronological overlap between the two periods will ultimately yield a validation of the downscaling performance on a time period that is chronologically independent from that of the calibration. Though this approach has merit in terms of establishing apparent confidence in the performance of the downscaling technique to predict climate in future time spans, it may be presented with limitations. Namely, the calibration of the Quantile-Quantile map will be restricted to the range of climate range only present in the calibration period. For example, the historical observations of the climate in Niamey indicate that the region recovered from a period of drought in the first portions of the obtained data's time span. If one were to choose to calibrate on the latter period, although able to reproduce statistical properties,

the Quantile-Quantile map would be limited in terms of capturing characteristics of a wet climate in a predicted future.

The second entails allocating two sets of time periods to both calibration and validation that are not necessarily chronologically independent. This approach allows for the calibration to span over the entire observed time span that is available. While this approach does not provide the apparent performance confidence the former approach may be able to, it permits the Quantile-Quantile map to be drawn on a greater spectrum of climate range.

The question of calibration approach is one that deserves its own study. The approach that seeks to use intercalated time spans for calibration and validation has been applied in this Thesis. Every second data point has been allocated to calibration and hence leaving the remainder half of the observed data for validation. Nonetheless, the former approach was applied for precipitation as well as minimum and maximum daily temperatures on two arbitrarily selected regional climate model outputs for comparison sake – CHMIALADIN, DMI-HIRHAM5 and INMRCA3.

As expected, the Quantile-Quantile downscaling approach is able to improve the agreement between observed and climate model simulation outputs regardless of the calibration approach. This is confirmed with visual evaluations of the various plots including: monthly distributions, binary probability scoring, monthly and annual plots as well as extreme event indices. The numerical results of the two-sample variant of the KS test also corroborate the latter conclusion. Moreover, the results are indicative that the approach applied in the Thesis yields better result. Higher agreement is noted between observed and downscaled climate data in 60% of the cases when calibrating on intercalated time slots as compared to the chronologically distinct approach. The comparison results are illustrated in Table 8 below where p values from KS test on the respective validation period after downscaling is applied.

Table 8 – Two sample KS test results (p-values) - evaluation of different calibration approaches on the validation period

Models	Variable	Cal. / Val. approach	Jan	Feb	Mar	Apr	May	Jun	Jul	Aug	Sep	Oct	Nov	Dec
CHMIALADIN	Daily precipitation	Intercalated	100.0%	100.0%	100.0%	100.0%	100.0%	100.0%	2.8%	15.1%	50.4%	100.0%	100.0%	100.0%
		Segregated	100.0%	100.0%	100.0%	100.0%	87.7%	49.4%	3.8%	3.8%	99.5%	100.0%	100.0%	100.0%
	Max. Daily Temperature	Intercalated	0.0%	0.5%	15.1%	0.1%	0.0%	70.9%	0.0%	25.5%	1.9%	0.0%	0.0%	0.4%
		Segregated	0.0%	0.0%	0.0%	25.1%	0.0%	8.9%	0.0%	0.0%	0.6%	0.0%	0.0%	0.0%
	Min. Daily Temperature	Intercalated	0.0%	1.5%	34.8%	0.2%	0.0%	0.9%	0.0%	0.3%	0.4%	0.1%	0.0%	0.0%
		Segregated	0.0%	0.0%	0.0%	42.5%	0.0%	1.4%	0.0%	0.0%	2.5%	0.1%	0.0%	0.1%
DMI-HIRHAM5	Daily precipitation	Intercalated	100.0%	100.0%	100.0%	100.0%	93.1%	33.5%	30.7%	19.2%	95.6%	96.2%	100.0%	100.0%
		Segregated	100.0%	100.0%	100.0%	100.0%	66.5%	50.1%	91.6%	66.5%	78.8%	100.0%	100.0%	100.0%
	Max. Daily Temperature	Intercalated	9.4%	0.0%	0.0%	0.4%	1.7%	38.7%	0.1%	0.3%	0.3%	0.0%	0.0%	6.1%
		Segregated	7.6%	0.0%	1.0%	0.1%	7.4%	71.8%	1.0%	0.3%	8.1%	0.8%	1.9%	2.2%
	Min. Daily Temperature	Intercalated	5.1%	0.0%	0.0%	0.0%	5.1%	0.3%	0.0%	0.0%	0.3%	0.0%	0.0%	22.1%
		Segregated	0.1%	0.0%	39.4%	31.9%	1.0%	22.6%	9.2%	11.3%	0.6%	0.0%	0.6%	1.0%
INMRCA3	Daily precipitation	Intercalated	100.0%	100.0%	100.0%	100.0%	77.3%	75.5%	22.9%	15.9%	56.9%	86.9%	100.0%	100.0%
		Segregated	100.0%	100.0%	100.0%	100.0%	97.2%	2.0%	43.5%	3.3%	0.6%	100.0%	100.0%	100.0%
	Max. Daily Temperature	Intercalated	1.3%	1.0%	0.2%	0.1%	0.1%	0.3%	0.6%	40.1%	0.9%	3.4%	0.6%	0.2%
		Segregated	0.0%	0.0%	23.7%	0.6%	2.8%	0.0%	11.8%	0.0%	0.0%	0.0%	2.1%	0.0%
	Min. Daily Temperature	Intercalated	3.5%	0.4%	0.0%	5.8%	0.0%	1.7%	1.7%	10.0%	5.8%	5.0%	0.4%	0.0%
		Segregated	14.2%	1.1%	0.0%	0.5%	0.0%	0.8%	0.0%	0.0%	0.1%	0.0%	0.0%	7.0%

6.6 Conclusion

The graphical illustrations of the probability density functions confirm the stipulation that the Quantile-Quantile downscaling approach indeed matches probability distributions; the probability density functions for the calibration period indicate quasi-complete agreement between observed and modeled data sets once subjected to Quantile-Quantile downscaling for all climate variables. A more interesting observation is perhaps the ability of the Quantile-Quantile method to influence probability distributions on the validation period; which is presumed to be an independent portion of the data set. Downscaled outputs of the regional climate models have seen their monthly distribution modified such that their mean and spread match those of the observed historical data sets. Moreover, we can notice that the downscaling method used is able

to match percentiles; i.e. count of wet days (precipitation over 1 mm), heavy precipitation days (over 10 mm) and very heavy precipitation days (over 20 mm) is maintained through the Quantile-Quantile downscaling process. Similarly, we can observe that climate indices such as dry and wet spells are conserved (count of consecutive days no precipitation and with precipitation, respectively).

Chapter 7. THE WEB PORTAL: AN INTERFACE FOR CLIMATE CHANGE DATA DISSEMINATION

Web based systems provide entry to climate change associated information for a broad variety of end-users. The particular complexity associated with climate change information in the actual development of user-friendly applications remains a challenge (Lawrence et al., 2005; Stephens et al., 2012; Woolf, Haines, & Liu, 2003). Thus, an end-user requires appropriate web-based interface for easy access to climate change data. A major challenge for climate data web-interface revolves around accessibility (Reusser et al., 2011; Wrobel & Reusser, 2012).

Although, monthly downscaled data are available to the general public (Tabor & Williams, 2010), a challenge remains in providing access to daily downscaled data. Moreover, the volume of GCM data scattered over the net is overwhelming on its own. IPCC initiatives such as the Coupled Model Intercomparison Project (CMIP)for example are putting forth close to two petabytes of GCM data each. It is imperative to bridge the gap between the available GCM output data and the required location scale daily climate change information.

Another major drawback identified with existing climate change data sets is their one-dimensional nature: a dominant portion of the available data is merely presented as mean temperature increase or possibilities of drought and flood misfortunes. This matter in particular is hindering to most climate change impact evaluators in different sectors who are non-specialists. As identified earlier in the present thesis, different end-users of climate change data require the information be presented to them in specific manners with well-defined metrics. Visual representations and seasonal pattern identifications coupled with meaningful climate indicators including temporal distribution and extreme climate indices are fundamental.

To allow ease of portability, the web-based interface was implemented as a standalone application that require very minimal effort for configuration. The downloadable lightweight application remotely accesses the database housing the downscaled climate data. The database is built using Oracle MySQL technology. The data portal's main goal is to offer readily available climate change projections as well as analysis tools in a format suitable for end-use for impact assessment across various sectors.

The *Daily Climate Change Data Portal* application comprises of three main components: it offers visual representation of daily climate data; it also provides impact assessment tools and features the ability to allow users to download daily climate data for the station of their choosing. Figure 168 below is the main window of the *Daily Climate Change Data Portal* where the user may select a combination desired climate station, variable and regional climate model.

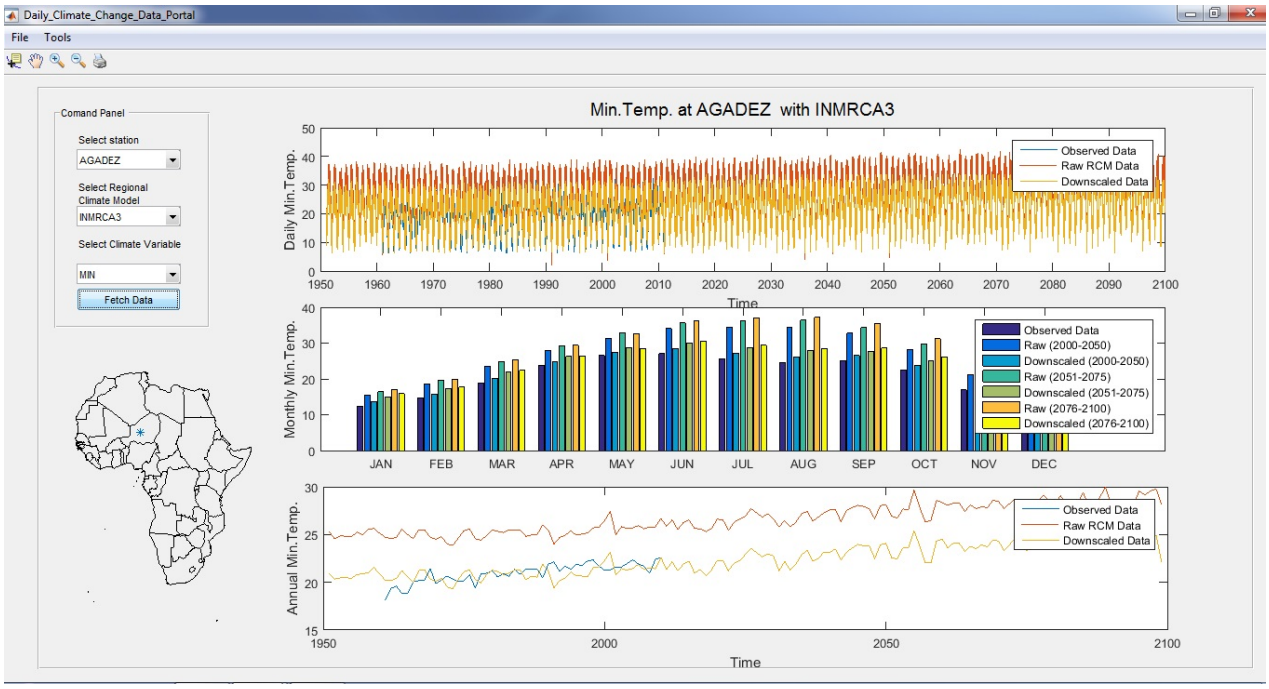

Figure 168 – The Web Portal for downscaled Daily Climate Change Data

The leading climate change information of this project is daily climate variable data downscaled to a specific location. The list of climate variables incorporated includes:

- Daily total precipitating in millimeters (mm);
- Daily maximum temperature in degree Celsius (^{o}C);
- Daily minimum temperature in degree Celsius (^{o}C);
- Daily relative humidity in percentage (%);
- Daily relative wind speed in meters per second (m/s);
- Daily solar radiation in Watts per square meter (W/m^{2});

Figure 169 below is a sample illustration of multiple climate model plots. It features daily minimum temperature values from historic observations at Agadez, Niger and downscaled outputs from the regional climate models at the daily, monthly and annual scales.

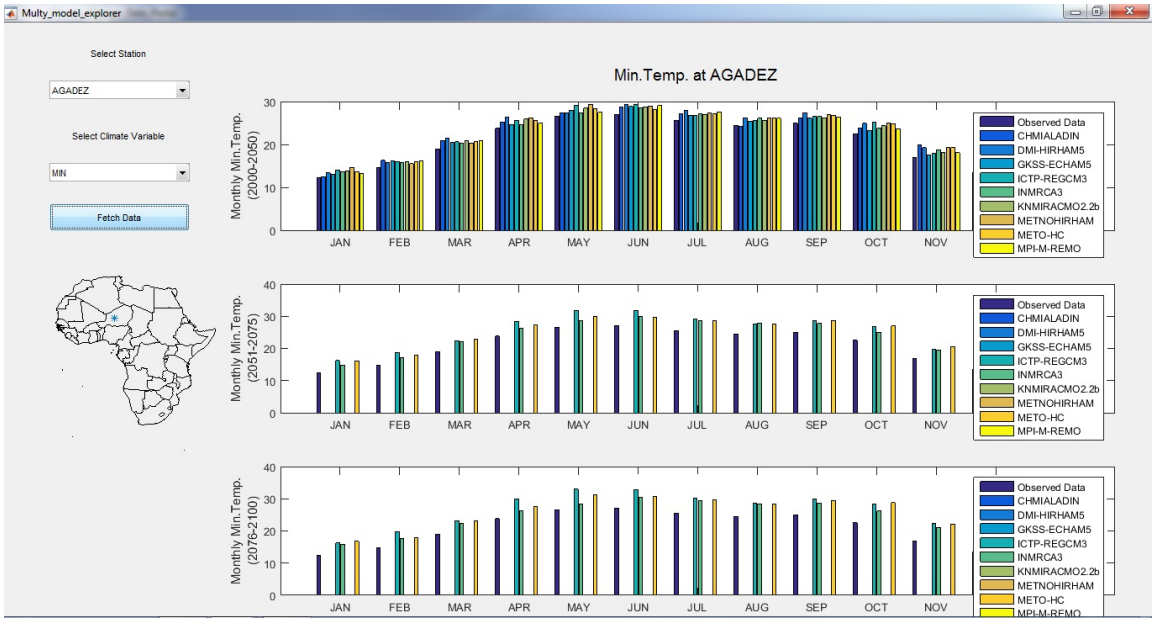

Figure 169 - Web Portal – Multi-model plot

Sample illustrations of monthly probability distribution plots and are shown in Figure 170 below.

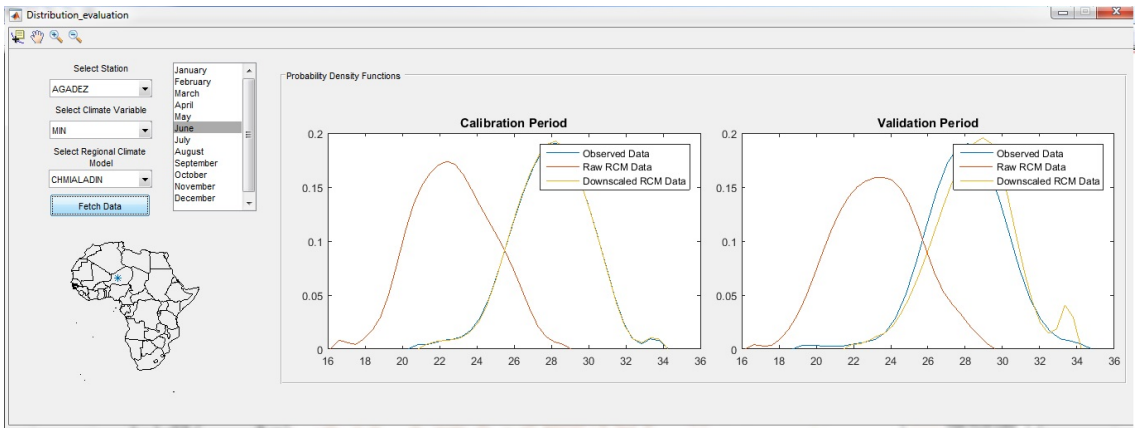

Figure 170 - Web Portal - Annual Mean plot

Figure 171 below illustrates the extreme climate event indices calculator that is offered with the data portal. This tools allows the end-user to compute indices for extreme events for a large number of scenarios by varying the given parameters.

Figure 171 - Web Portal – Extreme climate event indices calculator

The *Daily Climate Change Data Portal* enables users to perform probability distribution analysis for each of the climate variables listed above. The user has also the ability to compare and contrast distribution characteristics between historical observations of climate variables and their

simulated future. Perhaps one of the most valuable aspects of the *Daily Climate Change Data Portal* is the comparisons offered over the calibration and validation periods. This allows the end-user to put the downscaled outputs to test and evaluate them based on standards expected for a given sectorial impact assessment. Moreover, outputs from multiple regional climate models are downscaled and made available for each station to allow for a broader perspective that encompasses various plausible scenarios for our climate's future.

The *Daily Climate Change Data Portal* hopes to alleviate the burden of downscaling coarse climate change data and allow for improved impact assessment efforts across all sectors. Notably, we expect studies from various fields to yield coherent results and collectively present viable solutions. It is vital that policy makers have scientific and reliable information before they reach decisions and enact policies. Our goal is to have a better collective ability to deal with the ever-pressing issue that is climate change and plan to adapt to it. The *Daily Climate Change Data Portal* is available for download from http://daily-climatechangedata.com – a website dedicated for the dissemination of research outputs from this thesis.

Chapter 8. CONCLUSIONS

The limited amount of quality data available to end-users is a crucial problem nowadays, and the use of web-based interface in climate impact assessment can help deal with it. In this thesis, a user-friendly interactive web-based interface with multiple functionalities such as capacity to process information, capacity to search, sort, retrieve and filter data and download features is presented. It enables users to manipulate data and access climate change data for multiples seasons.

The Quantile-Quantile approach is used to downscale outputs from regional climate models of the AMMA-Ensemble; results from the downscaling effort have proven to be satisfactory when measured against the set performance evaluation metrics. Different temporal scales namely daily, monthly and yearly graphs of model simulations are accessible to end-users. Additionally, downscaled data sets can be downloaded by end-users. Furthermore, impact assessment tools such as monthly probability distributions as well as binary probability scoring for precipitation occurrence are made available. Finally, extreme climate indices from the ETCCDI are also explored.

As aforementioned, access to daily climate data is compelling to the general public; nonetheless handling climate and environmental data across networks can be a daunting task. Securing a universal solution to climatic change data can thus be a challenge (Woolf et al., 2003). Climate change data is prone to frequent changes (Court, 1957) and, therefore, need a dynamic web-based interface (Fitz-Rodríguez et al., 2010). Real time processing by streaming data directly along with model comparison can be a significant tool in impact analysis (Pantelimon, Pop, & Cristea, 2007). Consequently, climatic web interfaces should be implemented with a robust

scalable architecture. It is hence of the author's opinion that the survival and evolution of this initiative and others like it is crucial to the global need for adjusting to climate change.

BIBLIOGRAPHY

Abrate, T., Hubert, P., & Sighomnou, D. (2013). A study on hydrological series of the Niger River. *Hydrological Sciences Journal* .

Adeleke, O., & Otoo, E. J. (2013). An integrated metadata access infrastructure for a network of federated curated data repositories. *Integrated metadata access infrastructure* .

Amhed, K. F., Wang, G., Silander, J., Wilson, A. M., Allen, J. M., Horton, R., et al. (2013). Statistical downscaling and bias correction of climate model outputs for climate change impact assessment in the U.S. northeast. *Global and Planetary Change* (100), 320-332.

Arnell, N. W. (1999). Climate change and global water resources. *Global Environmental Change* , 31-49.

Beatty, T., & Shmishack, J. P. (2013). The Impact of Climate Change Information: New Evidence from the Stock Market. *The B.E. Journal of Economic Analysis & Policy , 10* (1).

Bessou, C., Ferchaud, F., Gabrielle, B., & Mary, B. (2011). Biofuels, greenhouse gases and climate change. A review. *Agrin. Sustain* .

Boucher, M., Favreau, G., Descloitres, M., Voullamoz, J.-M., Massuel, S., Nazoumou, Y., et al. (2009). Contribution of geophysical surveys to groundwater modelling of a porous aquifer in semiarid Niger: An overview. *Science Direct* , 800-809.

Boyer, C., Chaumont, D., Chartier, I., & Roy, A. G. (2010). Impact of climate change on the hydrology of St. Lawrence tributaries. *Journal of Hydrology* (384), 65-83.

Cappelaere, B., Descroix, L., Lebel, T., Boulain, N., Ramier, D., Laurent, J.-P., et al. (2009). The AMMA-CATCH experiment in the cultivated Sahelian area of south-west Niger – Investigating

water cycle response to a fluctuating climate and changing environment. *Journal of Hydrology* (375), 34-51.

Ceren Onur, A., & Tezer, A. (2015). Ecosystem services based spatial planning decision making for adaptation to climate changes. *Habitat International* (47), 267-278.

Change, I. P. (2000). *SUmmary for Policymakers - Emissions Scenarios.* IPCC, Working group III.

Chen, J., Brissette, F. P., & Leconte, R. (2012). Coupling statistical and dynamical methods for spatial downscaling of precipitation. *Climatic Change* (114), 509-526.

Chen, J., Brissette, F. P., & Leconte, R. (2011). Uncertainty of downscaling method in quantifying the impact of climate change on hydrology. *Journal of Hydrology* (401), 190-202.

Chen, J., Brissette, F. P., Chaumont, D., & Braun, M. (2013). Performance and uncertainty evaluation of empirical downscaling methods in quantifying the climate change impacts on hydrology over two North American river basins. *Journal of Hydrology* (479), 200-214.

Cheneau-Loquay, A. (2007). From networks to uses patterns: the digital divide as seen from Africa. *GeoJournal* (68), 55-70.

Chilingar, G. V., Sorokhtin, O. G., Khilyuk, L., & Gorfunkel, M. V. (2009). Greenhouse gases and greenhouse effect. *Environ Geol* (58), 1207-1213.

Danuor, S., Gaye, A., Yacouba, H., Mariko, A., Bouzou, M. I., Maiga, M. M., et al. (2011). Education in meteorology and climate sciences in West Africa. *Atmospheric Science Letters* , 155-159.

DeFries, R., Achard, F., Brown, S., Herold, M., Murdiyarso, D., Schlamadinger, B., et al. (2007). Earth observations for estimating greenhouse gas emissions from deforestation in developing countries. *Environmnetal Science and Policy* , 385-394.

Delire, C., Ngomanda, A., & Jolly, D. (2008). Possible impacts of 21st century climate on vegetation in Central and West Africa. *Global and Planetary Chnage* (64), 3-15.

Descroix, L., Genthon, P., Amogu, O., Rajot, J.-L., Sighomnou, D., & Vauclin, M. (2012). Change in Sahelian Rivers hydrograph: The case of recent red floods of the Niger River in the Niamey region. *Global Planetary Change* .

Dixon, G. R. (2012). Climate change – impact on crop growth and food production, and plant pathogens.

Dufersne, J.-L., & et. al. (2013). Climate change projections using the IPSL-CM5 Earth System Model: from CMIP3 to CMIP5. *Clim Dyn* , 2123-2165.

Estrada, F., Guerrero, V. M., Gay-Garcia, C., & Martinez-Lopez, B. (2013). A cautionary note on automated statistical downscaling methods for climate change. *Climatic Change* (120), 263-276.

Evangelista, P., Young, N., & Burnett, J. (2013). How will climate change spatially affect agriculture production in Ethiopia? Case studies of important cereal crops. *Climatic Change* , 855-873.

Ficket, A. D., Myrick, C. A., & Hansen, L. J. (2007). Potential impacts of global climate change on freshwater fisheries. 581-613.

Ford, M. D. (2007). Technologizing Africa: On the bumpy information highway. *Science Direct* (24), 302-316.

Fowler, H. J., Blenkinshop, S., & Tebaldi, C. (2007). Linking climate change modelling to impacts studies: recent advances in downscaling techniques for hydrological modelling. *International Journal of Climatology* (27), 1547-1578.

Froster, P., & Ramasamy, V. (2007). Changes in Atmospheric Constituents and Radiative Forcing. In *he Physical Science Basis. Contribution of Working Group I to the Fourth Assessment Report of the Intergovernmental Panel on Climate Change* . Cambrige, UK.

Gibbs, H. K., & Herold, M. (2007). Tropical deforestation and greenhouse gas emissions. *Enviromental research Letters* .

Gudmundsson, L., Bremnes, J., Haugen, J. E., & Engen-Skaugen, T. (2012). Technical Note: Downscaling RCM precipitation to the station scale using statistical transformations – a comparison of methods. *Hydrology and Earth System Sciences* (16), 3383-3390.

Hathaway, M. E. (2014). Connected Choices: How the Internet Is Challenging Sovereign Decisions. *American Foreign Policy Interests* (36), 300-313.

Hessami, M., Gachon, P., Ouarda, T. B., & St. Hilaire, A. (2008). Automated regression-based statistical downscaling tool. *Science Direct* , 813-834.

Hinson, R. E., & Adjasi, C. K. (2009). The Internet and Export: Some Cross-Country Evidence from Selected African Countries. *Journal of Internet Commerce* (8), 309-324.

Hope Sr, K. R. (2009). Climate change and poverty in Africa. *International Journal of Sustainable Development & World Ecology , 16*, 451-461.

Jorgensen, S. V., Hauschild, M. Z., & Nielsen, P. H. (2014). Assessment of urgent impacts of greenhouse gas emissions—the climate tipping potential (CTP). *Internalional Journal of Cycle Assessment* (19), 919-930.

Kjellsrtrom, T., Butler, A. J., Lucas, R. M., & Bonita, R. (2010). Public health impact of global heating due to climate change: potential effects on chronic non-communicable diseases. *International Journal of Public Health* (55), 97-103.

Koukidis, E. N., & Berg, A. A. (2010). Sensitivity of the Statistical DownScaling Model (SDSM) to reanalysis products. *Atmosphere-Ocean* .

Kysely, J., & Beranova, R. (2009). Climate-change effects on extreme precipitation in central Europe: uncertainties of scenarios based on regional climate models. *Theories of Applied Climatology* (95), 361-374.

Lieberman, D., Jonas, M., & Wniniwater, W. (2007). Accounting for Climate Change: Introduction. *Water Air Soul Pollut: Focus* , 421-424.

Loginov, V. F. (2013). Global and Regional Changes of Climate: Causes, Consequences and Adaptation of the Economic Activities. *Geography and National Resources , 35*, 13-24.

Ly, M., Traore, S. B., Alhassane, A., & Sarr, B. (2013). Evolution of some observed climate extremes in the West African Sahel. *Weather and Climate Extremes* (1), 19-25.

Maguire, M. C. (2013). An analysis of specialist and non-specialist user requirements for geographic climate change information. *Applied Ergonomics* (44), 874-885.

Maraun, D., Wetterhal, F., Ireson, A. M., Chandler, R. E., Kendon, E. J., Windmann, M., et al. (2010). PRECIPITATION DOWNSCALING UNDER CLIMATE CHANGE: RECENT DEVELOPMENTS TO BRIDGE THE GAP BETWEEN DYNAMICAL MODELS AND THE END USER. *Reviews of Geophisics* .

McGregor, G. R. (2011). Human biometeorology.

McKague, D., Zurubchen, T. H., Donjakowski, T., Ervin, J., Heckathorn, D., & Morgan, K. (2009). Imagin Africa: Providing Internet to the Developing World.

Mertz, O., D'haen, S., Maiga, A., Moussa, B. I., Barbier, B., Diouf, A., et al. (2012). Climate Variability and Environmental Stress in the Sudan-Sahel Zone of West Africa.

Mertz, O., Halsnaes, K., & Olsen, J. E. (2009). Adaptation to Climate Change in Developing Countries. *Environmental Managment* (43), 743-752.

Mohamed, A. B. (2011). Climate change risks in Sahelian Africa. *Reg. Envriron. Change* (11), 109-117.

Ngaira, J. W. (2007). Impact of climate change on agriculture in Africa by 2030. *Scientific Research and Essays* , 238-243.

Nissen, K. M., Leckebush, G. C., Pinto, J. G., & Ulbrich, U. (2014). Mediterranean cyclones and windstorms in a changing climate. *Reg. Environ. Change* (14), 1873-1890.

Njau, L. N. (2011). Seasonal-to-Interannual Climate Variability in the Context of Development and Delivery of Science-based Climate Prediction and Information Services Worldwide for the Benefit of Society. *Science Direct* , 411-420.

O'Neill, G. A., Hamann, A., & Wang, T. (2008). Accounting for population variation improves estimates of the impact of climate change on species' growth and distribution. *Journal of Applied Ecology* (45), 1040-1049.

Pegram, G., & Bardossy, A. (2013). Downscaling Regional Circulation Model rainfall to gauge sites using recorrelation and circulation pattern dependent quantile–quantile transforms for quantifying climate change. *Journal of Hydrology* (504), 142-159.

Quadrelli, R., & Peterson, S. (2007). he energy–climate challenge: Recent trends in CO2 emissions from fuel combustion. *Energy Policy* (35), 5938-5953.

Redelsperger, J.-L., Thorncroft, C. D., Diedhiou, A., Lebel, T., Parker, D. K., & Polcher, J. (1973). African Monsoon Multidisplinary Analysis - An International Reaseach Project and field Campaing. *American Meterological Society* .

Reenberg, A., Maman, I., & Oksen, P. (2013). Twenty years of land use and livelihood changes in SE-Niger: Obsolete and short- sighted adaptation to climatic and demographic pressures? *journal of Arid Environments* , 47-58.

Rose, K. (2010). Africa Shifts Focus from Infrastructure to Interconnection. *Expanding the Global Internet* .

Roudier, P., Sultan, B., Quirion , P., & Berg, A. (2011). The impact of future climate change on West African crop yields: What does the recent literature say? *Global Environmental Change* (21), 1073-1083.

Roy, D. P., Ju, J., Mbow, C., Frost, P., & Loveland, T. (2010). Accessing free Landsat data via the Internet: Africa's challenge. *Remote Sensing Letters , 1* (2), 111-117.

Salas, J. D., & Obeysekera, J. (2014). Revisiting the Concepts of Return Period and Risk for Nonstationary Hydrologic Extreme Events. *Journal of Hydrologic Engineering* .

Salathe jr, E. P. (2003). COMPARISON OF VARIOUS PRECIPITATION DOWNSCALING METHODS FOR THE SIMULATION OF STREAMFLOW IN A RAINSHADOW RIVER BASIN†. *International Journal of Climatology* , 887-901.

Salvi, K., Kannan, S., & Ghosh, S. (2013). High-resolution multisite daily rainfall projections in India with statistical downscaling for climate change impacts assessment. *Journal of Geophiscal Research: Atmospheres , 118*, 3557-3578.

Scmidli, J., Frei, C., & Vidale, P. L. (2006). DOWNSCALING FROM GCM PRECIPITATION: A BENCHMARK FOR DYNAMICAL AND STATISTICAL DOWNSCALING METHODS. *Intenational Journal of Cimatology* (26), 679-689.

Seidou, O., Ramsay, A., & Ioan, N. (2012). Climate change impacts on extreme floods II: improving flood future peaks simulation using non-stationary frequency analysis. *Nat. Hazards* , 715-726.

Serinaldi, F. (2014). Dismissing return periods! *Stoch Environ Res Risk Assess* .

Serreze, M. C. (2009). Understanding Recent Climate Change. (S. Edition, Ed.) *Conservation Biology , 24*, 10-17.

Skelly, W. (1996). GRID BOX OR GRID POINT: WHAT TYPE OF DATA DO GCMs DELIVER TO CLIMATE IMPACTS RESEARCHERS? *International Journal of Climatorology , 16*, 1079-1086.

Spada, M. M. (2014). An overview of problematic Internet use. *Addictive Behaviours* (39), 3-6.

Stork, C., Calandro, E., & Gilwald, A. (2013). Internet going mobile: internet access and use in 11 African countries. *15* (5), 24-51.

Stork, C., Clandro, E., & Gamage, R. (2014). The future of broadband in Africa. *16* (1), 76-93.

Strauss, F., Formayer, H., & Schimd, E. (2013). High resolution climate data for Austria in the period 2008-240 from a statistical climate chnage model. *International journal of climatology* , 430-443.

Sultan, B. (2012). Global warming threatens agricultural productivity in Africa and South Asia. *Environmental Research Letters* (7).

Tareghian, R., & Rasmussen, P. F. (2013). Statistical downscaling of precipitation using quantile regression. *Journal of Hydrology* (487), 122-135.

Thembel, M. J., Gobiet, A., & Heinrich, G. (2011). Empirical-statistical downscaling and error correction of regional climate models and its impact on the climate change signal. *Climatic Change* .

Thomas, D. S., Burrough, S. L., & Adrian, P. G. (2012). Extreme events as drivers of early human behaviour in Africa? The case for variability, not catastrophic drought. *Journal of Quaternary Science* , 7-12.

Timbal, B., Wang, Y., & Evans, A. (2011). Downscaling climate change information: an essential ingredient to incorporate uncertainties into adaptation policies. *International Congress on Modeling and Simulation* .

Van Vuuren, D. P., Riahi, K., Moss, R., Edmonds, J., Thomson, A., Nakicenovic, N., et al. (2012). A proposal for a new scenario framework to support research and assessment in different climate research communities. *Gloabl Environmental Chnage* (22), 21-35.

Vrac, M., Stein, M. L., Hayhoe, K., & Liang, X.-Z. (2007). A general method for validating statistical downscaling methods under future climate change. *Geophisical Research Letters , 34*.

Wilby, R. L., & Dawson, C. W. (2013). The Statistical DownScaling Model: insights from one decade of application. *international Journal of Climatology* , 1707-1719.

Wilby, R. L., & Wigley, T. (1997). Downscaling general circulation model output: a review of methods and limitations. *Progress in Physical Geography* , 530-548.

Wilby, R. L., Hay, L. E., & Leavesley, G. H. (1999). A comparison of downscaled and raw GCM output: implications for climate change scenarios in the San Juan River basin, Colorado. *Journal of Hydrology* , 67-91.

Wilby, R. L., Hay, L. E., & Leavesly, G. H. (1999). A Comparison of downscaled and raw GMC output: implications for climate change scenarios in the San Juan River, Colorado. *Journal of Hydrology* .

Williams, J. (2012). The impact of climate change on indigenous people – the implications for the cultural, spiritual, economic and legal rights of indigenous people. *The International Journal of Human Rights , 16*, 648-688.

Wood, A. W., Leung, L. R., Shridhar, V., & Letternmaier, D. P. (2004). HYDROLOGIC IMPLICATIONS OF DYNAMICAL AND STATISTICAL APPROACHES TO DOWNSCALING CLIMATE MODEL OUTPUTS. *Climatic Change* (62), 189-216.

Xu, C.-y. (1999). From GCMs to river flow: a review of downscaling methods and hydrologic modelling approaches. *Progress in Physical Geography* , 229-249.

APPENDIX A: PROBABILITY DENSITY FUNCTIONS OF OBSERVED, RAW AND DOWNSCALED RCM OUTPUTS.

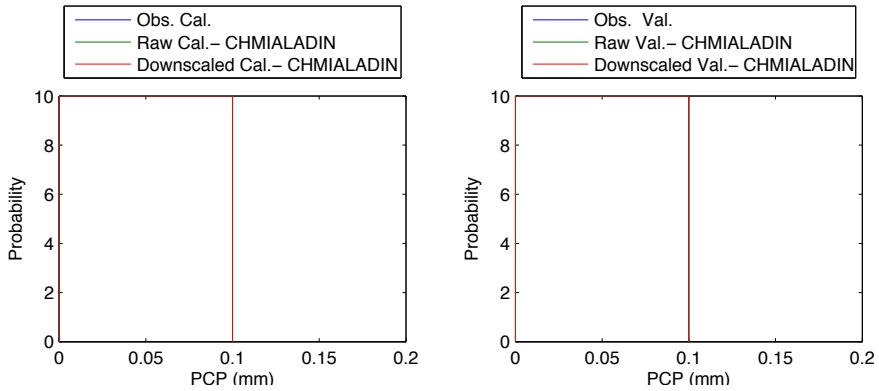

Figure 172 - Probability density of precipitation at Niamey airport with CHMIALADIN in January

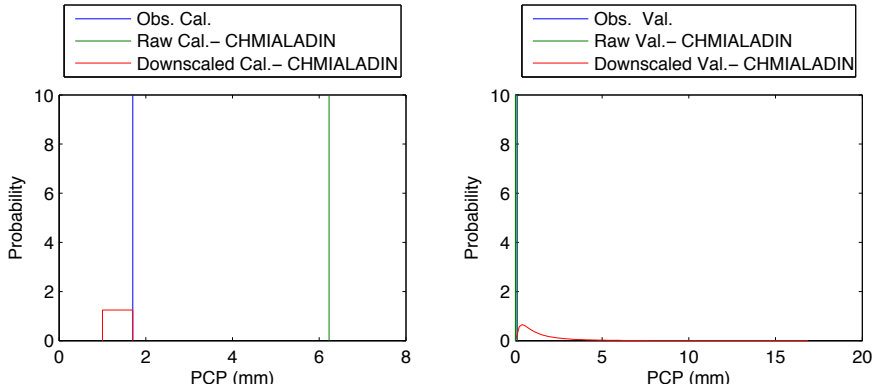

Figure 173 - Probability density of precipitation at Niamey airport with CHMIALADIN in February

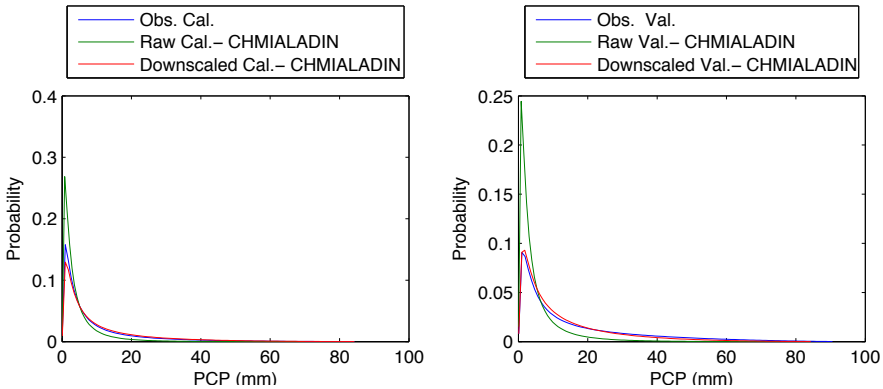

Figure 174 - Probability density of precipitation at Niamey airport with CHMIALADIN in March

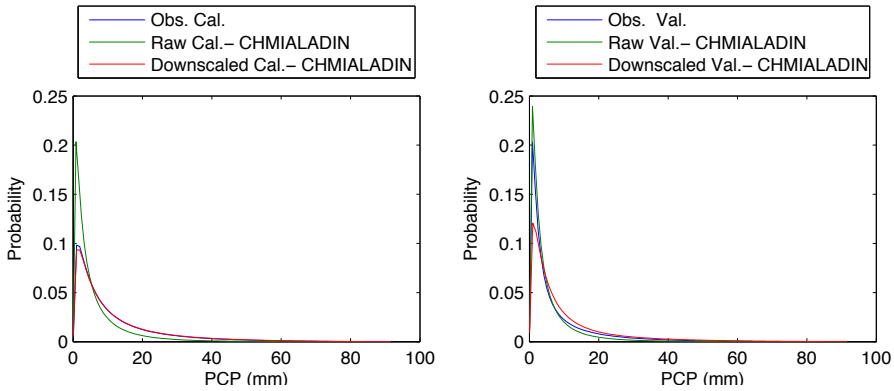

Figure 175 - Probability density of precipitation at Niamey airport with CHMIALADIN in April

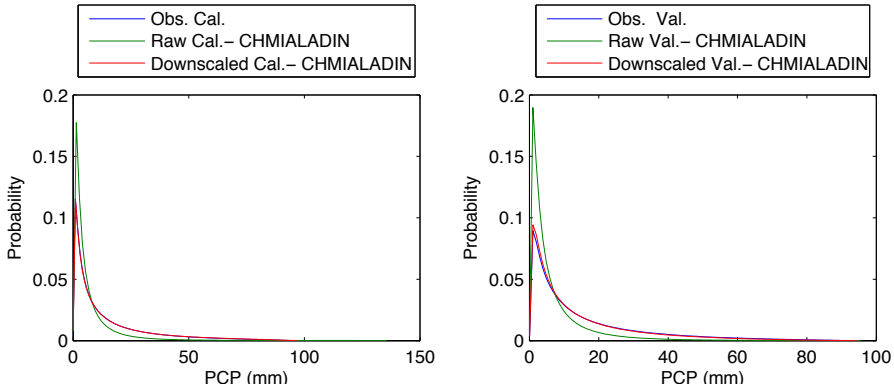

Figure 176 - Probability density of precipitation at Niamey airport with CHMIALADIN in May

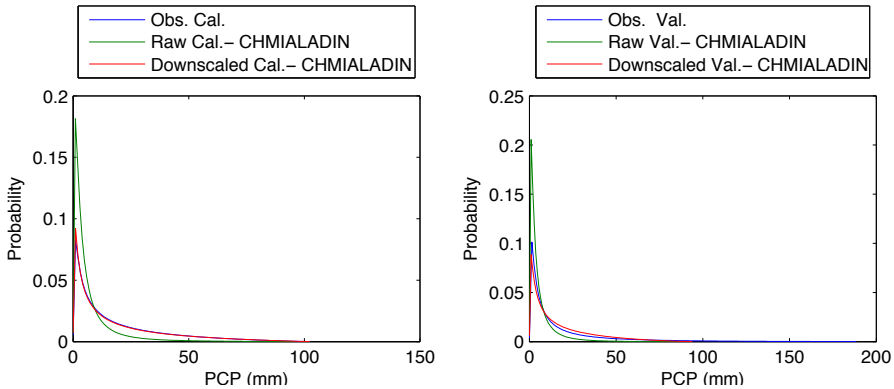

Figure 177 - Probability density of precipitation at Niamey airport with CHMIALADIN in June

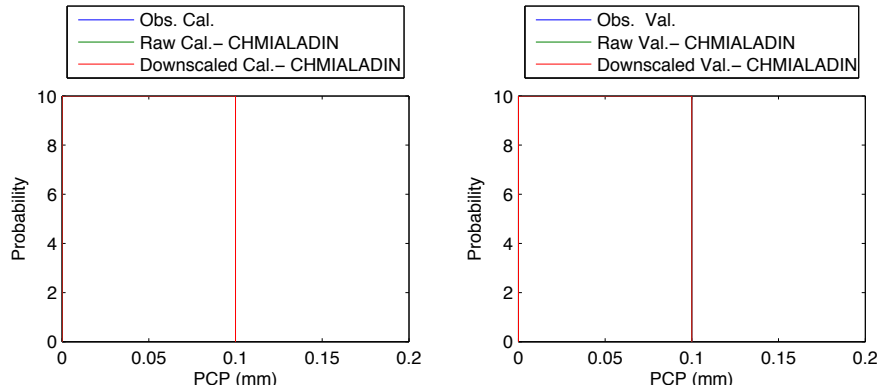

Figure 178 - Probability density of precipitation at Niamey airport with CHMIALADIN in July

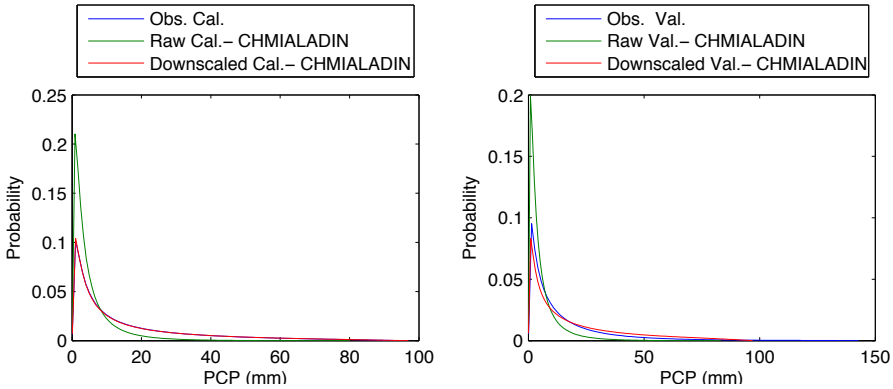

Figure 179 - Probability density of precipitation at Niamey airport with CHMIALADIN in August

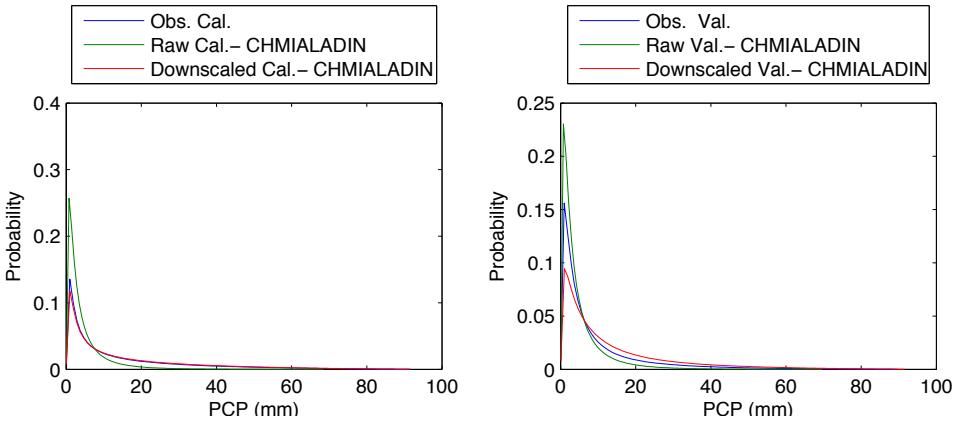

Figure 180 - Probability density of precipitation at Niamey airport with CHMIALADIN in September

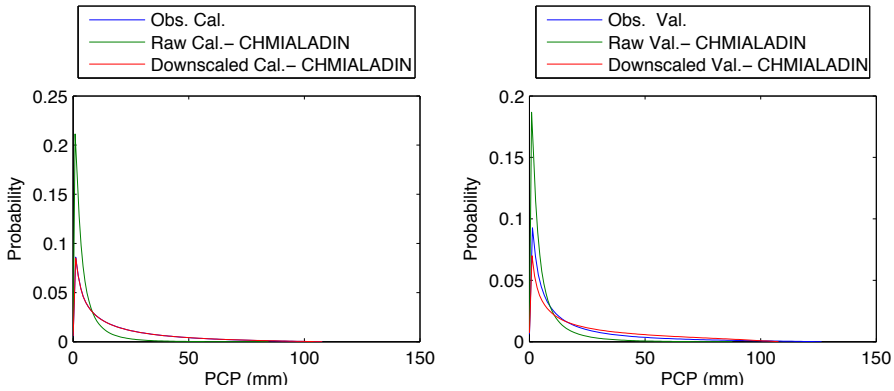

Figure 181 - Probability density of precipitation at Niamey airport with CHMIALADIN in October

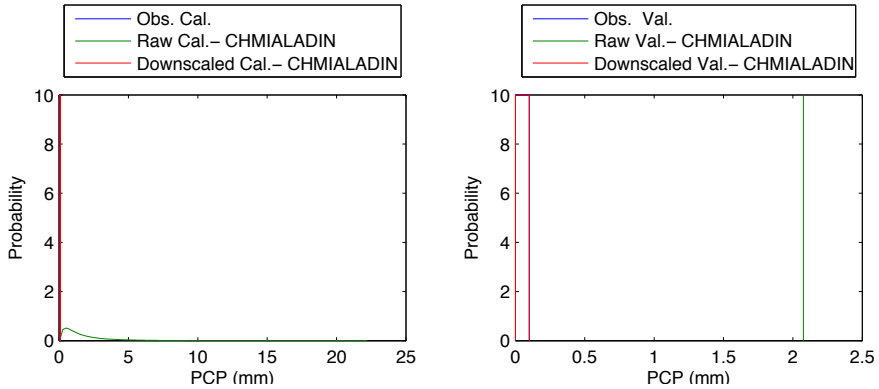

Figure 182 - Probability density of precipitation at Niamey airport with CHMIALADIN in November

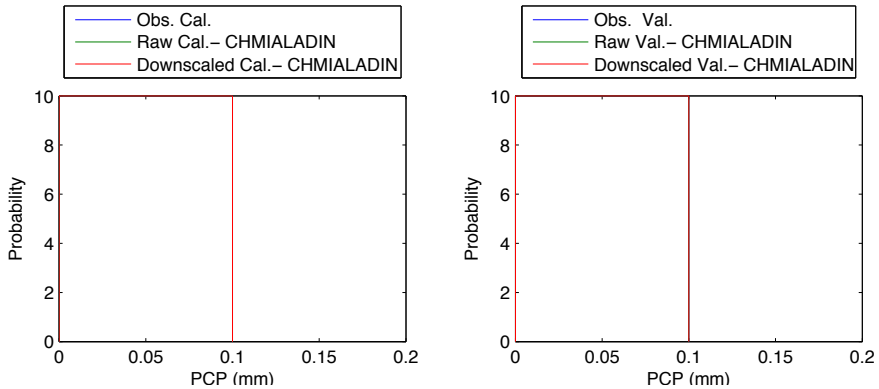

Figure 183 - Probability density of precipitation at Niamey airport with CHMIALADIN in December

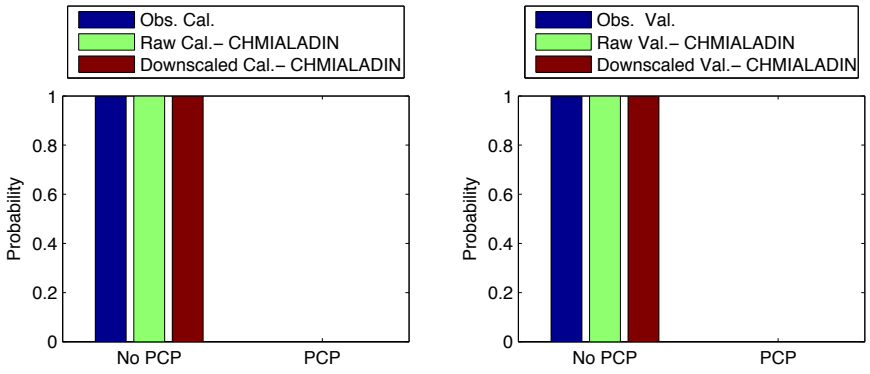

Figure 184 - Precipitation occurrence at Niamey airport with CHMIALADIN in January

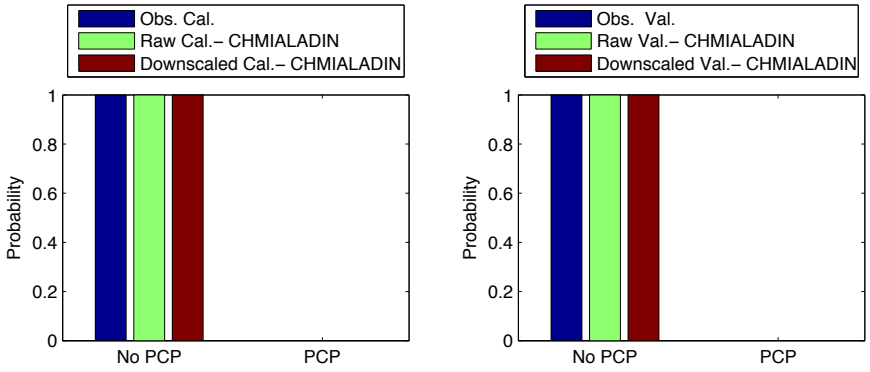

Figure 185 - Precipitation occurrence at Niamey airport with CHMIALADIN in February

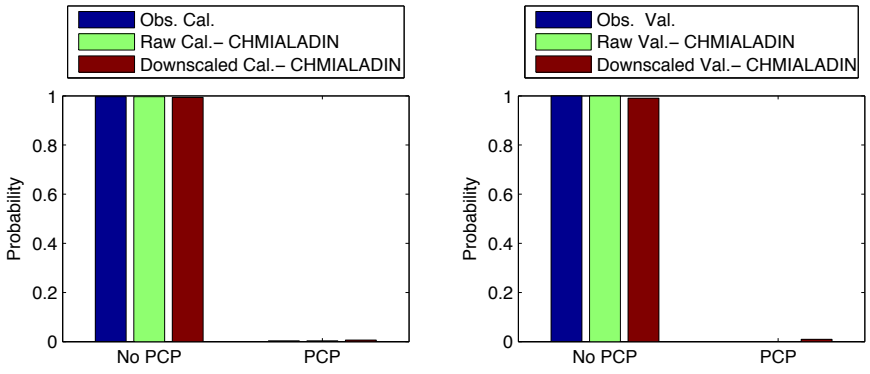

Figure 186 - Precipitation occurrence at Niamey airport with CHMIALADIN in March

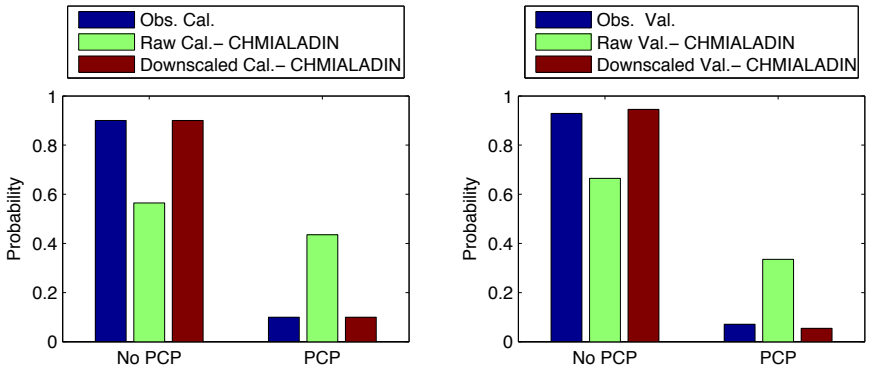

Figure 187 - Precipitation occurrence at Niamey airport with CHMIALADIN in April

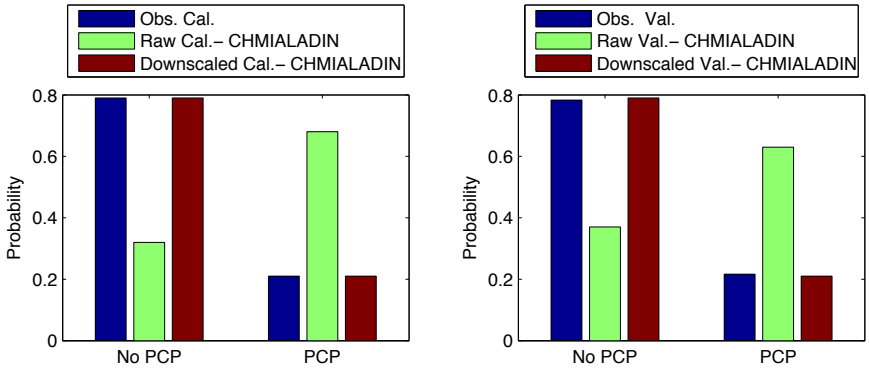

Figure 188 - Precipitation occurrence at Niamey airport with CHMIALADIN in May

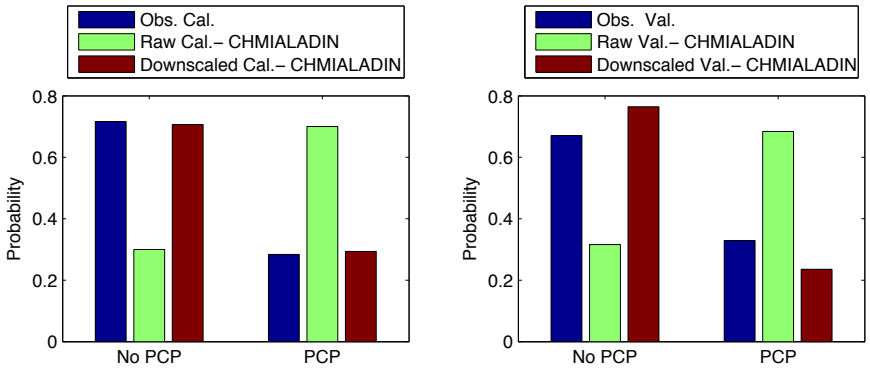

Figure 189 - Precipitation occurrence at Niamey airport with CHMIALADIN in June

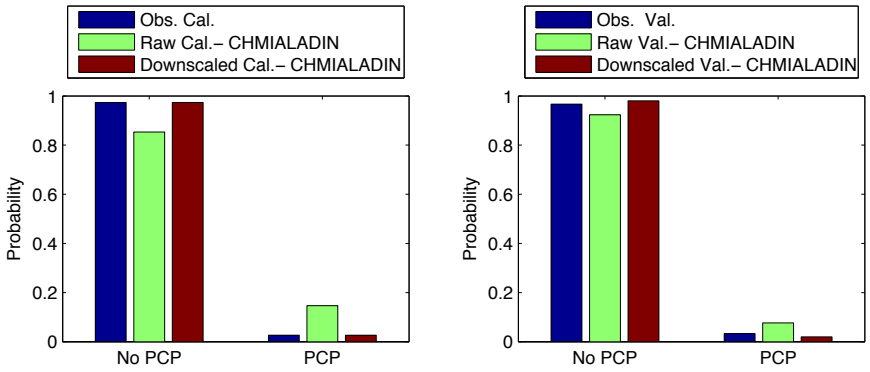

Figure 190 - Precipitation occurrence at Niamey airport with CHMIALADIN in July

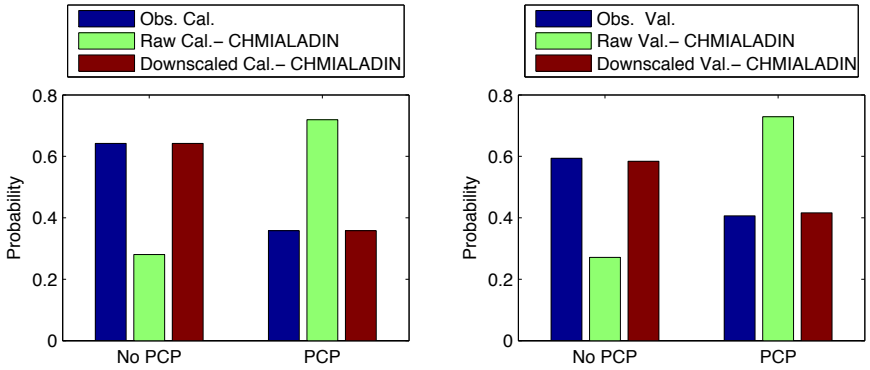

Figure 191 - Precipitation occurrence at Niamey airport with CHMIALADIN in August

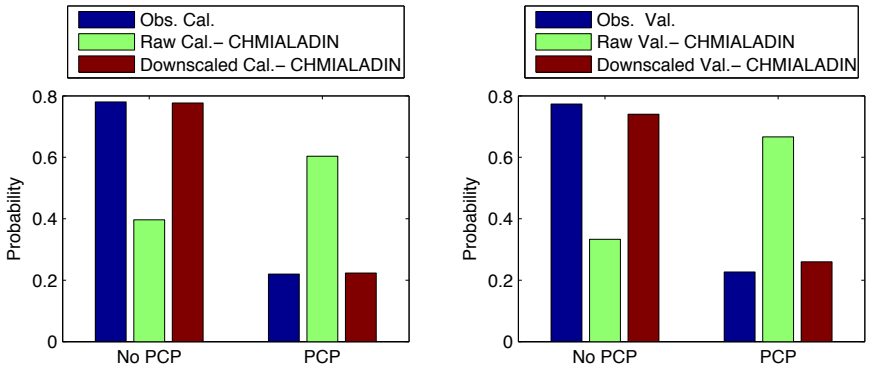

Figure 192 - Precipitation occurrence at Niamey airport with CHMIALADIN in September

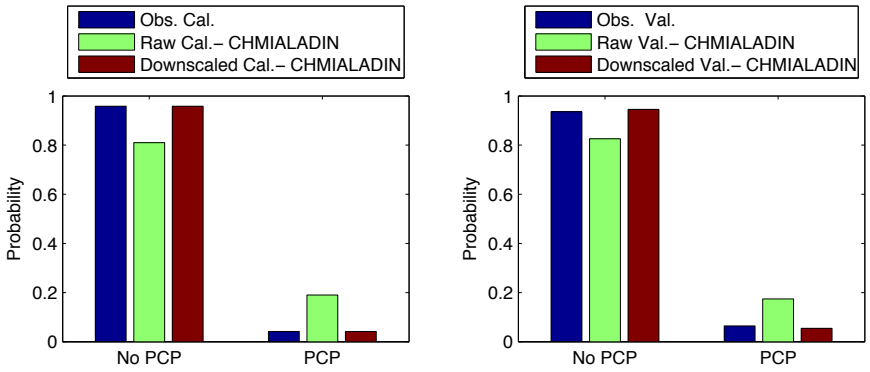

Figure 193 - Precipitation occurrence at Niamey airport with CHMIALADIN in October

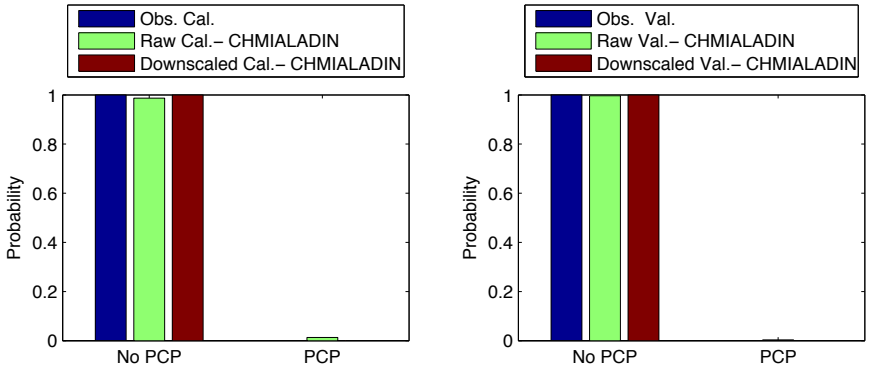

Figure 194 - Precipitation occurrence at Niamey airport with CHMIALADIN in November

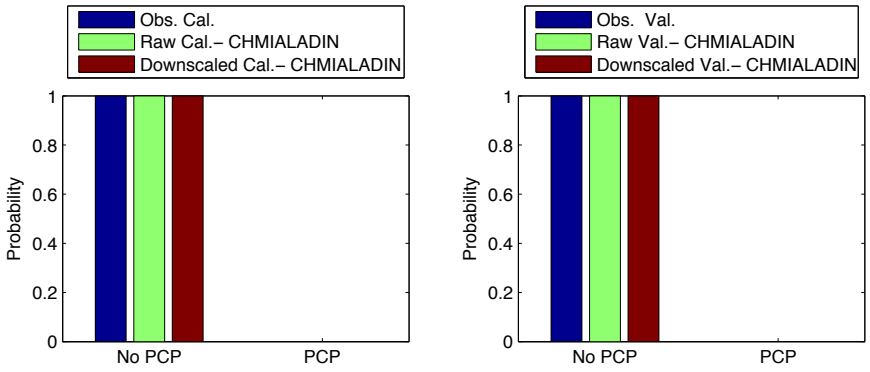

Figure 195 - Precipitation occurrence at Niamey airport with CHMIALADIN in December

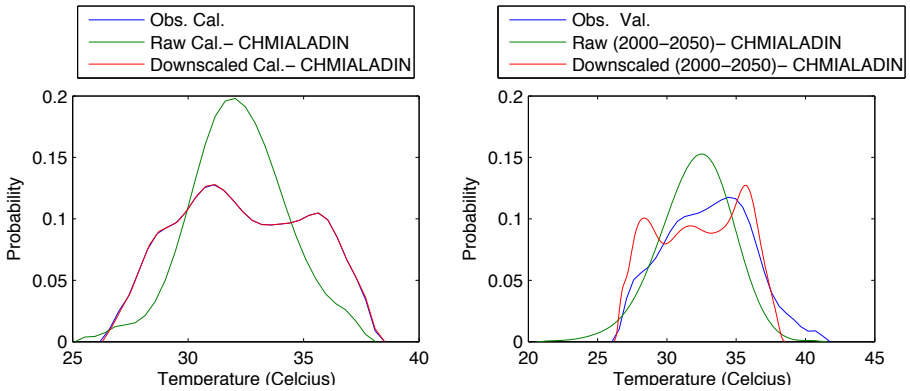

Figure 196 - Probability density for maximum temperature at Niamey airport with CHMIALADIN in January

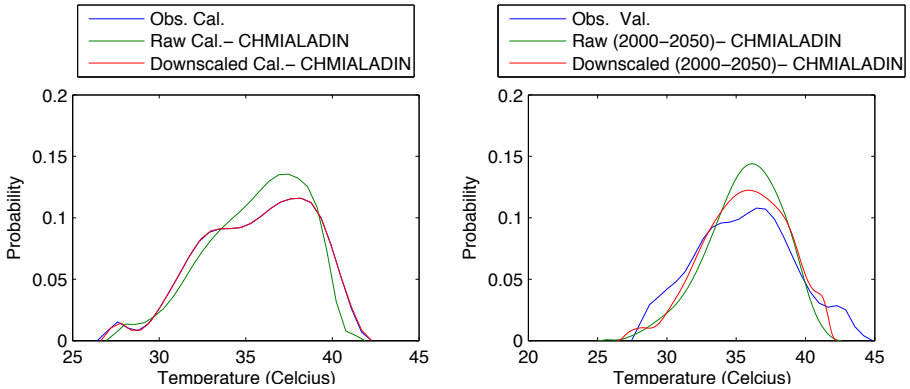

Figure 197 - Probability density for maximum temperature at Niamey airport with CHMIALADIN in February

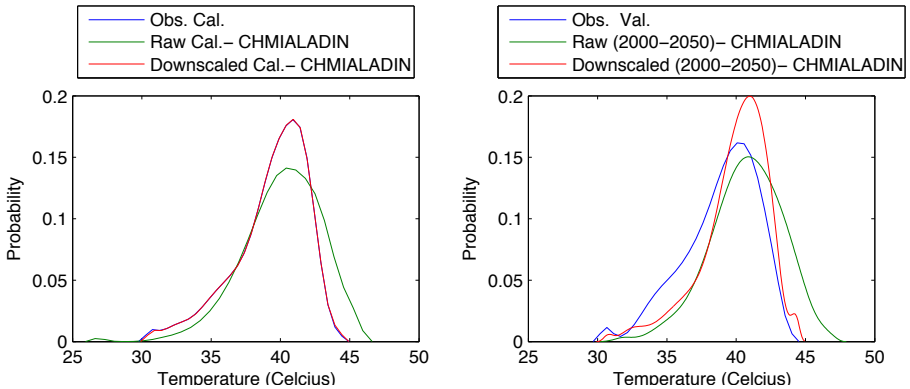

Figure 198 - Probability density for maximum temperature at Niamey airport with CHMIALADIN in March

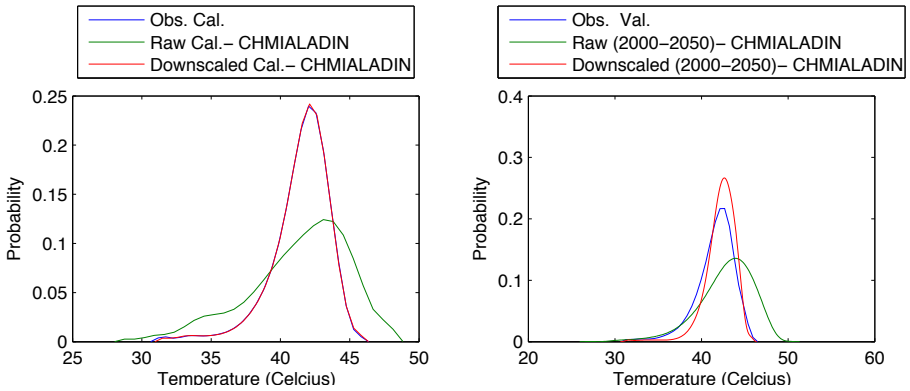

Figure 199 - Probability density for maximum temperature at Niamey airport with CHMIALADIN in April

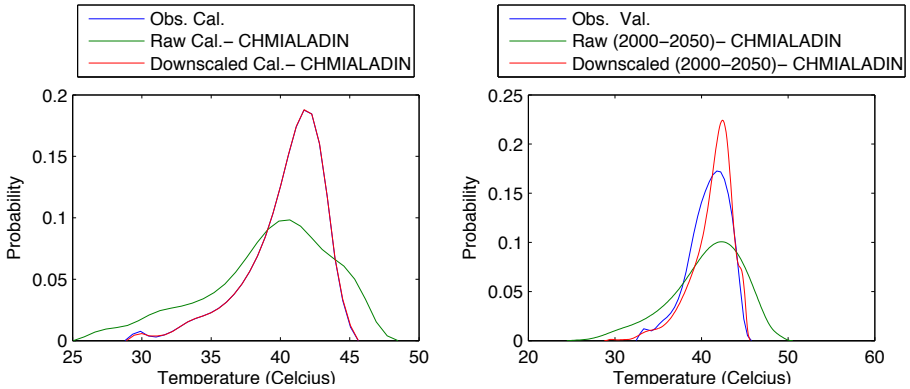

Figure 200 - Probability density for maximum temperature at Niamey airport with CHMIALADIN in May

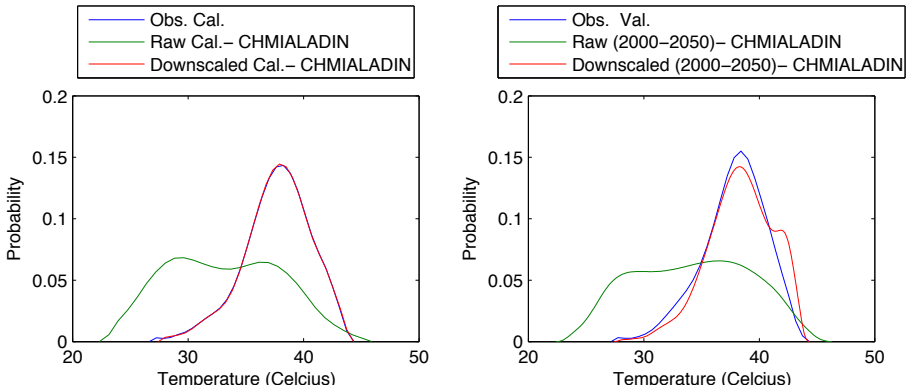

Figure 201 - Probability density for maximum temperature at Niamey airport with CHMIALADIN in June

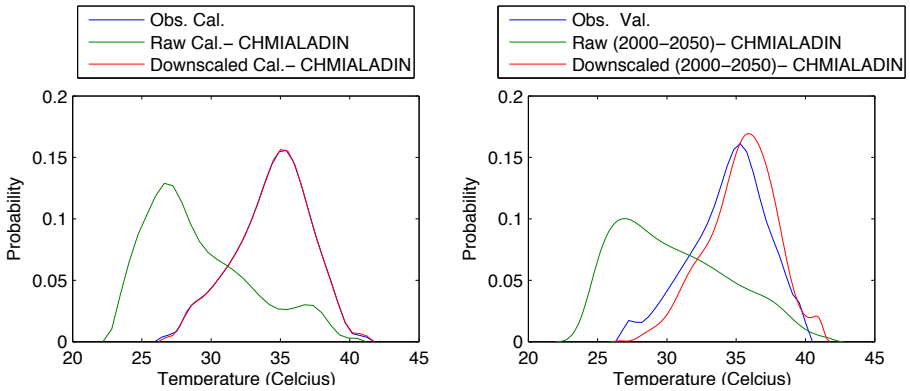

Figure 202 - Probability density for maximum temperature at Niamey airport with CHMIALADIN in July

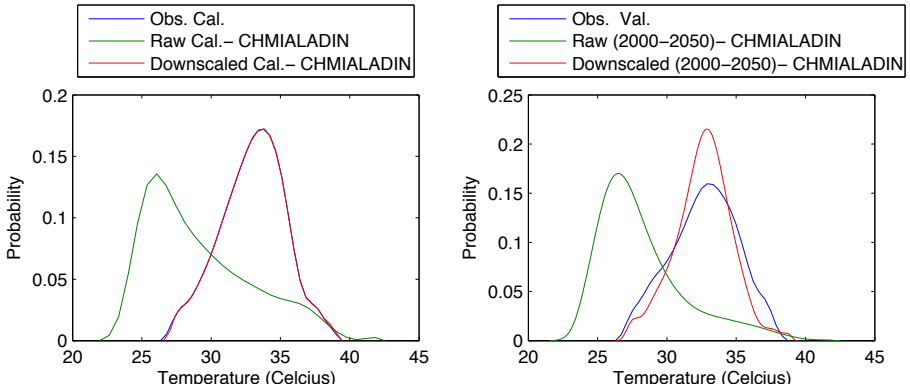

Figure 203 - Probability density for maximum temperature at Niamey airport with CHMIALADIN in August

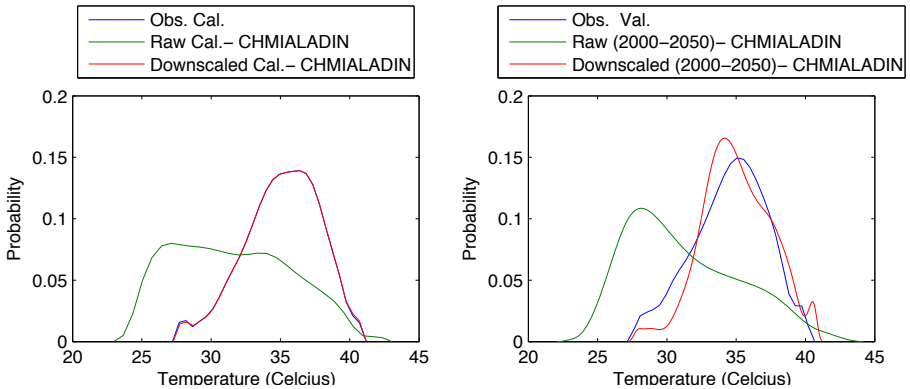

Figure 204 - Probability density for maximum temperature at Niamey airport with CHMIALADIN in September

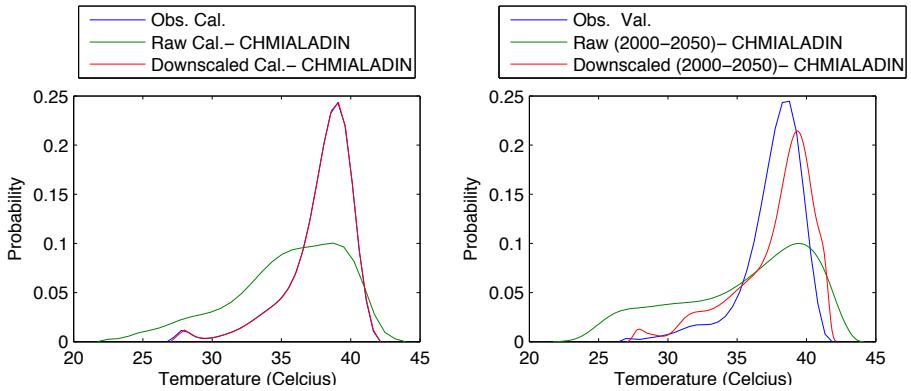

Figure 205 - Probability density for maximum temperature at Niamey airport with CHMIALADIN in October

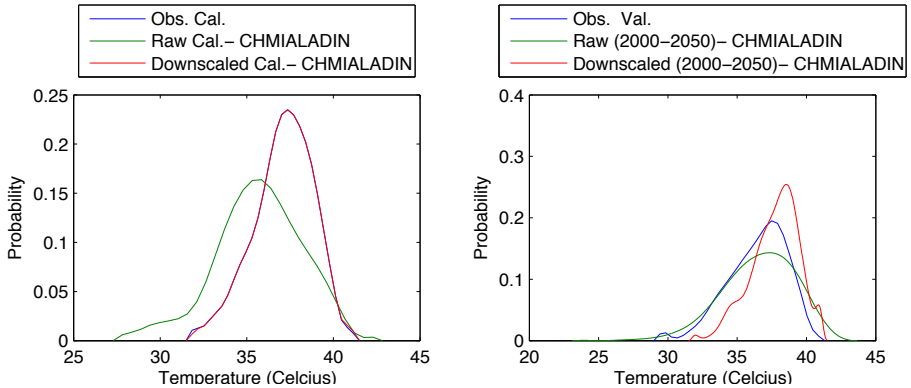

Figure 206 - Probability density for maximum temperature at Niamey airport with CHMIALADIN in November

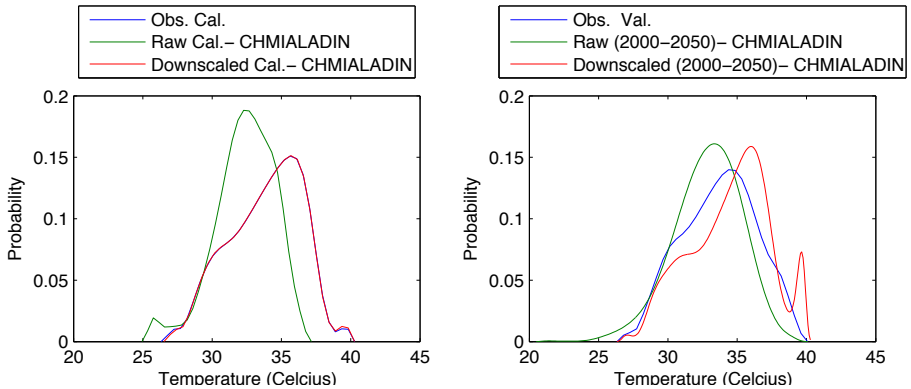

Figure 207 - Probability density for maximum temperature at Niamey airport with CHMIALADIN in December

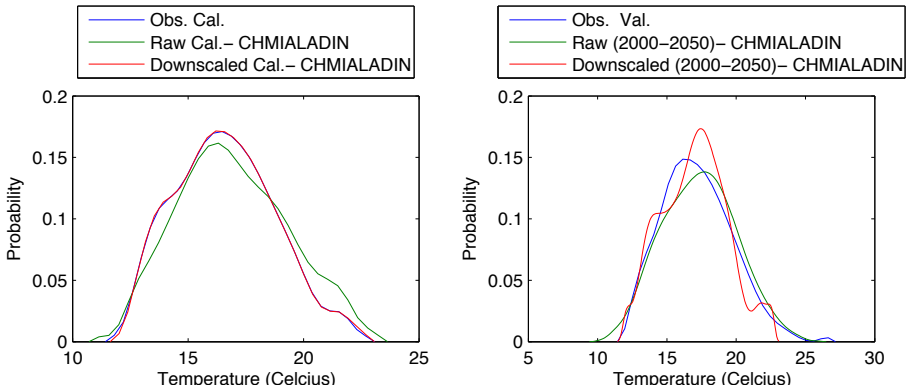

Figure 208 - Probability density for minimum temperature at Niamey airport with CHMIALADIN in January

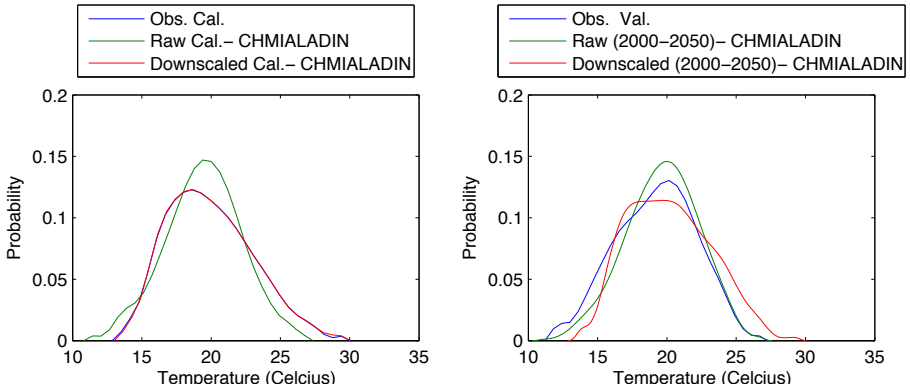

Figure 209 - Probability density for minimum temperature at Niamey airport with CHMIALADIN in February

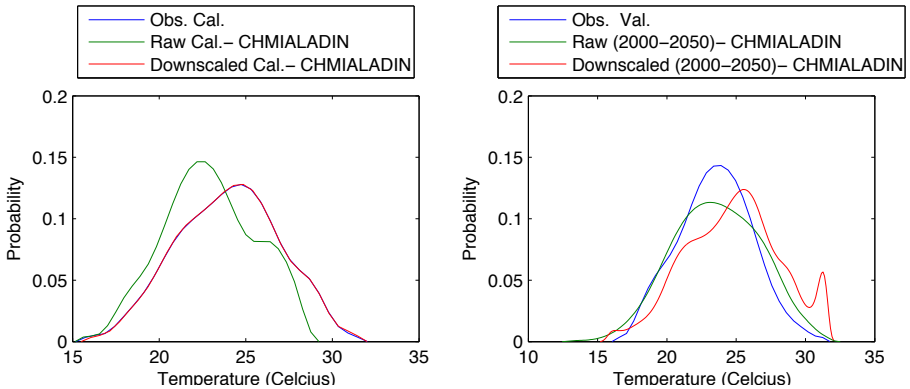

Figure 210 - Probability density for minimum temperature at Niamey airport with CHMIALADIN in March

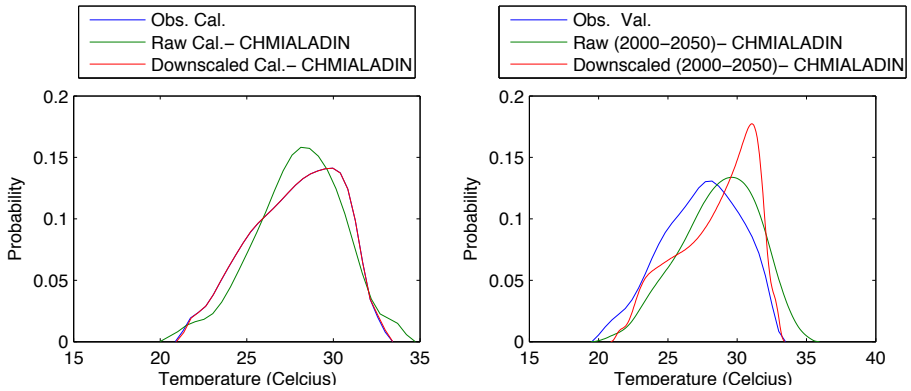

Figure 211 - Probability density for minimum temperature at Niamey airport with CHMIALADIN in April

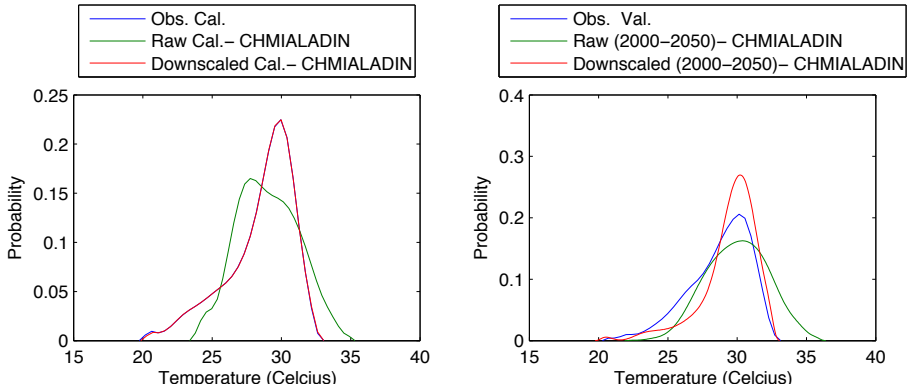

Figure 212 - Probability density for minimum temperature at Niamey airport with CHMIALADIN in May

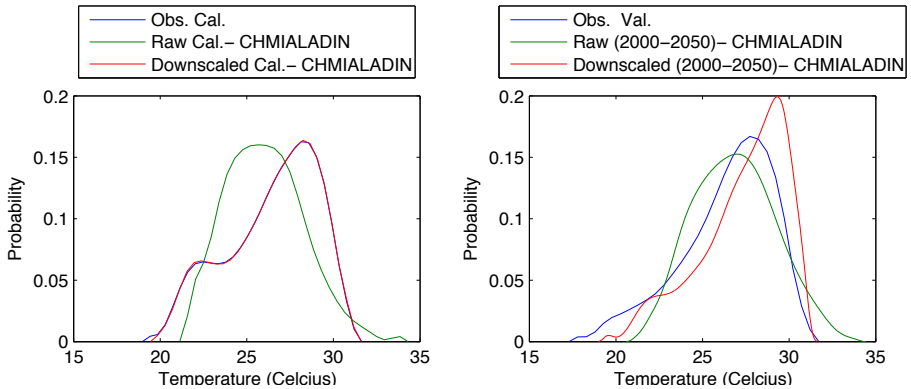

Figure 213 - Probability density for minimum temperature at Niamey airport with CHMIALADIN in June

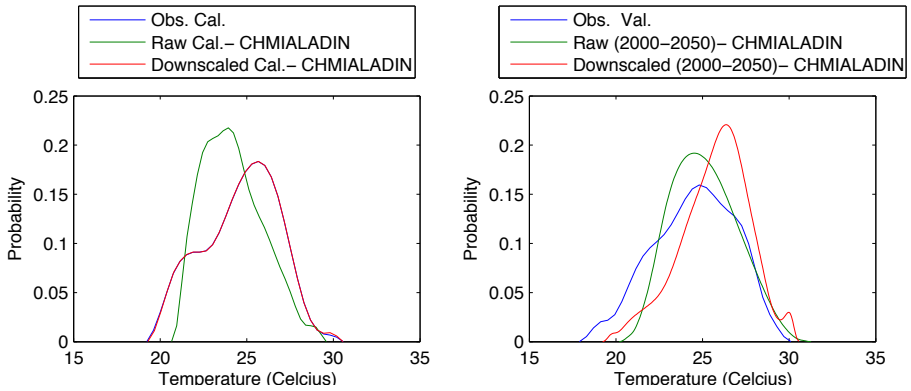

Figure 214 - Probability density for minimum temperature at Niamey airport with CHMIALADIN in July

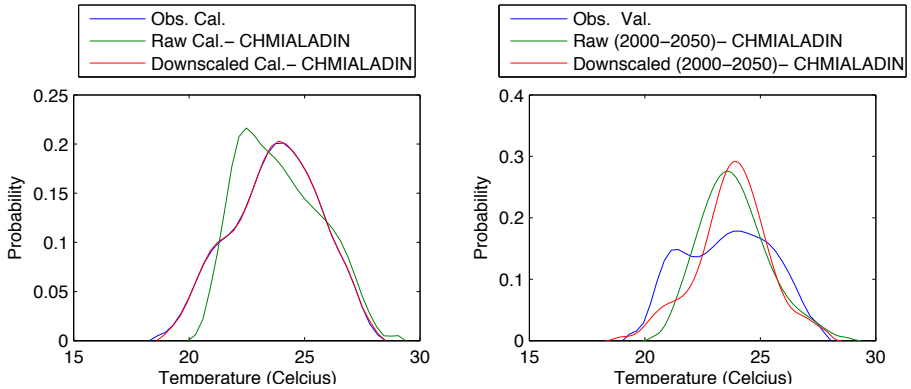

Figure 215 - Probability density for minimum temperature at Niamey airport with CHMIALADIN in August

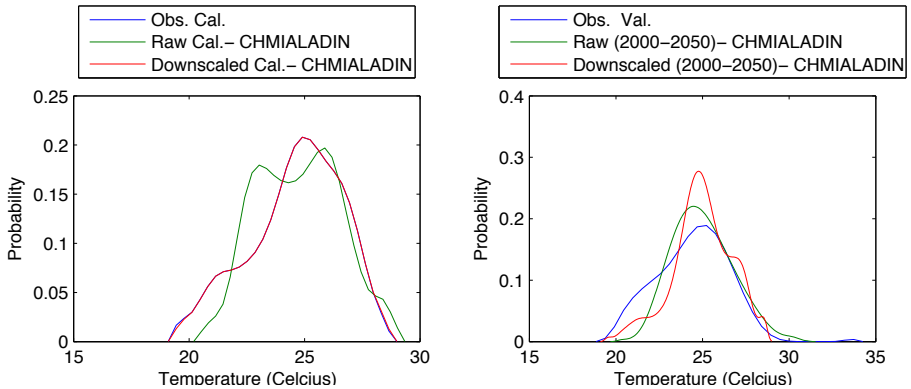

Figure 216 - Probability density for minimum temperature at Niamey airport with CHMIALADIN in September

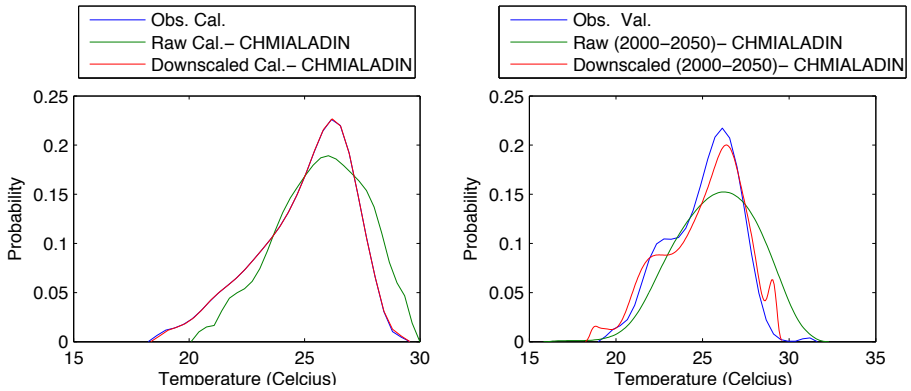

Figure 217 - Probability density for minimum temperature at Niamey airport with CHMIALADIN in October

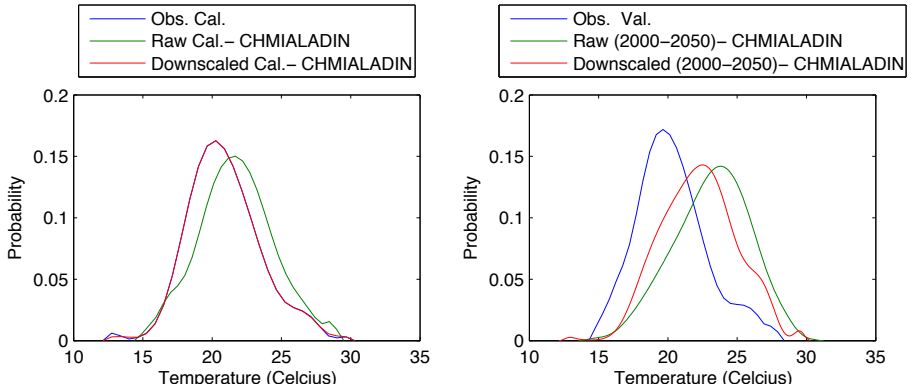

Figure 218 - Probability density for minimum temperature at Niamey airport with CHMIALADIN in November

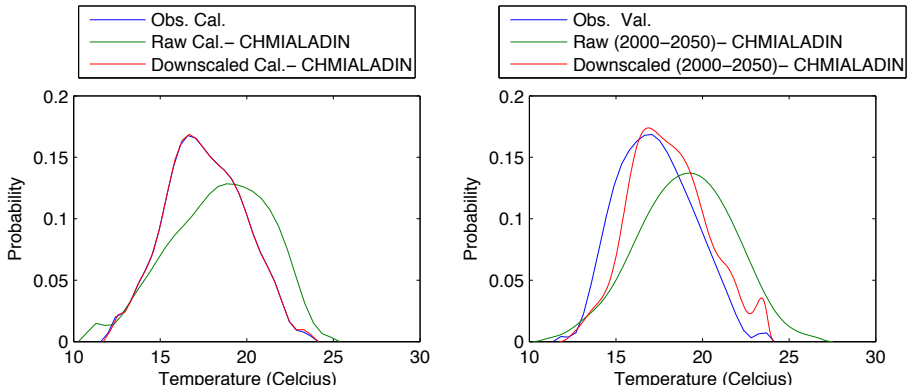

Figure 219 - Probability density for minimum temperature at Niamey airport with CHMIALADIN in December

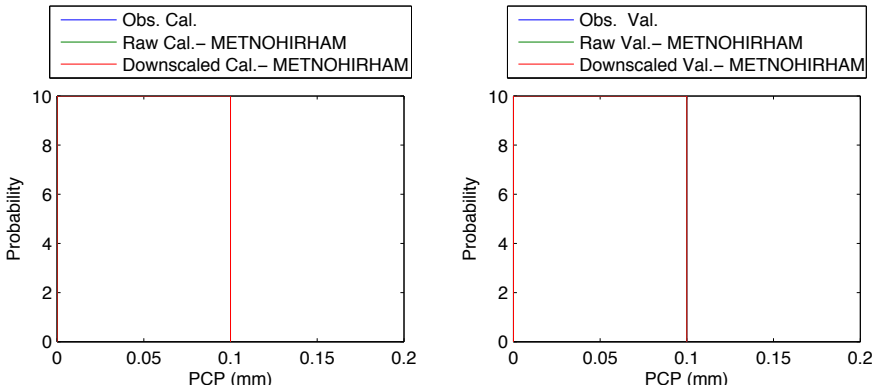

Figure 220 - Probability density of precipitation at Niamey airport with METNOHORHAM in January

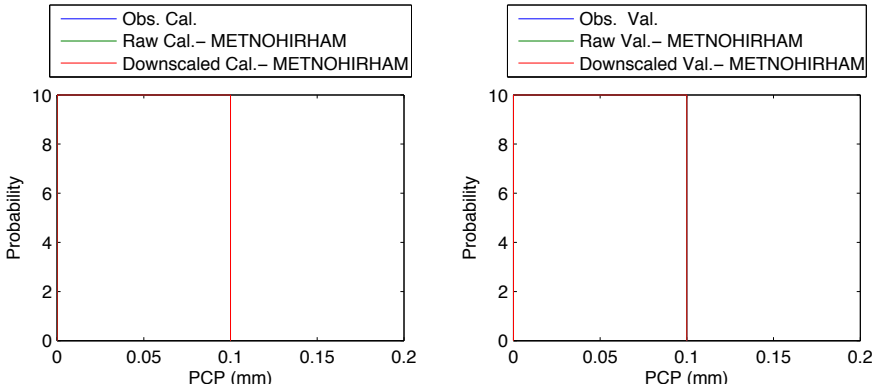

Figure 221 - Probability density of precipitation at Niamey airport with METNOHORHAM in February

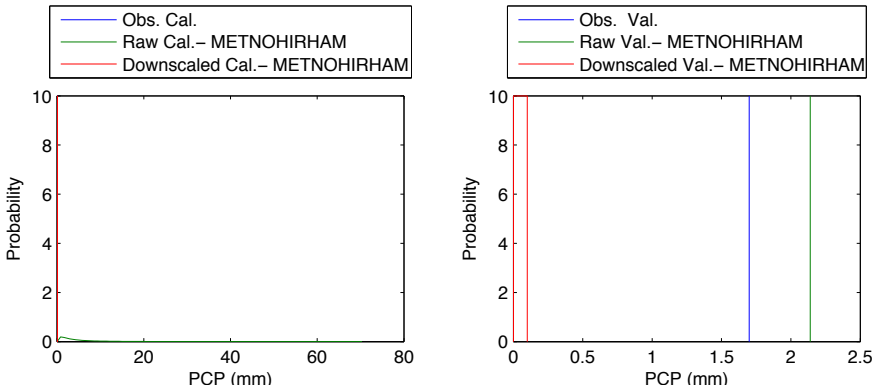

Figure 222 - Probability density of precipitation at Niamey airport with METNOHORHAM in March

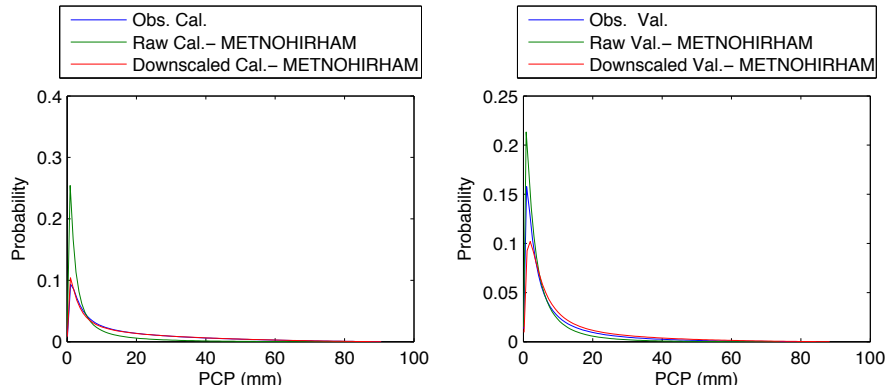

Figure 223 - Probability density of precipitation at Niamey airport with METNOHORHAM in April

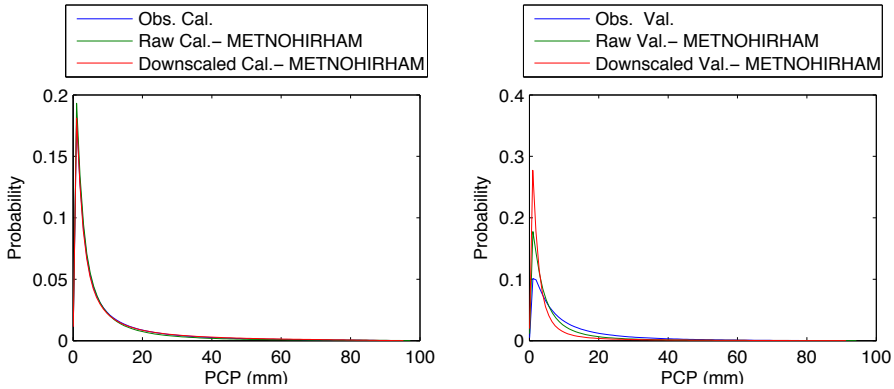

Figure 224 - Probability density of precipitation at Niamey airport with METNOHORHAM in May

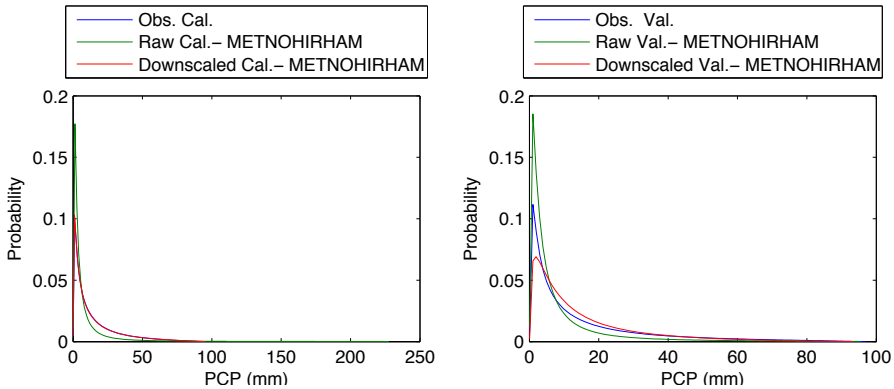

Figure 225 - Probability density of precipitation at Niamey airport with METNOHORHAM in June

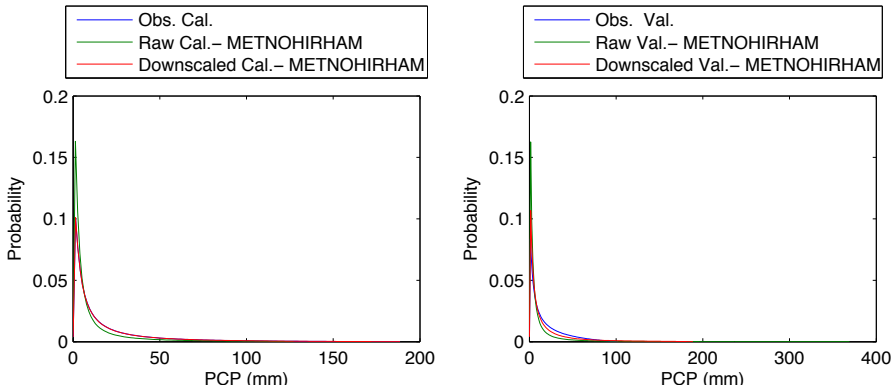

Figure 226 - Probability density of precipitation at Niamey airport with METNOHORHAM in July

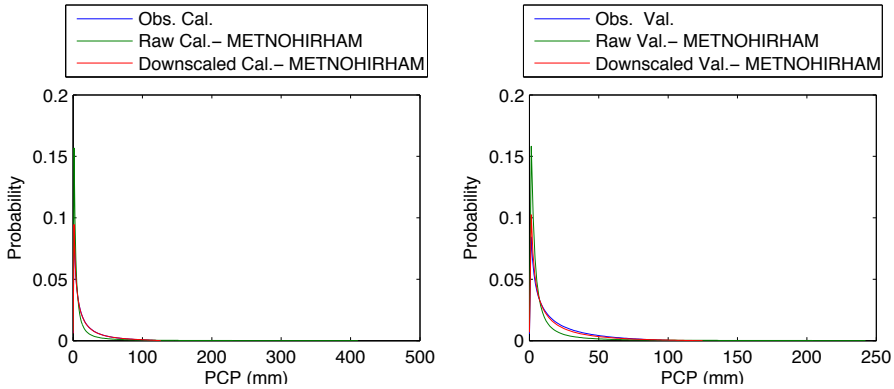

Figure 227 - Probability density of precipitation at Niamey airport with METNOHORHAM in August

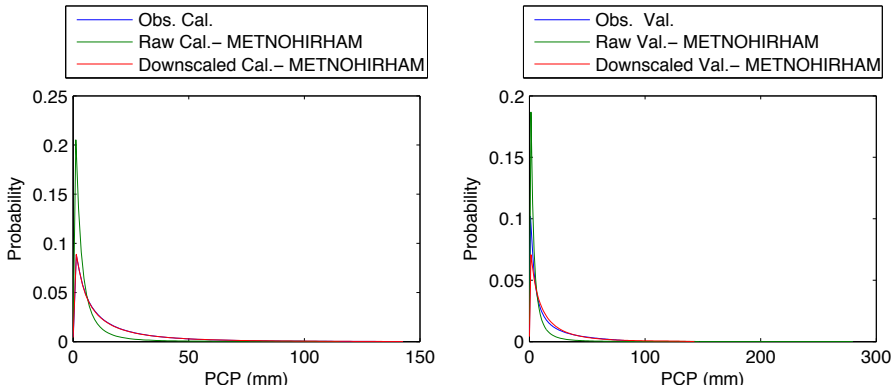

Figure 228 - Probability density of precipitation at Niamey airport with METNOHORHAM in September

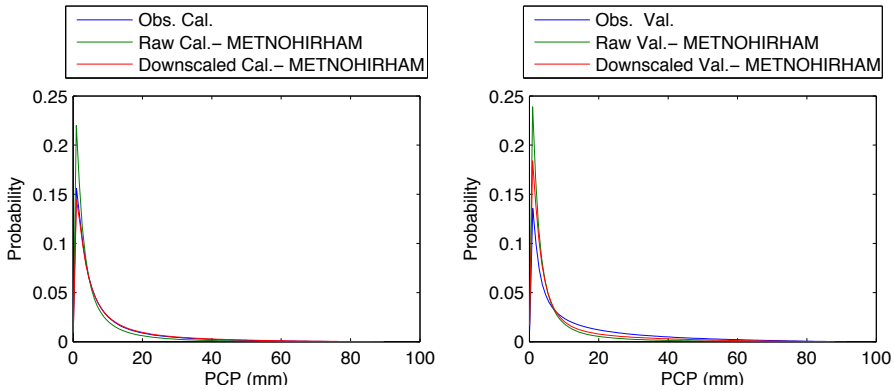

Figure 229 - Probability density of precipitation at Niamey airport with METNOHORHAM in October

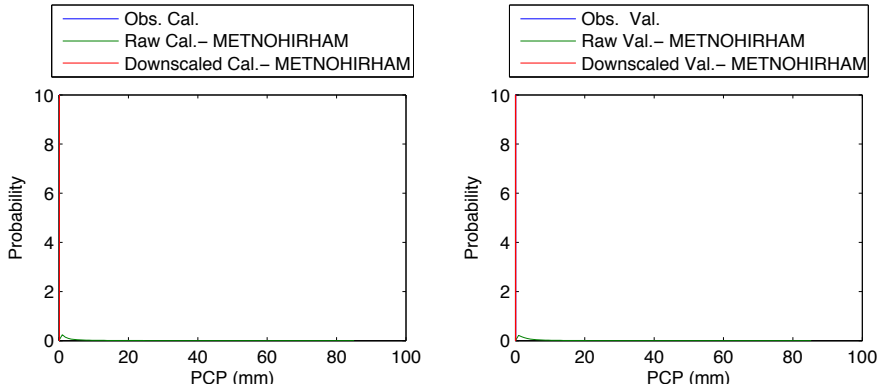

Figure 230 - Probability density of precipitation at Niamey airport with METNOHORHAM in November

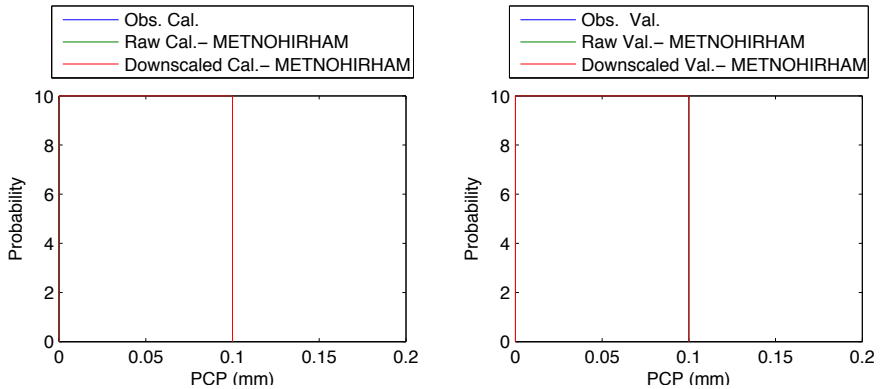

Figure 231 - Probability density of precipitation at Niamey airport with METNOHORHAM in December

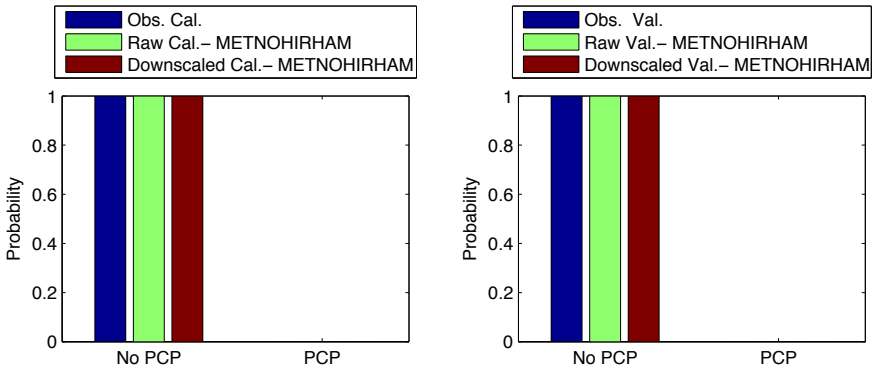

Figure 232 - Precipitation occurrence at Niamey airport with METNOHORHAM in January

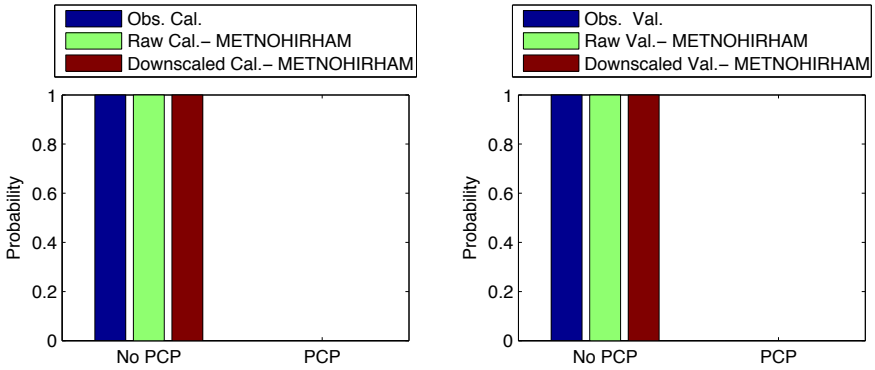

Figure 233 - Precipitation occurrence at Niamey airport with METNOHORHAM in February

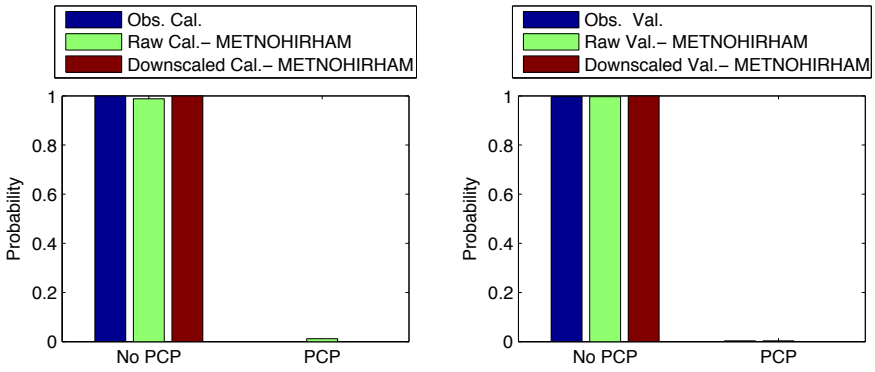

Figure 234 - Precipitation occurrence at Niamey airport with METNOHORHAM in March

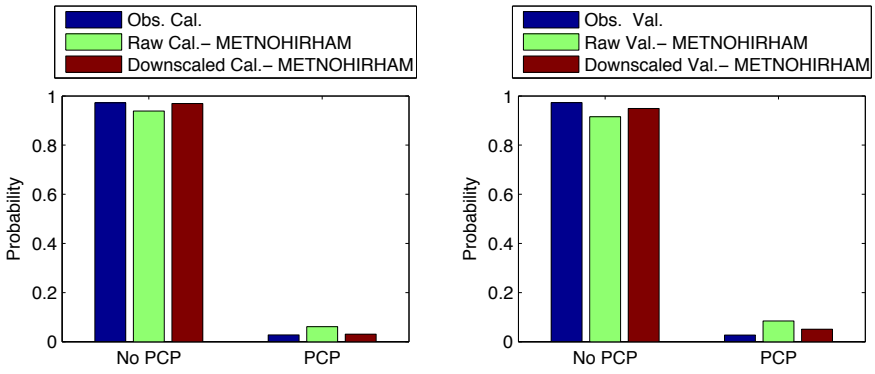

Figure 235 - Precipitation occurrence at Niamey airport with METNOHORHAM in April

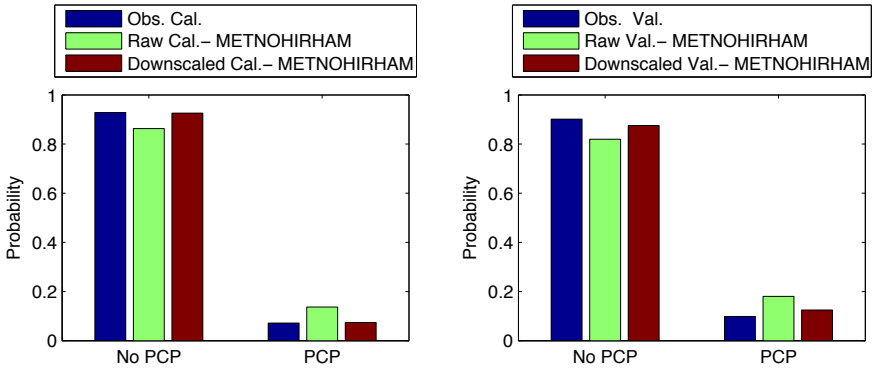

Figure 236 - Precipitation occurrence at Niamey airport with METNOHORHAM in May

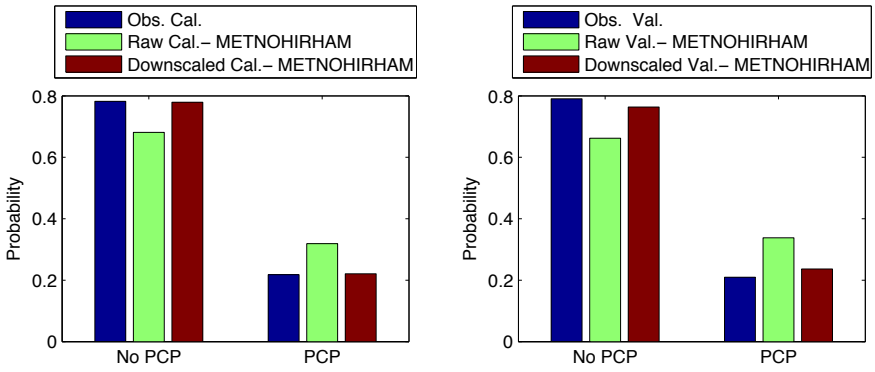

Figure 237 - Precipitation occurrence at Niamey airport with METNOHORHAM in June

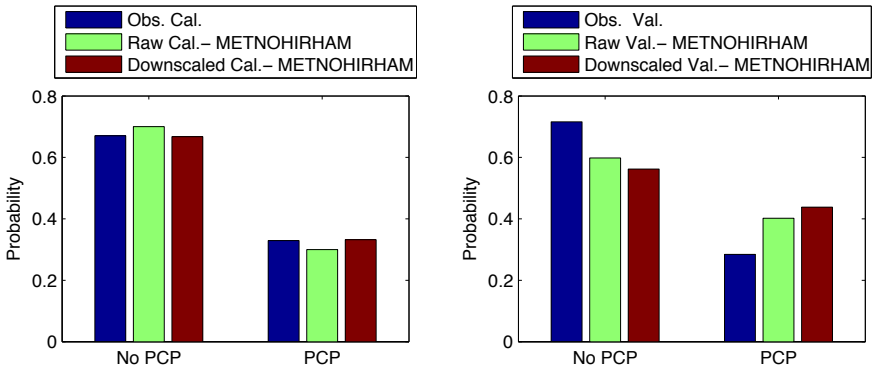

Figure 238 - Precipitation occurrence at Niamey airport with METNOHORHAM in July

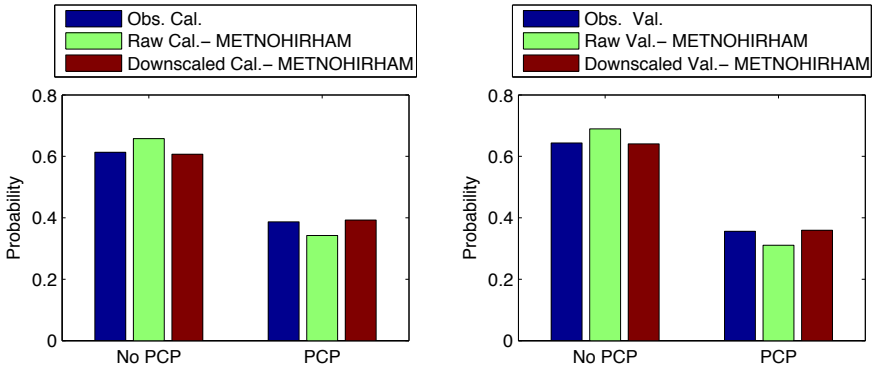

Figure 239 - Precipitation occurrence at Niamey airport with METNOHORHAM in August

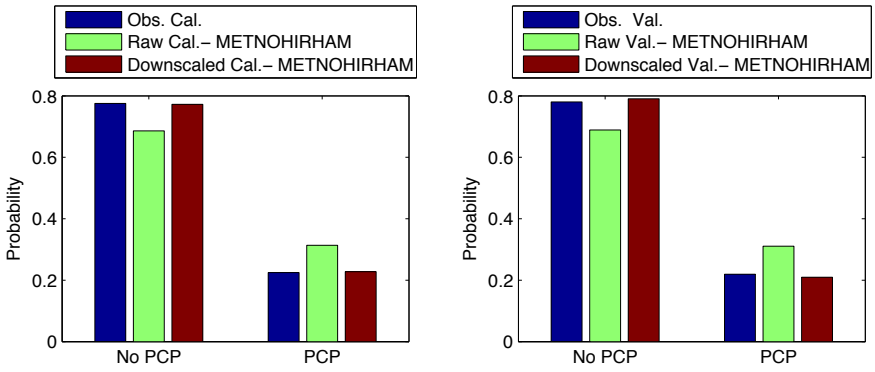

Figure 240 - Precipitation occurrence at Niamey airport with METNOHORHAM in September

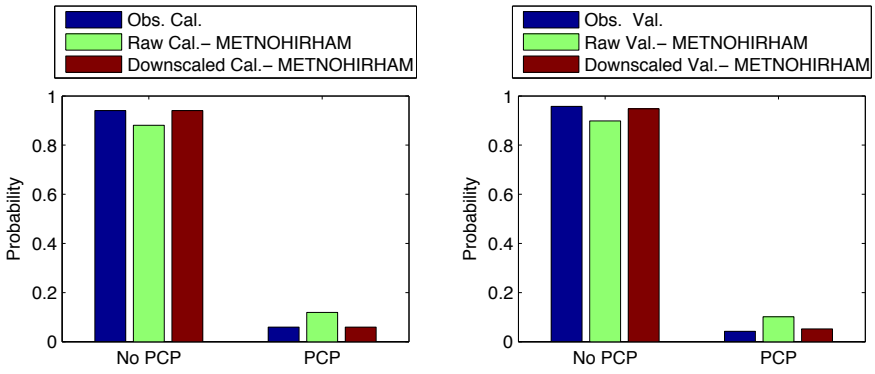

Figure 241 - Precipitation occurrence at Niamey airport with METNOHORHAM in October

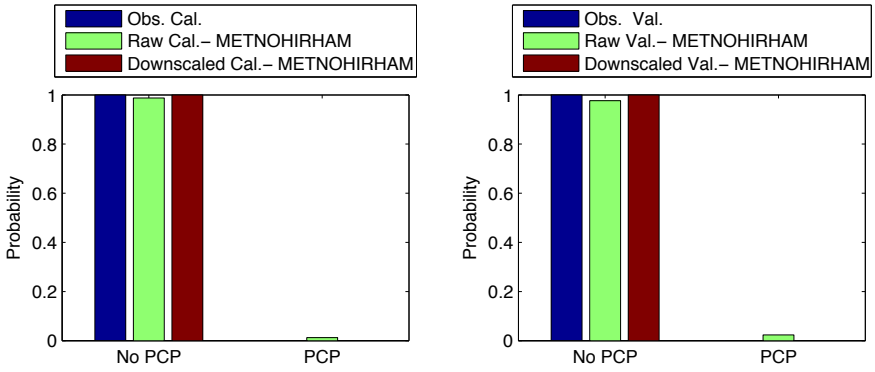

Figure 242 - Precipitation occurrence at Niamey airport with METNOHORHAM in November

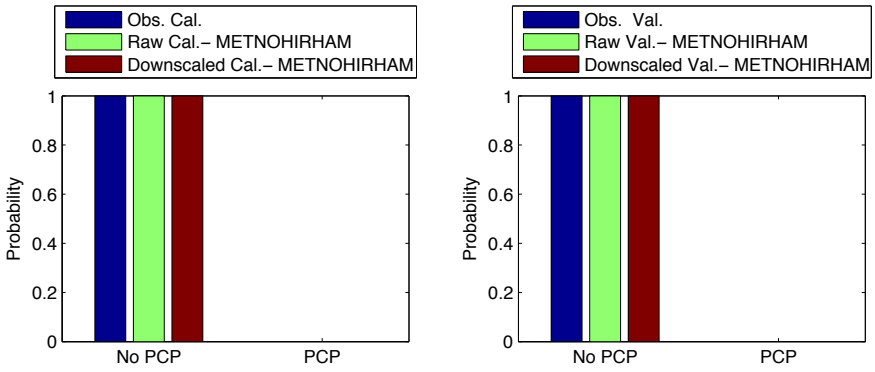

Figure 243 - Precipitation occurrence at Niamey airport with METNOHORHAM in December

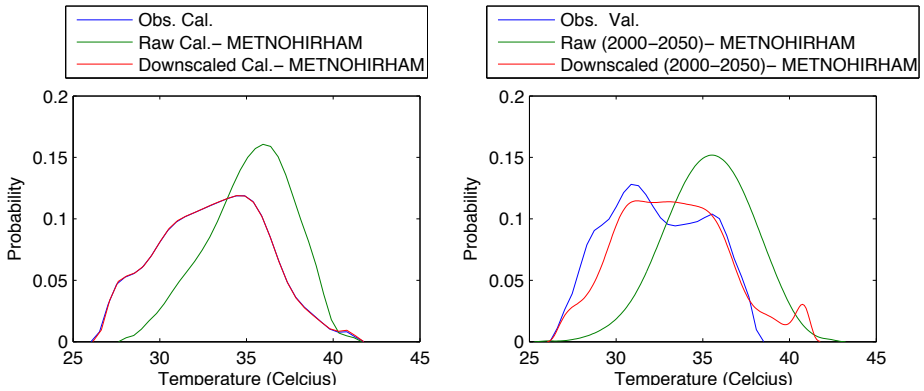

Figure 244 - Probability density for maximum temperature at Niamey airport with METNOHORHAM in January

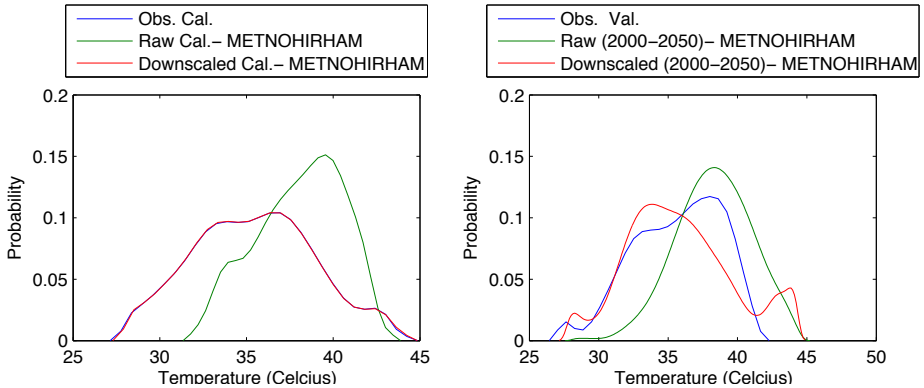

Figure 245 - Probability density for maximum temperature at Niamey airport with METNOHORHAM in February

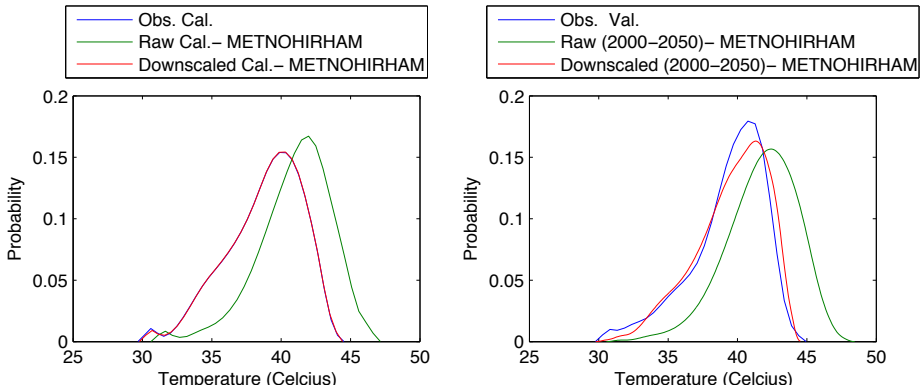

Figure 246 - Probability density for maximum temperature at Niamey airport with METNOHORHAM in March

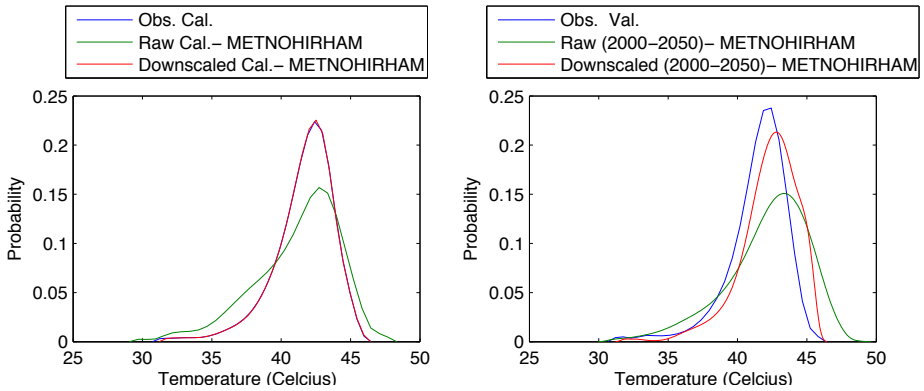

Figure 247 - Probability densities for maximum temperature at Niamey airport with METNOHORHAM in April

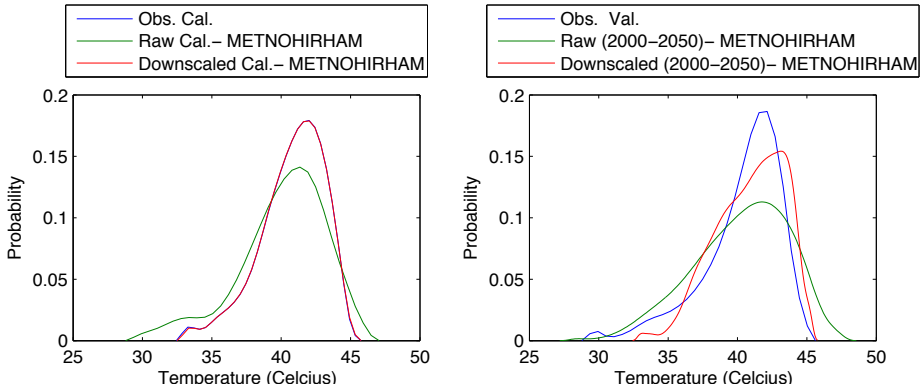

Figure 248 - Probability densities for maximum temperature at Niamey airport with METNOHORHAM in May

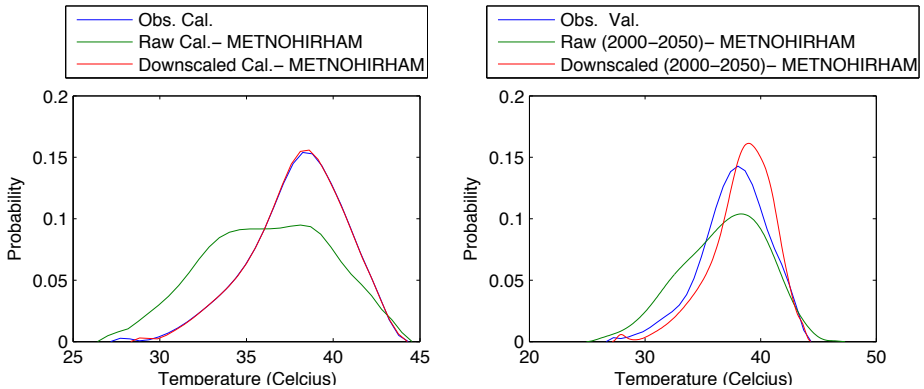

Figure 249 - Probability densities for maximum temperature at Niamey airport with METNOHORHAM in June

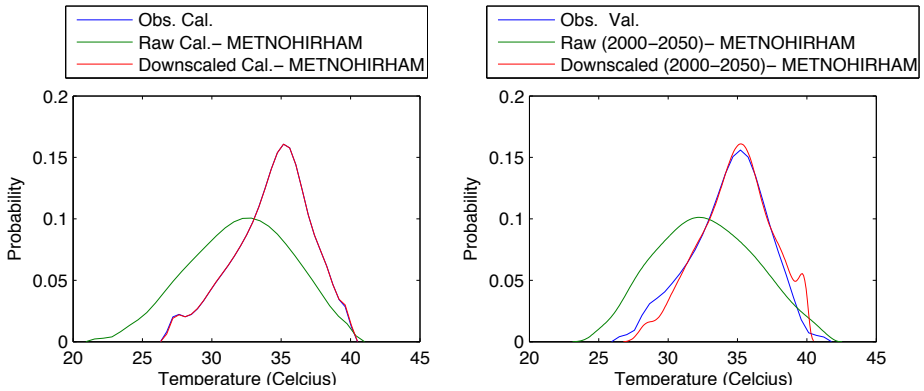

Figure 250 - Probability density for maximum temperature at Niamey airport with METNOHORHAM in July

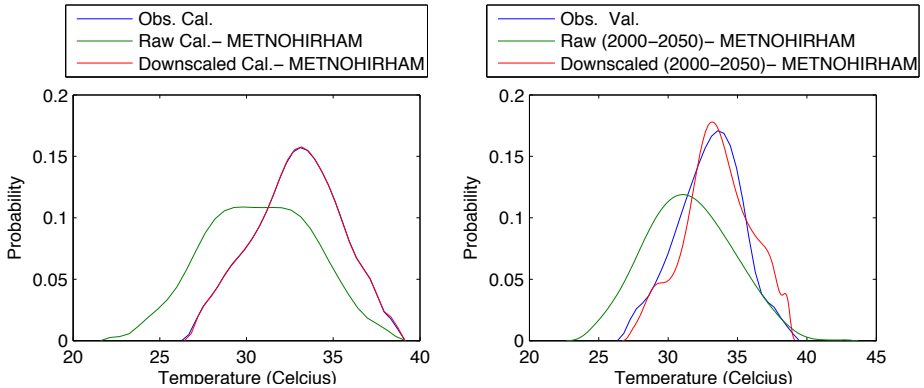

Figure 251 - Probability density for maximum temperature at Niamey airport with METNOHORHAM in August

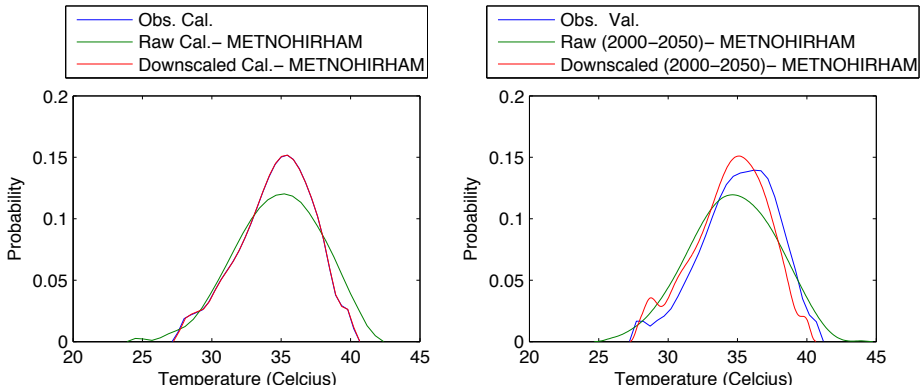

Figure 252 - Probability density for maximum temperature at Niamey airport with METNOHORHAM in September

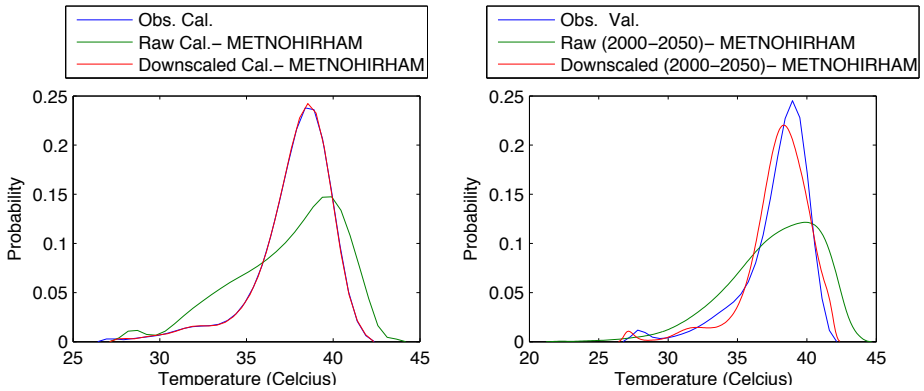

Figure 253 - Probability density for maximum temperature at Niamey airport with METNOHORHAM in October

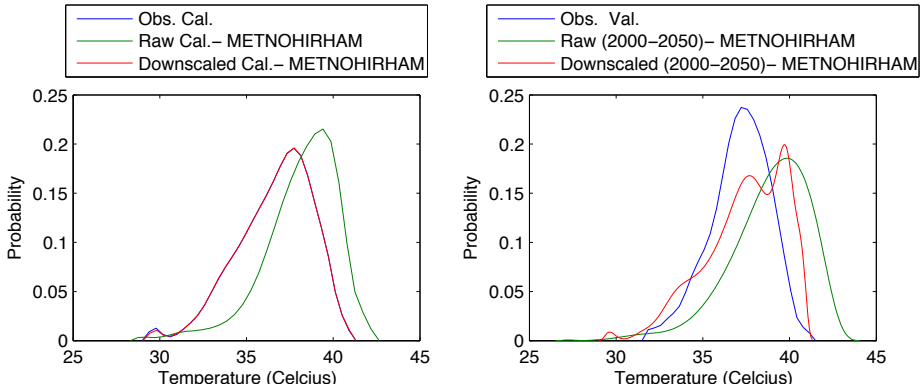

Figure 254 - Probability density for maximum temperature at Niamey airport with METNOHORHAM in November

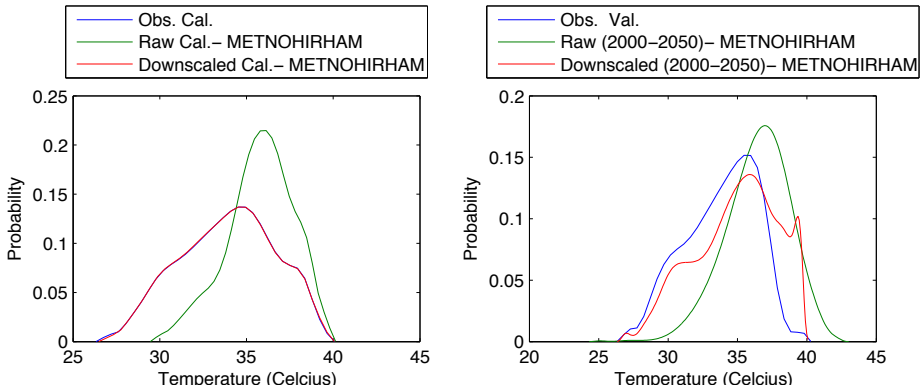

Figure 255 - Probability density for maximum temperature at Niamey airport with METNOHORHAM in December

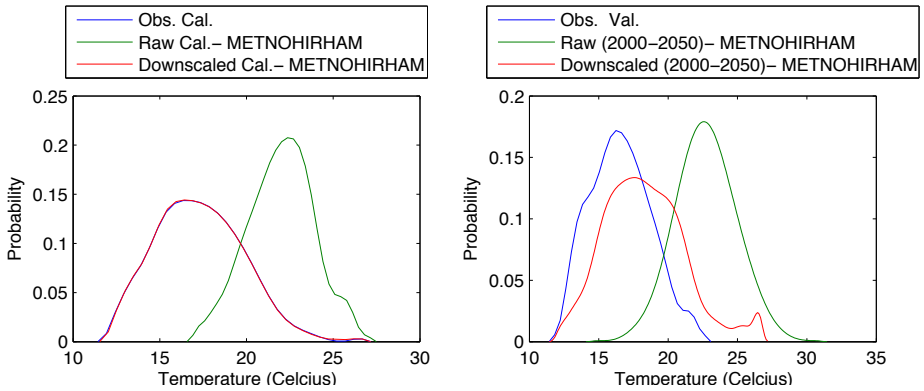

Figure 256 - Probability density for minimum temperature at Niamey airport with METNOHORHAM in January

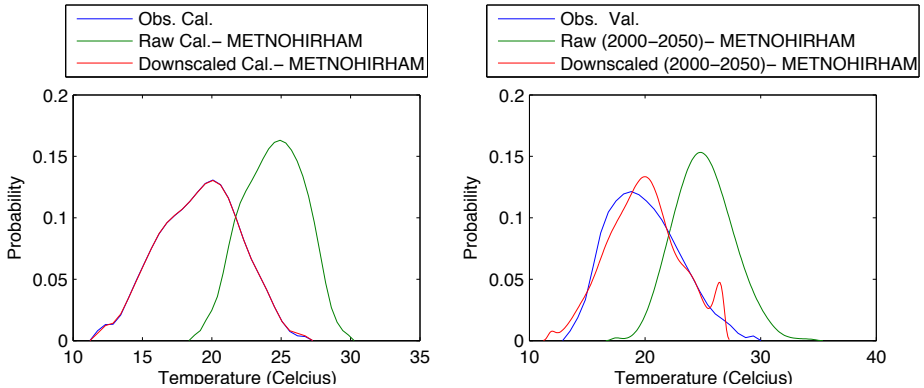

Figure 257 - Probability density for minimum temperature at Niamey airport with METNOHORHAM in February

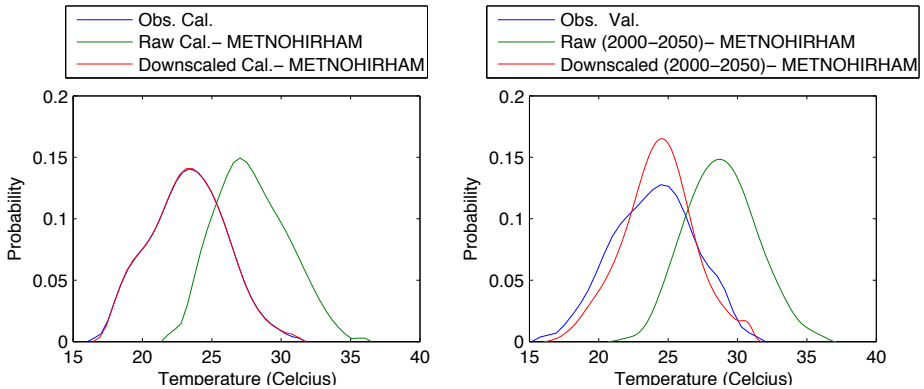

Figure 258 - Probability density for minimum temperature at Niamey airport with METNOHORHAM in March

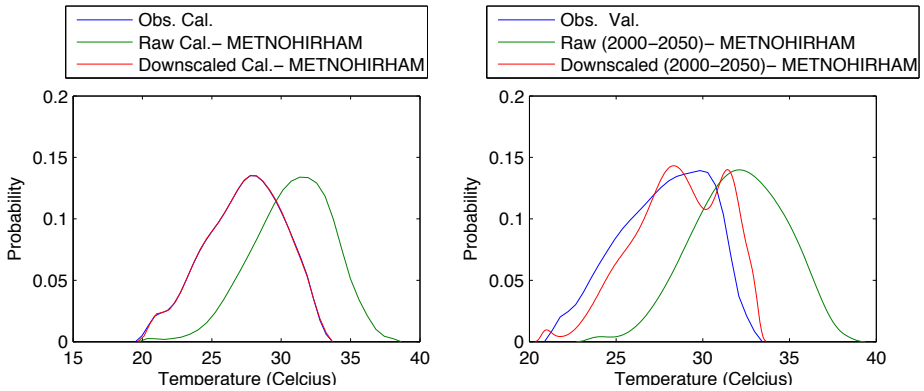

Figure 259 - Probability density for minimum temperature at Niamey airport with METNOHORHAM in April

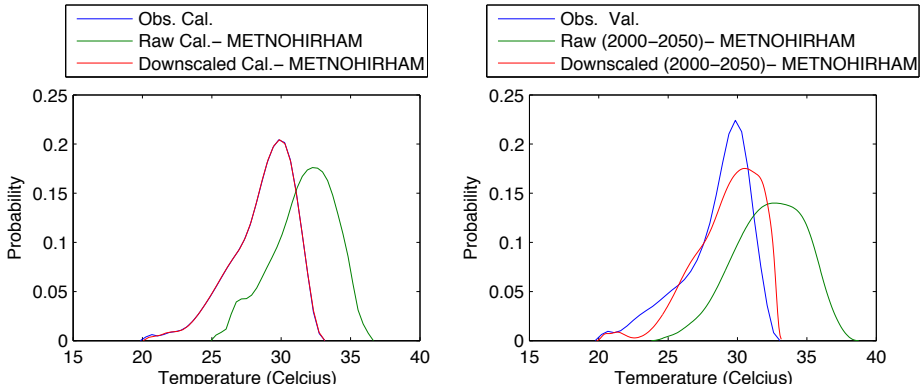

Figure 260 - Probability density for minimum temperature at Niamey airport with METNOHORHAM in May

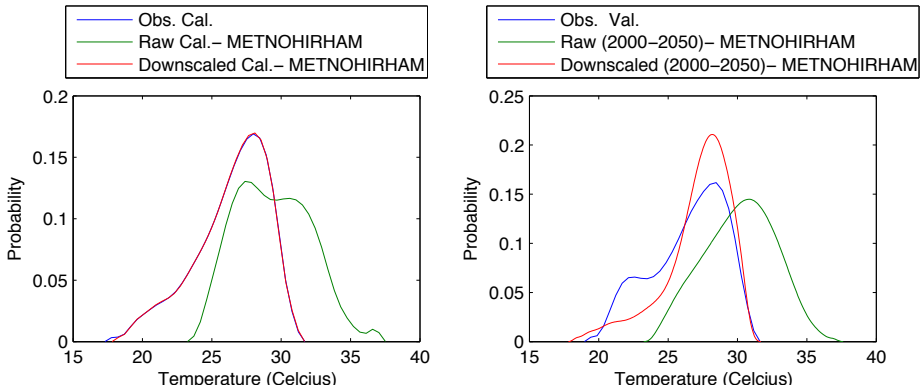

Figure 261 - Probability density for minimum temperature at Niamey airport with METNOHORHAM in June

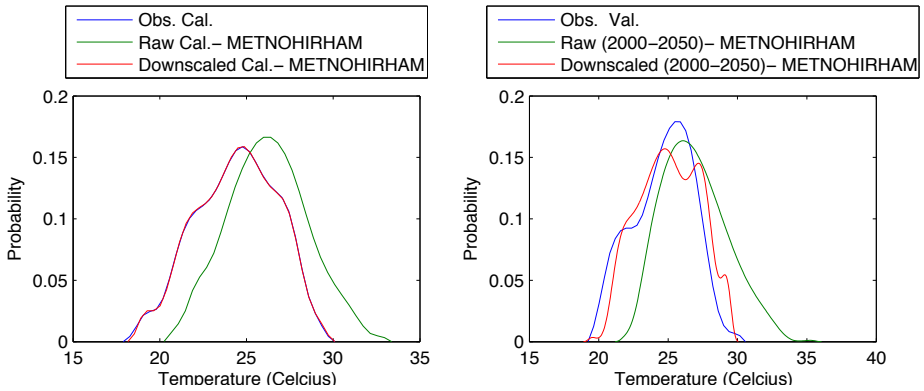

Figure 262 - Probability density for minimum temperature at Niamey airport with METNOHORHAM in July

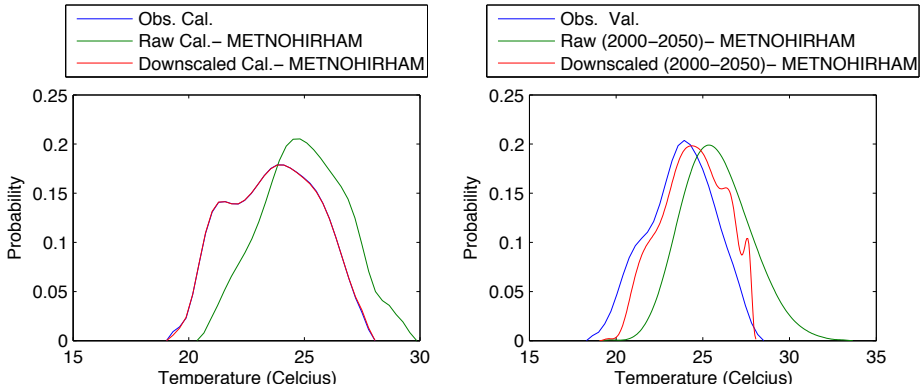

Figure 263 - Probability density for minimum temperature at Niamey airport with METNOHORHAM in August

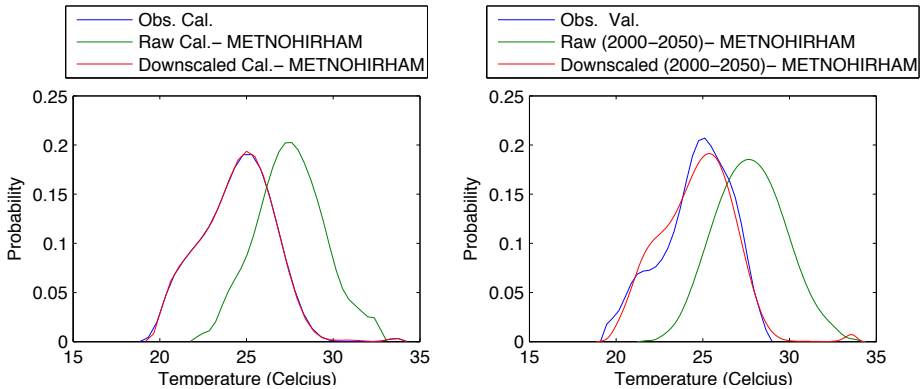

Figure 264 - Probability density for minimum temperature at Niamey airport with METNOHORHAM in September

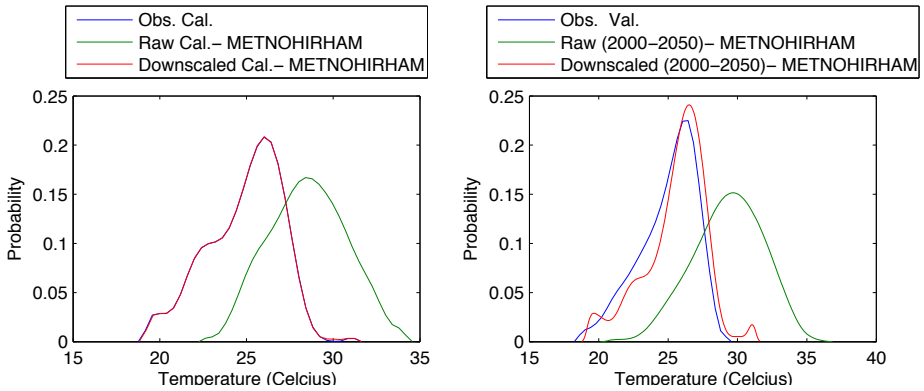

Figure 265 - Probability density for minimum temperature at Niamey airport with METNOHORHAM in October

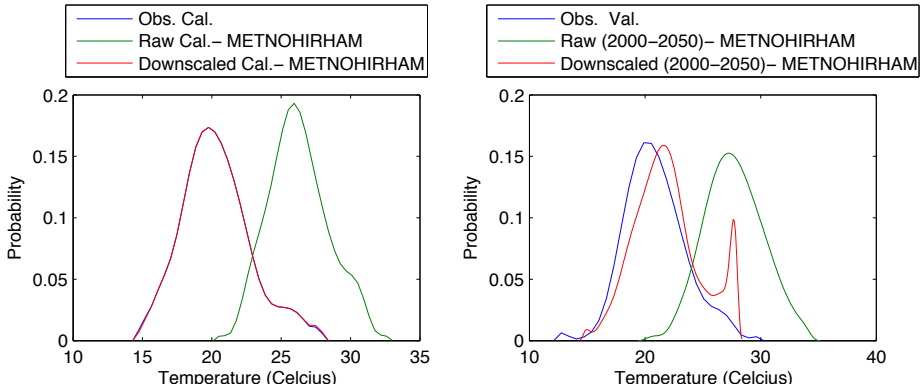

Figure 266 - Probability density for minimum temperature at Niamey airport with METNOHORHAM in November

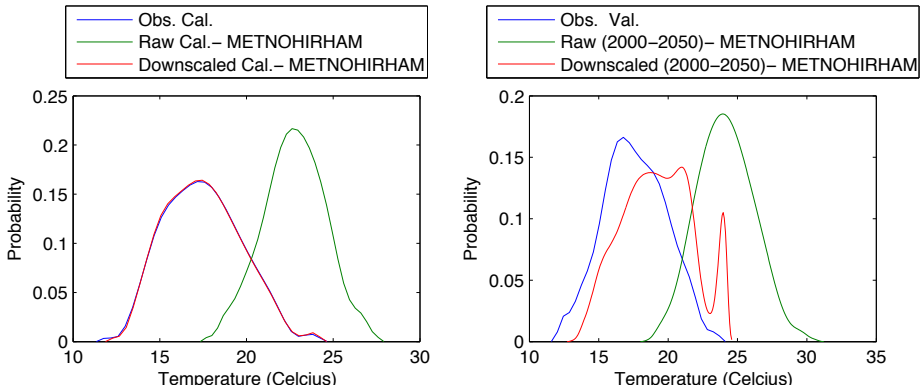

Figure 267 - Probability density for minimum temperature at Niamey airport with METNOHORHAM in December

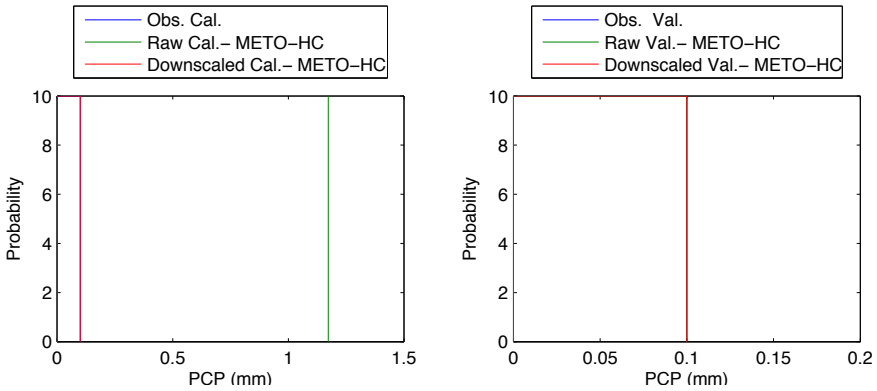

Figure 268 - Probability density of precipitation at Niamey airport with METO - HC in January

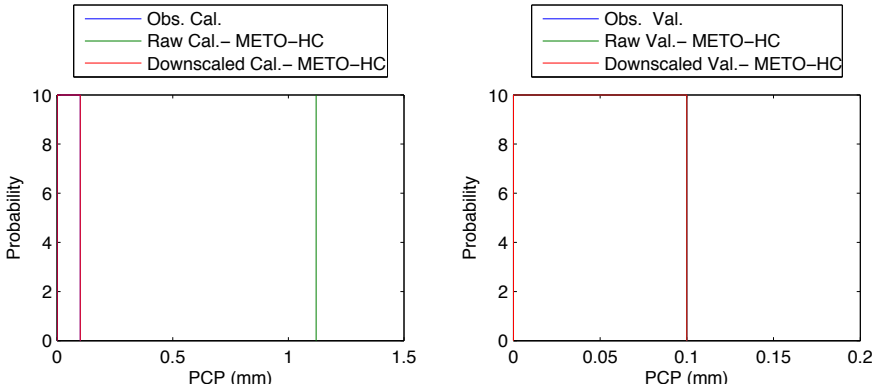

Figure 269 - Probability density of precipitation at Niamey airport with METO - HC in February

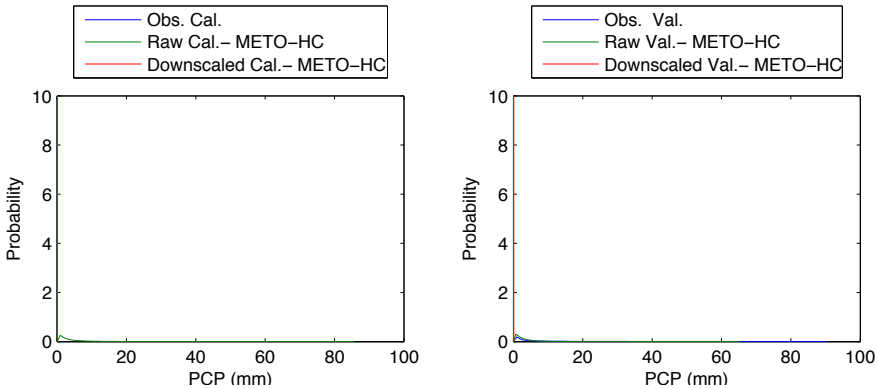

Figure 270 - Probability density of precipitation at Niamey airport with METO - HC in March

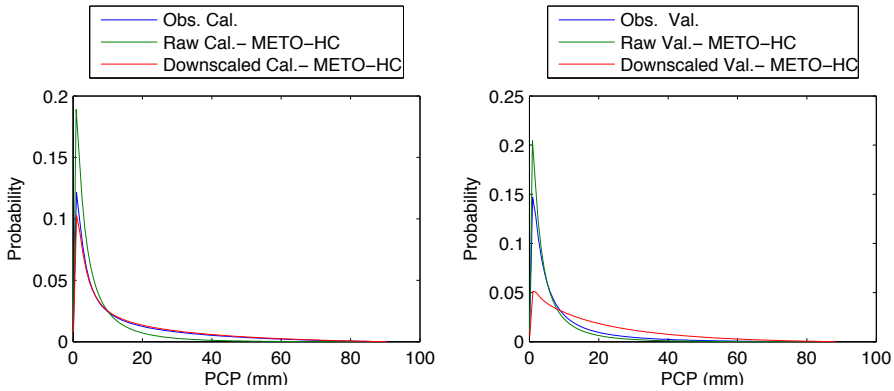

Figure 271 - Probability density of precipitation at Niamey airport with METO - HC in April

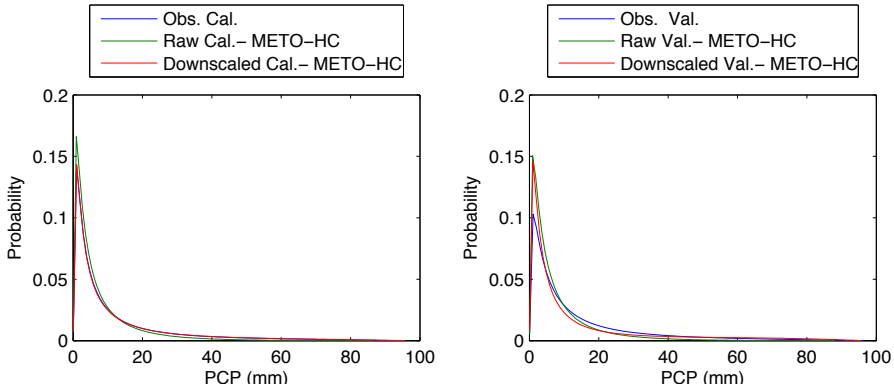

Figure 272 - Probability density of precipitation at Niamey airport with METO - HC in May

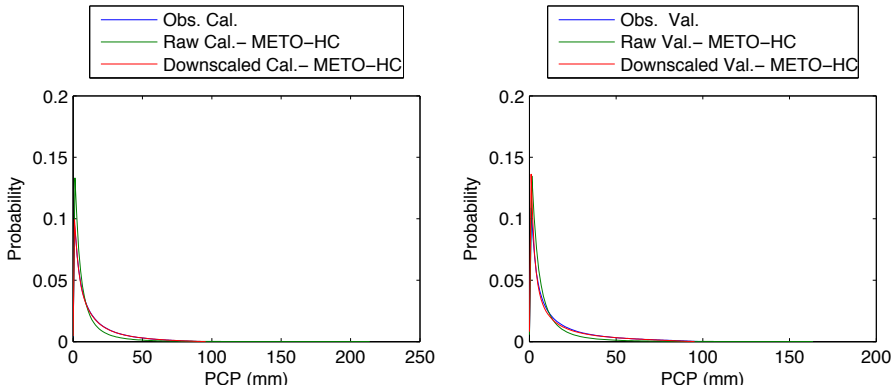

Figure 273 - Probability density of precipitation at Niamey airport with METO - HC in June

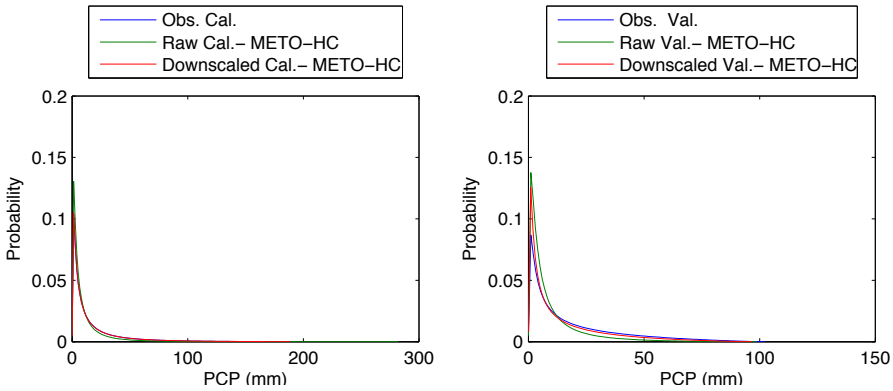

Figure 274 - Probability density of precipitation at Niamey airport with METO - HC in July

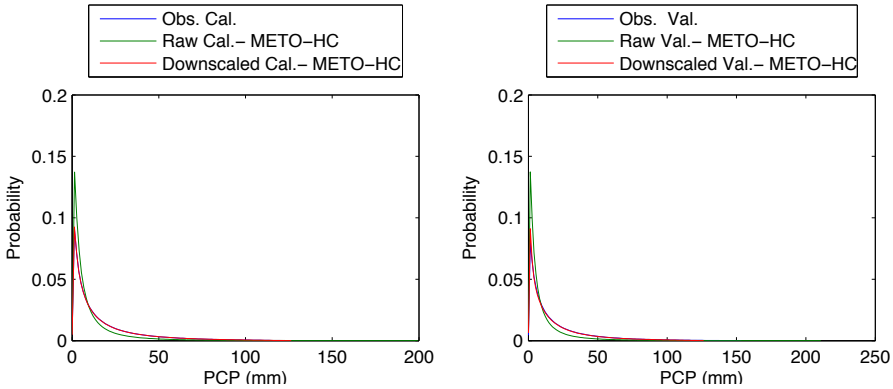

Figure 275 - Probability density of precipitation at Niamey airport with METO - HC in August

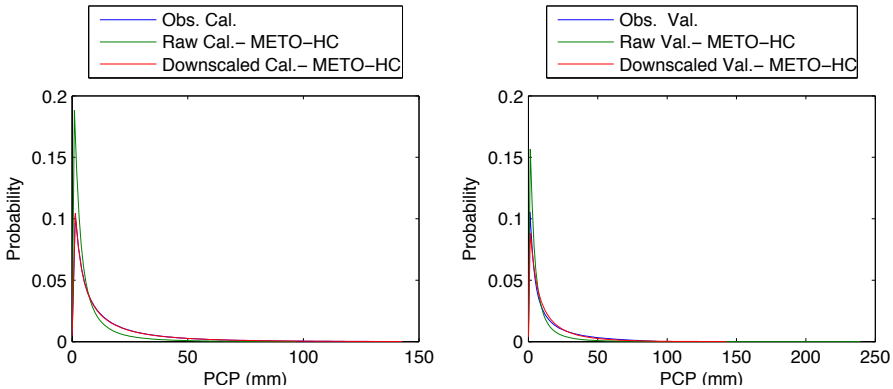

Figure 276 - Probability density of precipitation at Niamey airport with METO - HC in September

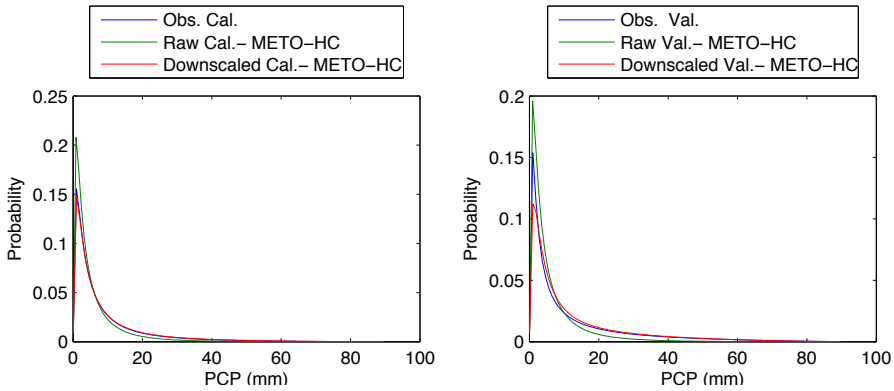

Figure 277 - Probability density of precipitation at Niamey airport with METO - HC in October

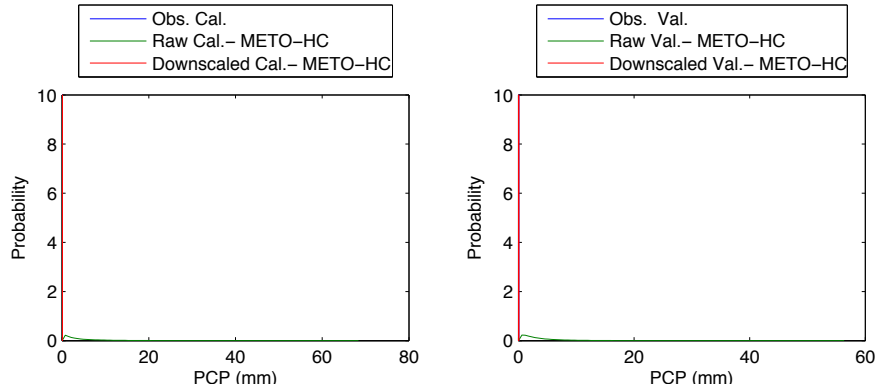

Figure 278 - Probability density of precipitation at Niamey airport with METO - HC in November

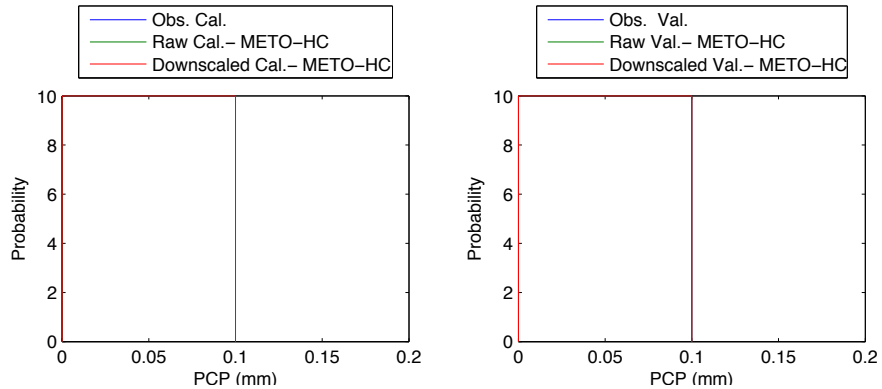

Figure 279 - Probability density of precipitation at Niamey airport with METO - HC in December

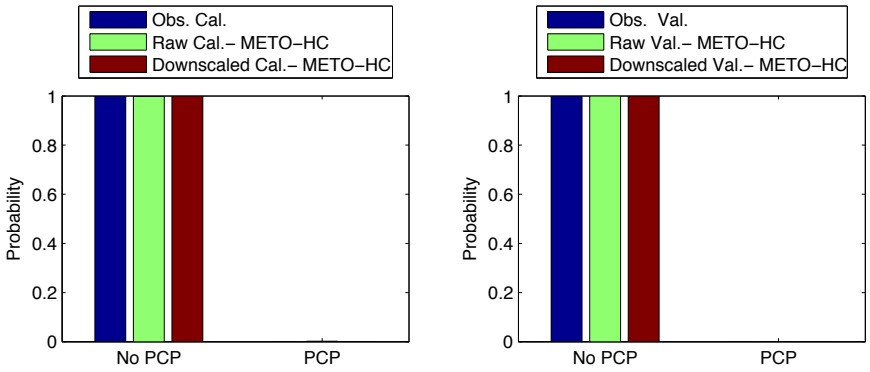

Figure 280 - Precipitation occurrence at Niamey airport with METO - HC in January

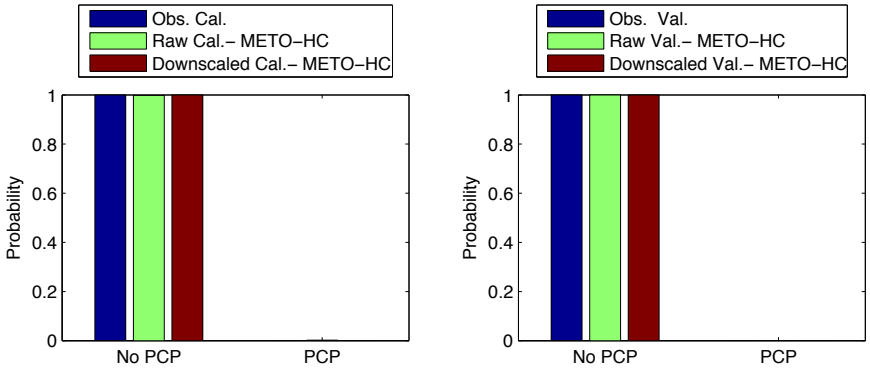

Figure 281 - Precipitation occurrence at Niamey airport with METO - HC in February

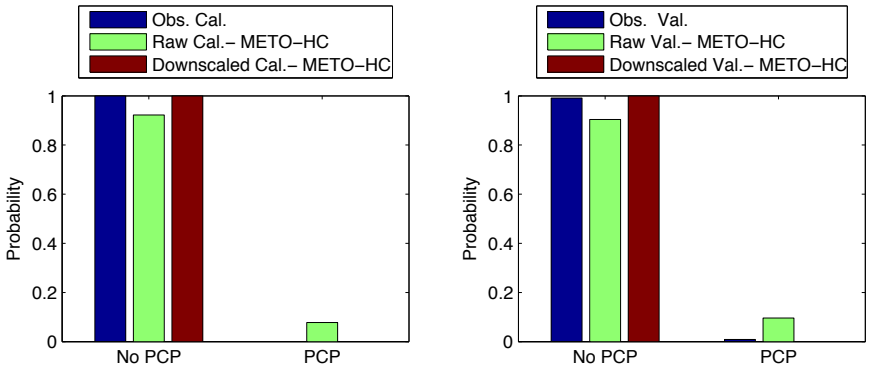

Figure 282 - Precipitation occurrence at Niamey airport with METO - HC in March

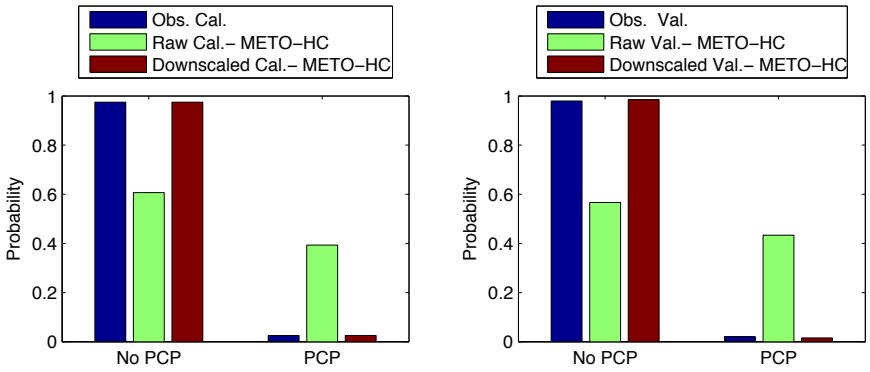

Figure 283 - Precipitation occurrence at Niamey airport with METO - HC in April

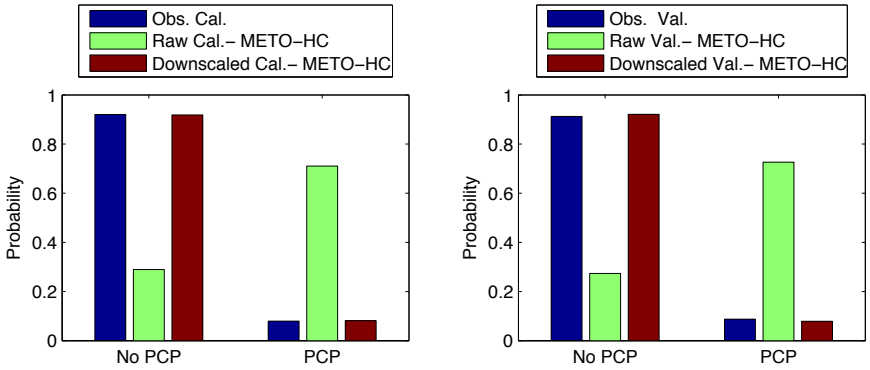

Figure 284 - Precipitation occurrence at Niamey airport with METO - HC in May

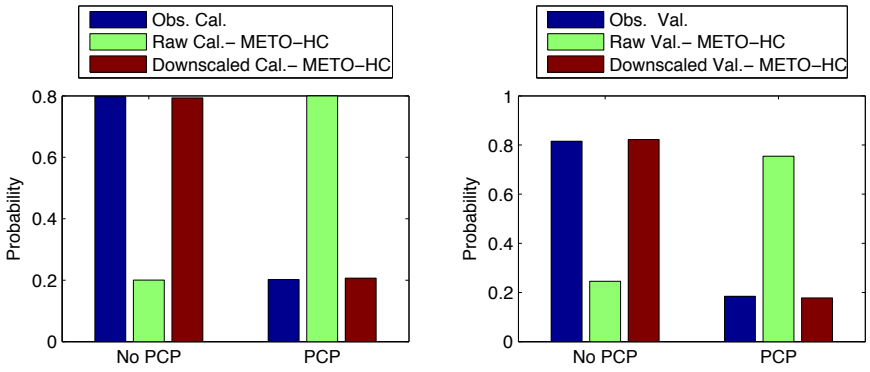

Figure 285 - Precipitation occurrence at Niamey airport with METO - HC in June

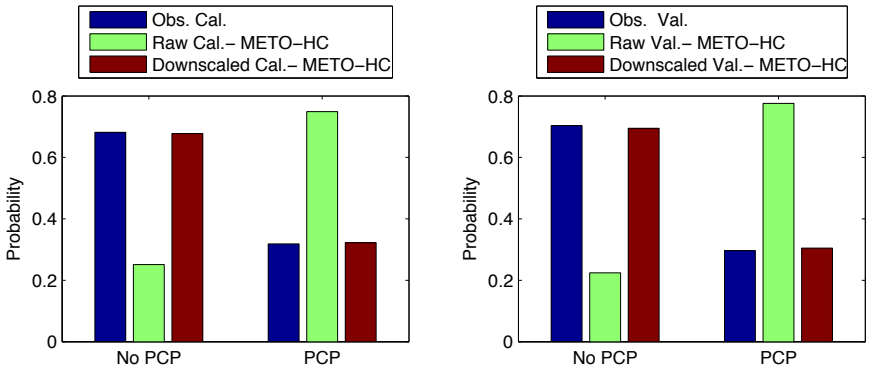

Figure 286 - Precipitation occurrence at Niamey airport with METO - HC in July

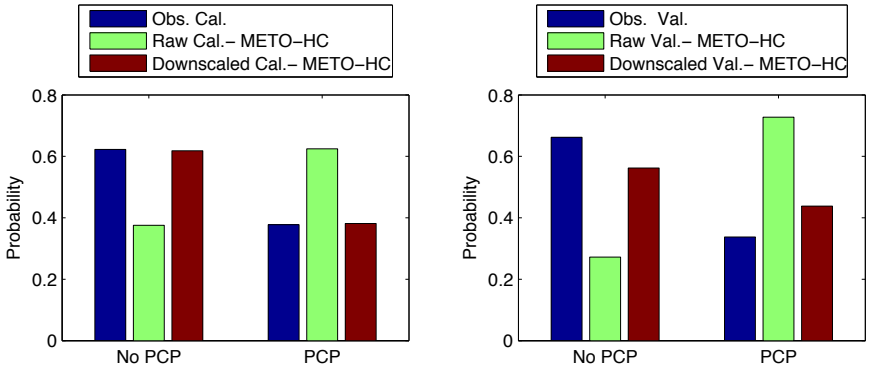

Figure 287 - Precipitation occurrence at Niamey airport with METO - HC in August

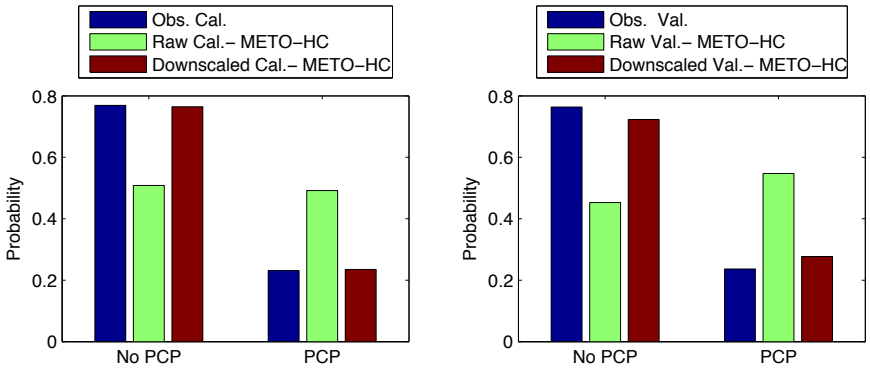

Figure 288 - Precipitation occurrence at Niamey airport with METO - HC in September

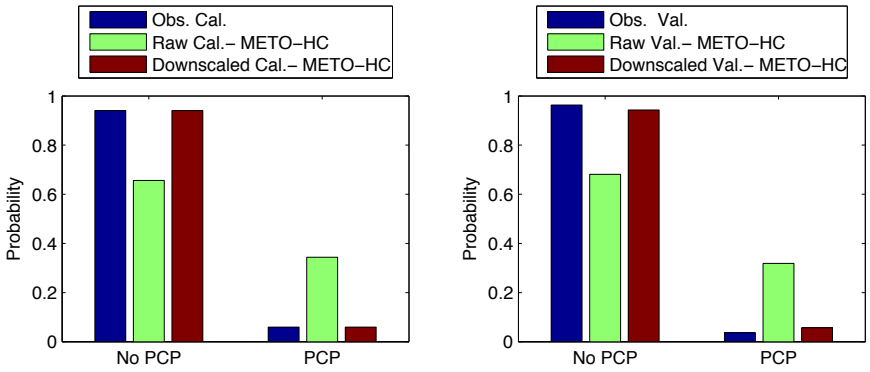

Figure 289 - Precipitation occurrence at Niamey airport with METO - HC in October

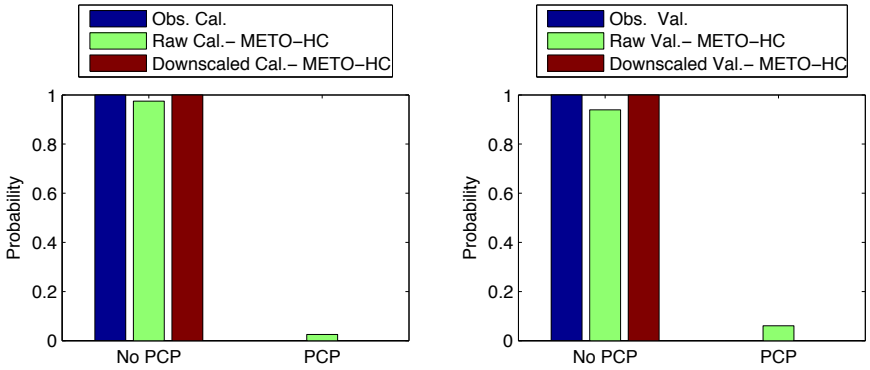

Figure 290 - Precipitation occurrence at Niamey airport with METO - HC in November

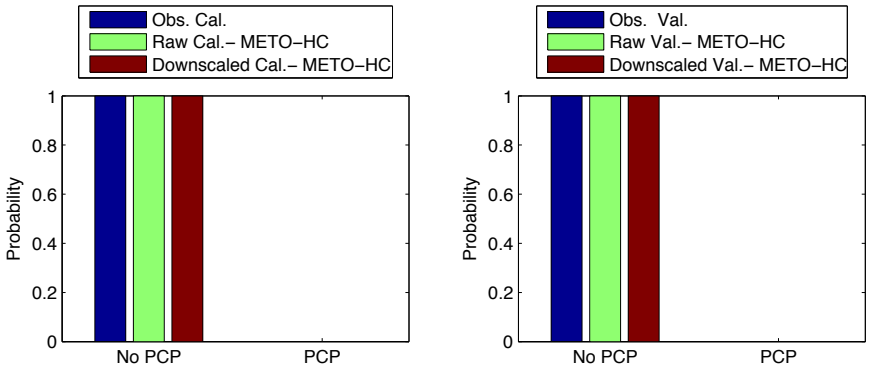

Figure 291 - Precipitation occurrence at Niamey airport with METO - HC in December

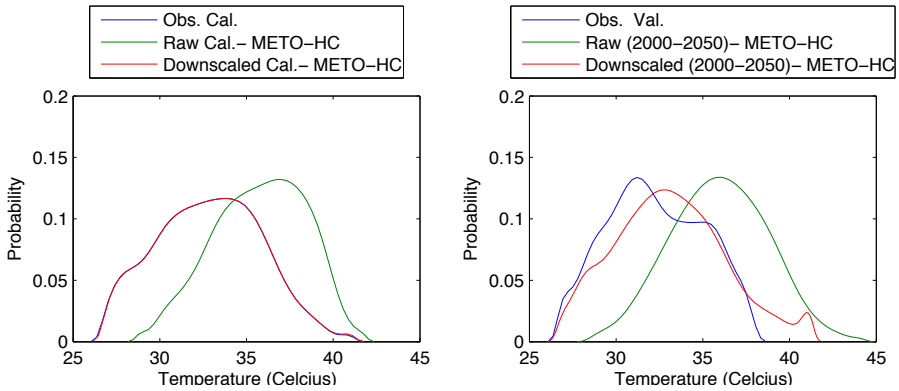

Figure 292 - Probability density for maximum temperature at Niamey airport with METO - HC in January

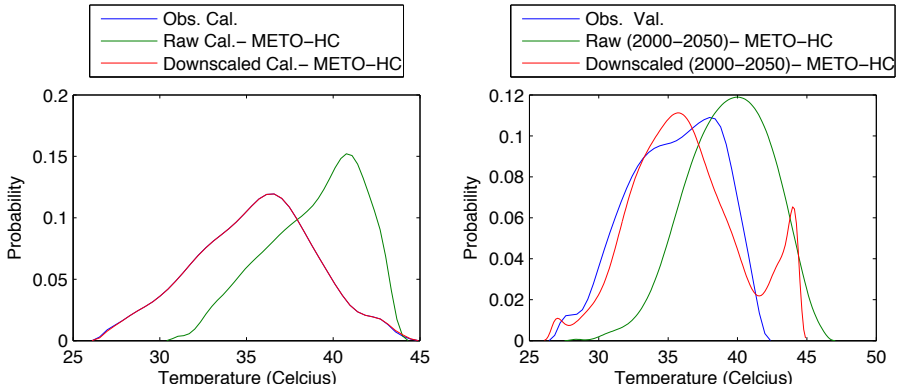

Figure 293 - Probability density for maximum temperature at Niamey airport with METO - HC in February

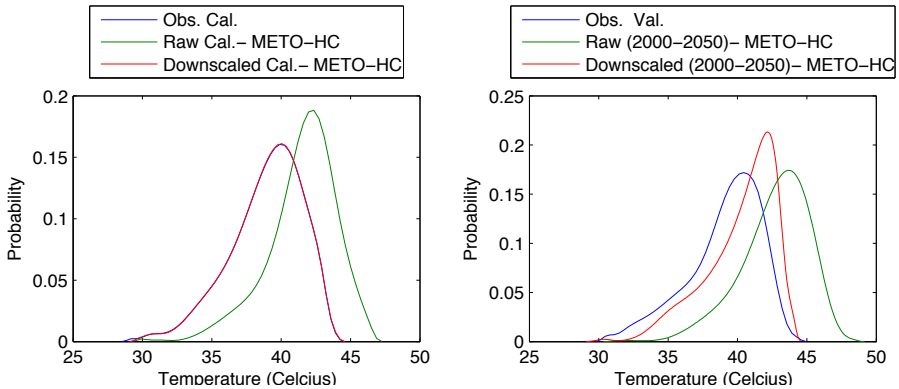

Figure 294 - Probability density for maximum temperature at Niamey airport with METO - HC in March

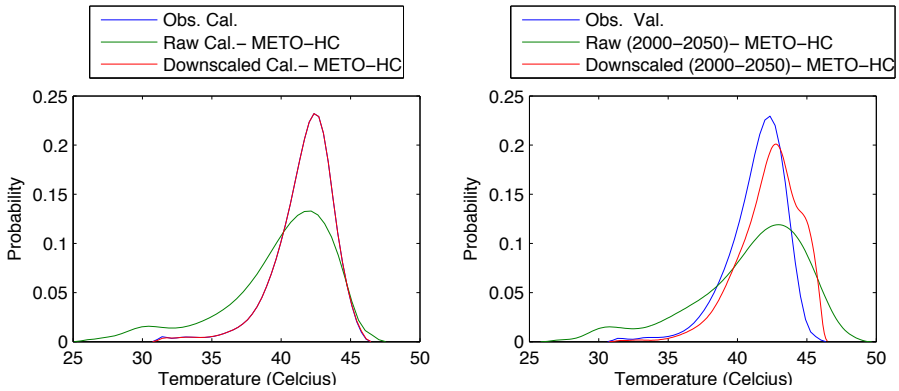

Figure 295 - Probability density for maximum temperature at Niamey airport with METO - HC in April

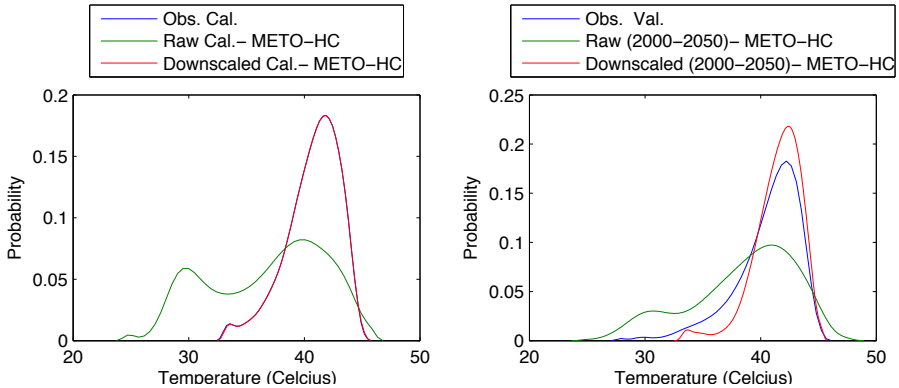

Figure 296 - Probability density for maximum temperature at Niamey airport with METO - HC in May

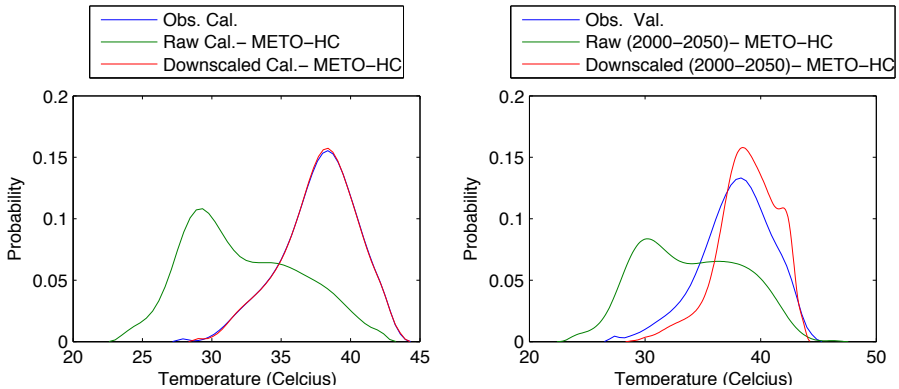

Figure 297 - Probability density for maximum temperature at Niamey airport with METO - HC in June

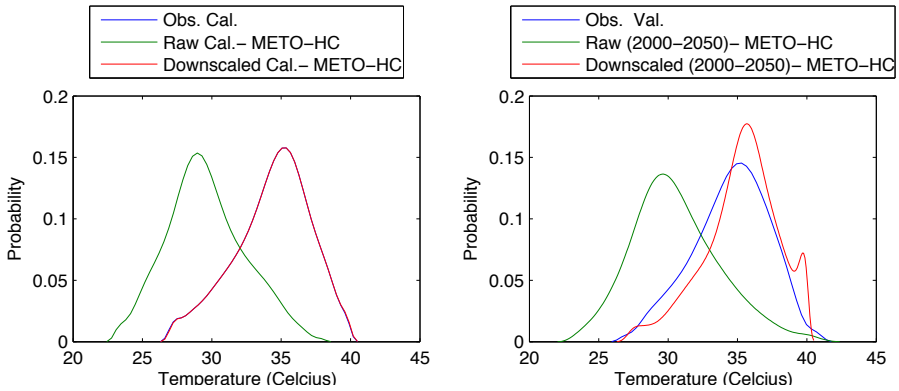

Figure 298 - Probability density for maximum temperature at Niamey airport with METO - HC in July

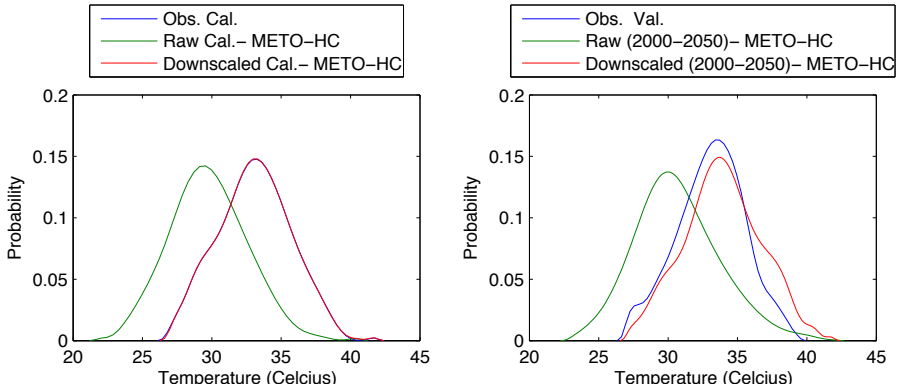

Figure 299 - Probability density for maximum temperature at Niamey airport with METO - HC in August

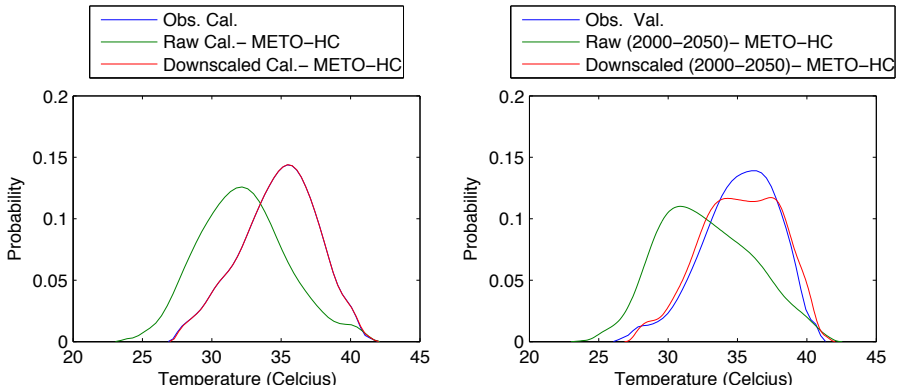

Figure 300 - Probability density for maximum temperature at Niamey airport with METO - HC in September

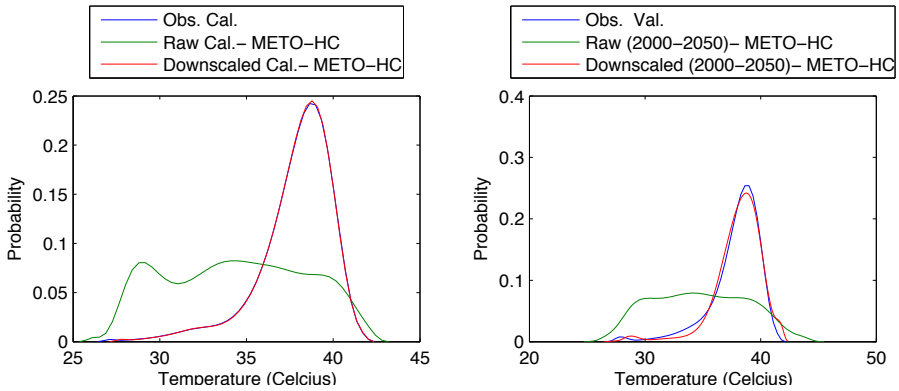

Figure 301 - Probability density for maximum temperature at Niamey airport with METO - HC in October

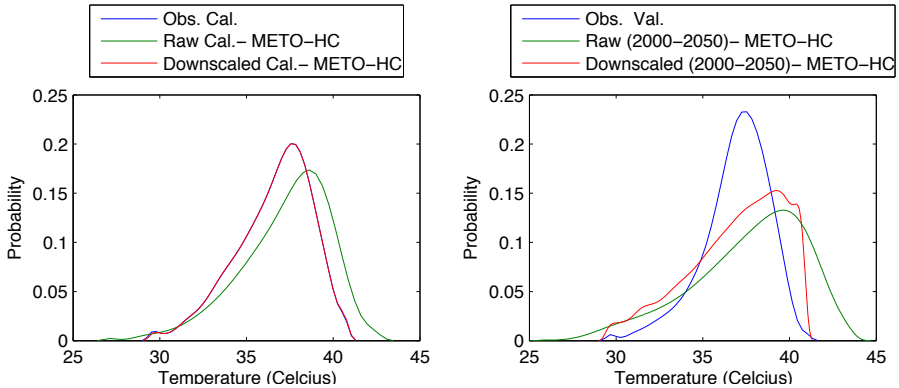

Figure 302 - Probability density for maximum temperature at Niamey airport with METO - HC in November

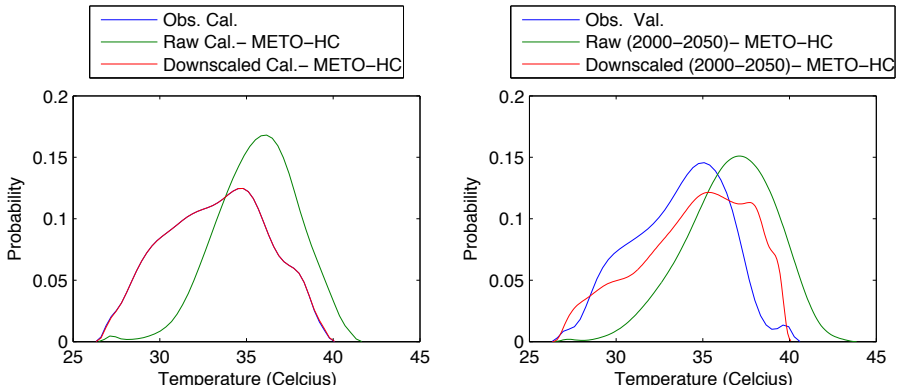

Figure 303 - Probability density for maximum temperature at Niamey airport with METO - HC in December

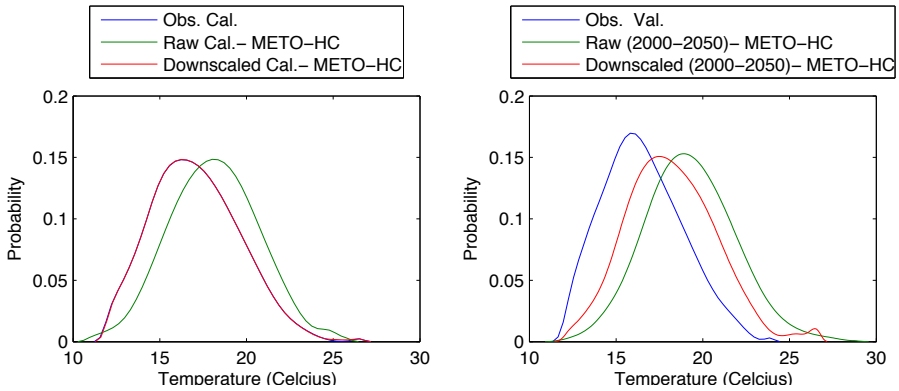

Figure 304 - Probability density for minimum temperature at Niamey airport with METO - HC in January

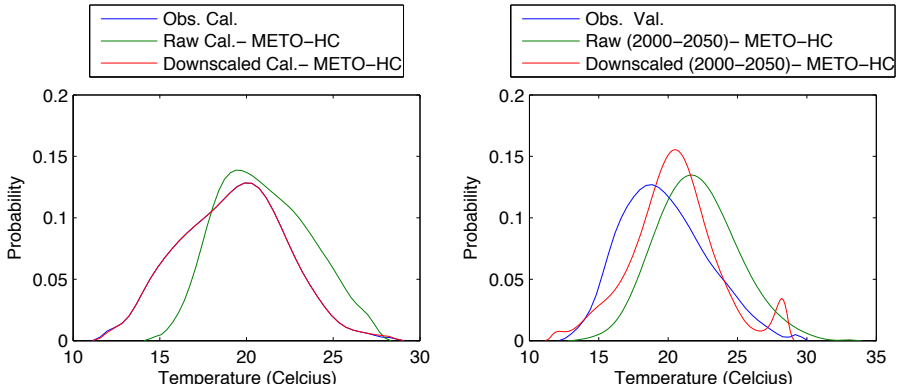

Figure 305 - Probability density for minimum temperature at Niamey airport with METO - HC in February

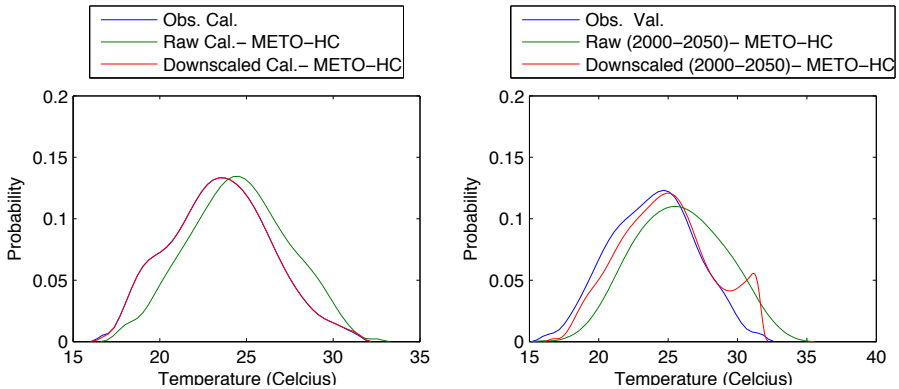

Figure 306 - Probability density for minimum temperature at Niamey airport with METO - HC in March

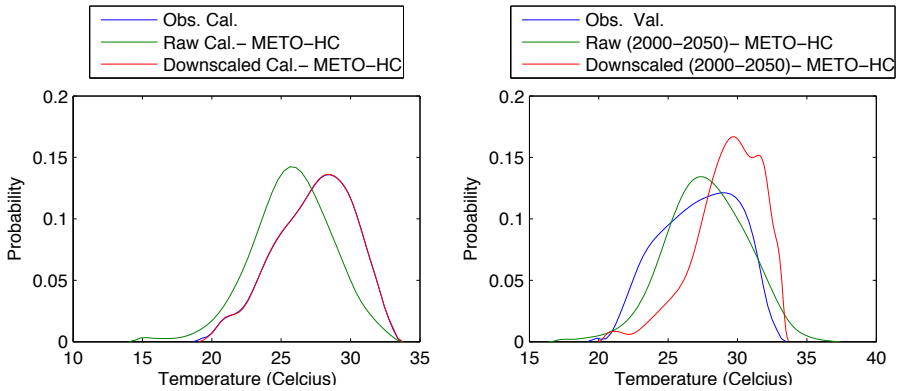

Figure 307 - Probability density for minimum temperature at Niamey airport with METO - HC in April

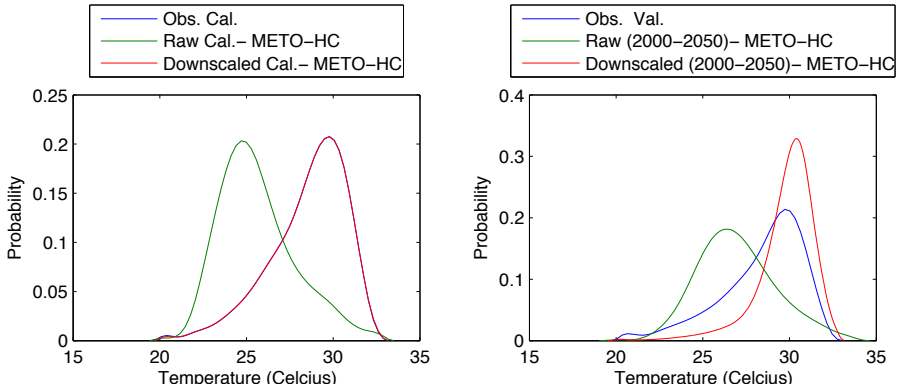

Figure 308 - Probability density for minimum temperature at Niamey airport with METO - HC in May

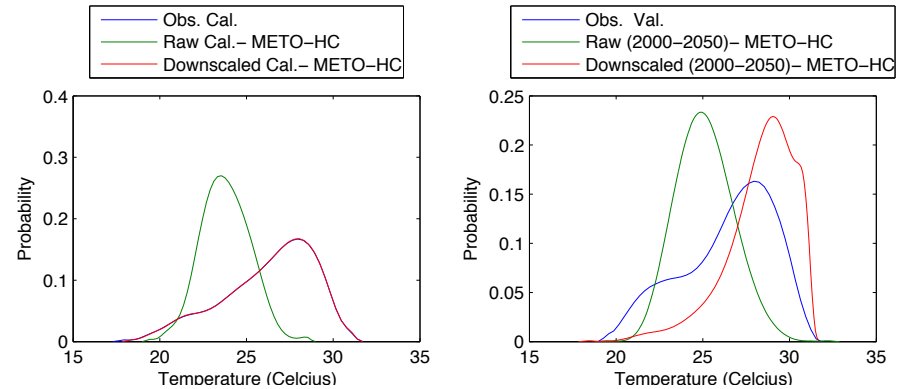

Figure 309 - Probability density for minimum temperature at Niamey airport with METO - HC in June

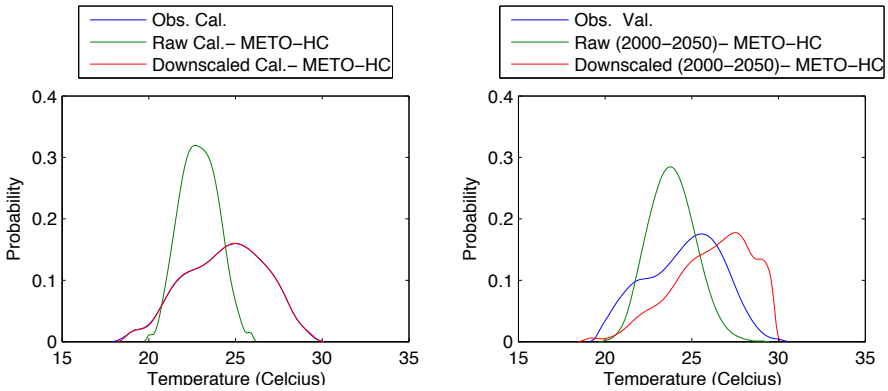

Figure 310 - Probability density for minimum temperature at Niamey airport with METO - HC in July

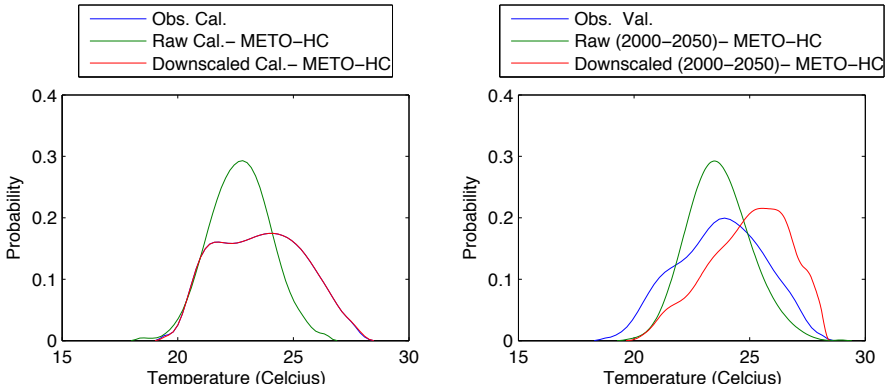

Figure 311 - Probability density for minimum temperature at Niamey airport with METO - HC in August

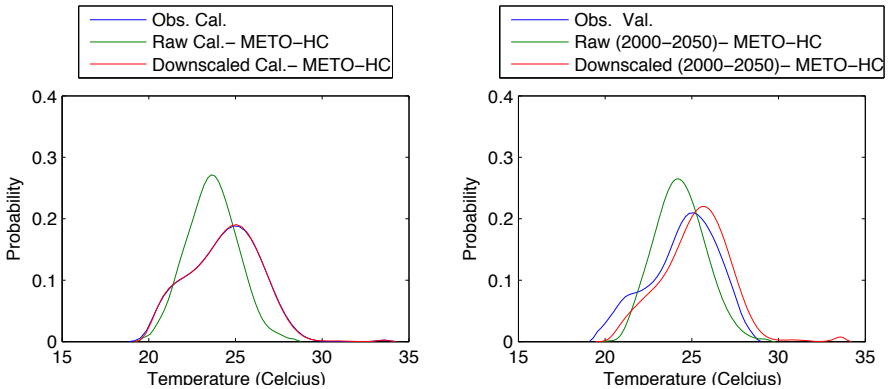

Figure 312 - Probability density for minimum temperature at Niamey airport with METO - HC in September

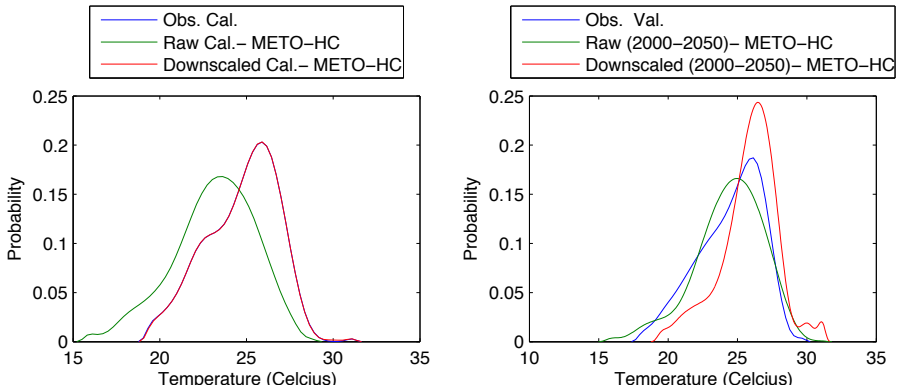

Figure 313 - Probability density for minimum temperature at Niamey airport with METO - HC in October

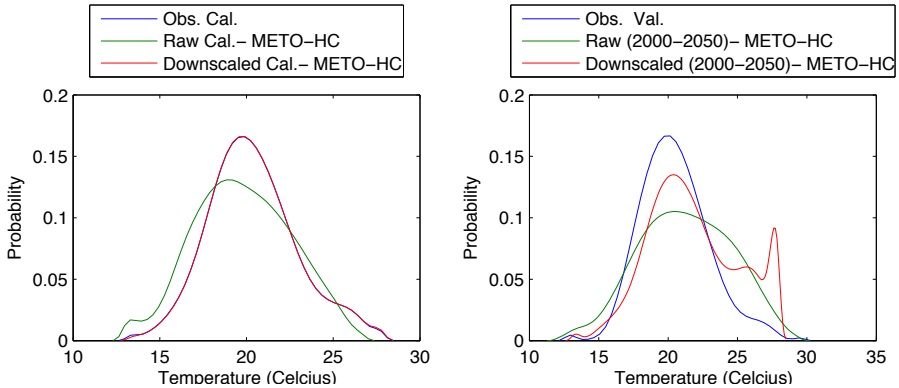

Figure 314 - Probability density for minimum temperature at Niamey airport with METO - HC in November

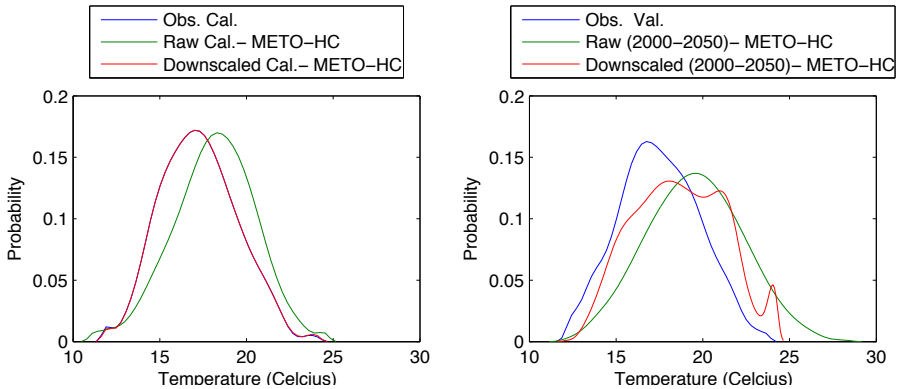

Figure 315 - Probability density for minimum temperature at Niamey airport with METO - HC in December

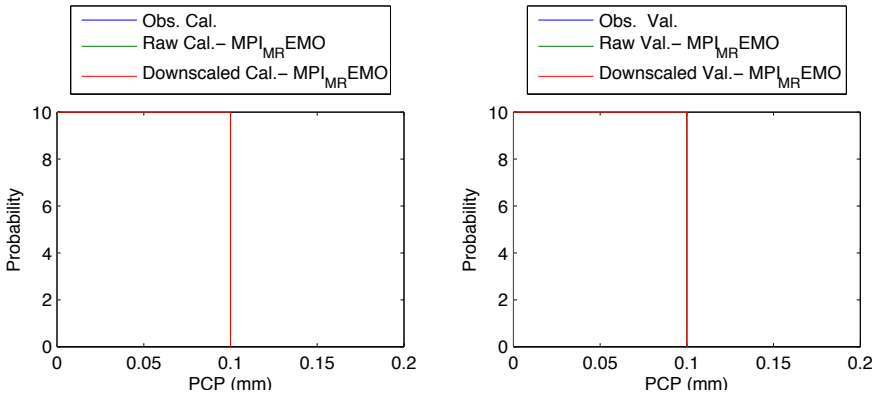

Figure 316 - Probability density of precipitation at Niamey airport with MPI - M - REMO in January

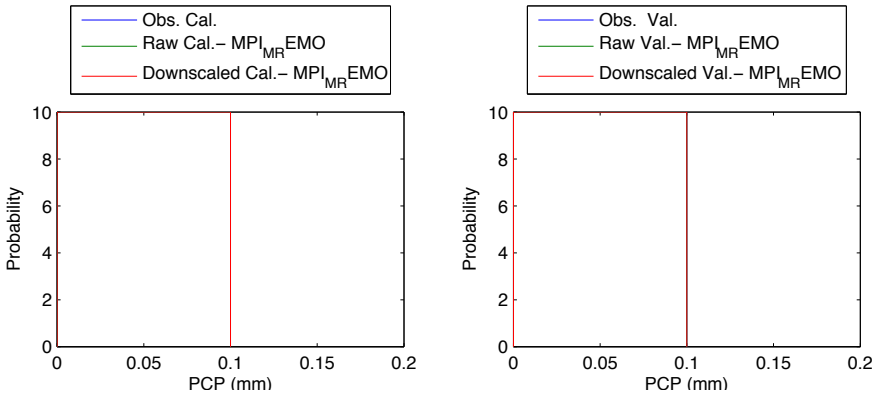

Figure 317 - Probability density of precipitation at Niamey airport with MPI - M - REMO in February

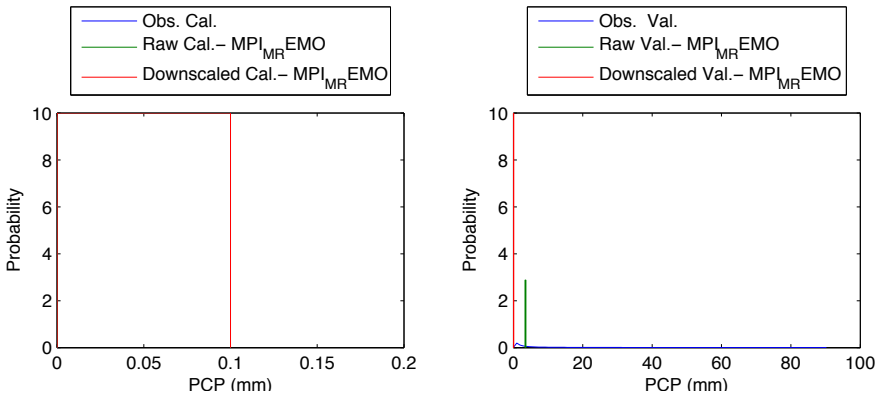

Figure 318 - Probability density of precipitation at Niamey airport with MPI - M - REMO in March

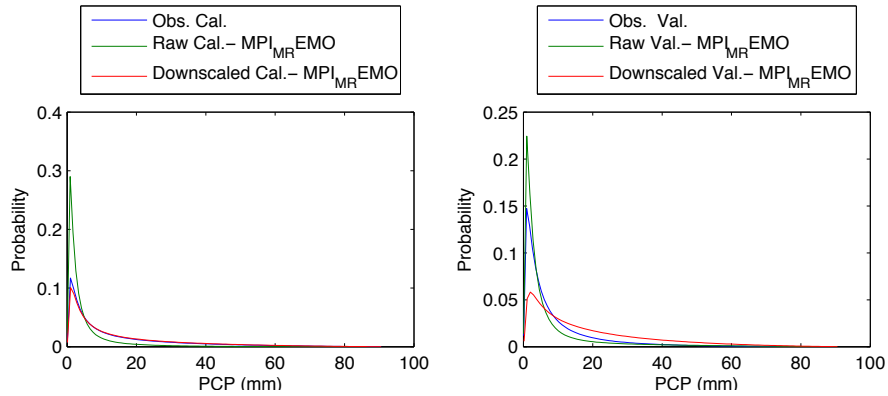

Figure 319 - Probability density of precipitation at Niamey airport with MPI - M - REMO in April

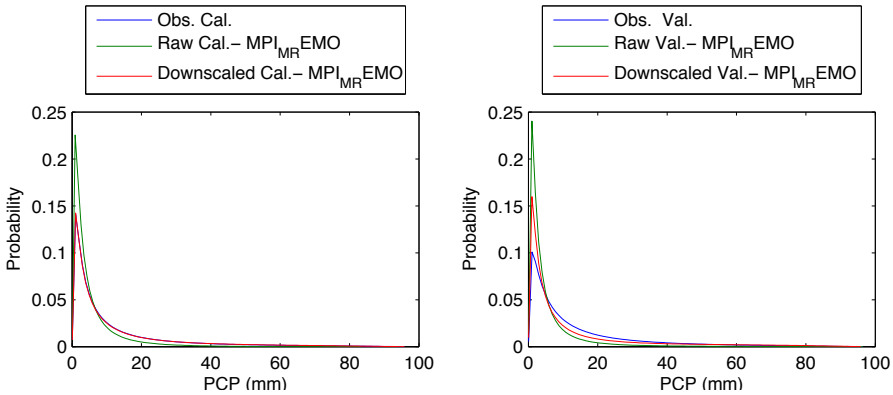

Figure 320 - Probability density of precipitation at Niamey airport with MPI - M - REMO in May

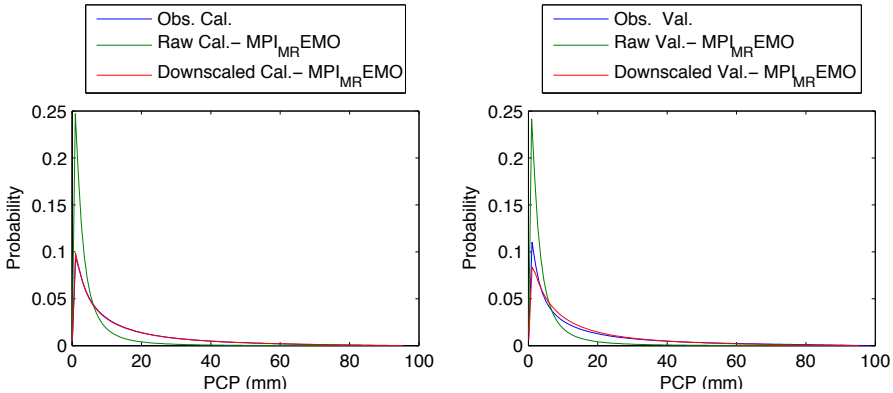

Figure 321 - Probability density of precipitation at Niamey airport with MPI - M - REMO in June

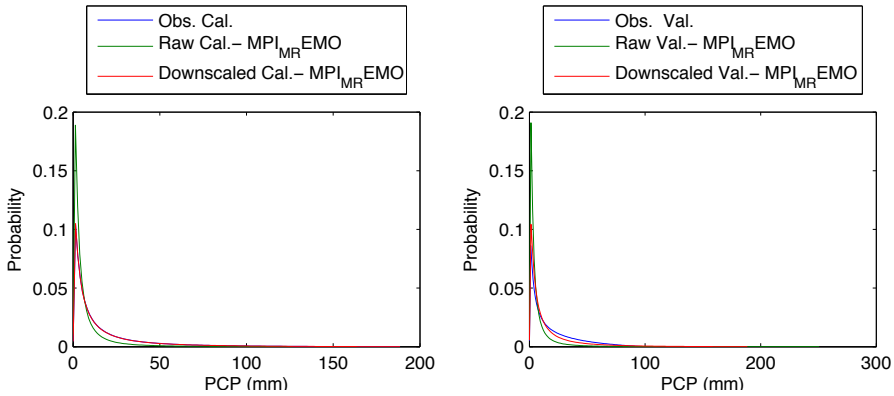

Figure 322 - Probability density of precipitation at Niamey airport with MPI - M - REMO in July

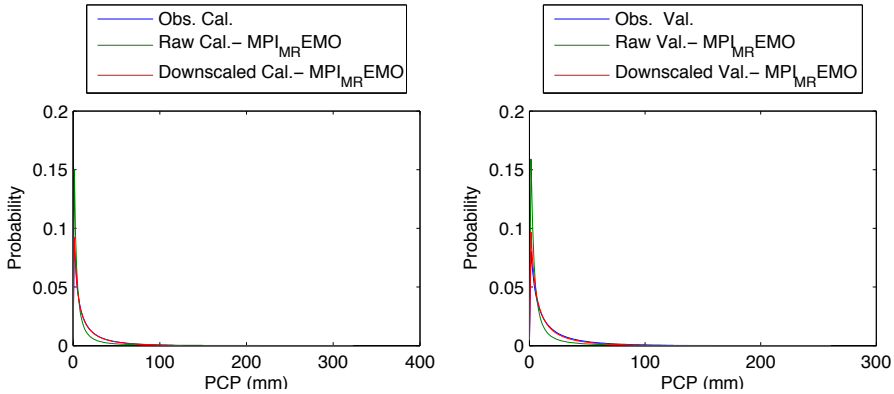

Figure 323 - Probability density of precipitation at Niamey airport with MPI - M - REMO in August

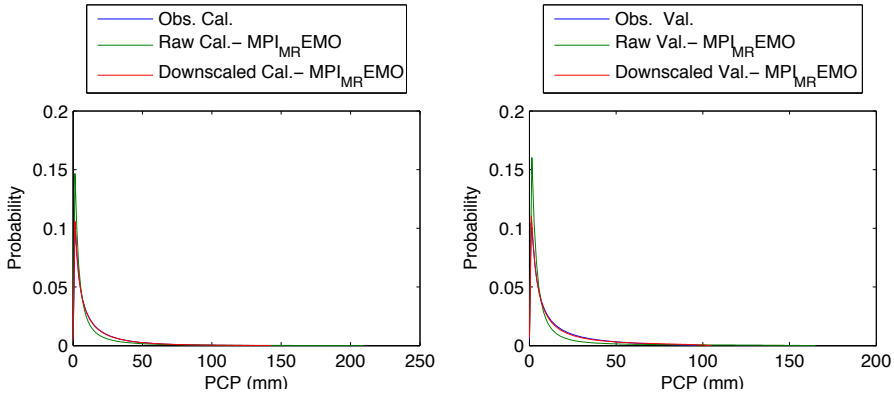

Figure 324 - Probability density of precipitation at Niamey airport with MPI - M - REMO in September

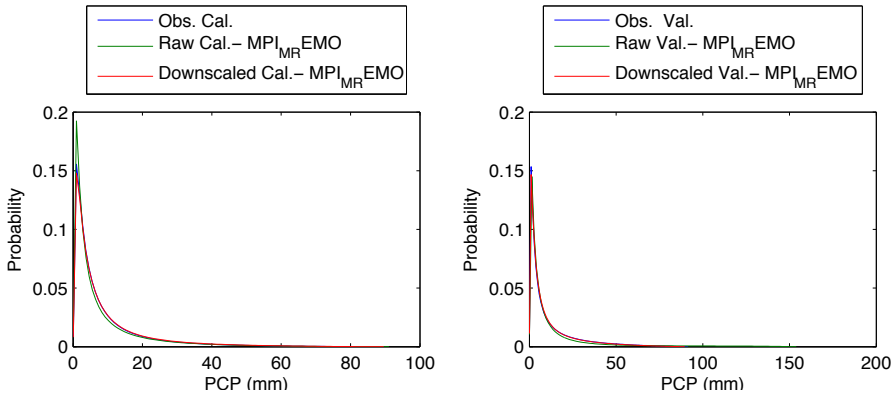

Figure 325 - Probability density of precipitation at Niamey airport with MPI - M - REMO in October

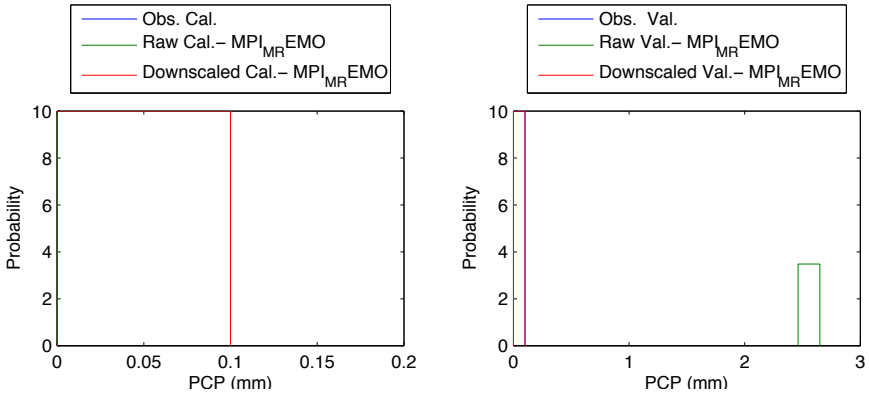

Figure 326 - Probability density of precipitation at Niamey airport with MPI - M - REMO in November

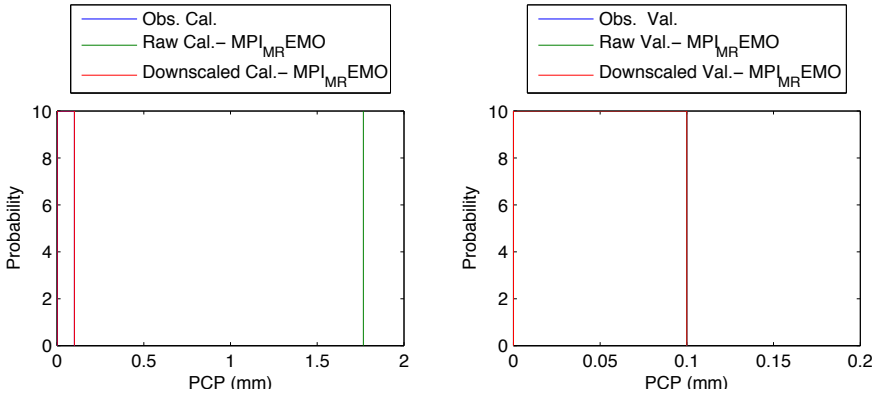

Figure 327 - Probability density of precipitation at Niamey airport with MPI - M - REMO in December

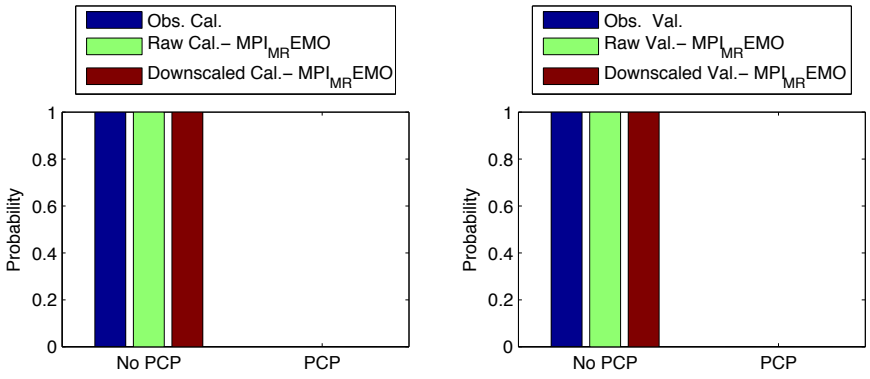

Figure 328 - Precipitation occurrence at Niamey airport with MPI - M - REMO in January

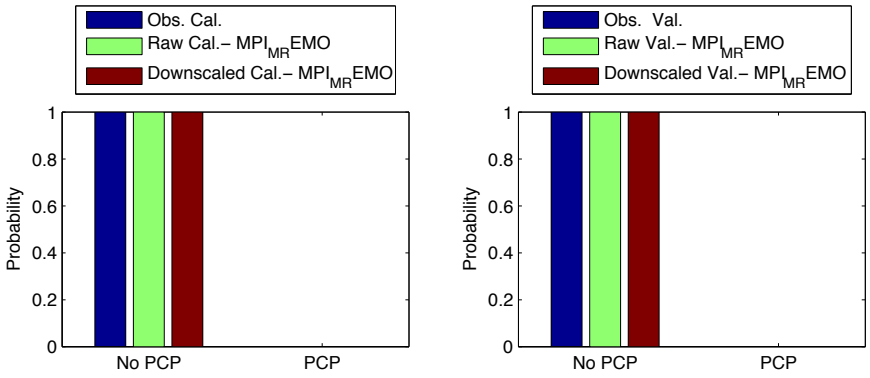

Figure 329 - Precipitation occurrence at Niamey airport with MPI - M - REMO in February

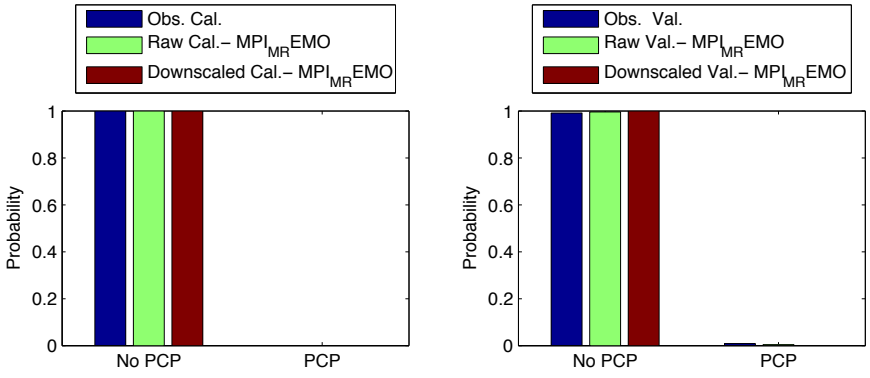

Figure 330 - Precipitation occurrence at Niamey airport with MPI - M - REMO in March

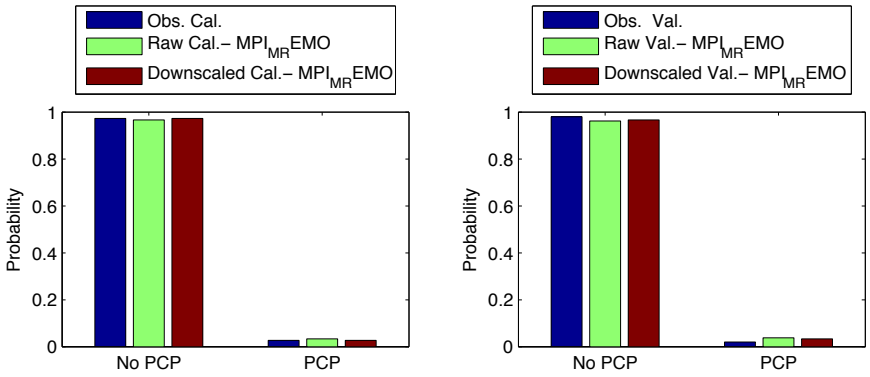

Figure 331 - Precipitation occurrence at Niamey airport with MPI - M - REMO in April

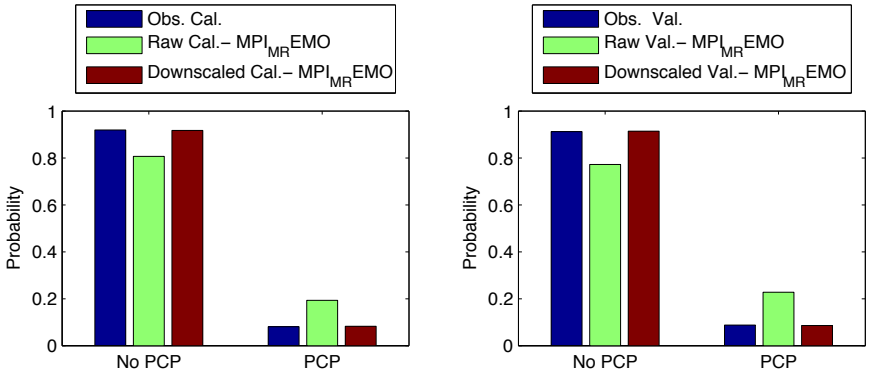

Figure 332 - Precipitation occurrence at Niamey airport with MPI - M - REMO in May

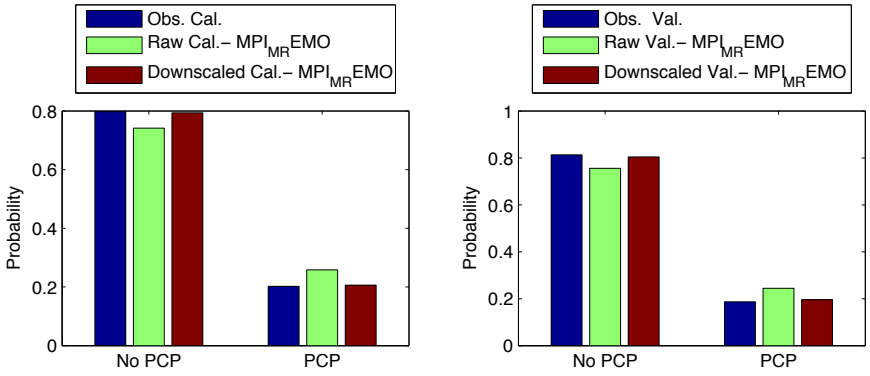

Figure 333 - Precipitation occurrence at Niamey airport with MPI - M - REMO in June

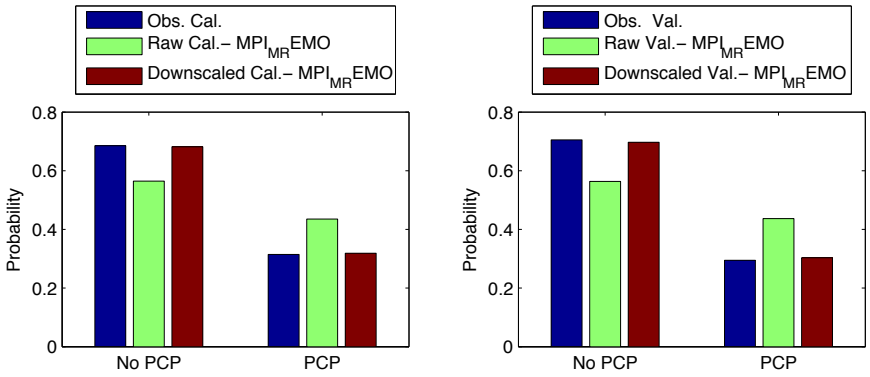

Figure 334 - Precipitation occurrence at Niamey airport with MPI - M - REMO in July

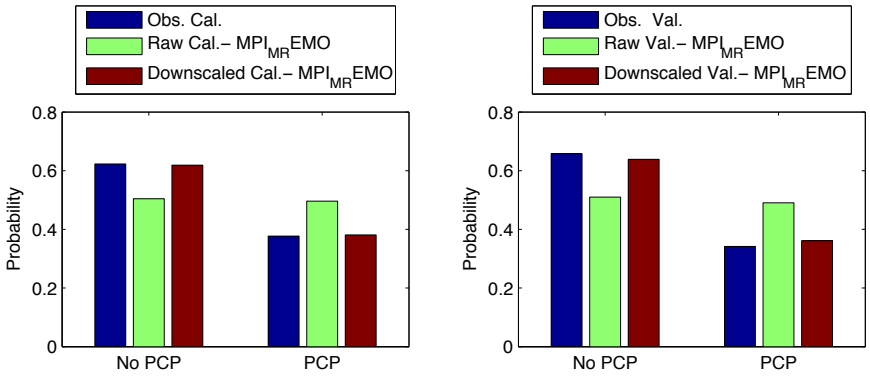

Figure 335 - Precipitation occurrence at Niamey airport with MPI - M - REMO in August

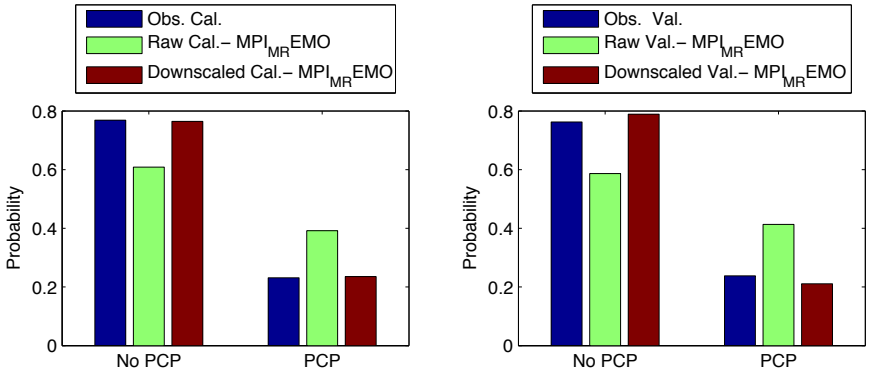

Figure 336 - Precipitation occurrence at Niamey airport with MPI - M - REMO in September

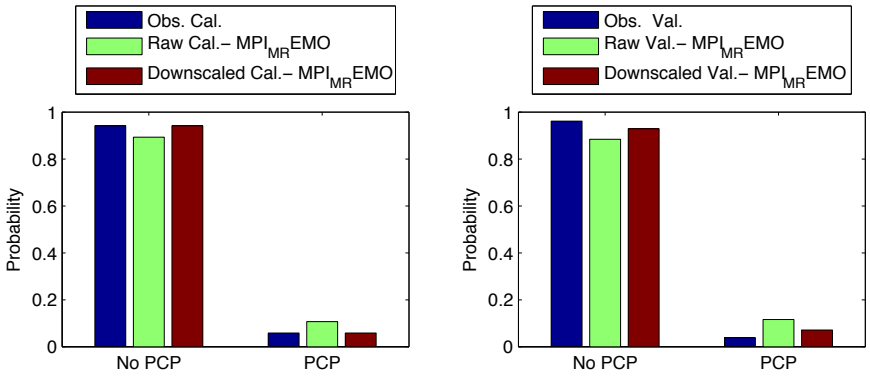

Figure 337 - Precipitation occurrence at Niamey airport with MPI - M - REMO in October

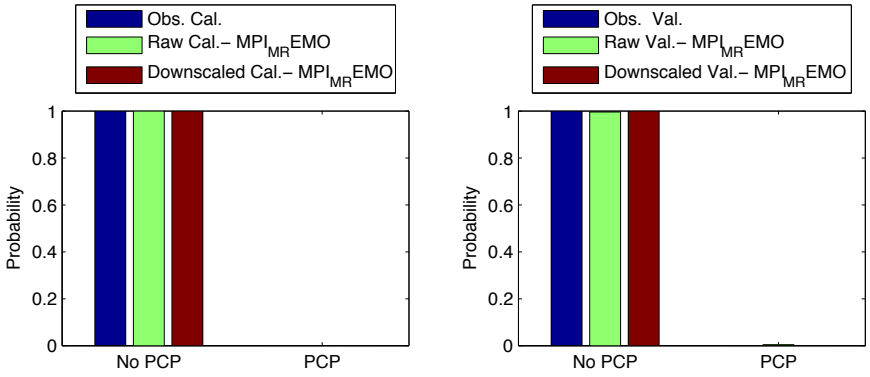

Figure 338 - Precipitation occurrence at Niamey airport with MPI - M - REMO in November

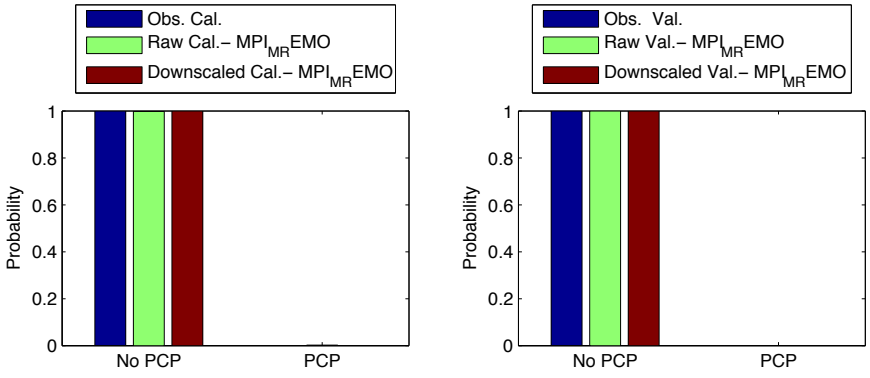

Figure 339 - Precipitation occurrence at Niamey airport with MPI - M - REMO in December

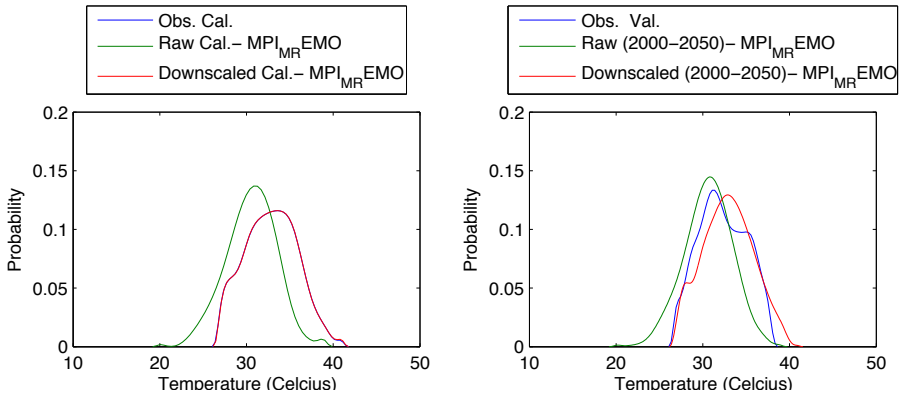

Figure 340 - Probability density for maximum temperature at Niamey airport with MPI - M - REMO in January

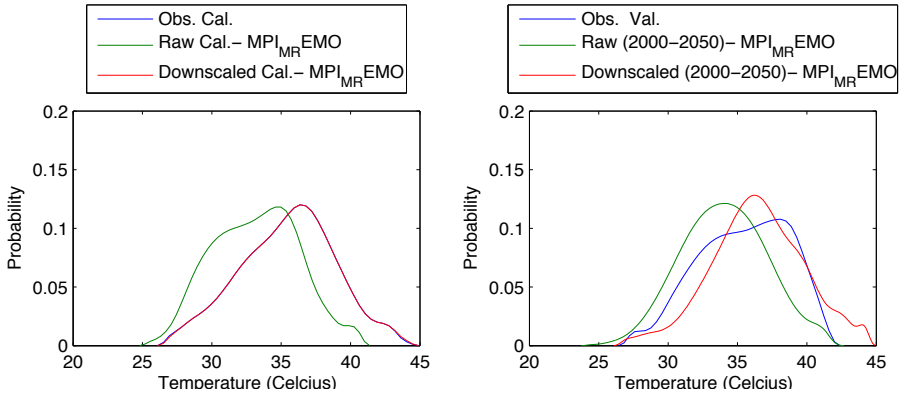

Figure 341 - Probability density for maximum temperature at Niamey airport with MPI - M - REMO in February

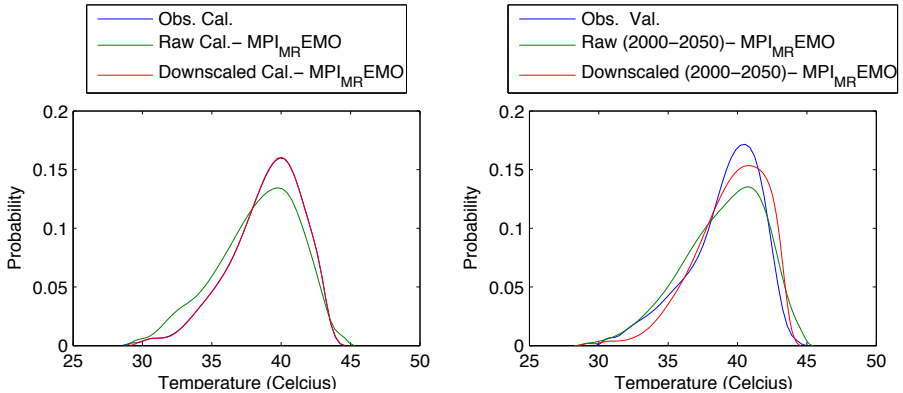

Figure 342 - Probability density for maximum temperature at Niamey airport with MPI - M - REMO in March

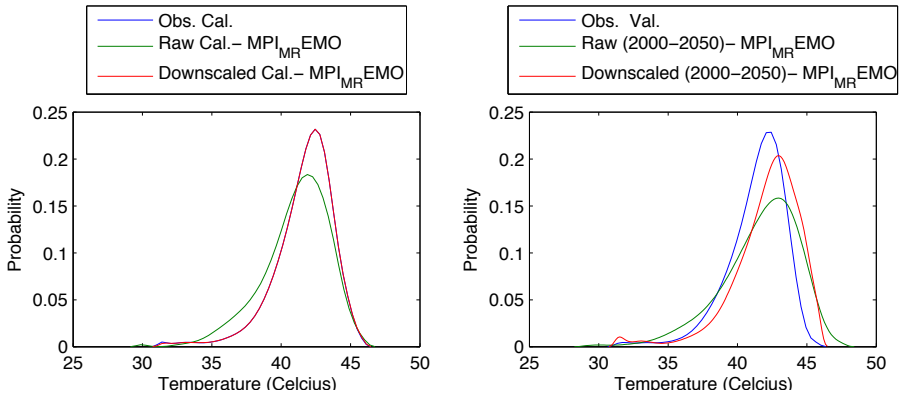

Figure 343 - Probability density for maximum temperature at Niamey airport with MPI - M - REMO in April

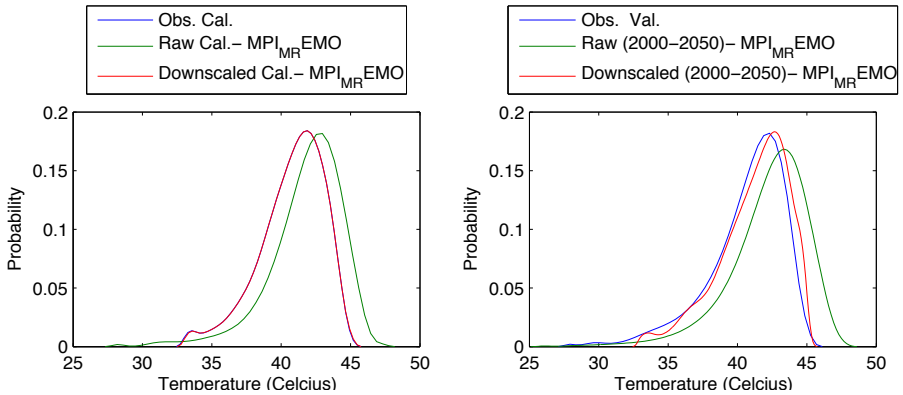

Figure 344 - Probability density for maximum temperature at Niamey airport with MPI - M - REMO in May

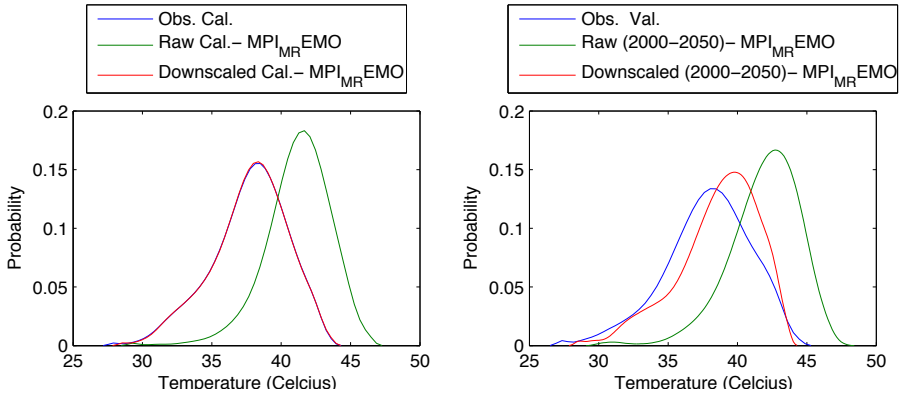

Figure 345 - Probability density for maximum temperature at Niamey airport with MPI - M - REMO in June

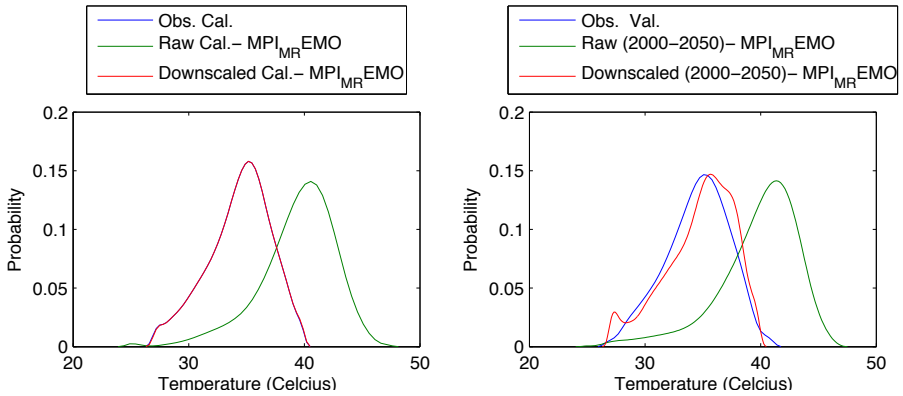

Figure 346 - Probability density for maximum temperature at Niamey airport with MPI - M - REMO in July

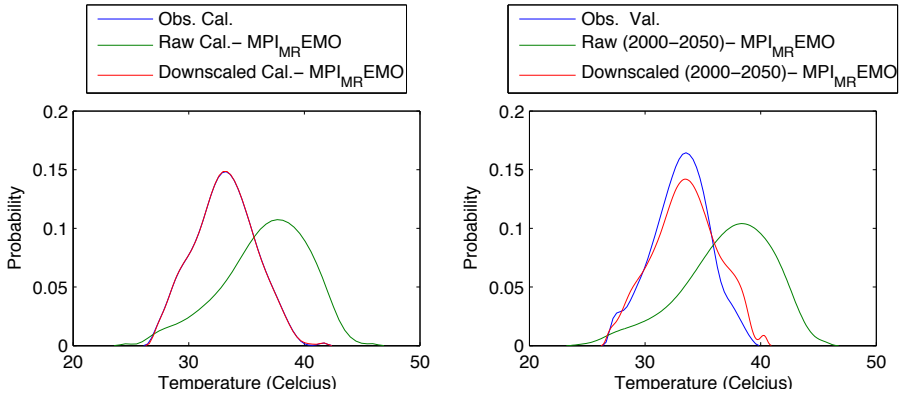

Figure 347 - Probability density for maximum temperature at Niamey airport with MPI - M - REMO in August

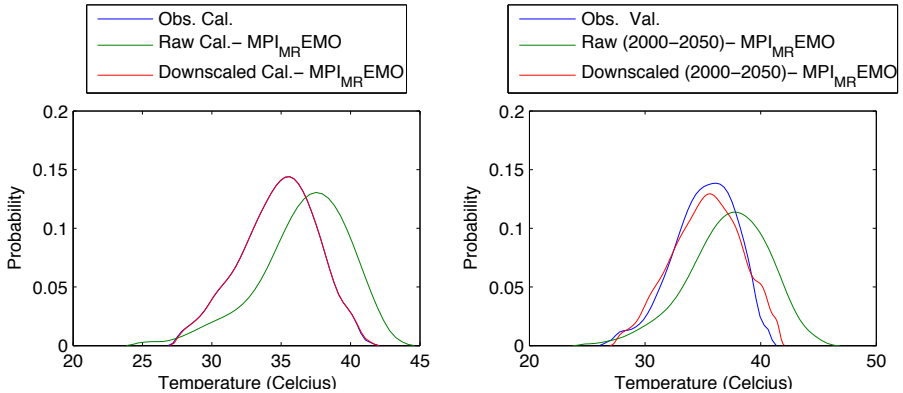

Figure 348 - Probability density for maximum temperature at Niamey airport with MPI - M - REMO in September

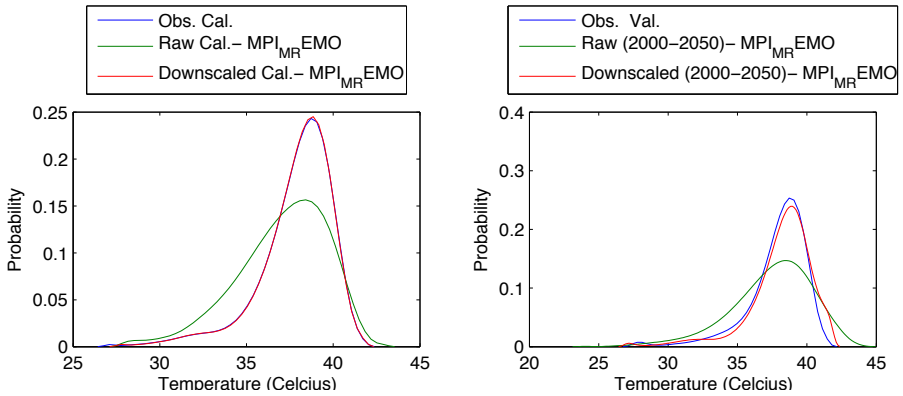

Figure 349 - Probability density for maximum temperature at Niamey airport with MPI - M - REMO in October

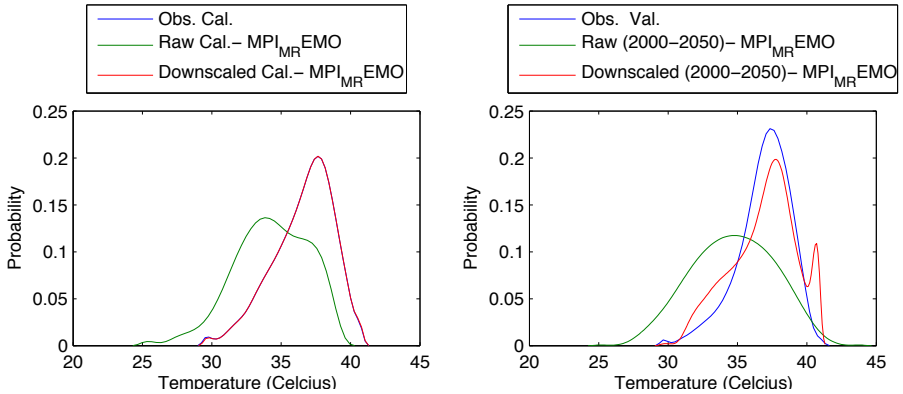

Figure 350 - Probability density for maximum temperature at Niamey airport with MPI - M - REMO in November

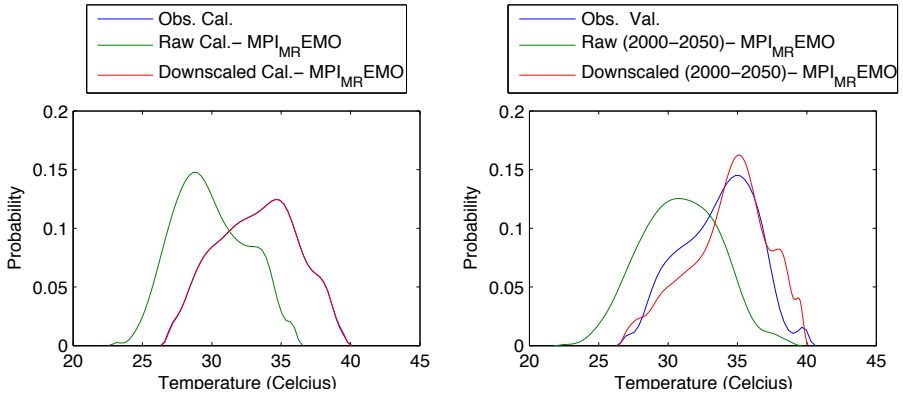

Figure 351 - Probability density for maximum temperature at Niamey airport with MPI - M - REMO in December

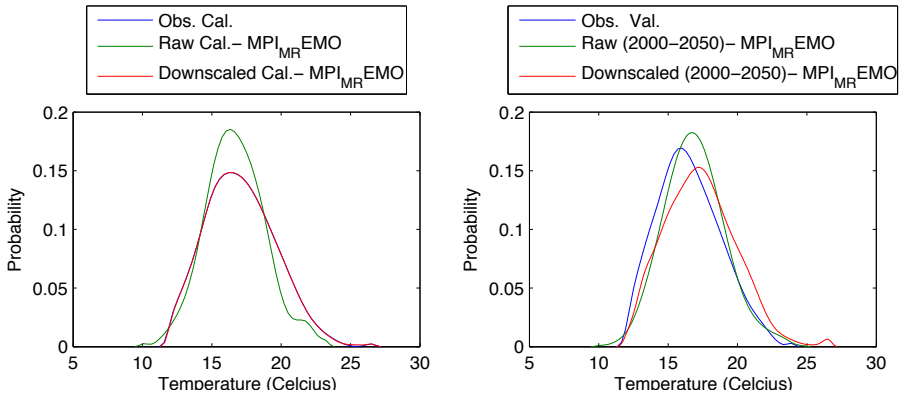

Figure 352 - Probability density for minimum temperature at Niamey airport with MPI - M - REMO in January

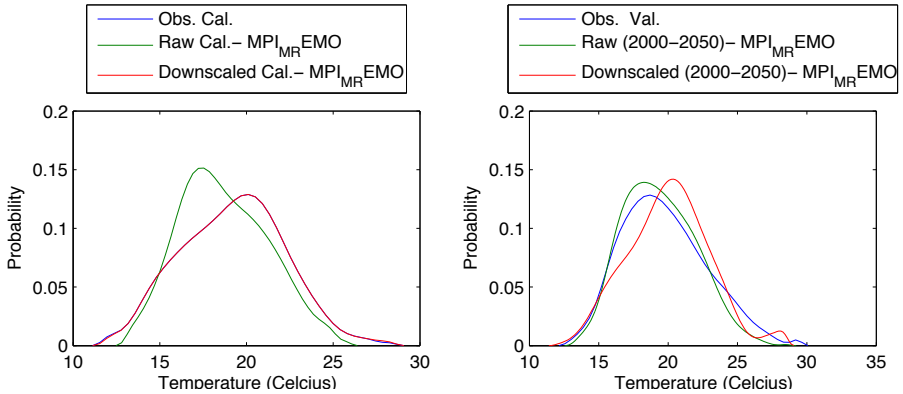

Figure 353 - Probability density for minimum temperature at Niamey airport with MPI - M - REMO in February

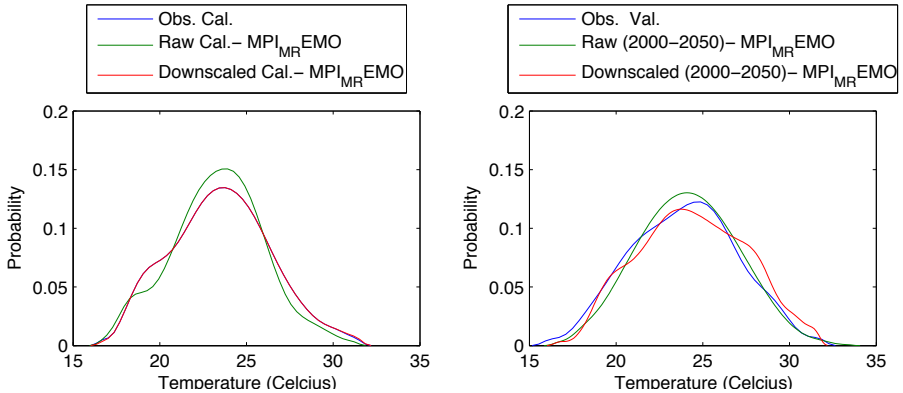

Figure 354 - Probability density for minimum temperature at Niamey airport with MPI - M - REMO in March

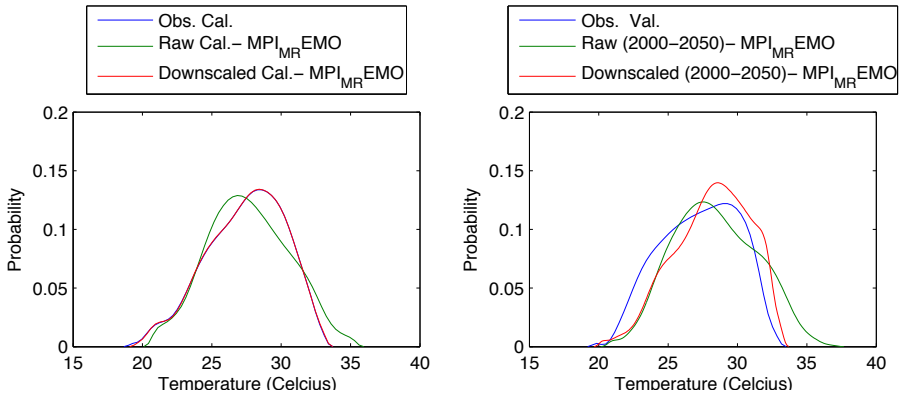

Figure 355 - Probability density for minimum temperature at Niamey airport with MPI - M - REMO in April

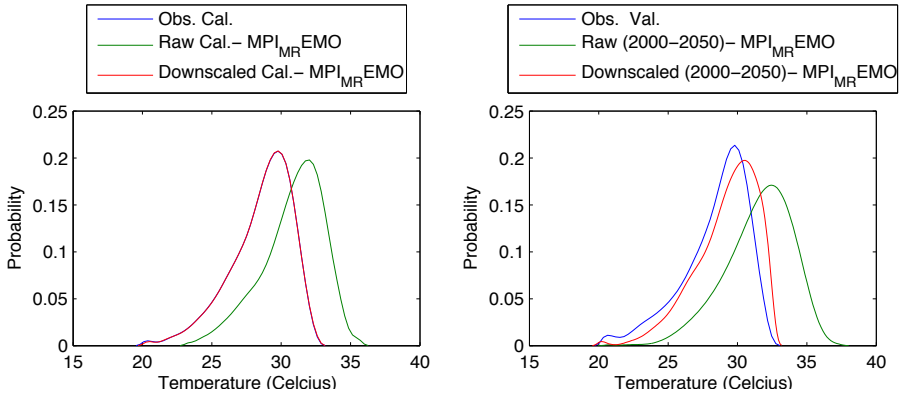

Figure 356 - Probability density for minimum temperature at Niamey airport with MPI - M - REMO in May

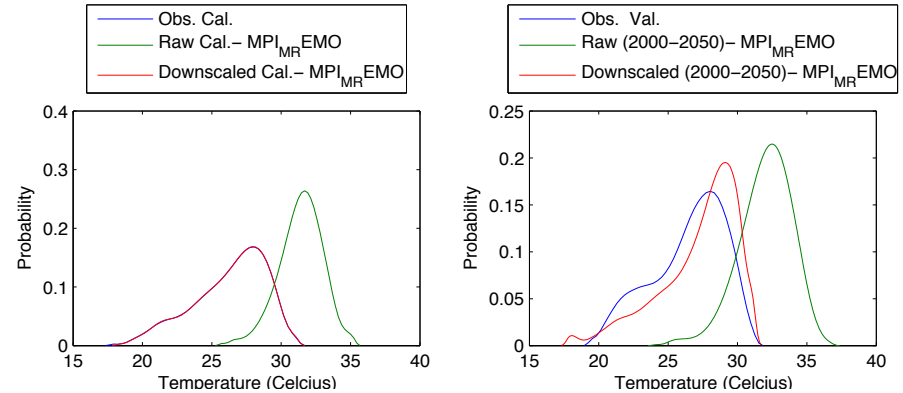

Figure 357 - Probability density for minimum temperature at Niamey airport with MPI - M - REMO in June

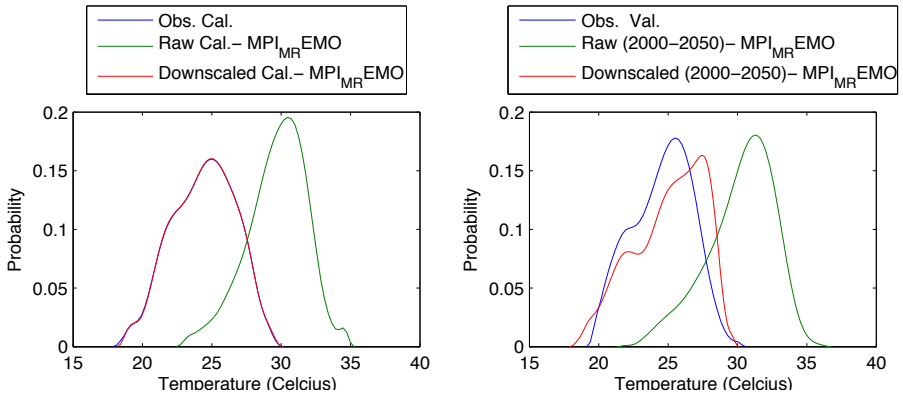

Figure 358 - Probability density for minimum temperature at Niamey airport with MPI - M - REMO in July

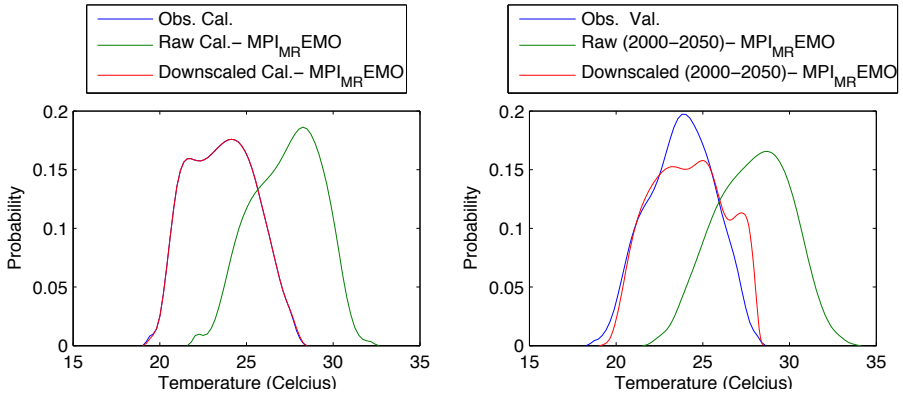

Figure 359 - Probability density for minimum temperature at Niamey airport with MPI - M - REMO in August

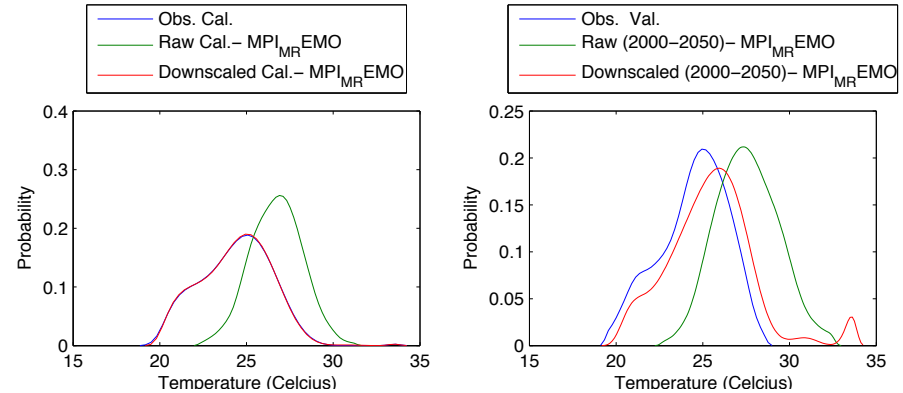

Figure 360 - Probability density for minimum temperature at Niamey airport with MPI - M - REMO in September

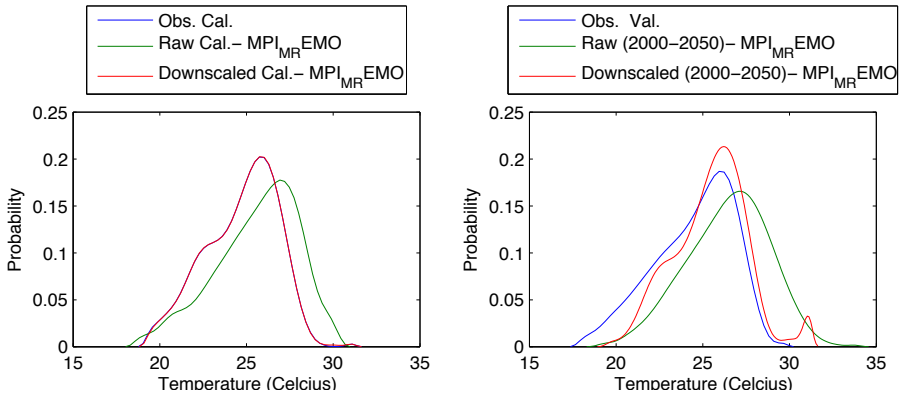

Figure 361 - Probability density for minimum temperature at Niamey airport with MPI - M - REMO in October

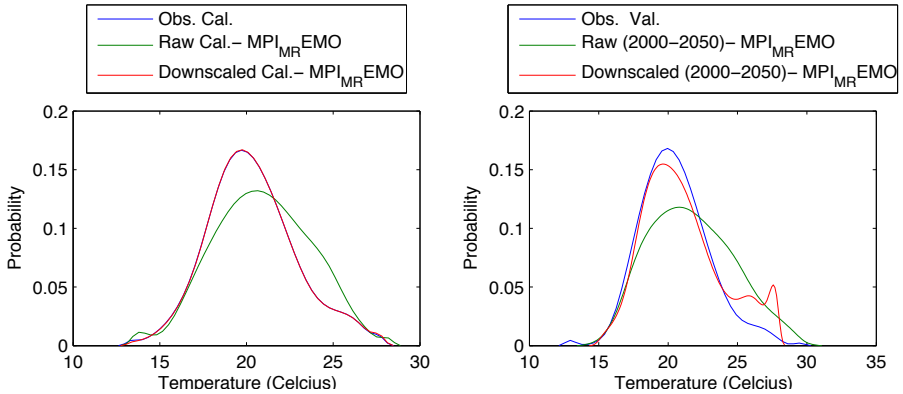

Figure 362 - Probability density for minimum temperature at Niamey airport with MPI - M - REMO in November

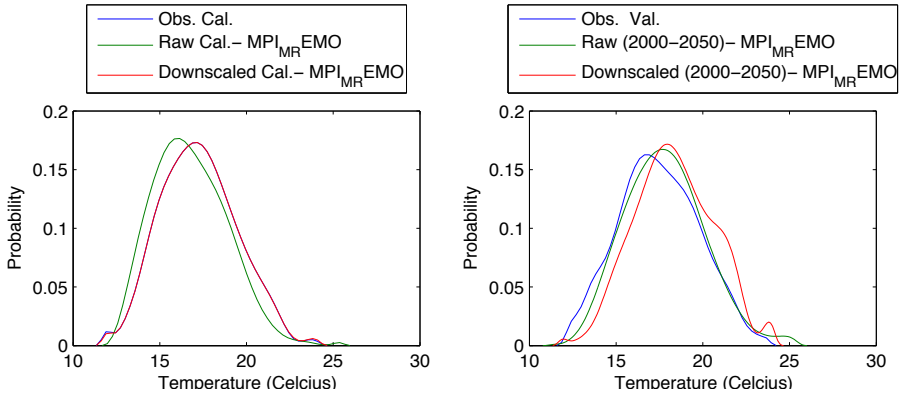

Figure 363 - Probability density for minimum temperature at Niamey airport with MPI - M - REMO in December

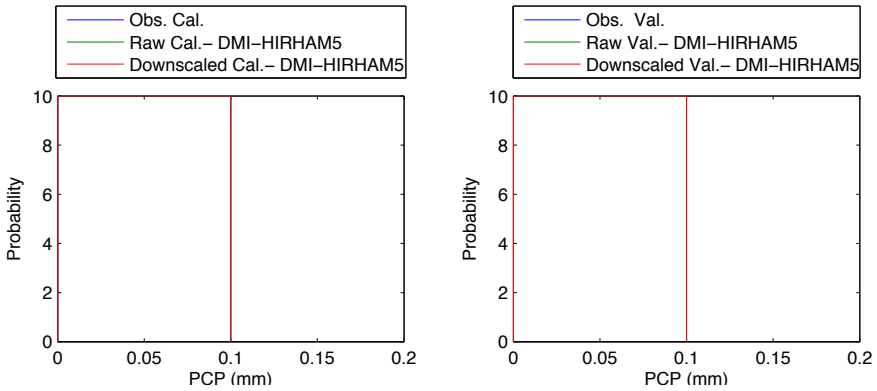

Figure 364 - Probability density of precipitation at Niamey airport with DMI - HIRHAM 5 in January

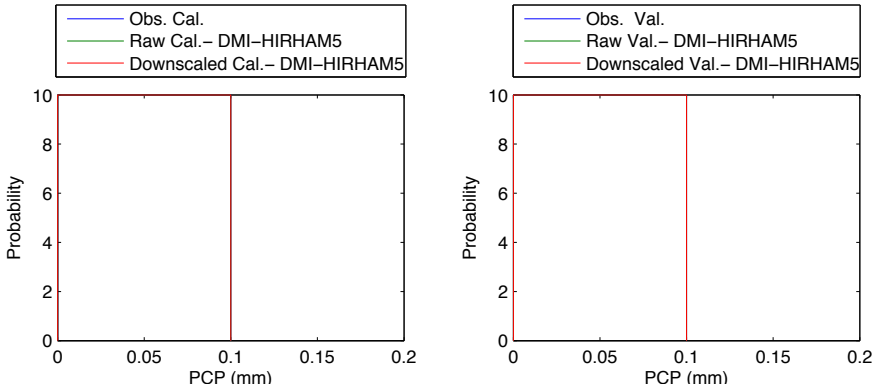

Figure 365 - Probability density of precipitation at Niamey airport with DMI - HIRHAM 5 in February

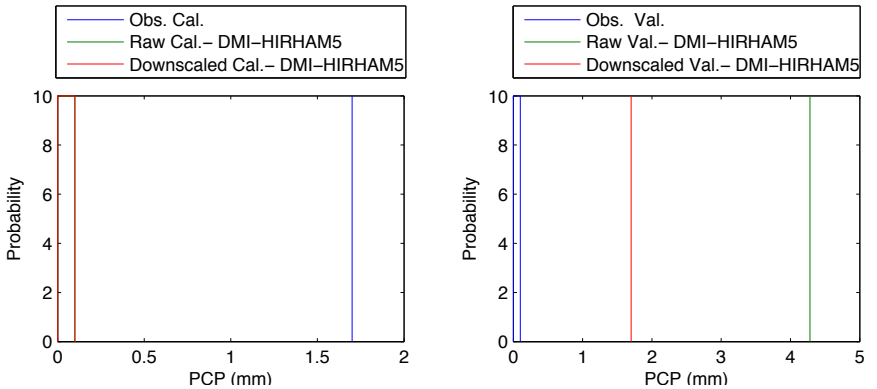

Figure 366 - Probability density of precipitation at Niamey airport with DMI - HIRHAM 5 in March

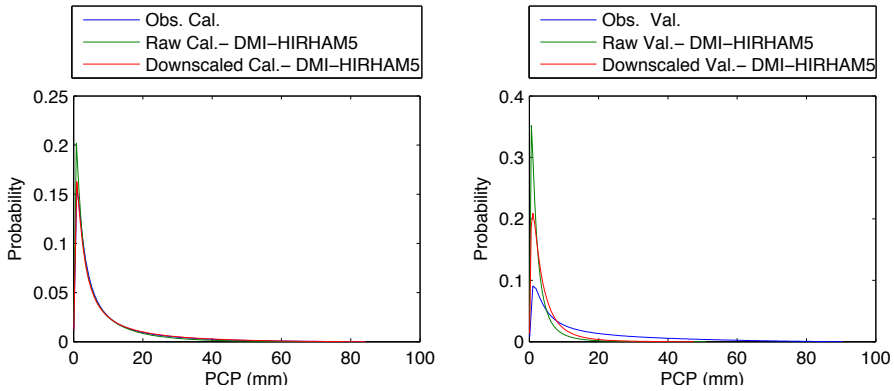

Figure 367 - Probability density of precipitation at Niamey airport with DMI - HIRHAM 5 in April

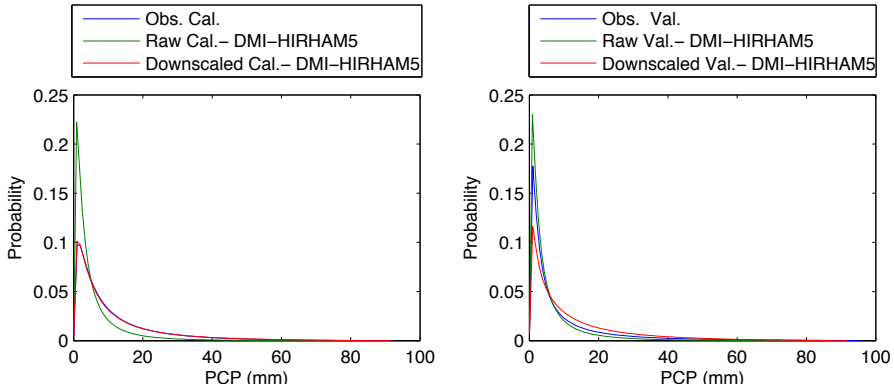

Figure 368 - Probability density of precipitation at Niamey airport with DMI - HIRHAM 5 in May

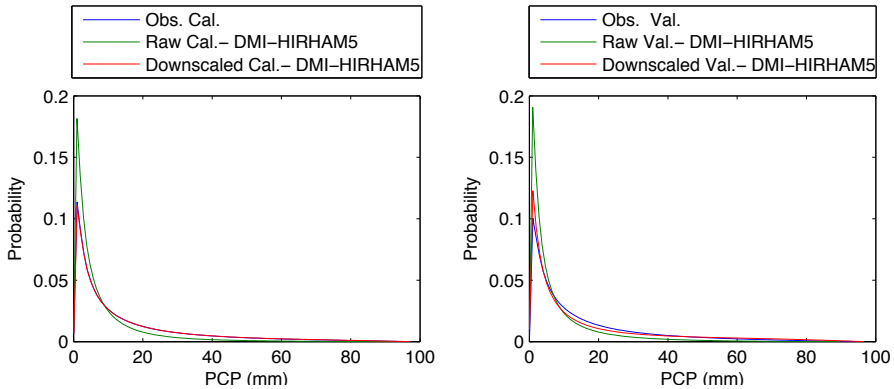

Figure 369 - Probability density of precipitation at Niamey airport with DMI - HIRHAM 5 in June

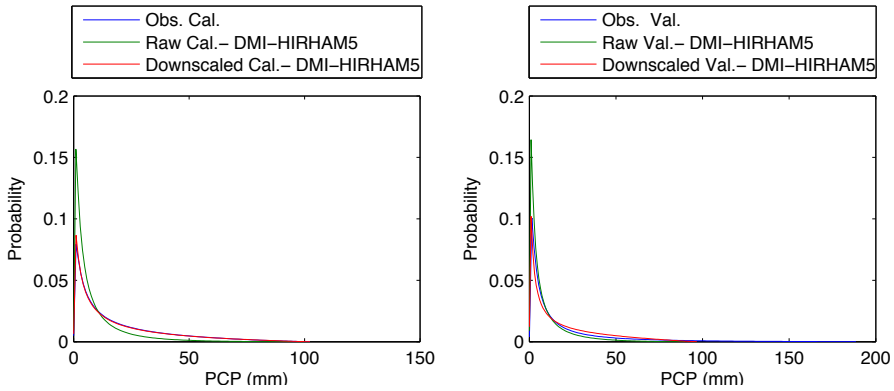

Figure 370 - Probability density of precipitation at Niamey airport with DMI - HIRHAM 5 in July

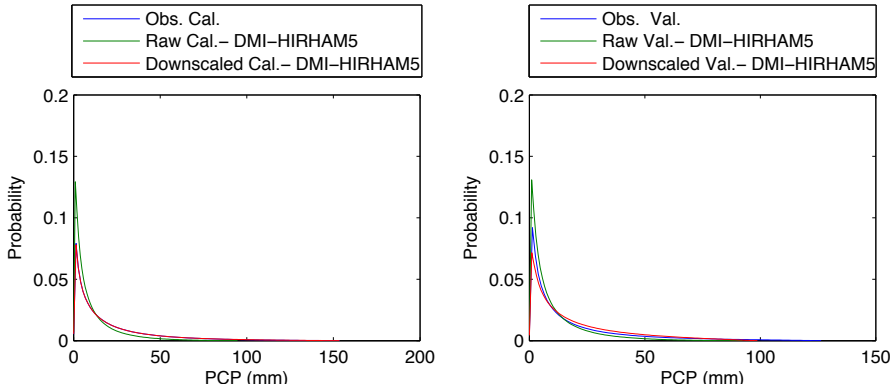

Figure 371 - Probability density of precipitation at Niamey airport with DMI - HIRHAM 5 in August

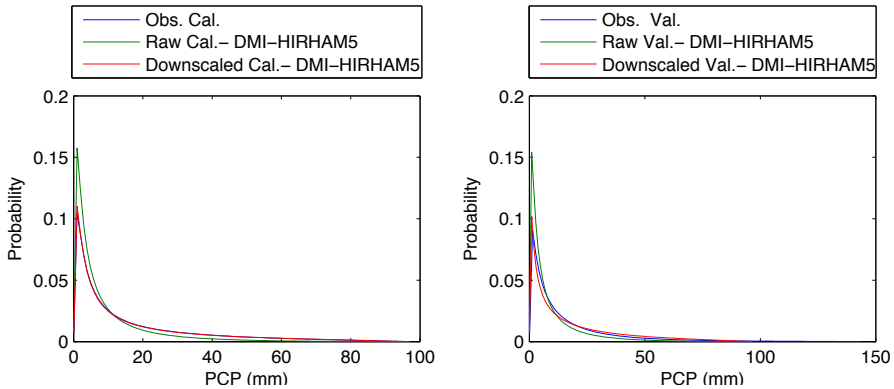

Figure 372 - Probability density of precipitation at Niamey airport with DMI - HIRHAM 5 in September

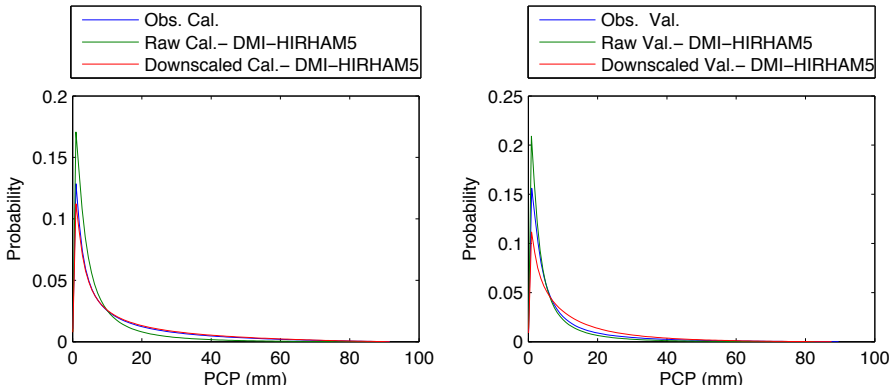

Figure 373 - Probability density of precipitation at Niamey airport with DMI - HIRHAM 5 in October

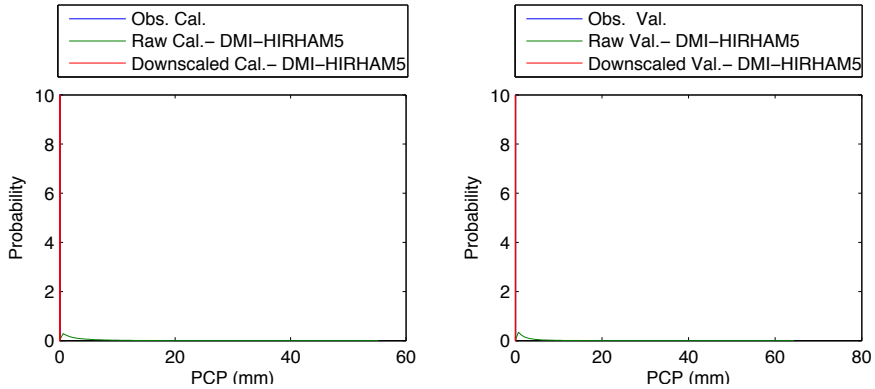

Figure 374 - Probability density of precipitation at Niamey airport with DMI - HIRHAM 5 in November

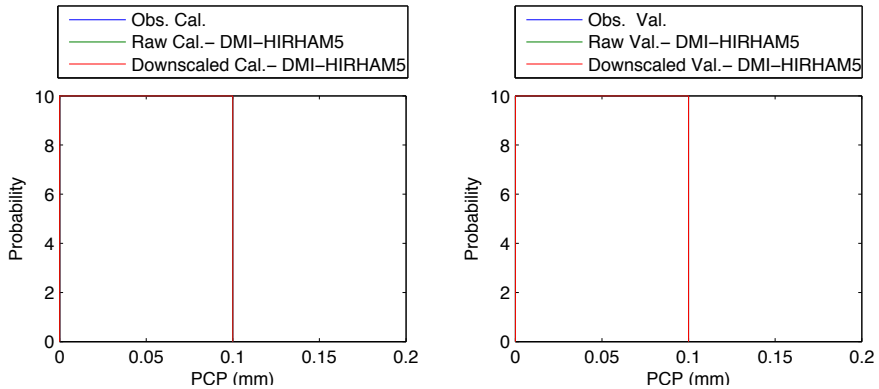

Figure 375 - Probability density of precipitation at Niamey airport with DMI - HIRHAM 5 in December

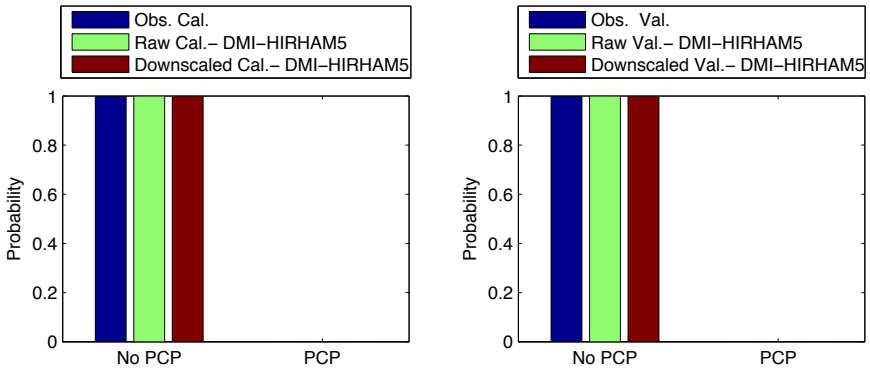

Figure 376 - Precipitation occurrence at Niamey airport with DMI - HIRHAM 5 in January

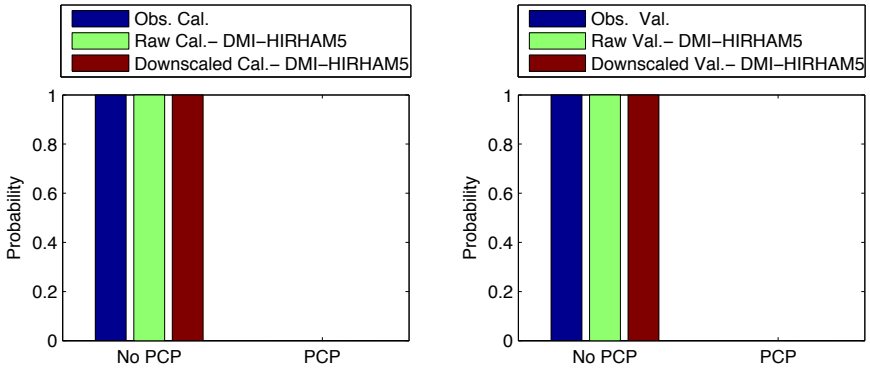

Figure 377 - Precipitation occurrence at Niamey airport with DMI - HIRHAM 5 in February

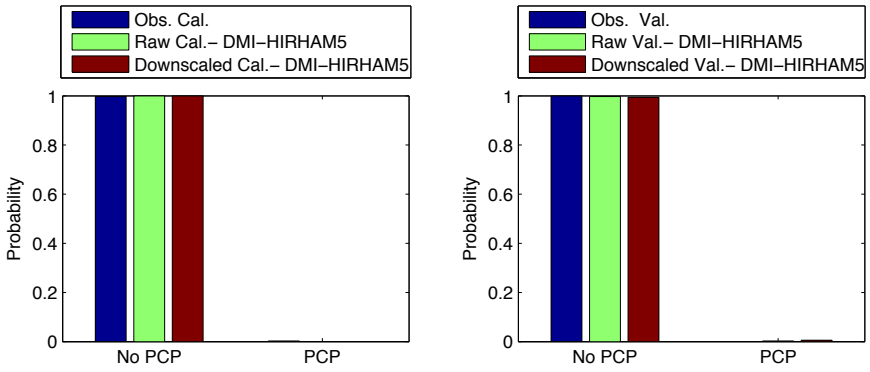

Figure 378 - Precipitation occurrence at Niamey airport with DMI - HIRHAM 5 in March

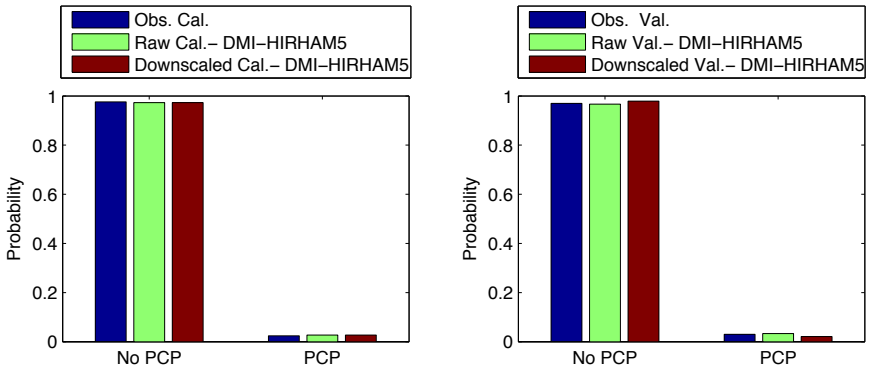

Figure 379 - Precipitation occurrence at Niamey airport with DMI - HIRHAM 5 in April

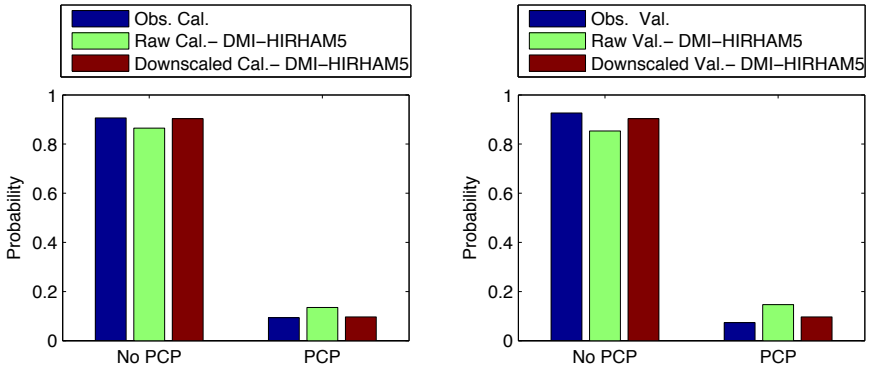

Figure 380 - Precipitation occurrence at Niamey airport with DMI - HIRHAM 5 in May

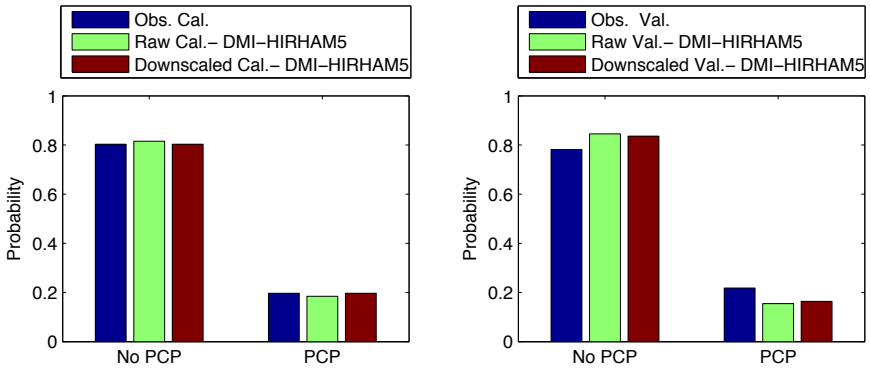

Figure 381 - Precipitation occurrence at Niamey airport with DMI - HIRHAM 5 in June

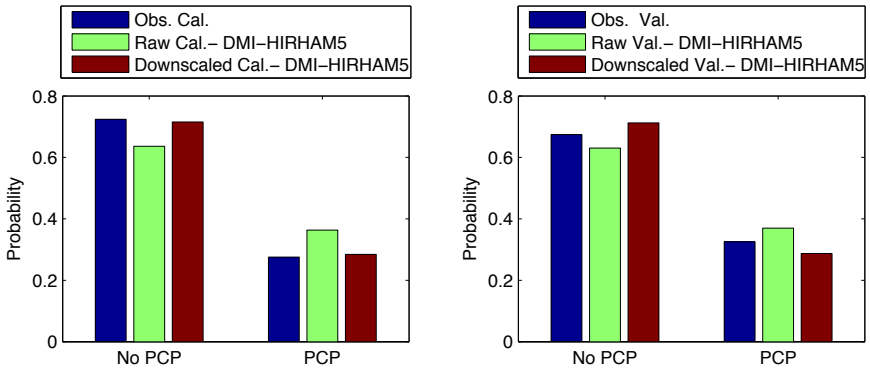

Figure 382 - Precipitation occurrence at Niamey airport with DMI - HIRHAM 5 in July

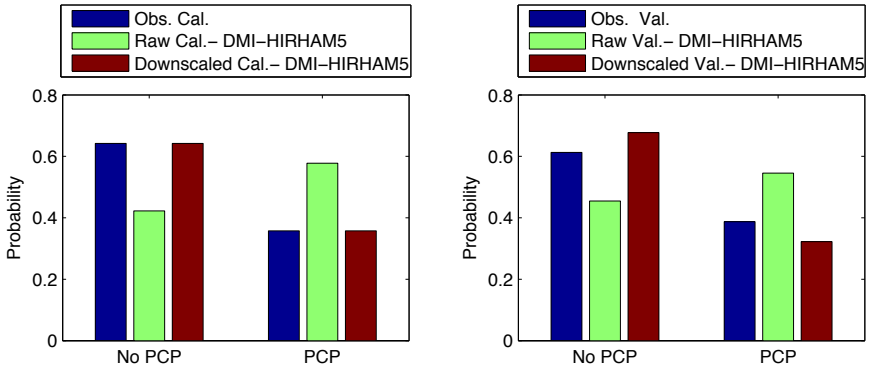

Figure 383 - Precipitation occurrence at Niamey airport with DMI - HIRHAM 5 in August

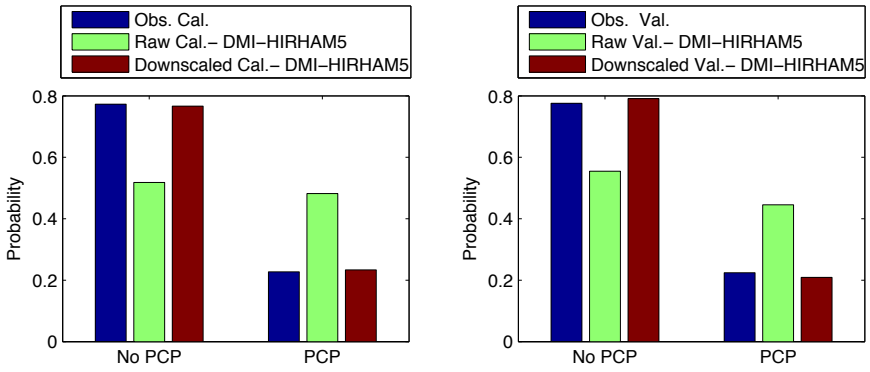

Figure 384 - Precipitation occurrence at Niamey airport with DMI - HIRHAM 5 in September

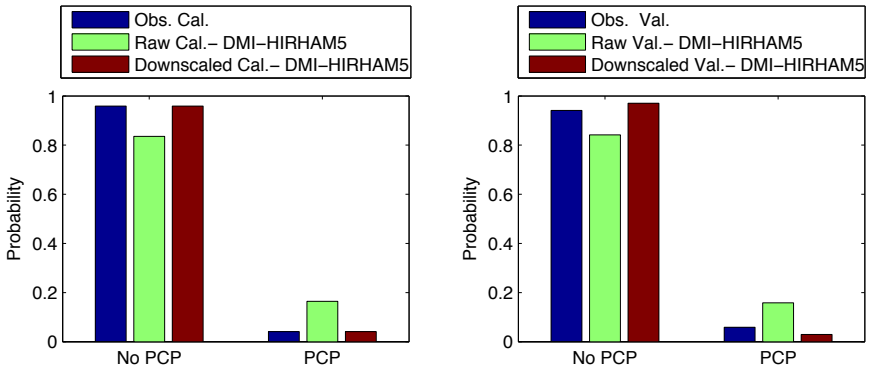

Figure 385 - Precipitation occurrence at Niamey airport with DMI - HIRHAM 5 in October

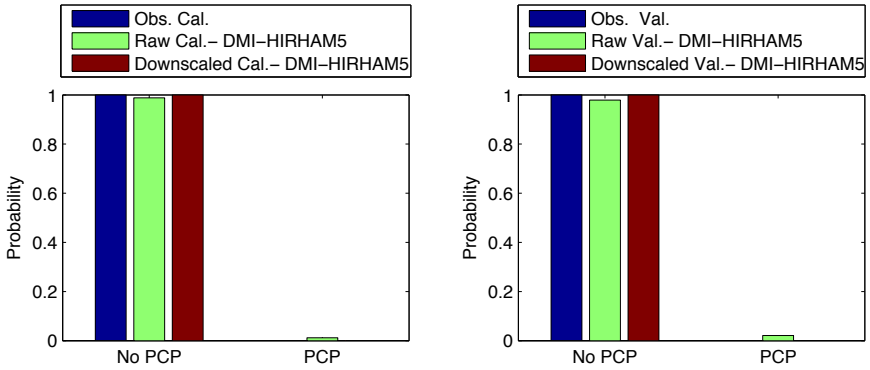

Figure 386 - Precipitation occurrence at Niamey airport with DMI - HIRHAM 5 in November

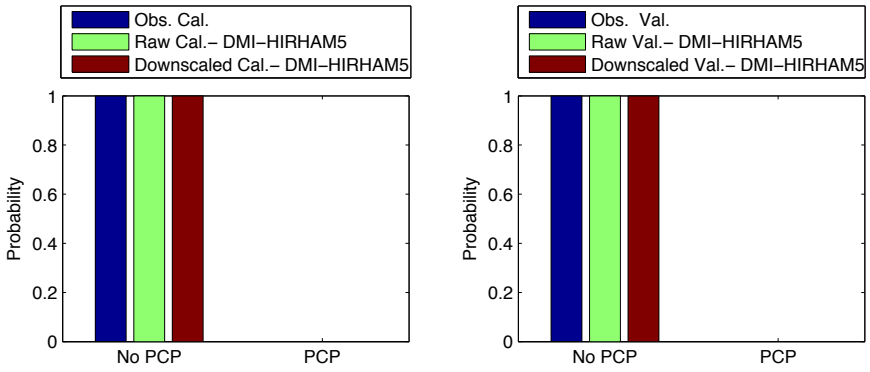

Figure 387 - Precipitation occurrence at Niamey airport with DMI - HIRHAM 5 in December

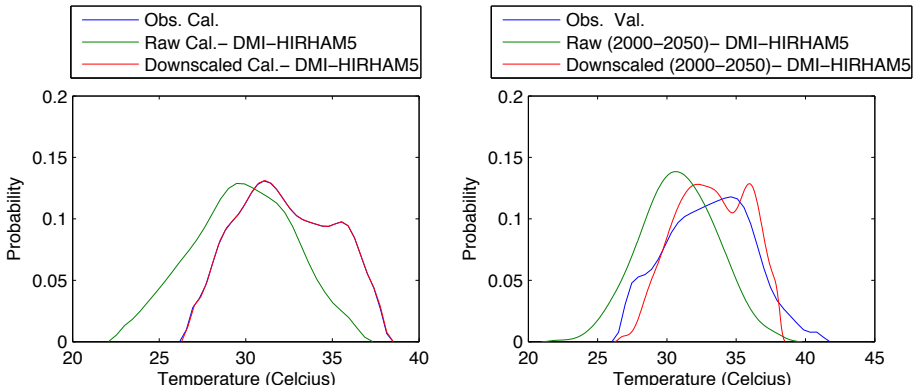

Figure 388 - Probability density for maximum temperature at Niamey airport with DMI - HIRHAM 5 in January

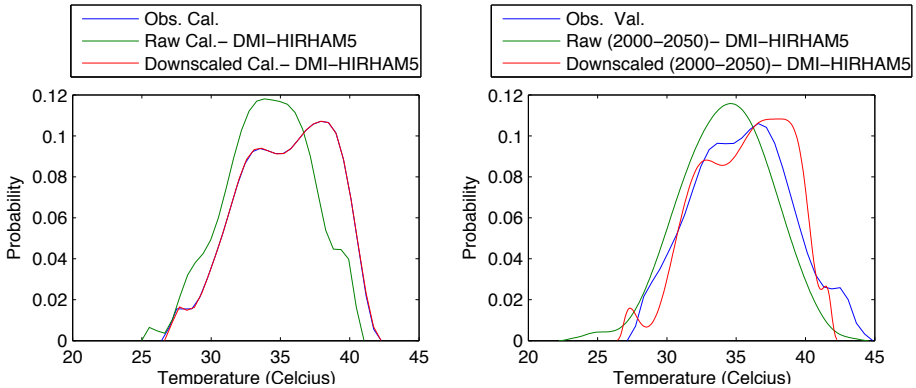

Figure 389 - Probability density for maximum temperature at Niamey airport with DMI - HIRHAM 5 in February

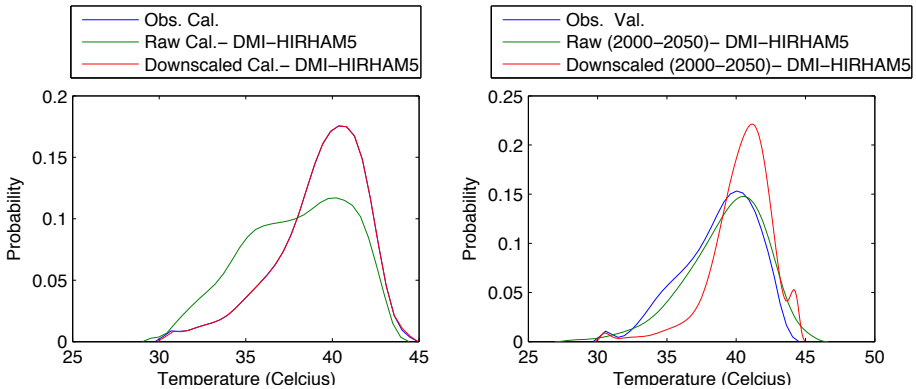

Figure 390 - Probability density for maximum temperature at Niamey airport with DMI - HIRHAM 5 in March

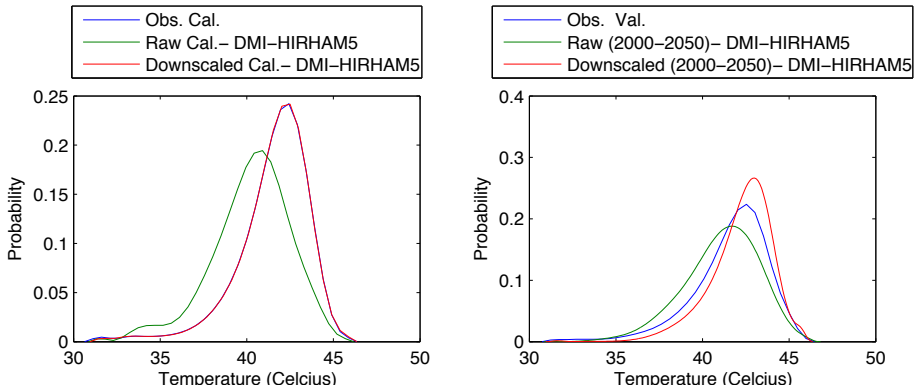

Figure 391 - Probability density for maximum temperature at Niamey airport with DMI - HIRHAM 5 in April

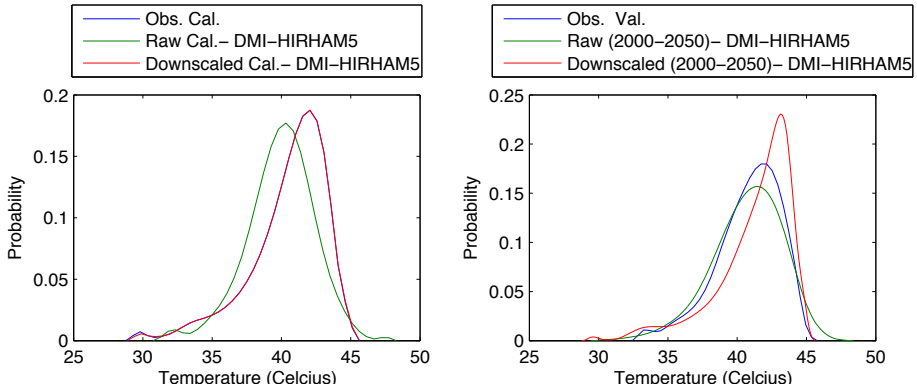

Figure 392 - Probability density for maximum temperature at Niamey airport with DMI - HIRHAM 5 in May

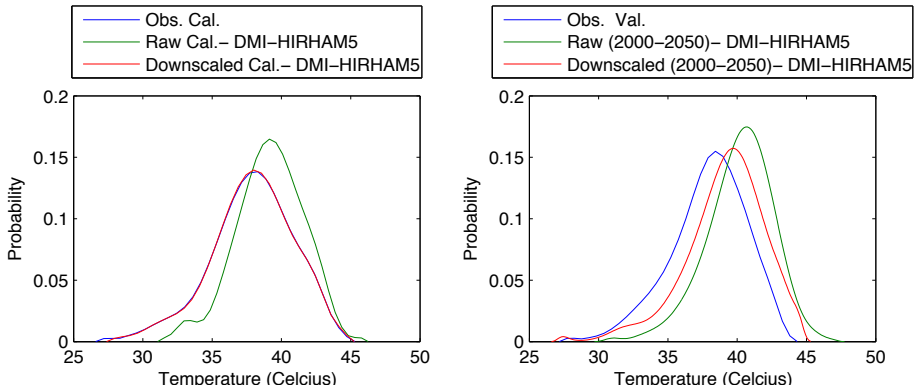

Figure 393 - Probability density for maximum temperature at Niamey airport with DMI - HIRHAM 5 in June

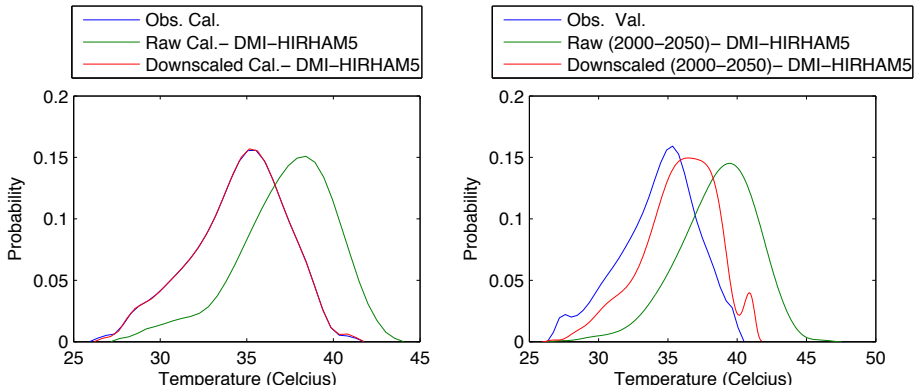

Figure 394 - Probability density for maximum temperature at Niamey airport with DMI - HIRHAM 5 in July

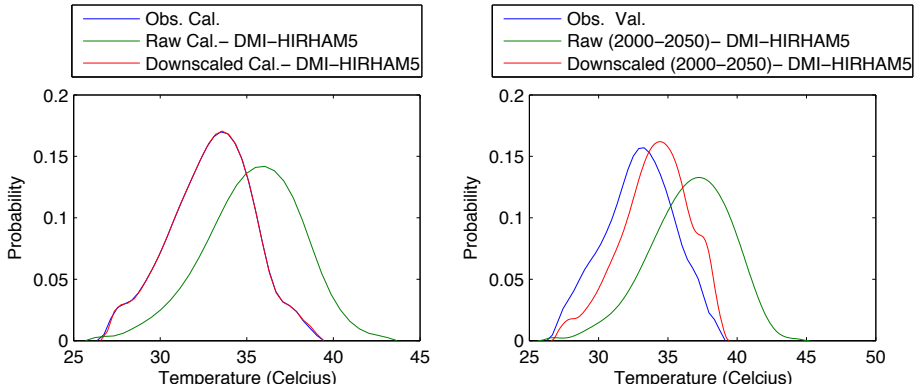

Figure 395 - Probability density for maximum temperature at Niamey airport with DMI - HIRHAM 5 in August

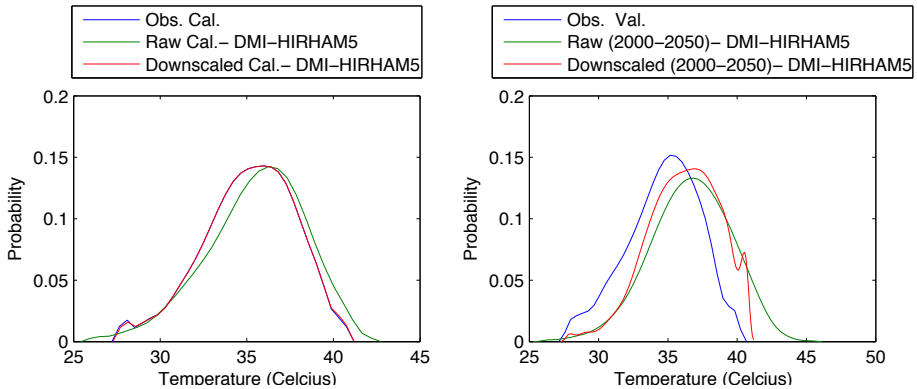

Figure 396 - Probability density for maximum temperature at Niamey airport with DMI - HIRHAM 5 in September

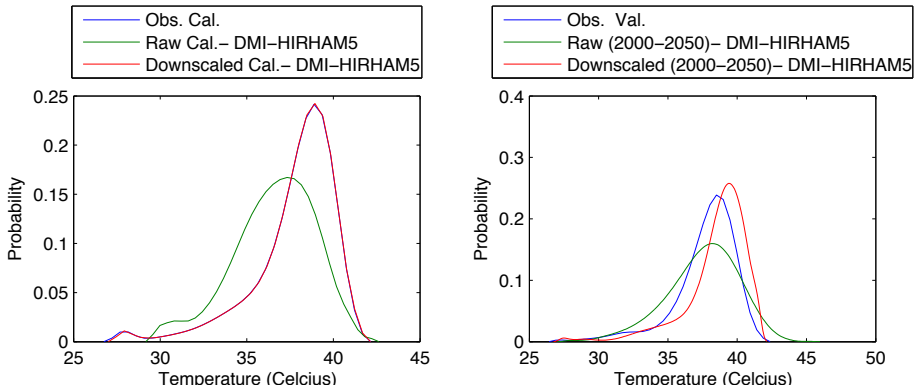

Figure 397 - Probability density for maximum temperature at Niamey airport with DMI - HIRHAM 5 in October

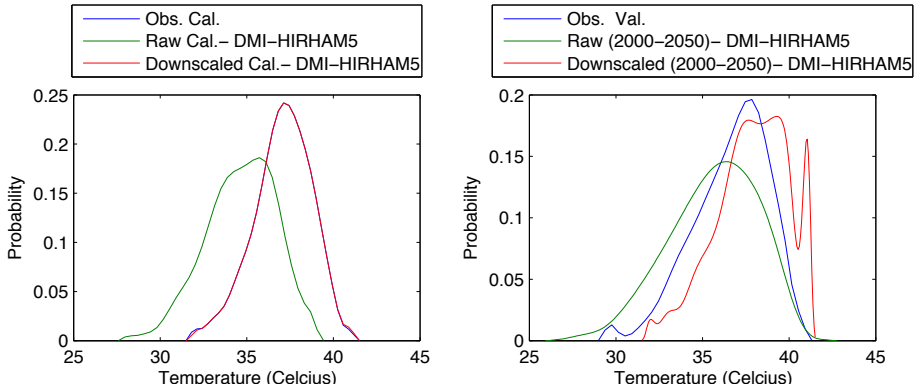

Figure 398 - Probability density for maximum temperature at Niamey airport with DMI - HIRHAM 5 in November

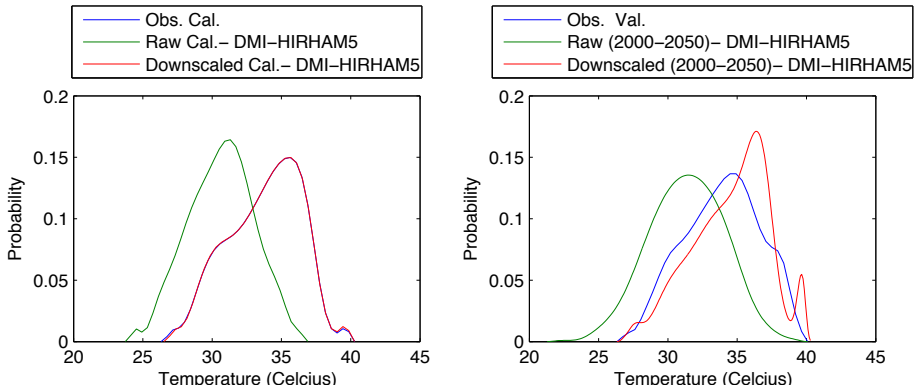

Figure 399 - Probability density for maximum temperature at Niamey airport with DMI - HIRHAM 5 in December

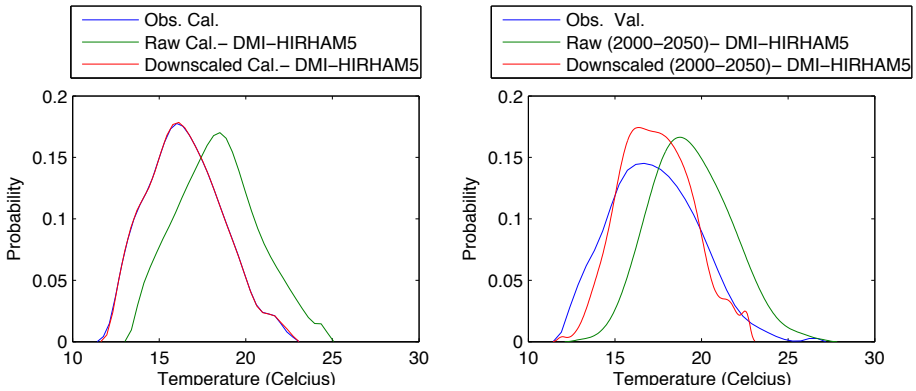

Figure 400 - Probability density for minimum temperature at Niamey airport with DMI - HIRHAM 5 in January

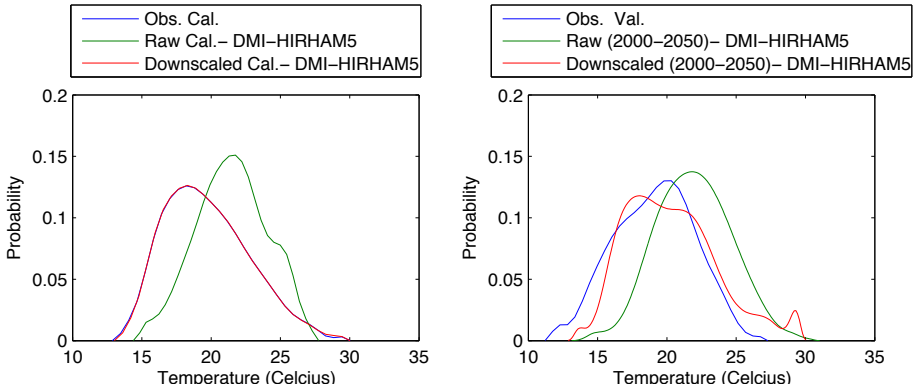

Figure 401 - Probability density for minimum temperature at Niamey airport with DMI - HIRHAM 5 in February

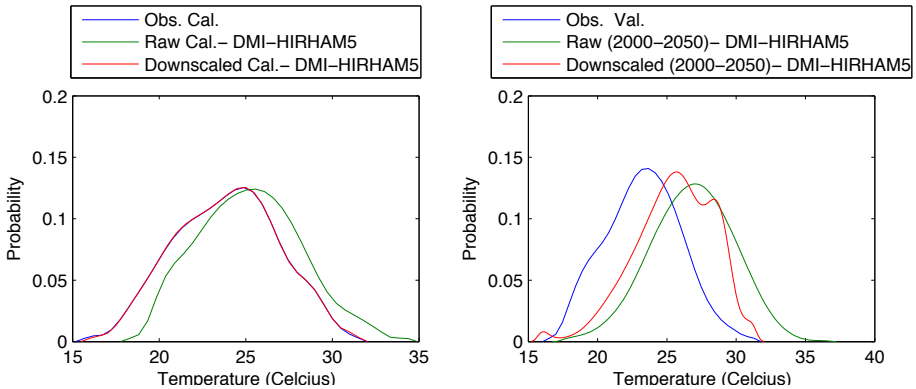

Figure 402 - Probability density for minimum temperature at Niamey airport with DMI - HIRHAM 5 in March

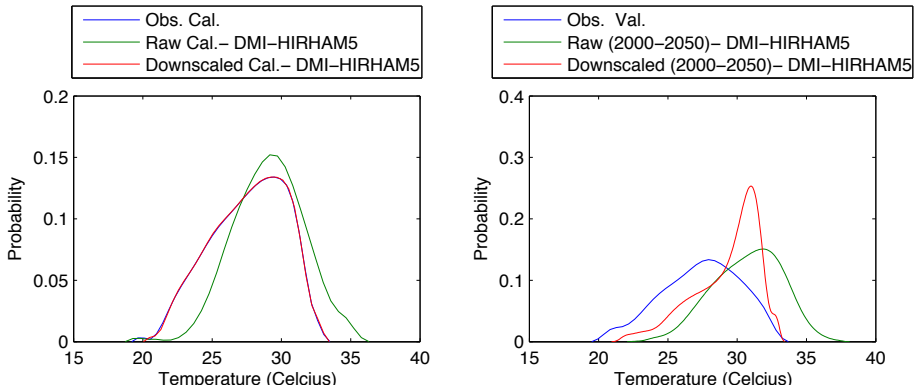

Figure 403 - Probability density for minimum temperature at Niamey airport with DMI - HIRHAM 5 in April

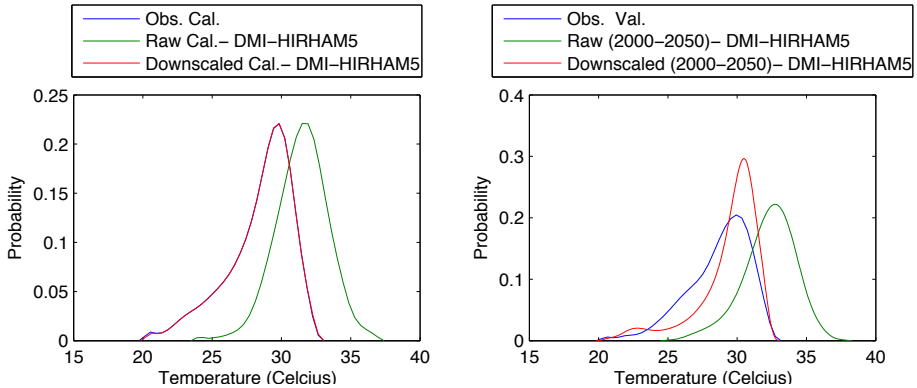

Figure 404 - Probability density for minimum temperature at Niamey airport with DMI - HIRHAM 5 in May

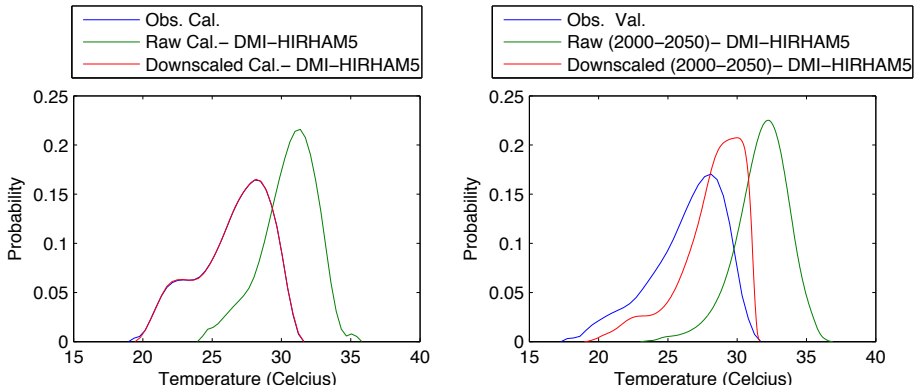

Figure 405 - Probability density for minimum temperature at Niamey airport with DMI - HIRHAM 5 in June

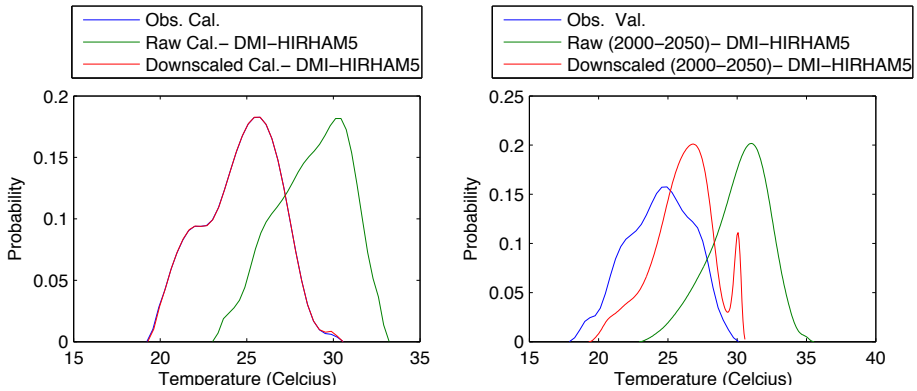

Figure 406 - Probability density for minimum temperature at Niamey airport with DMI - HIRHAM 5 in July

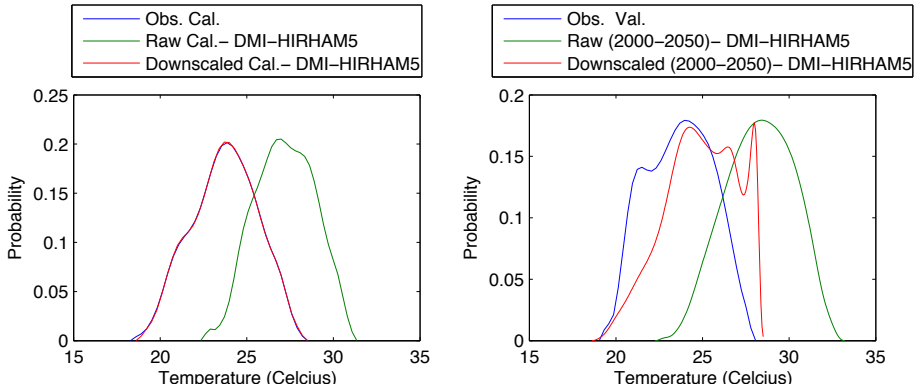

Figure 407 - Probability density for minimum temperature at Niamey airport with DMI - HIRHAM 5 in August

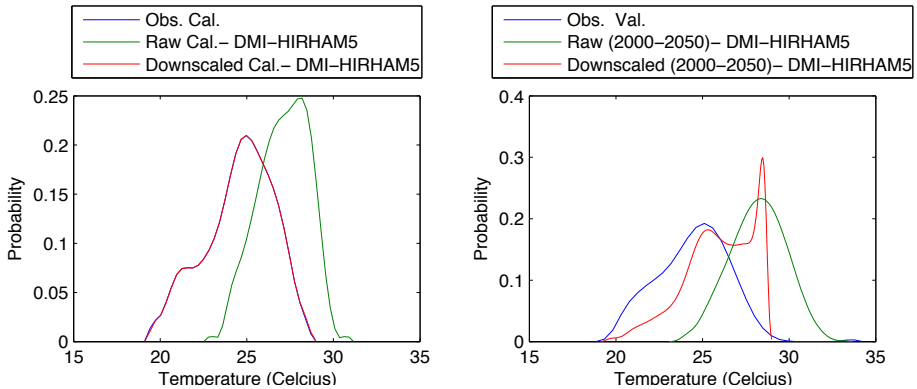

Figure 408 - Probability density for minimum temperature at Niamey airport with DMI - HIRHAM 5 in September

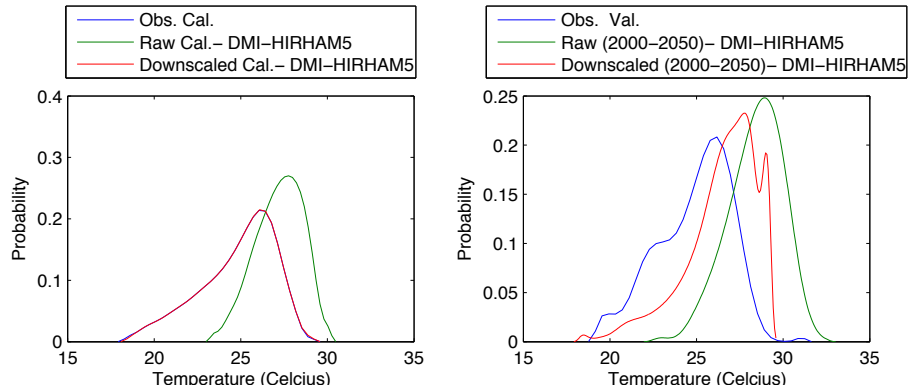

Figure 409 - Probability density for minimum temperature at Niamey airport with DMI - HIRHAM 5 in October

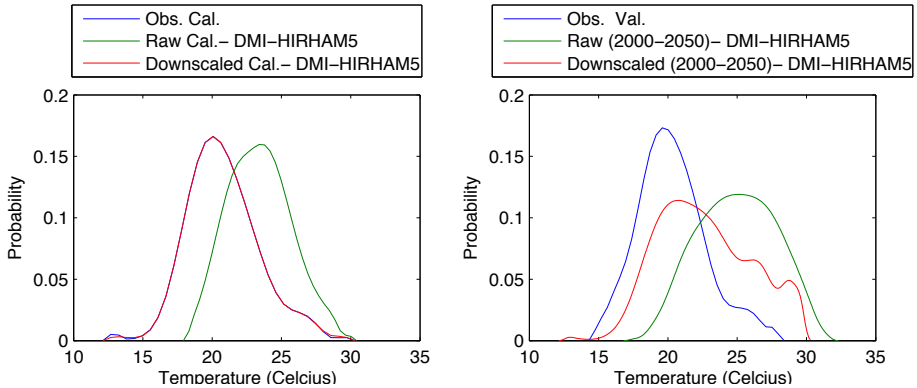

Figure 410 - Probability density for minimum temperature at Niamey airport with DMI - HIRHAM 5 in November

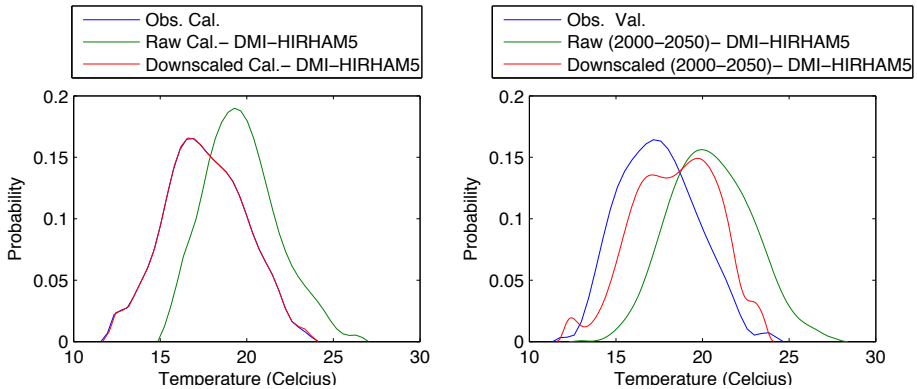

Figure 411 - Probability density for minimum temperature at Niamey airport with DMI - HIRHAM 5 in December

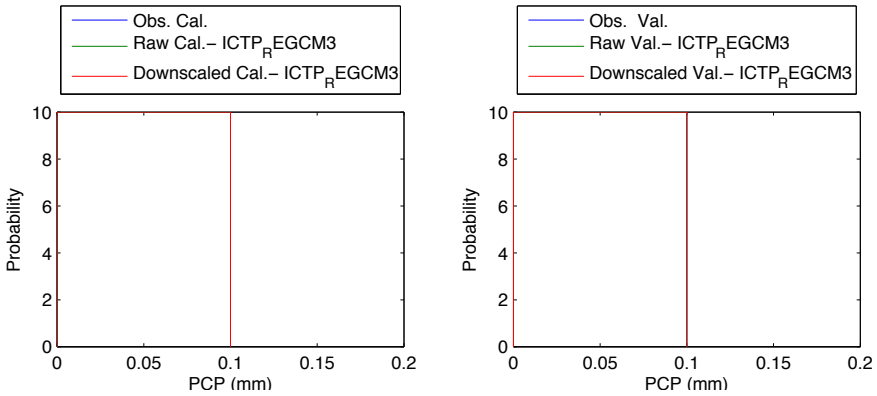

Figure 412 - Probability density of precipitation at Niamey airport with ICTP - REGCM 3 in January

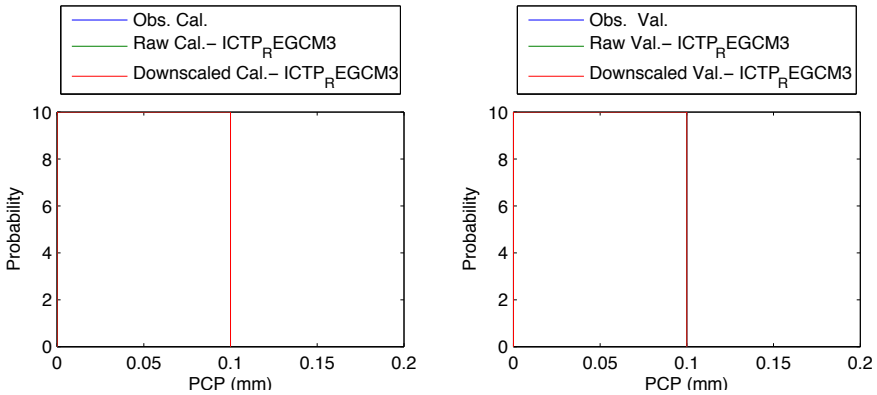

Figure 413 - Probability density of precipitation at Niamey airport with ICTP - REGCM 3 in February

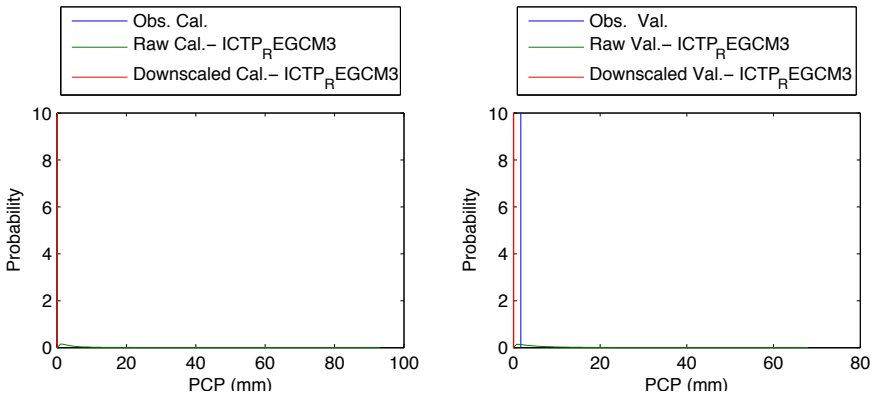

Figure 414 - Probability density of precipitation at Niamey airport with ICTP - REGCM 3 in March

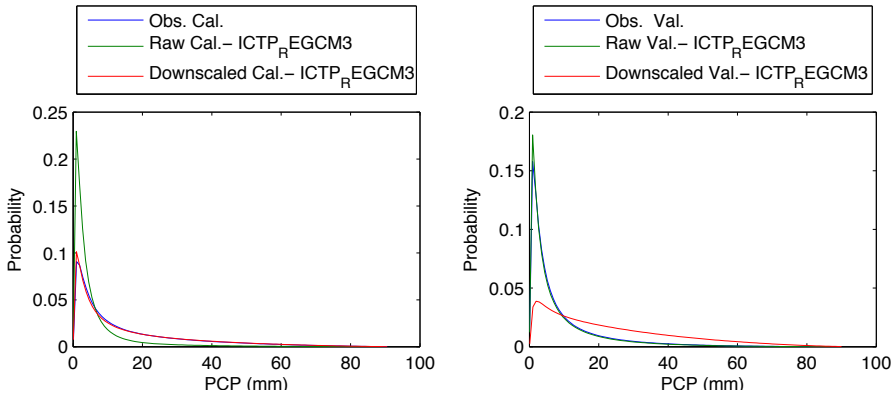

Figure 415 - Probability density of precipitation at Niamey airport with ICTP - REGCM 3 in April

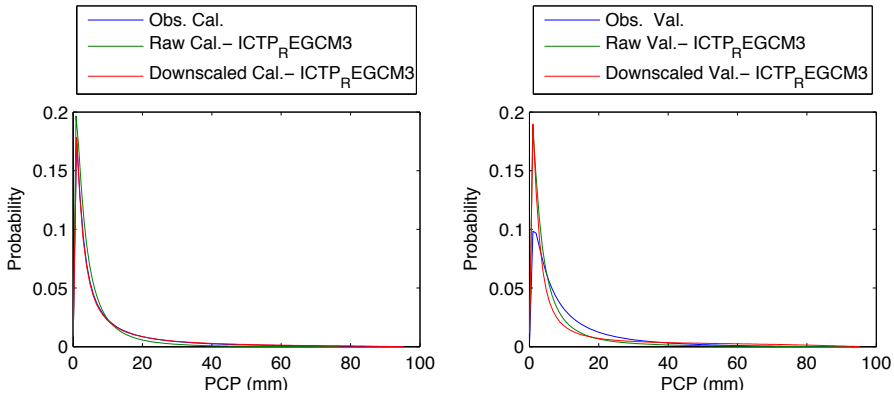

Figure 416 - Probability density of precipitation at Niamey airport with ICTP - REGCM 3 in May

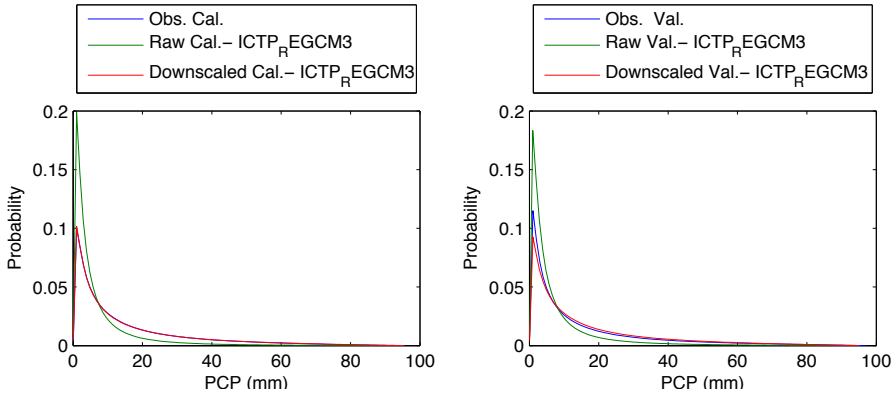

Figure 417 - Probability density of precipitation at Niamey airport with ICTP - REGCM 3 in June

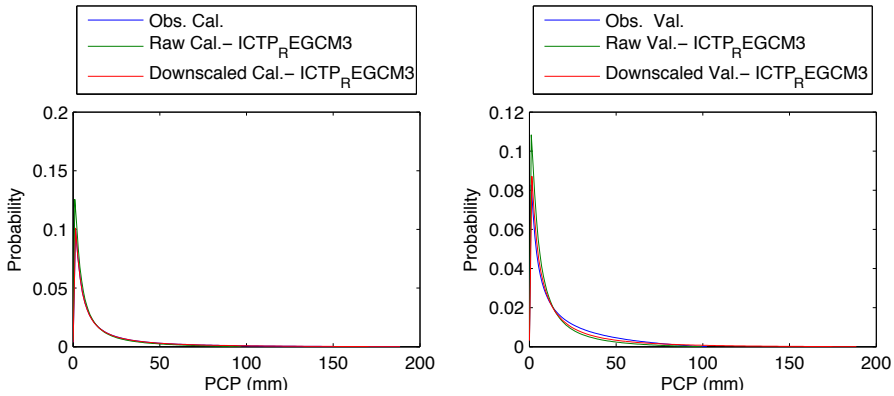

Figure 418 - Probability density of precipitation at Niamey airport with ICTP - REGCM 3 in July

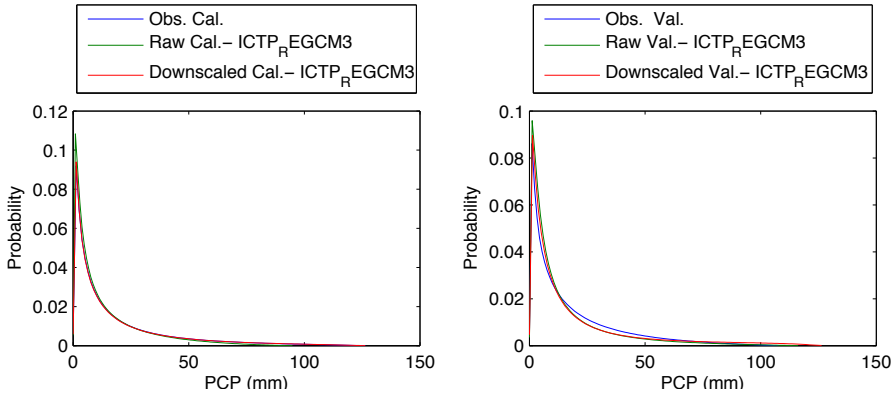

Figure 419 - Probability density of precipitation at Niamey airport with ICTP - REGCM 3 in August

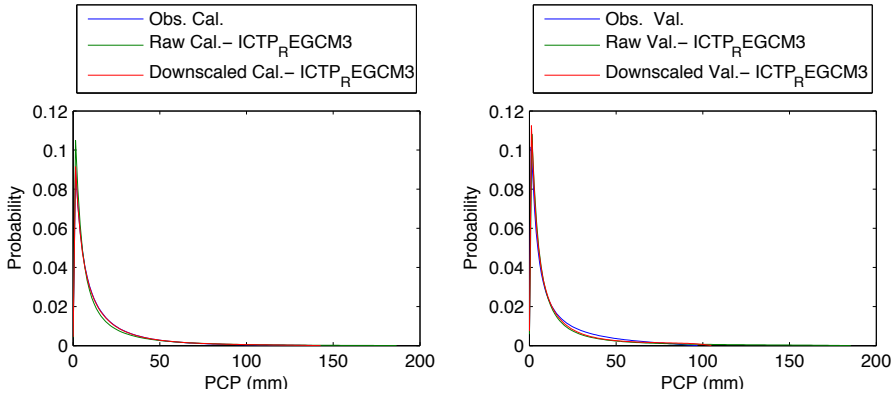

Figure 420 - Probability density of precipitation at Niamey airport with ICTP - REGCM 3 in September

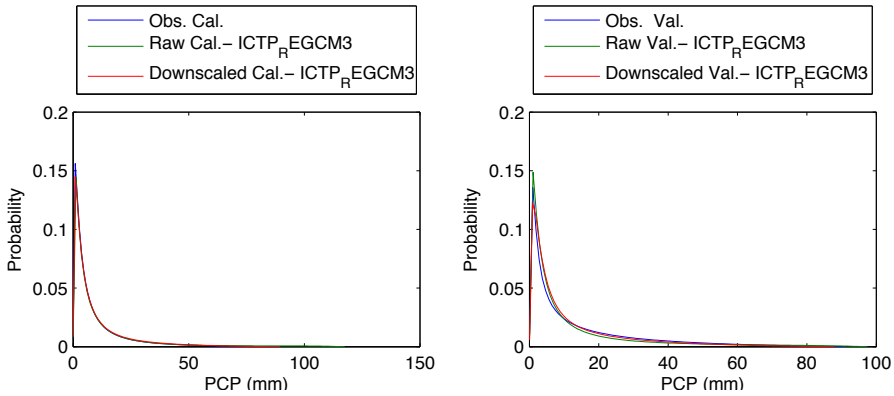

Figure 421 - Probability density of precipitation at Niamey airport with ICTP - REGCM 3 in October

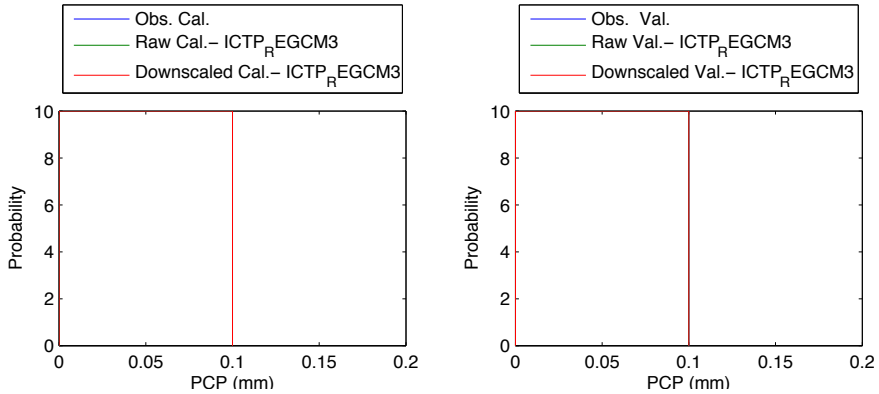

Figure 422 - Probability density of precipitation at Niamey airport with ICTP - REGCM 3 in November

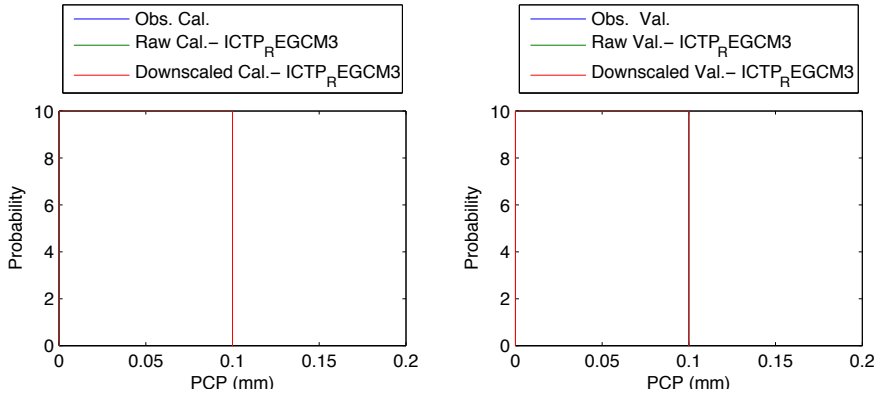

Figure 423 - Probability density of precipitation at Niamey airport with ICTP - REGCM 3 in December

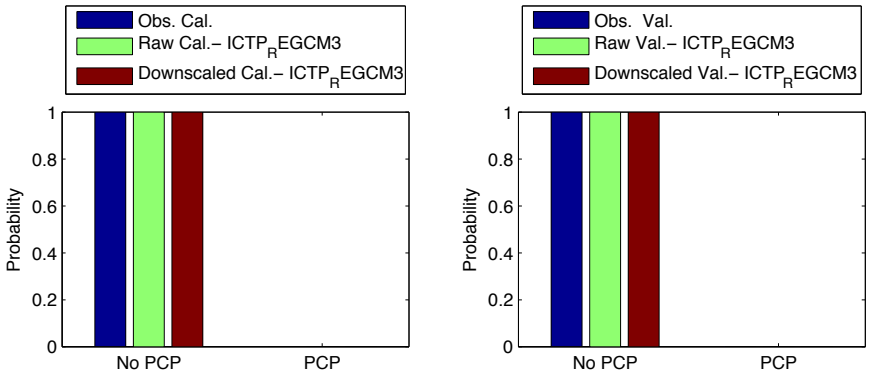

Figure 424 - Precipitation occurrence at Niamey airport with ICTP - REGCM 3 in January

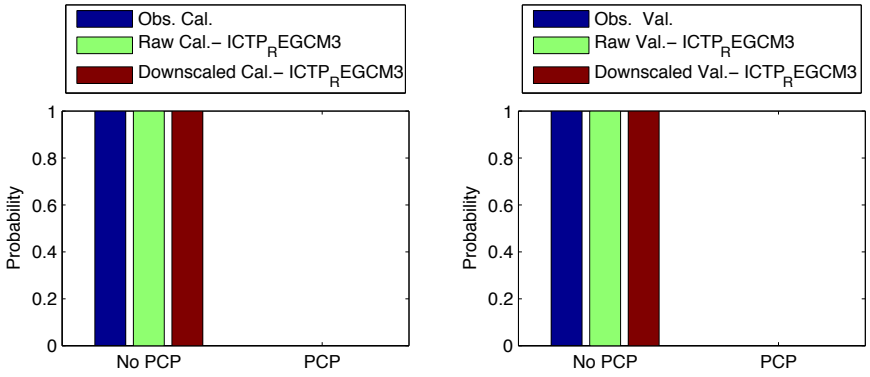

Figure 425 - Precipitation occurrence at Niamey airport with ICTP - REGCM 3 in February

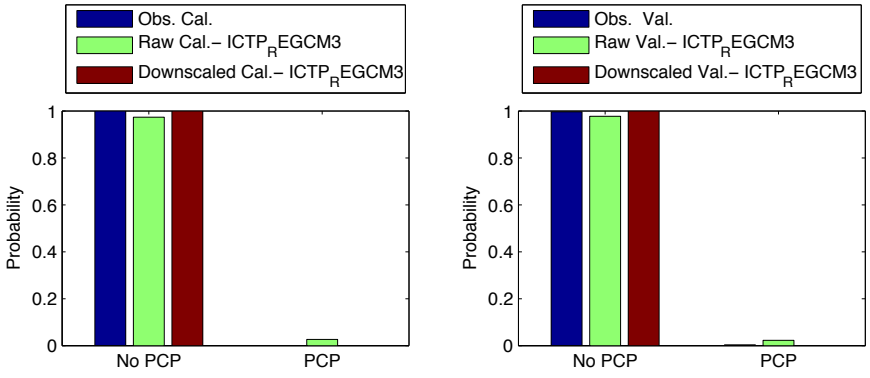

Figure 426 - Precipitation occurrence at Niamey airport with ICTP - REGCM 3 in March

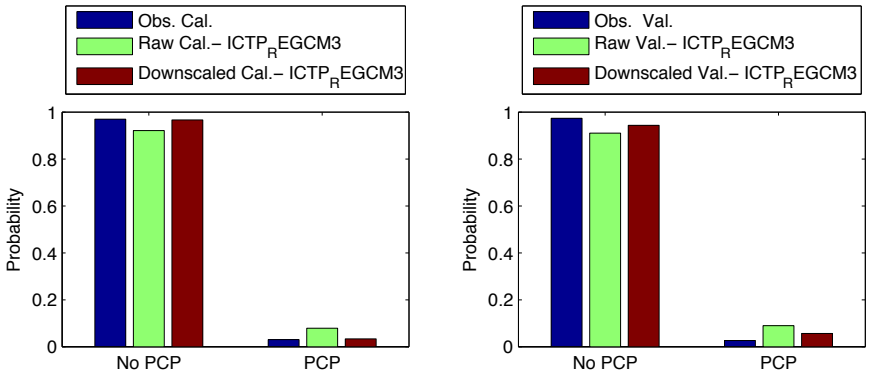

Figure 427 - Precipitation occurrence at Niamey airport with ICTP - REGCM 3 in April

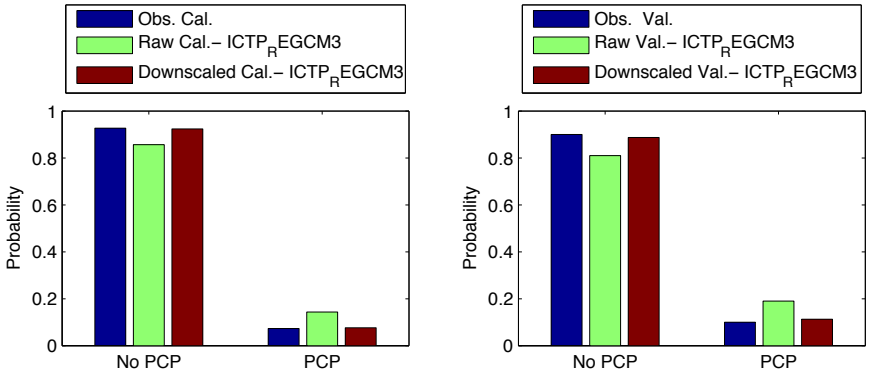

Figure 428 - Precipitation occurrence at Niamey airport with ICTP - REGCM 3 in May

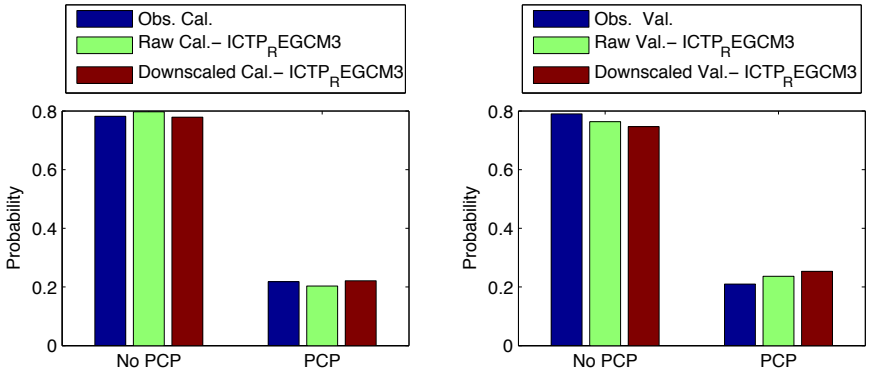

Figure 429 - Precipitation occurrence at Niamey airport with ICTP - REGCM 3 in June

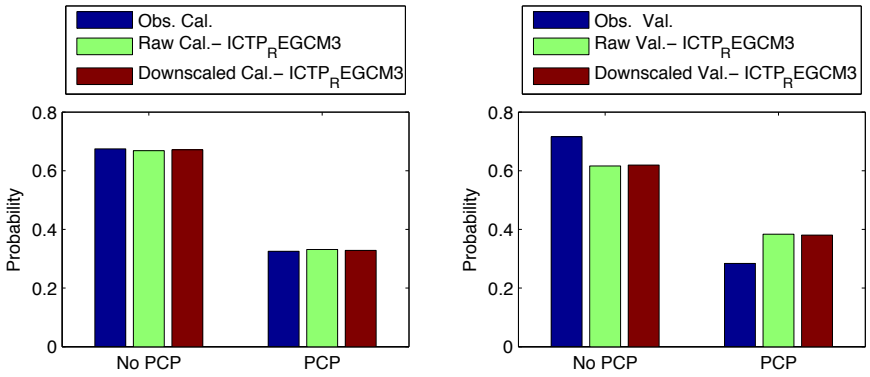

Figure 430 - Precipitation occurrence at Niamey airport with ICTP - REGCM 3 in July

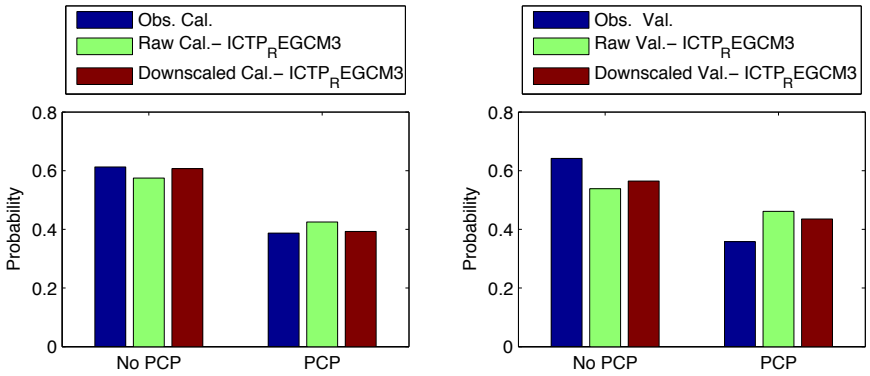

Figure 431 - Precipitation occurrence at Niamey airport with ICTP - REGCM 3 in August

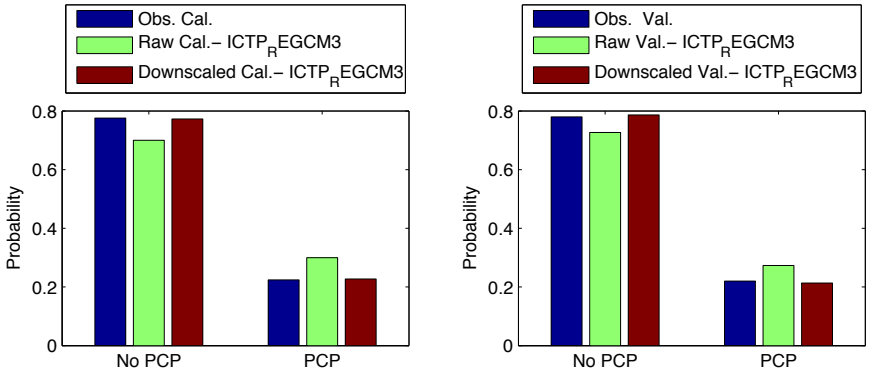

Figure 432 - Precipitation occurrence at Niamey airport with ICTP - REGCM 3 in September

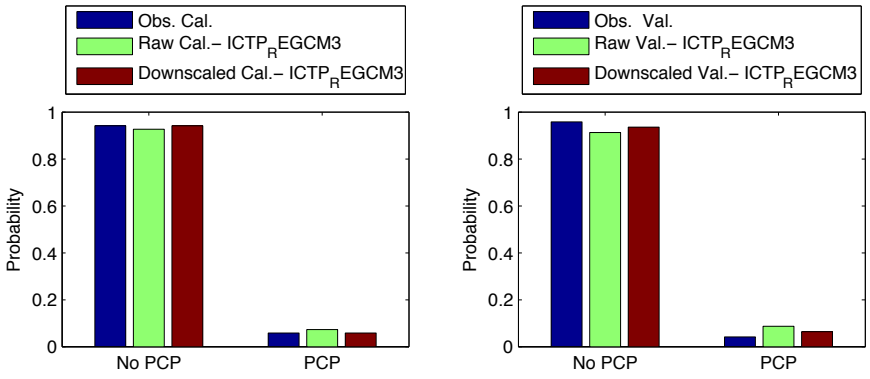

Figure 433 - Precipitation occurrence at Niamey airport with ICTP - REGCM 3 in October

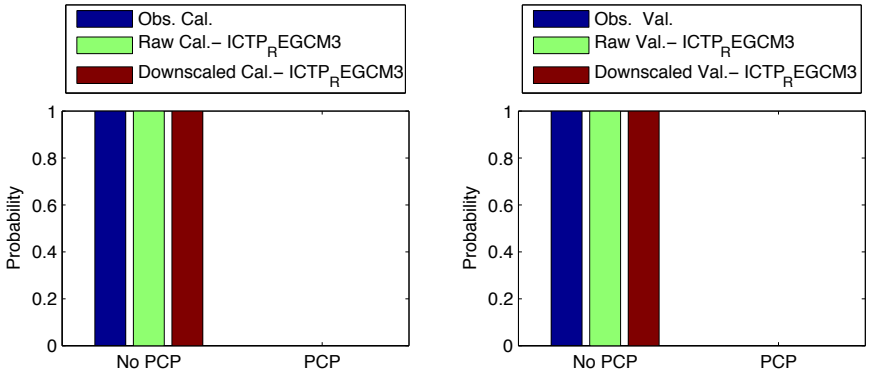

Figure 434 - Precipitation occurrence at Niamey airport with ICTP - REGCM 3 in November

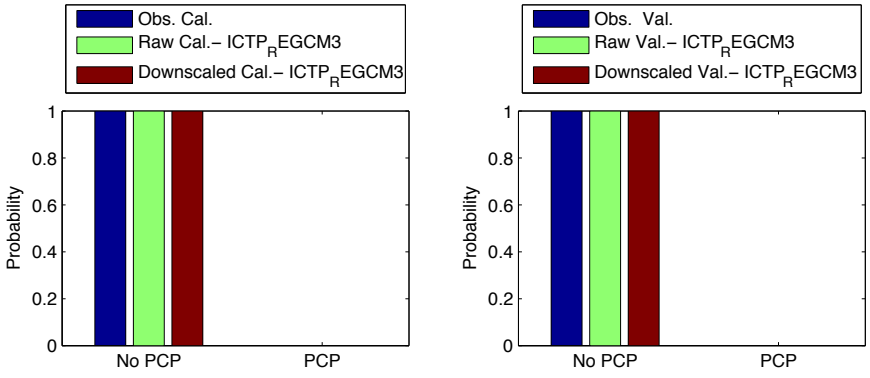

Figure 435 - Precipitation occurrence at Niamey airport with ICTP - REGCM 3 in December

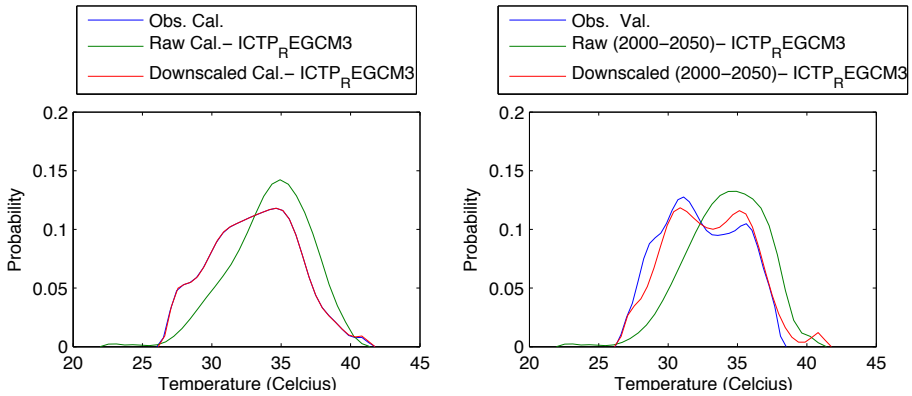

Figure 436 - Probability density for maximum temperature at Niamey airport with ICTP - REGCM 3 in January

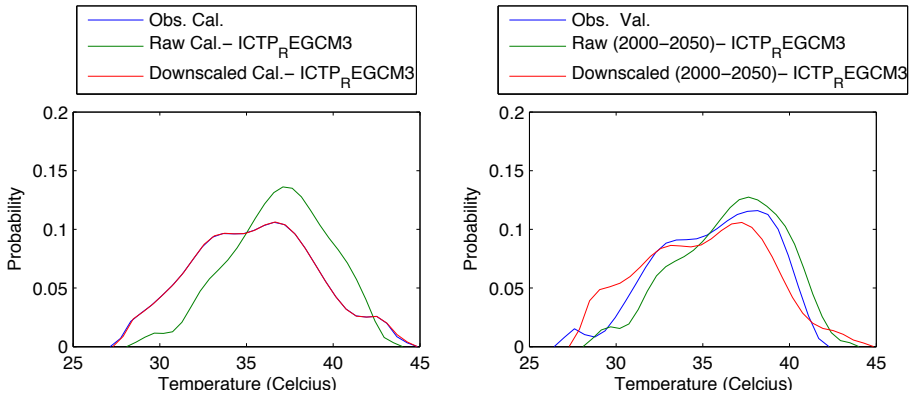

Figure 437 - Probability density for maximum temperature at Niamey airport with ICTP - REGCM 3 in February

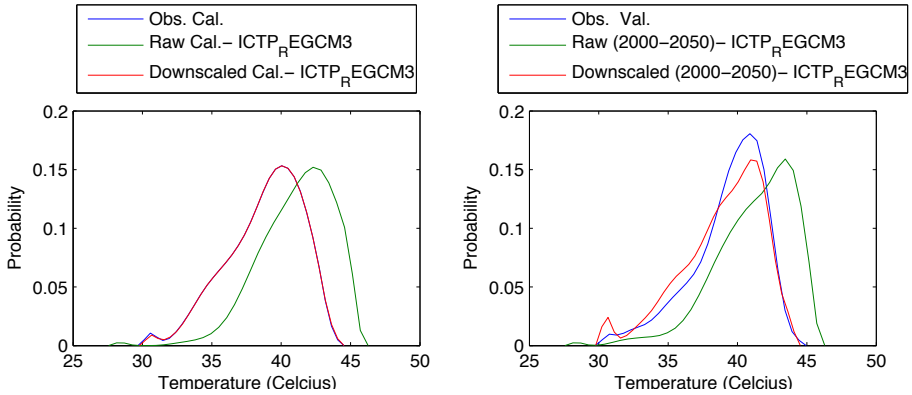

Figure 438 - Probability density for maximum temperature at Niamey airport with ICTP - REGCM 3 in March

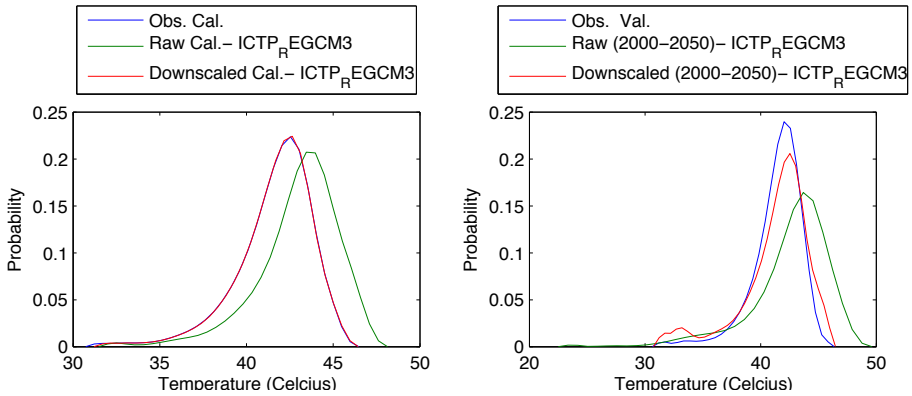

Figure 439 - Probability density for maximum temperature at Niamey airport with ICTP - REGCM 3 in April

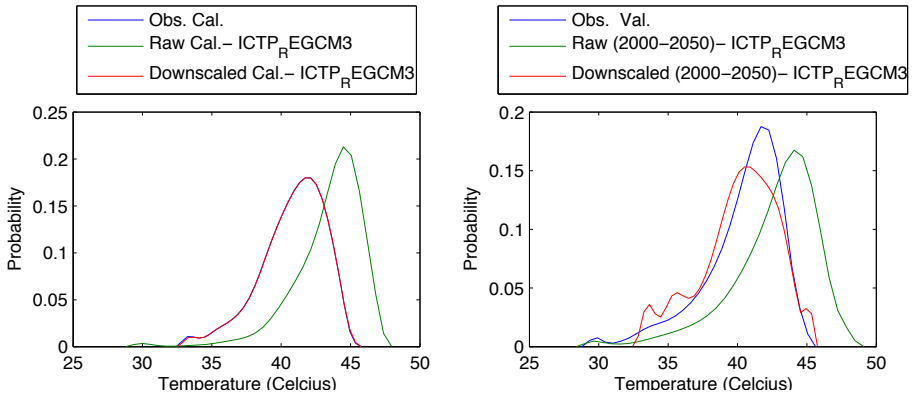

Figure 440 - Probability density for maximum temperature at Niamey airport with ICTP - REGCM 3 in May

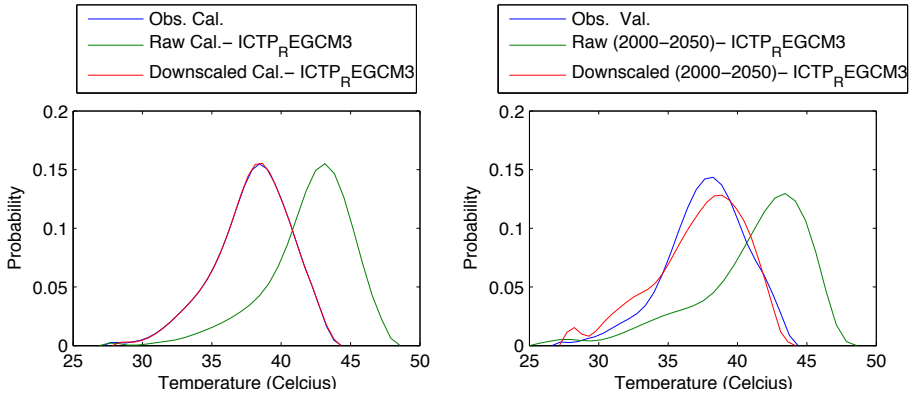

Figure 441 - Probability density for maximum temperature at Niamey airport with ICTP - REGCM 3 in June

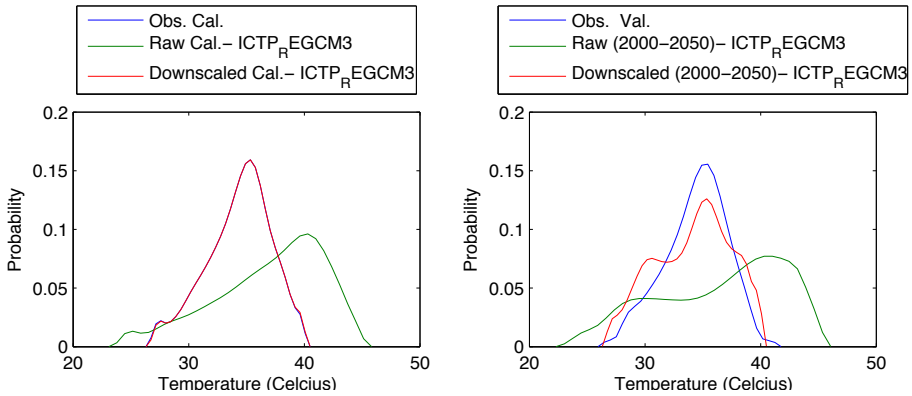

Figure 442 - Probability density for maximum temperature at Niamey airport with ICTP - REGCM 3 in July

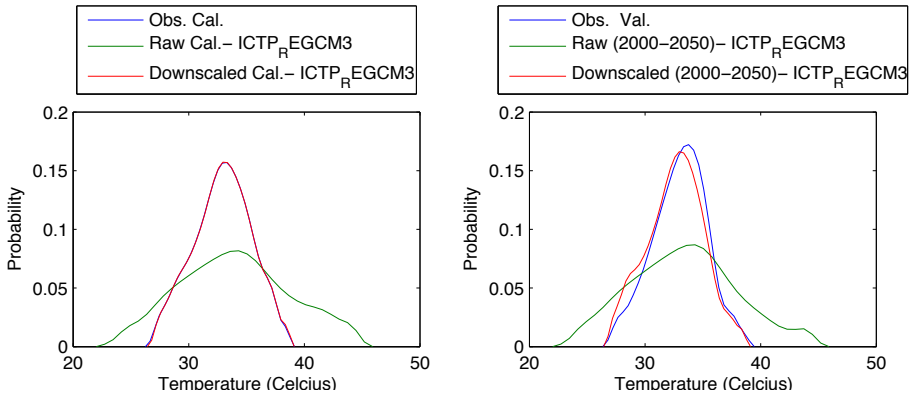

Figure 443 - Probability density for maximum temperature at Niamey airport with ICTP - REGCM 3 in August

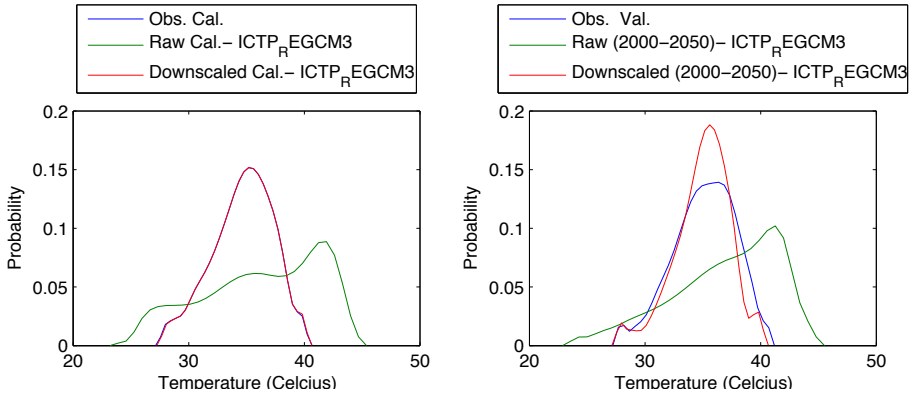

Figure 444 - Probability density for maximum temperature at Niamey airport with ICTP - REGCM 3 in September

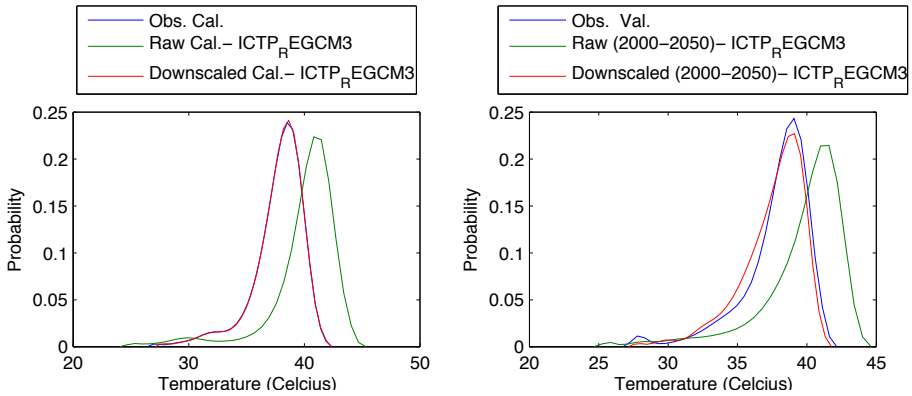

Figure 445 - Probability density for maximum temperature at Niamey airport with ICTP - REGCM 3 in October

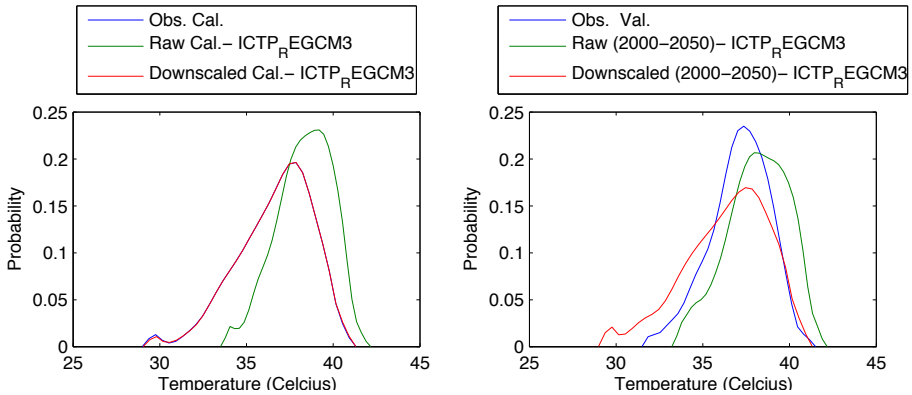

Figure 446 - Probability density for maximum temperature at Niamey airport with ICTP - REGCM 3 in November

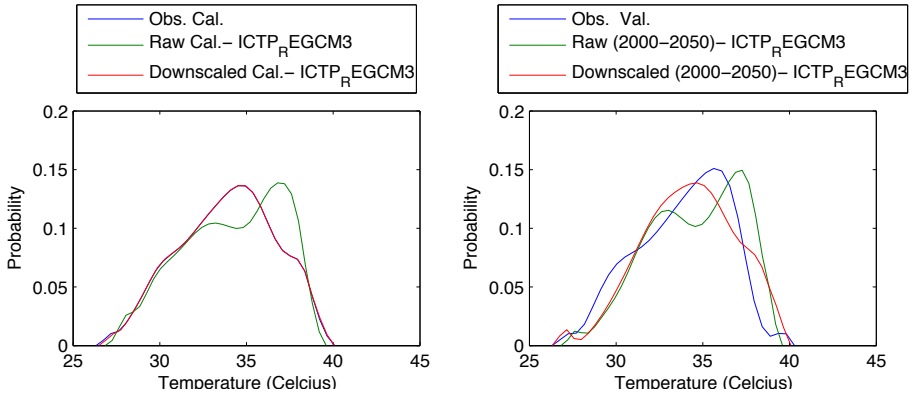

Figure 447 - Probability density for maximum temperature at Niamey airport with ICTP - REGCM 3 in December

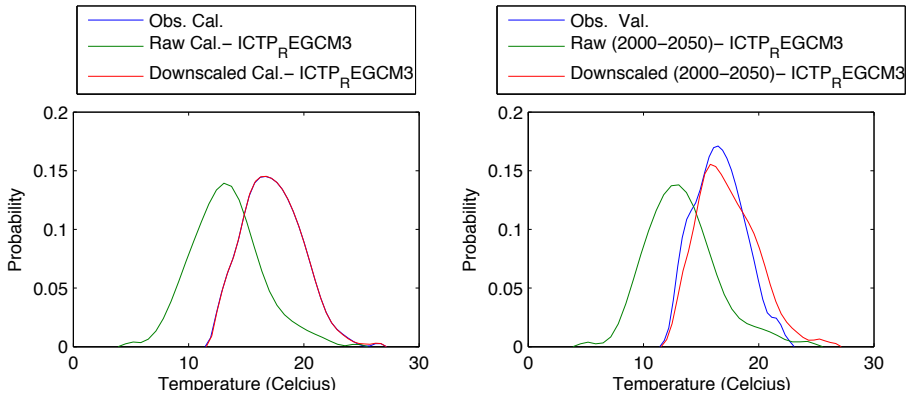

Figure 448 - Probability density for minimum temperature at Niamey airport with ICTP - REGCM 3 in January

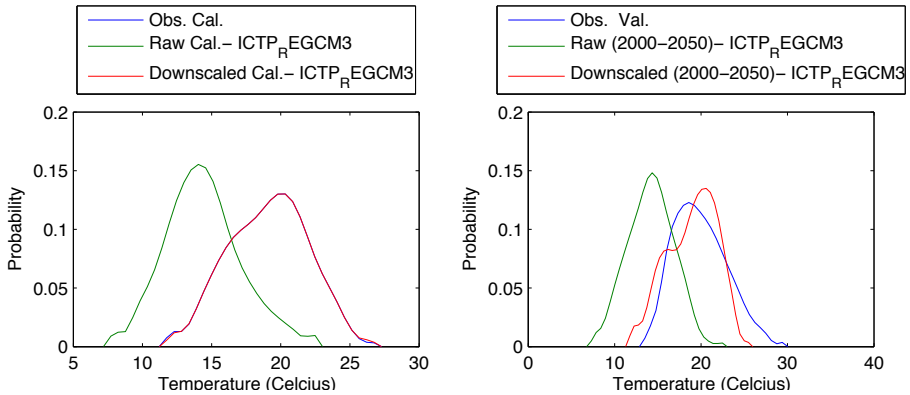

Figure 449 - Probability density for minimum temperature at Niamey airport with ICTP - REGCM 3 in February

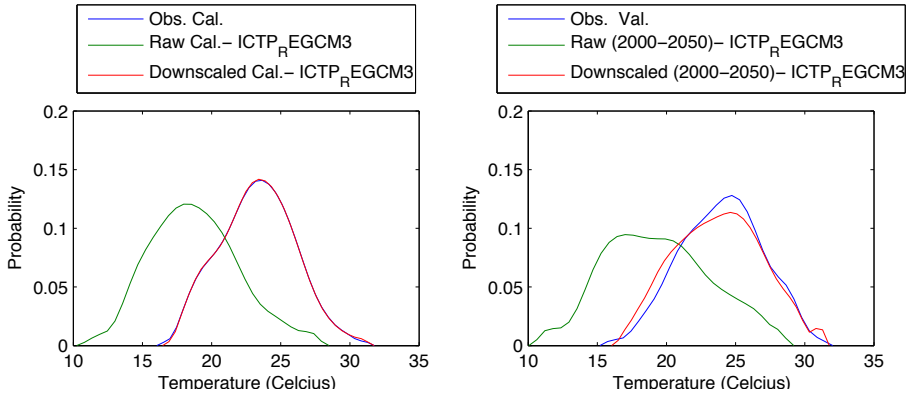

Figure 450 - Probability density for minimum temperature at Niamey airport with ICTP - REGCM 3 in March

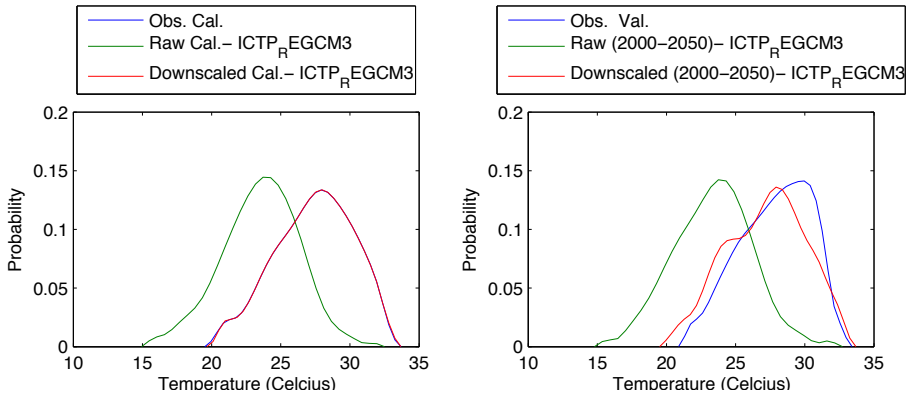

Figure 451 - Probability density for minimum temperature at Niamey airport with ICTP - REGCM 3 in April

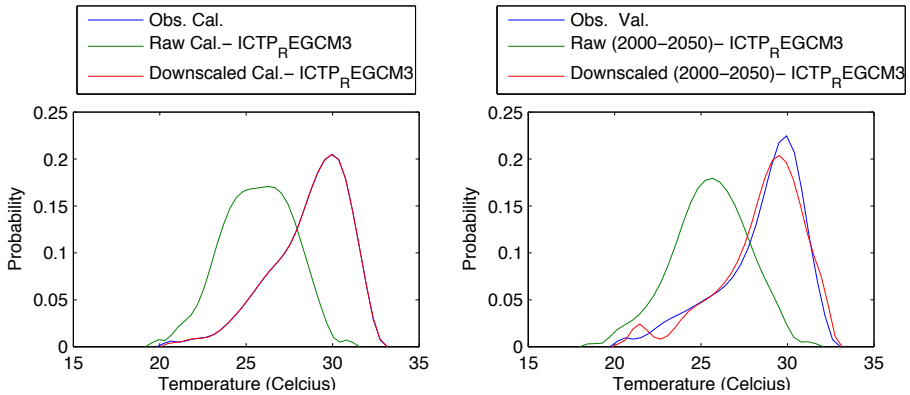

Figure 452 - Probability density for minimum temperature at Niamey airport with ICTP - REGCM 3 in May

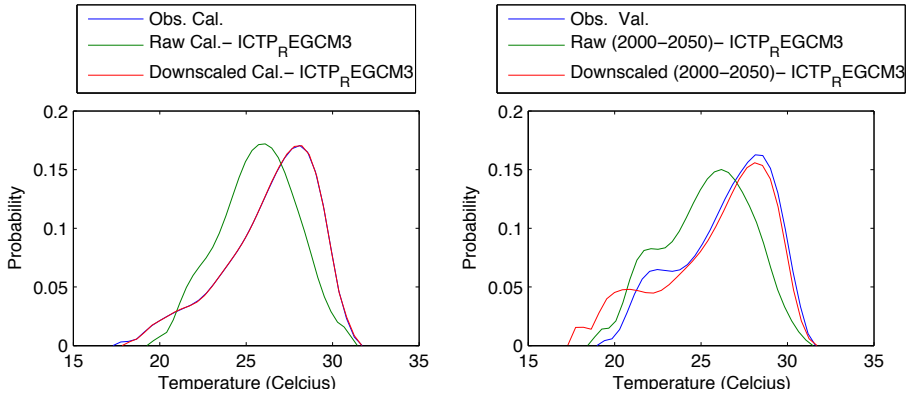

Figure 453 - Probability density for minimum temperature at Niamey airport with ICTP - REGCM 3 in June

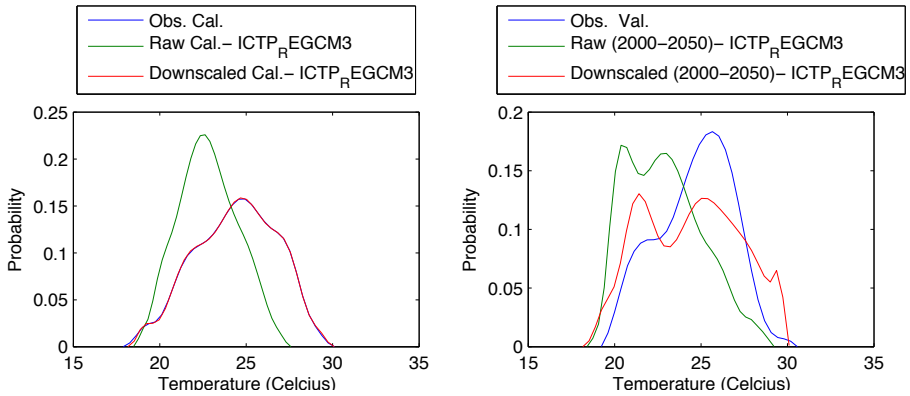

Figure 454 - Probability density for minimum temperature at Niamey airport with ICTP - REGCM 3 in July

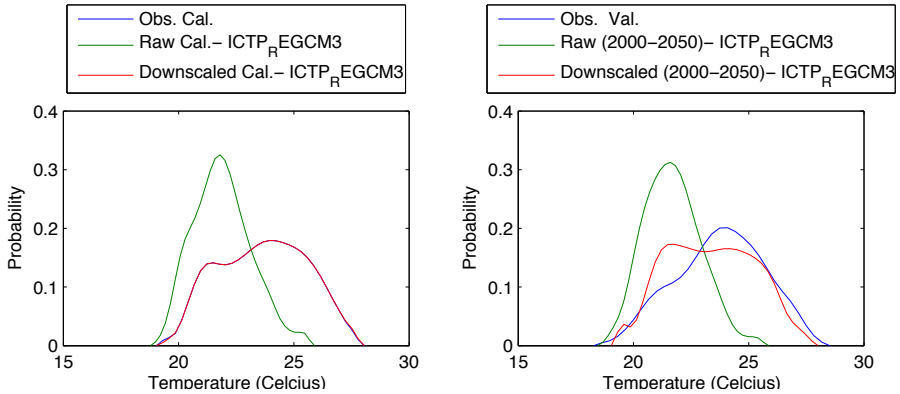

Figure 455 - Probability density for minimum temperature at Niamey airport with ICTP - REGCM 3 in August

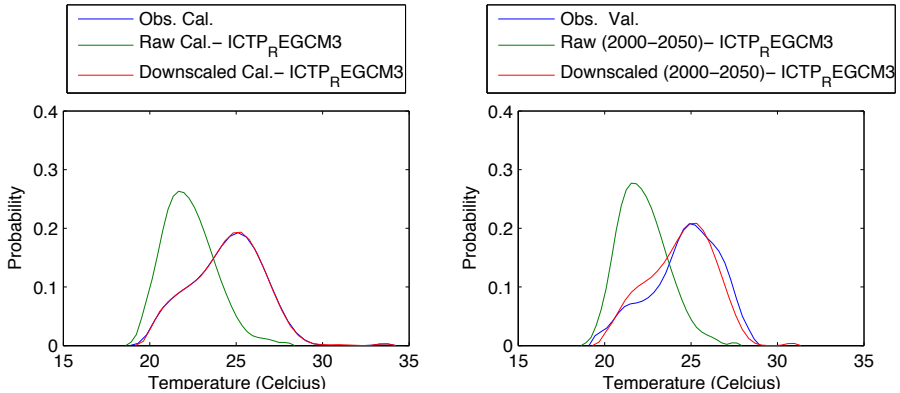

Figure 456 - Probability density for minimum temperature at Niamey airport with ICTP - REGCM 3 in September

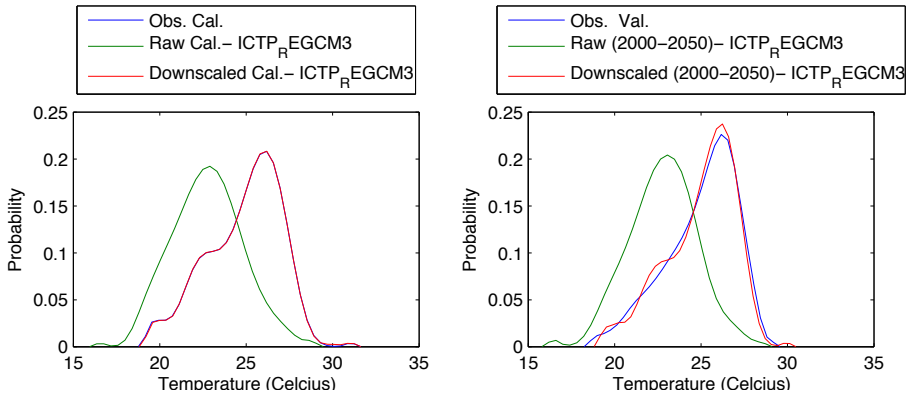

Figure 457 - Probability density for minimum temperature at Niamey airport with ICTP - REGCM 3 in October

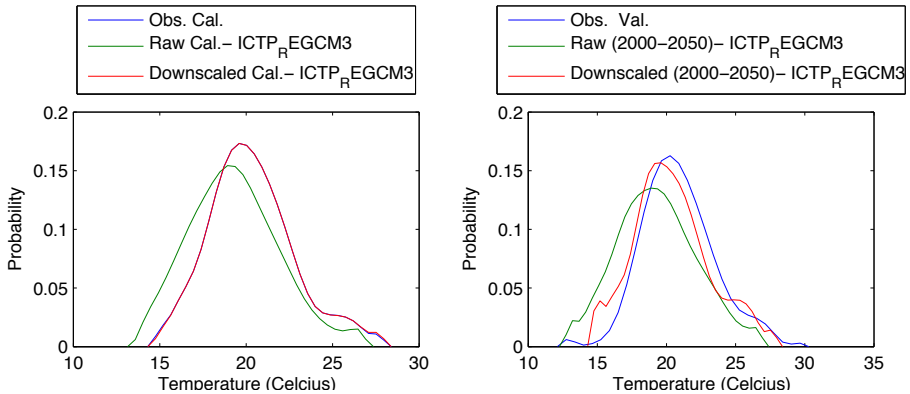

Figure 458 - Probability density for minimum temperature at Niamey airport with ICTP - REGCM 3 in November

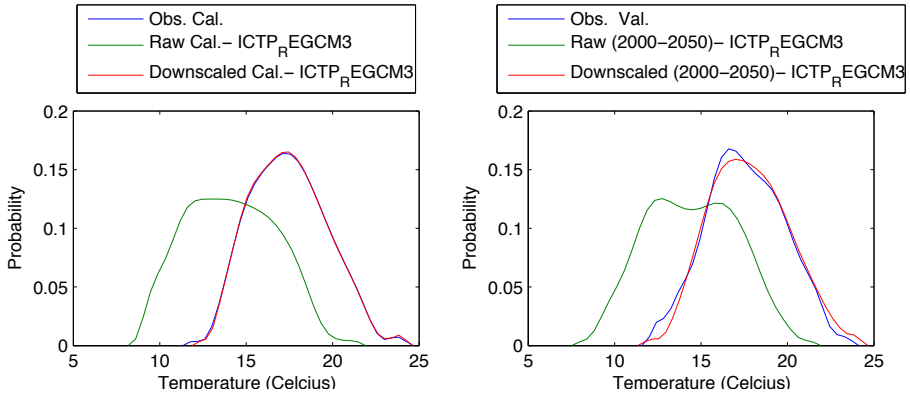

Figure 459 - Probability density for minimum temperature at Niamey airport with ICTP - REGCM 3 in December

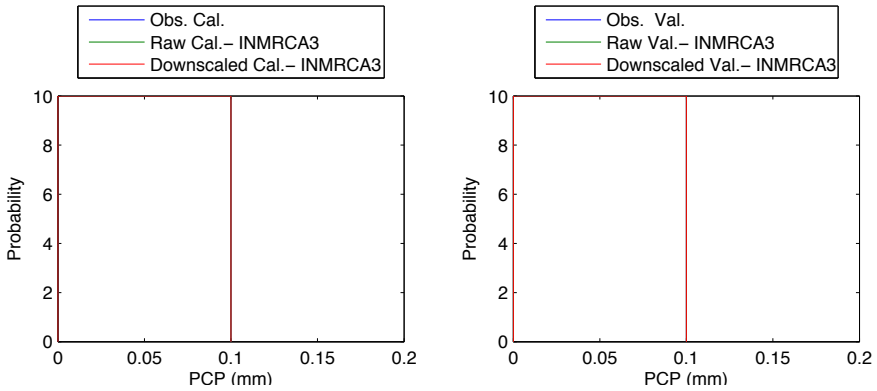

Figure 460 - Probability density of precipitation at Niamey airport with INMRCA 3 in January

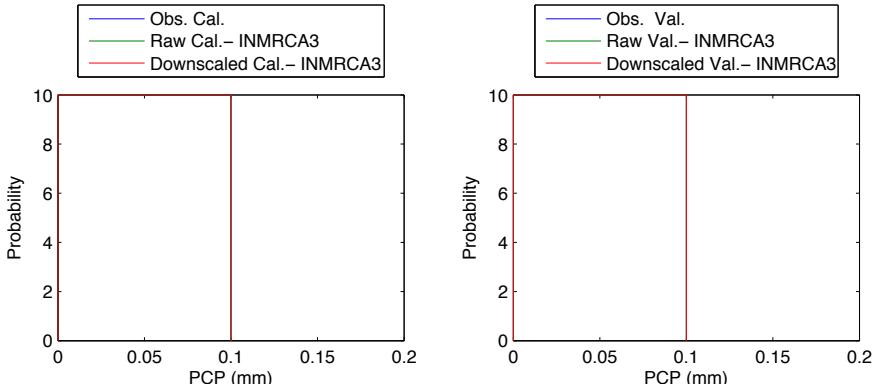

Figure 461 - Probability density of precipitation at Niamey airport with INMRCA 3 in February

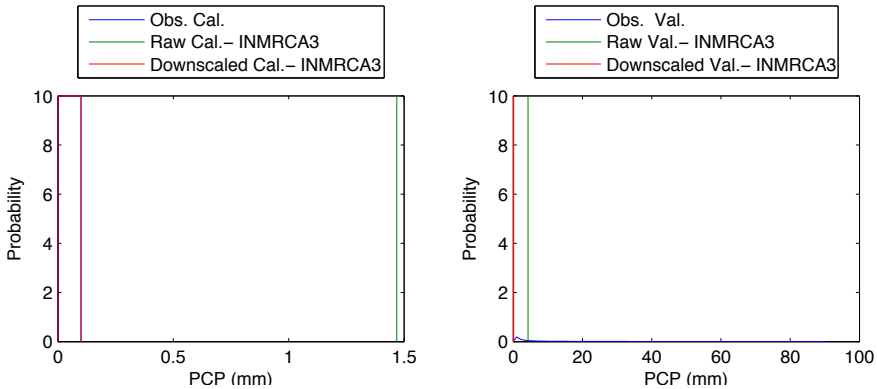

Figure 462 - Probability density of precipitation at Niamey airport with INMRCA 3 in March

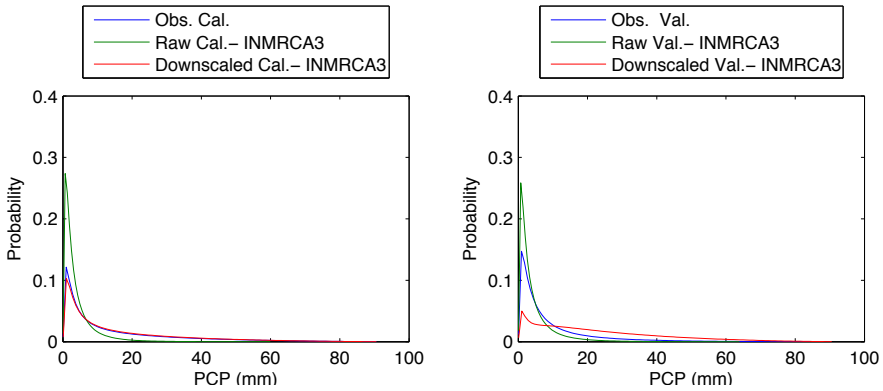

Figure 463 - Probability density of precipitation at Niamey airport with INMRCA 3 in April

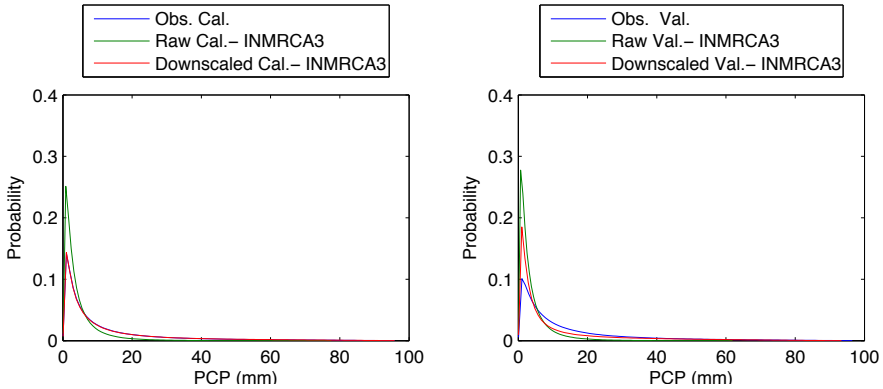

Figure 464 - Probability density of precipitation at Niamey airport with INMRCA 3 in May

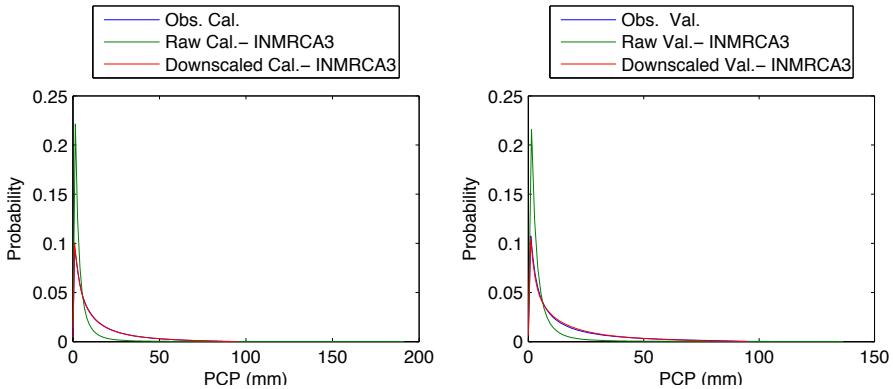

Figure 465 - Probability density of precipitation at Niamey airport with INMRCA 3 in June

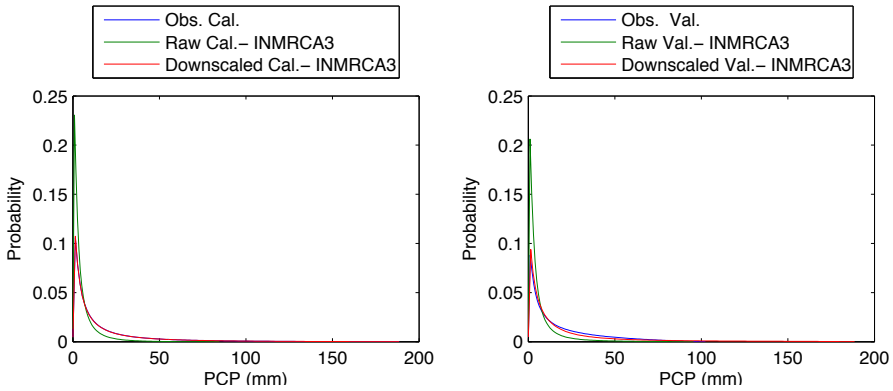

Figure 466 - Probability density of precipitation at Niamey airport with INMRCA 3 in July

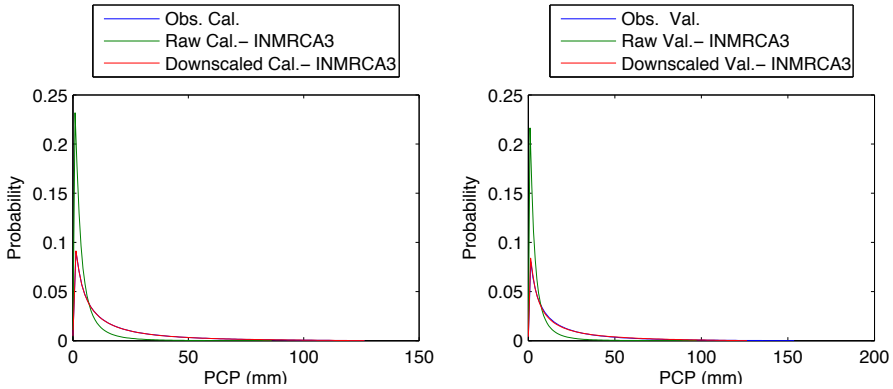

Figure 467 - Probability density of precipitation at Niamey airport with INMRCA 3 in August

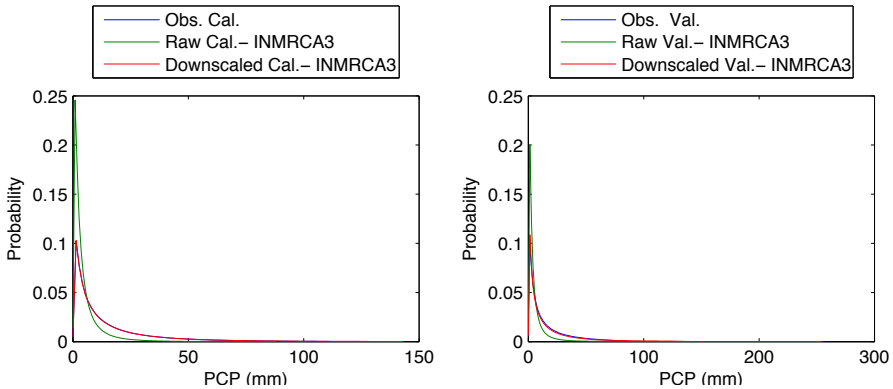

Figure 468 - Probability density of precipitation at Niamey airport with INMRCA 3 in September

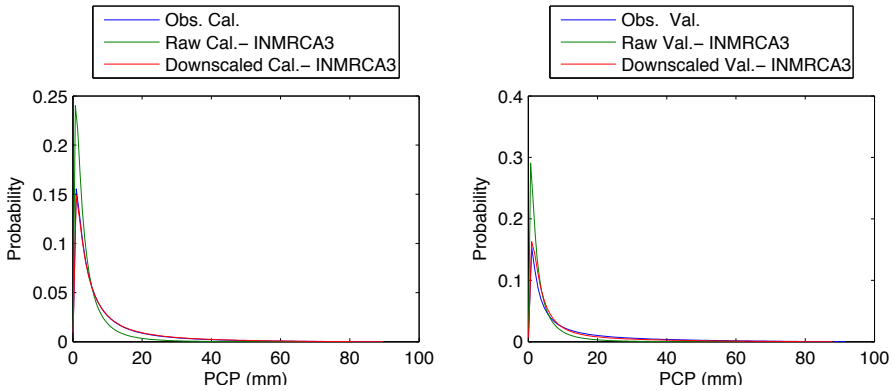

Figure 469 - Probability density of precipitation at Niamey airport with INMRCA 3 in October

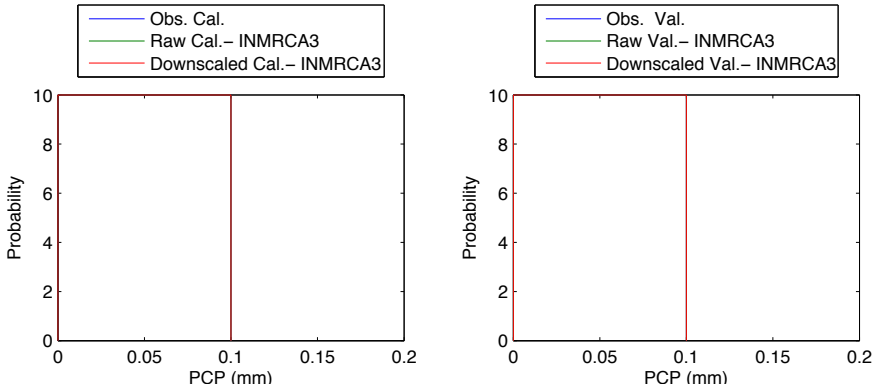

Figure 470 - Probability density of precipitation at Niamey airport with INMRCA 3 in November

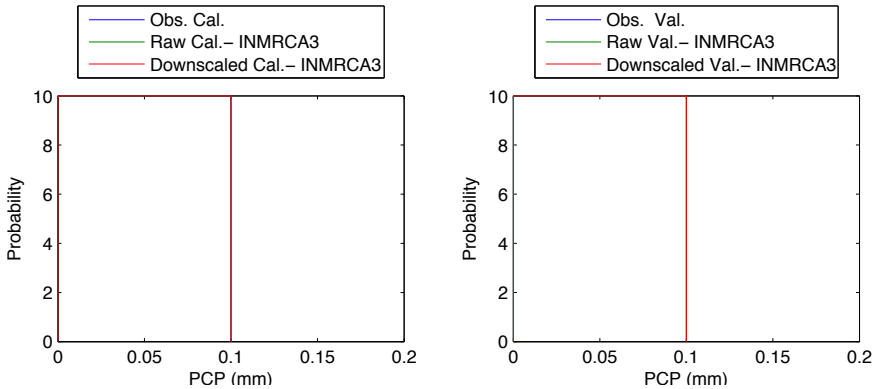

Figure 471 - Probability density of precipitation at Niamey airport with INMRCA 3 in December

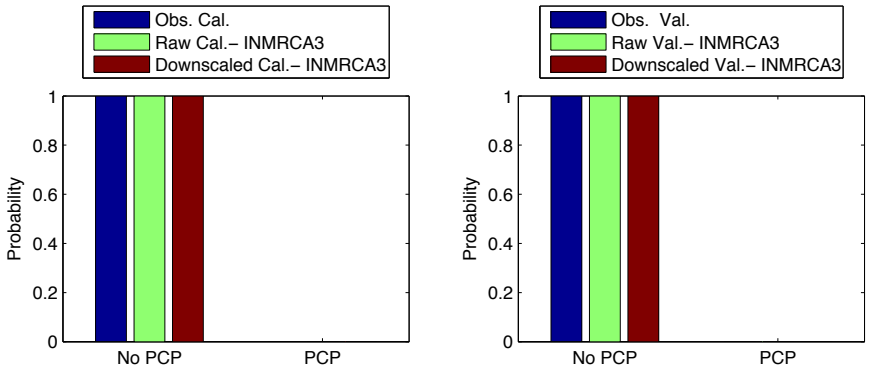

Figure 472 - Precipitation occurrence at Niamey airport with INMRCA 3 in January

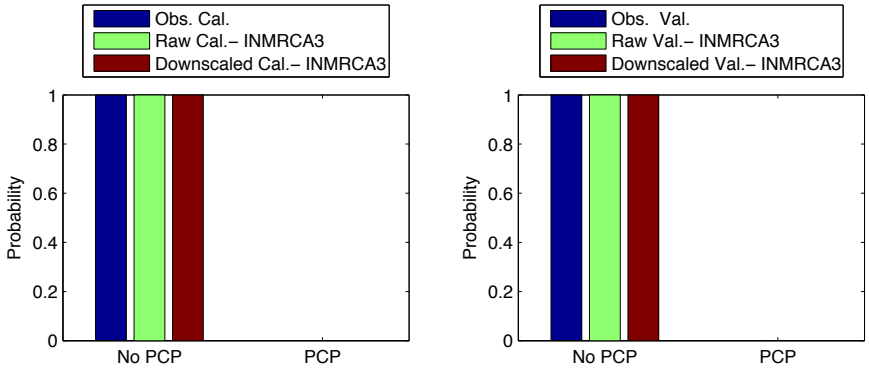

Figure 473 - Precipitation occurrence at Niamey airport with INMRCA 3 in February

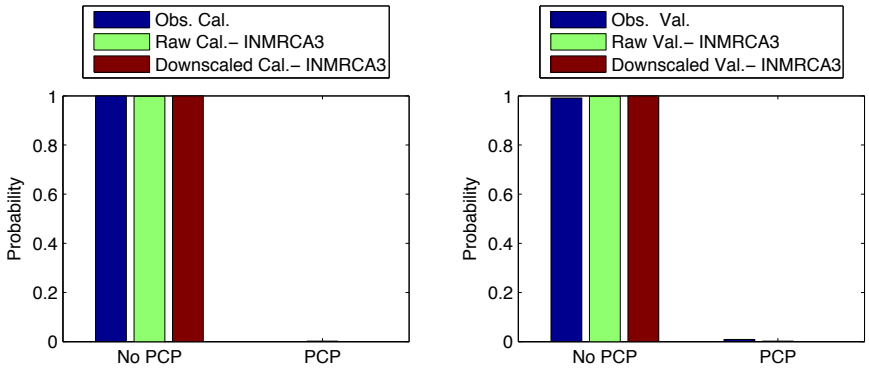

Figure 474 - Precipitation occurrence at Niamey airport with INMRCA 3 in March

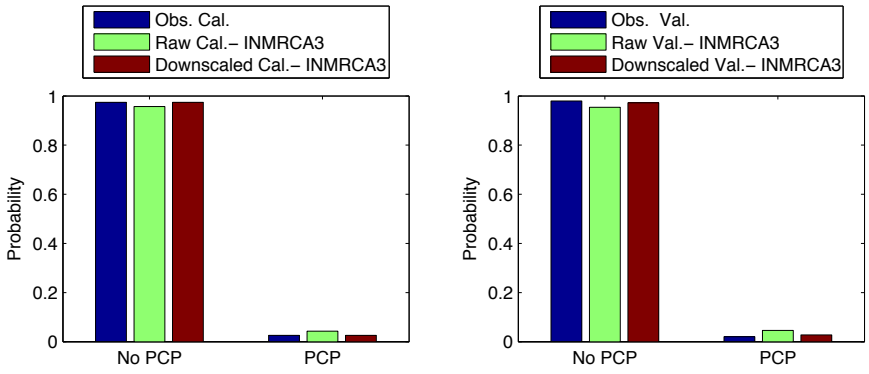

Figure 475 - Precipitation occurrence at Niamey airport with INMRCA 3 in April

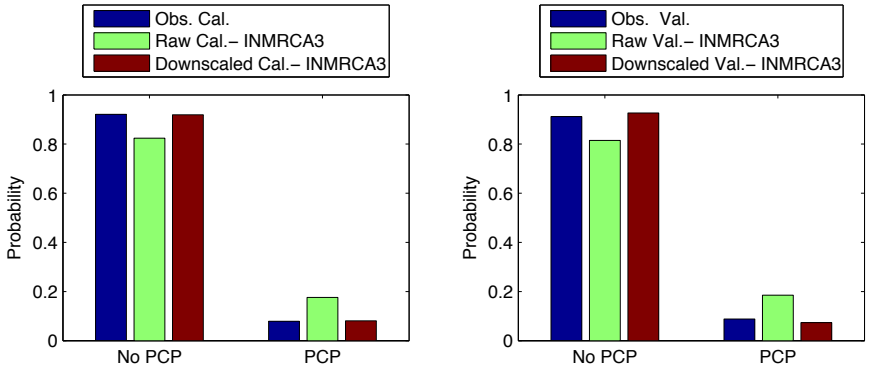

Figure 476 - Precipitation occurrence at Niamey airport with INMRCA 3 in May

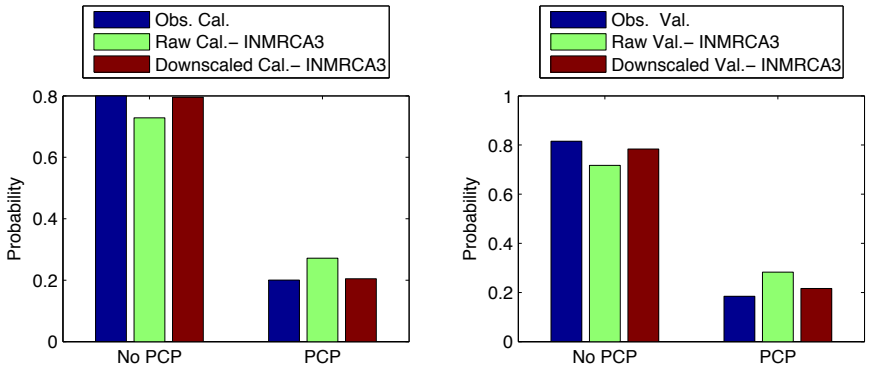

Figure 477 - Precipitation occurrence at Niamey airport with INMRCA 3 in June

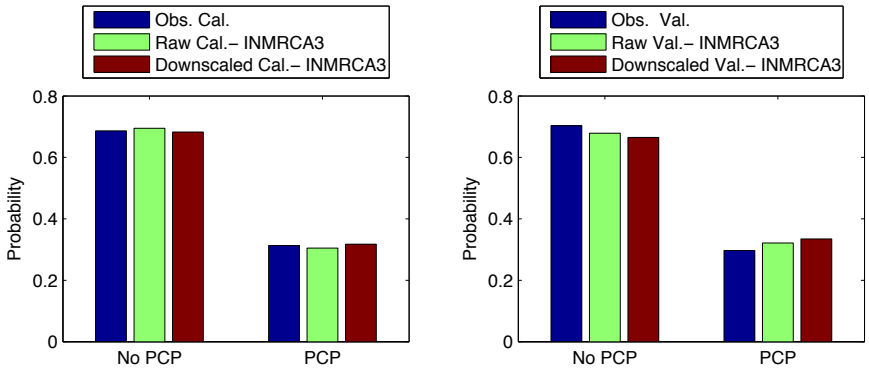

Figure 478 - Precipitation occurrence at Niamey airport with INMRCA 3 in July

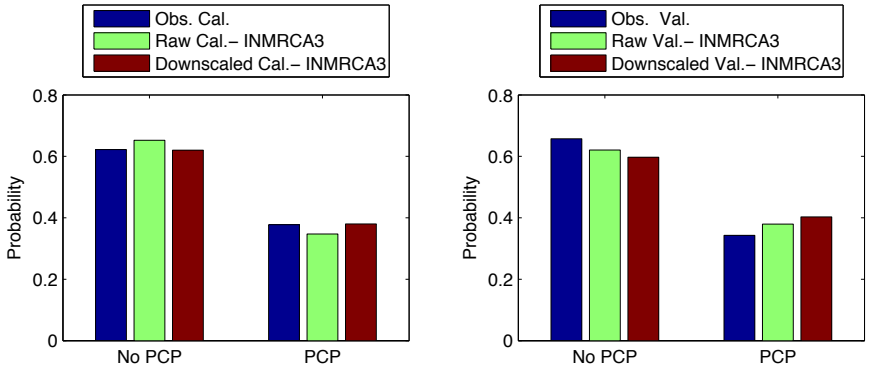

Figure 479 - Precipitation occurrence at Niamey airport with INMRCA 3 in August

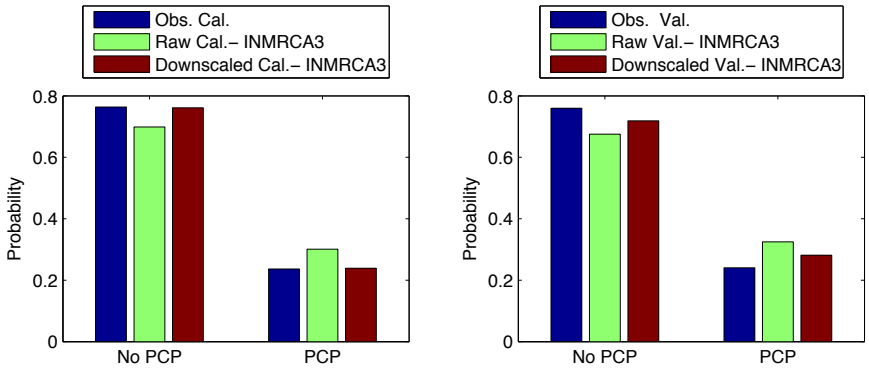

Figure 480 - Precipitation occurrence at Niamey airport with INMRCA 3 in September

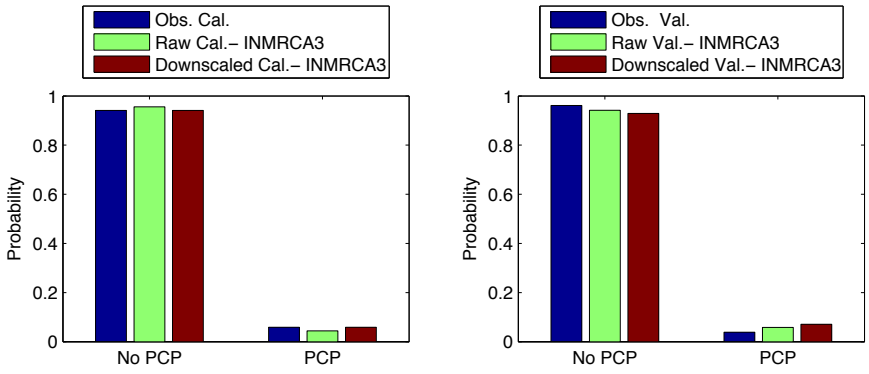

Figure 481 - Precipitation occurrence at Niamey airport with INMRCA 3 in October

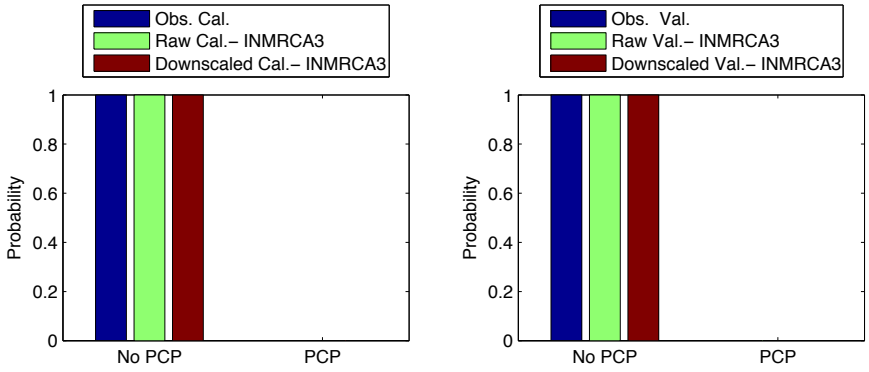

Figure 482 - Precipitation occurrence at Niamey airport with INMRCA 3 in November

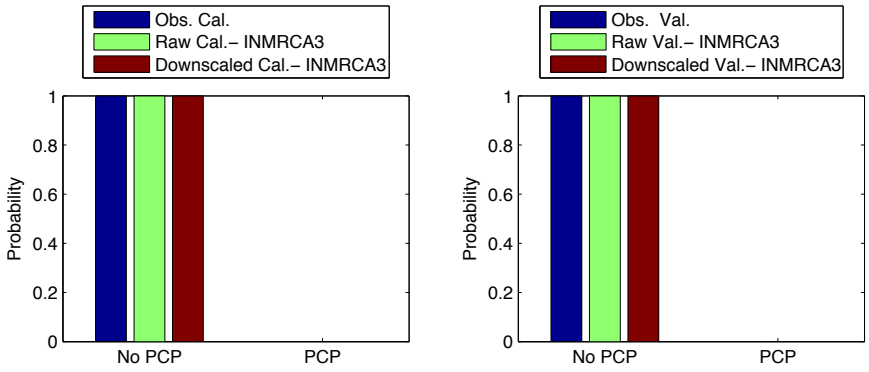

Figure 483 - Precipitation occurrence at Niamey airport with INMRCA 3 in December

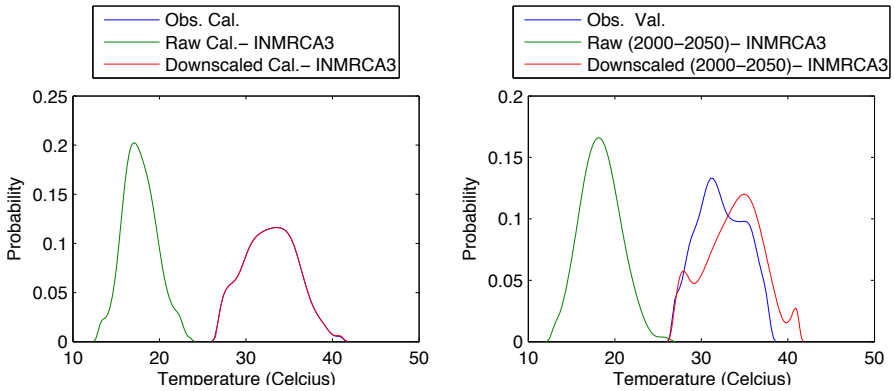

Figure 484 - Probability density for maximum temperature at Niamey airport with INMRCA 3 in January

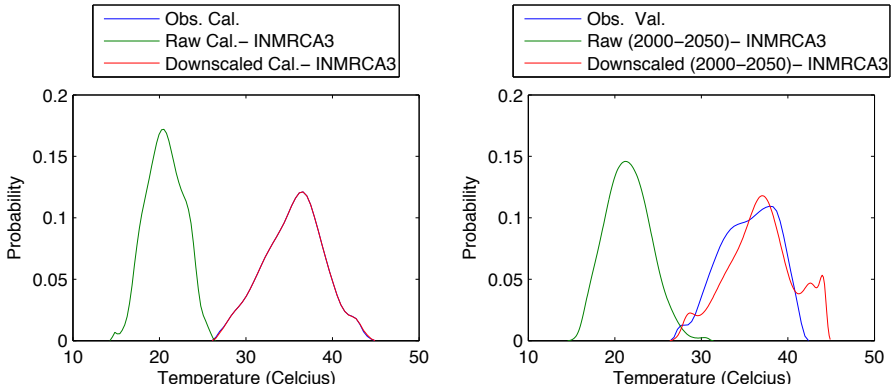

Figure 485 - Probability density for maximum temperature at Niamey airport with INMRCA 3 in February

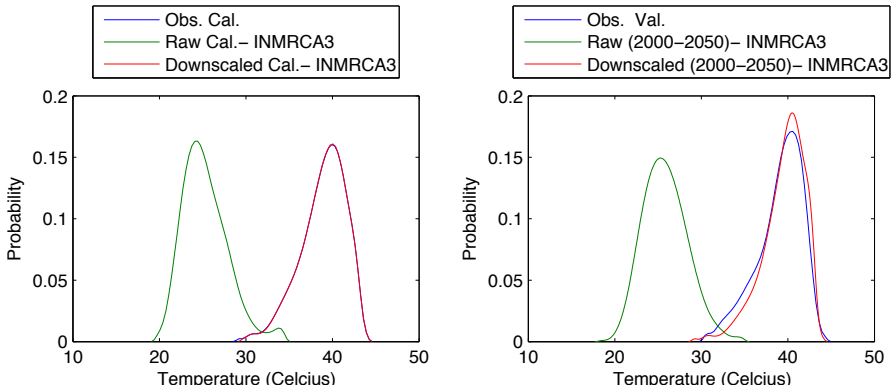

Figure 486 - Probability density for maximum temperature at Niamey airport with INMRCA 3 in March

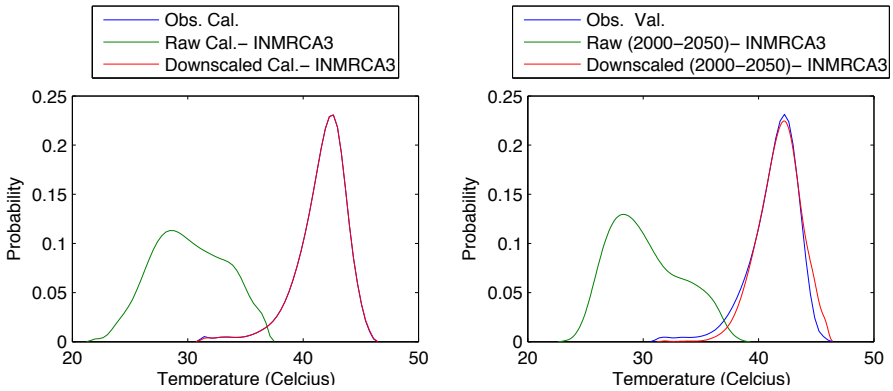

\

Figure 487 - Probability density for maximum temperature at Niamey airport with INMRCA 3 in April

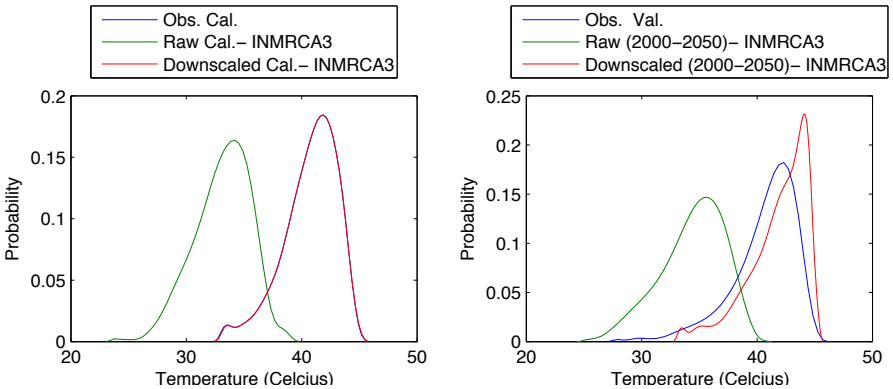

Figure 488 - Probability density for maximum temperature at Niamey airport with INMRCA 3 in May

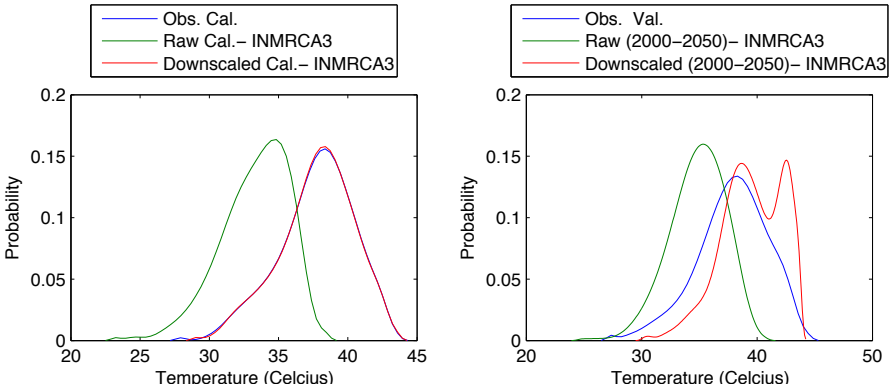

Figure 489 - Probability density for maximum temperature at Niamey airport with INMRCA 3 in June

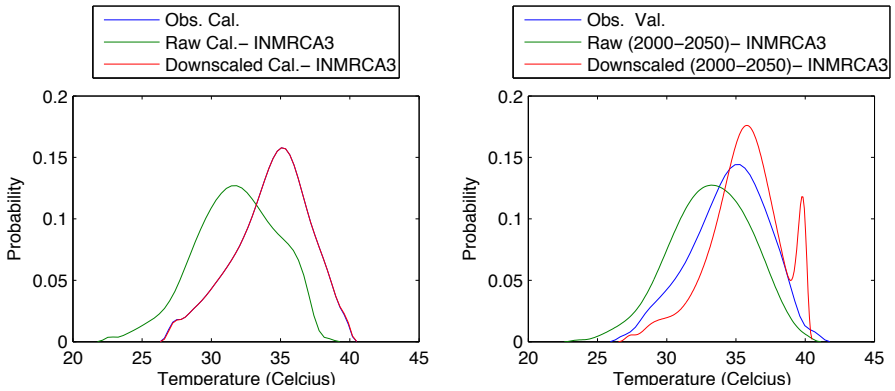

Figure 490 - Probability density for maximum temperature at Niamey airport with INMRCA 3 in July

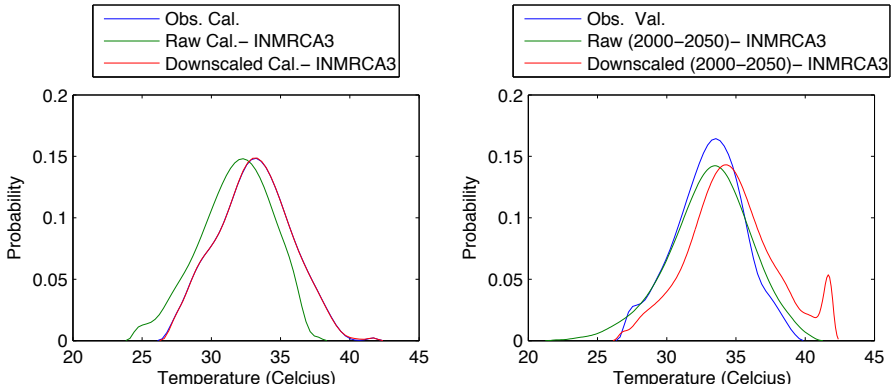

Figure 491 - Probability density for maximum temperature at Niamey airport with INMRCA 3 in August

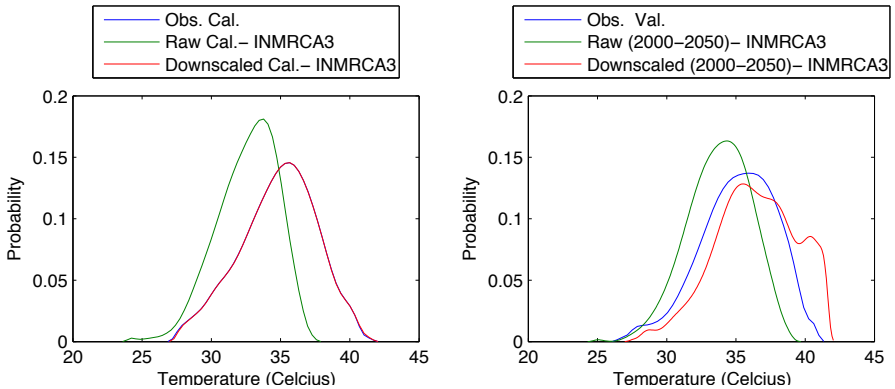

Figure 492 - Probability density for maximum temperature at Niamey airport with INMRCA 3 in September

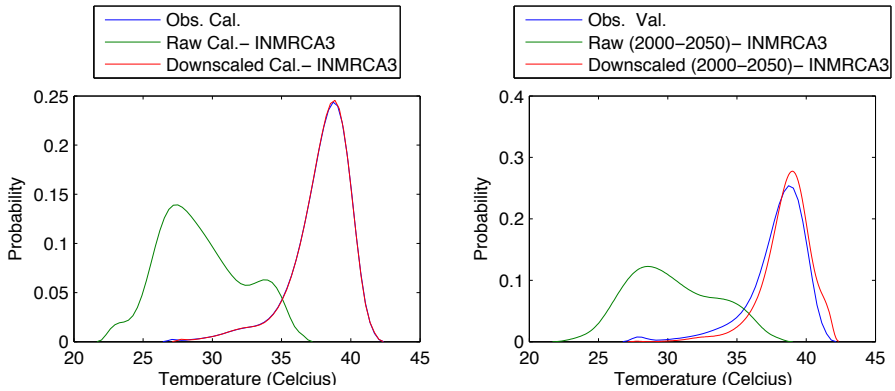

Figure 493 - Probability density for maximum temperature at Niamey airport with INMRCA 3 in October

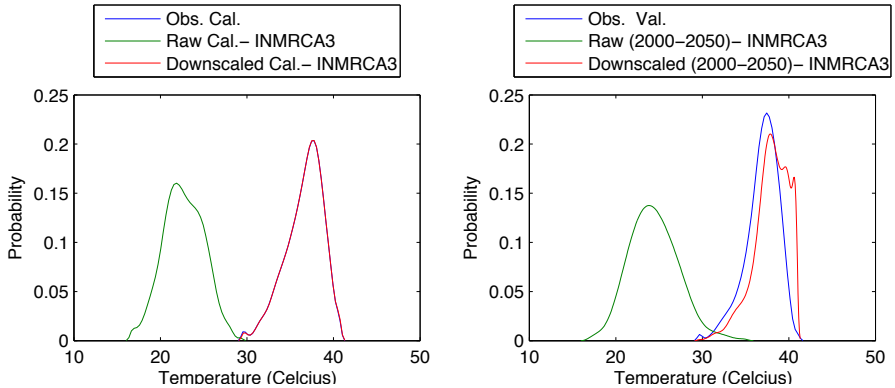

Figure 494 - Probability density for maximum temperature at Niamey airport with INMRCA 3 in November

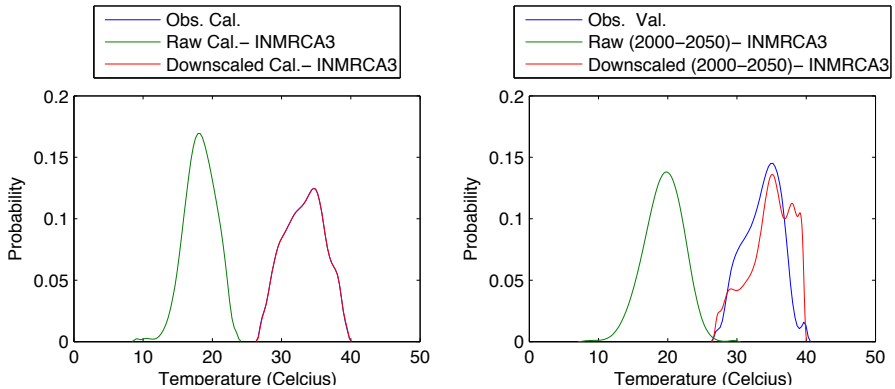

Figure 495 - Probability density for maximum temperature at Niamey airport with INMRCA 3 in December

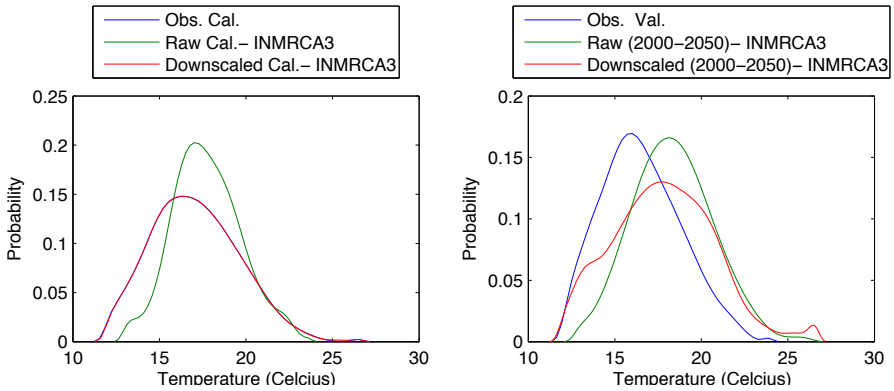

Figure 496 - Probability density for minimum temperature at Niamey airport with INMRCA 3 in January

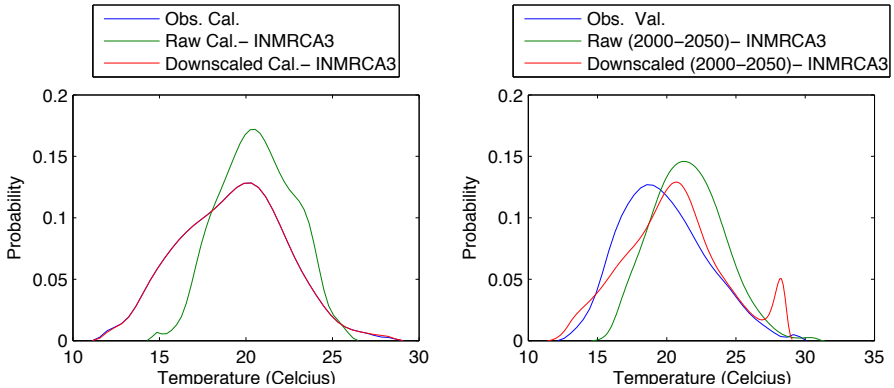

Figure 497 - Probability density for minimum temperature at Niamey airport with INMRCA 3 in February

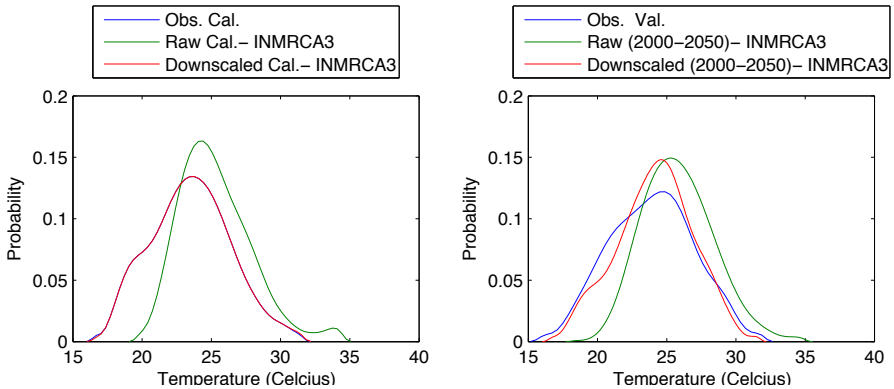

Figure 498 - Probability density for minimum temperature at Niamey airport with INMRCA 3 in March

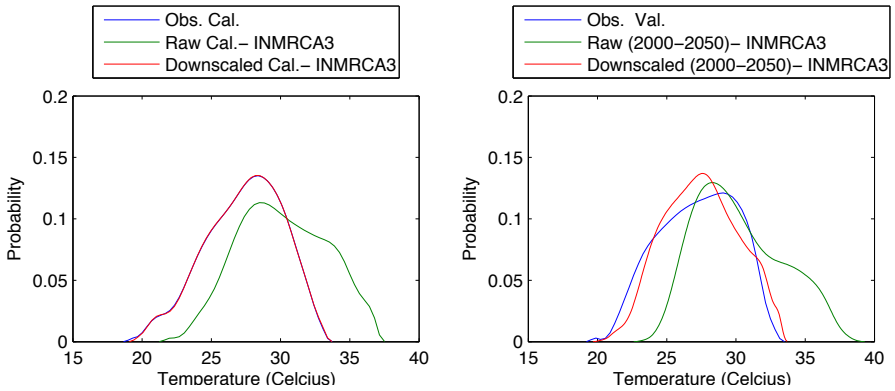

Figure 499 - Probability density for minimum temperature at Niamey airport with INMRCA 3 in April

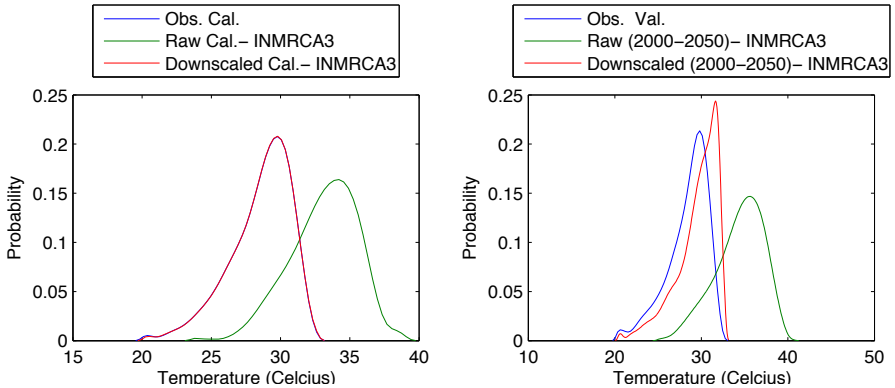

Figure 500 - Probability density for minimum temperature at Niamey airport with INMRCA 3 in May

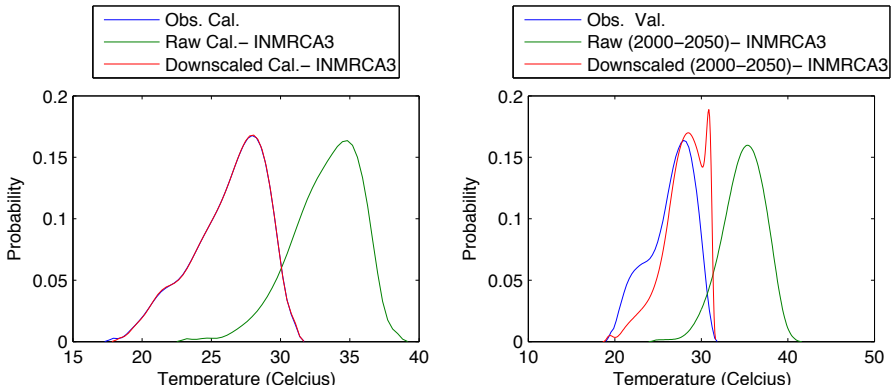

Figure 501 - Probability density for minimum temperature at Niamey airport with INMRCA 3 in June

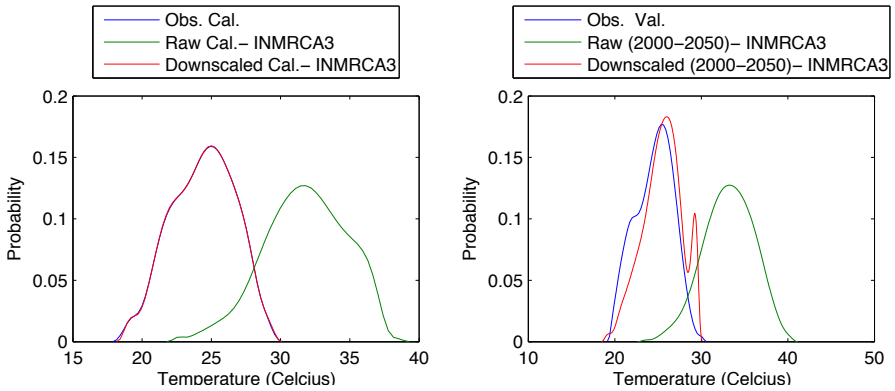

Figure 502 - Probability density for minimum temperature at Niamey airport with INMRCA 3 in July

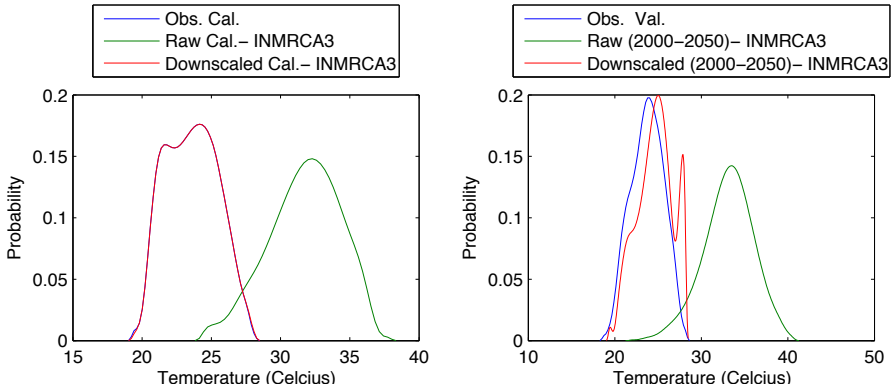

Figure 503 - Probability density for minimum temperature at Niamey airport with INMRCA 3 in August

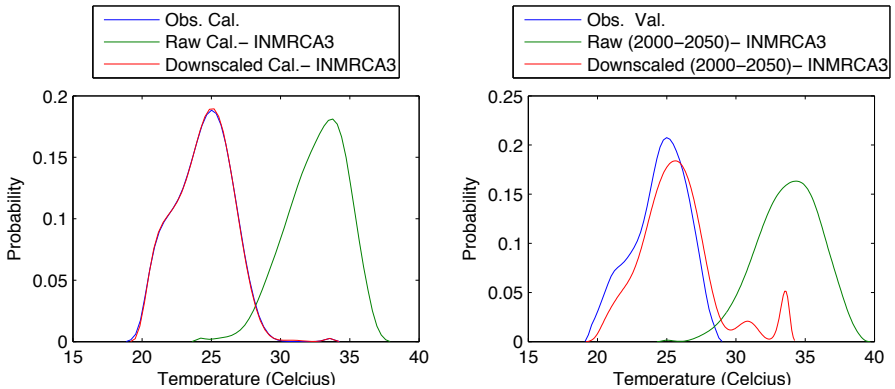

Figure 504 - Probability density for minimum temperature at Niamey airport with INMRCA 3 in September

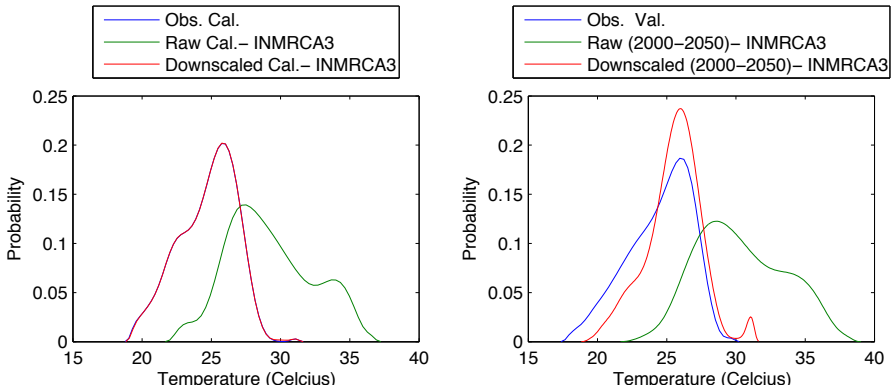

Figure 505 - Probability density for minimum temperature at Niamey airport with INMRCA 3 in October

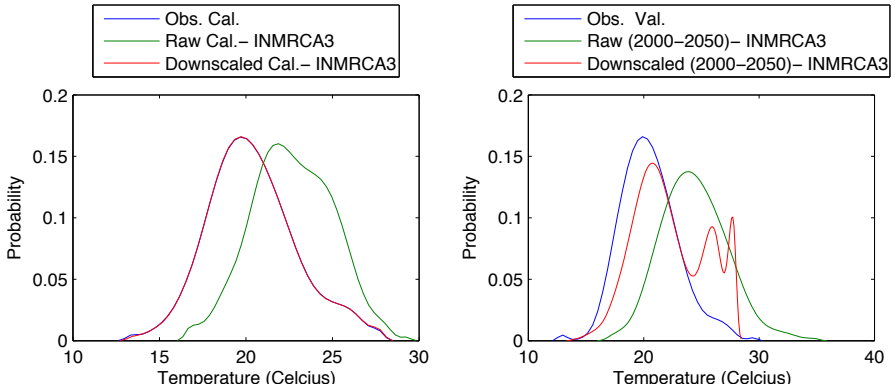

Figure 506 - Probability density for minimum temperature at Niamey airport with INMRCA 3 in November

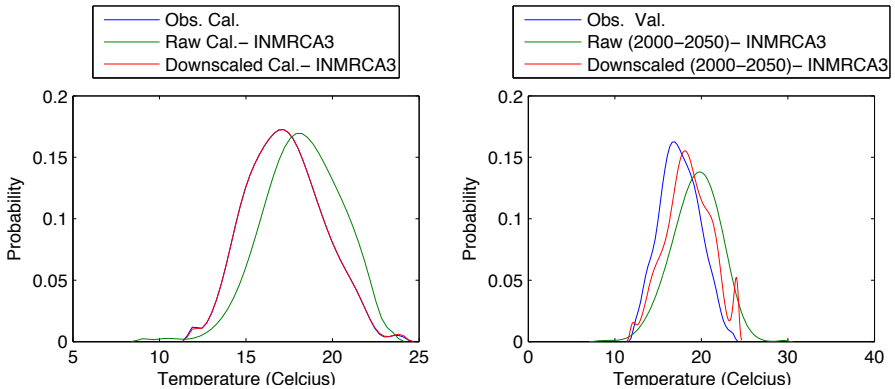

Figure 507 - Probability density for minimum temperature at Niamey airport with INMRCA 3 in December

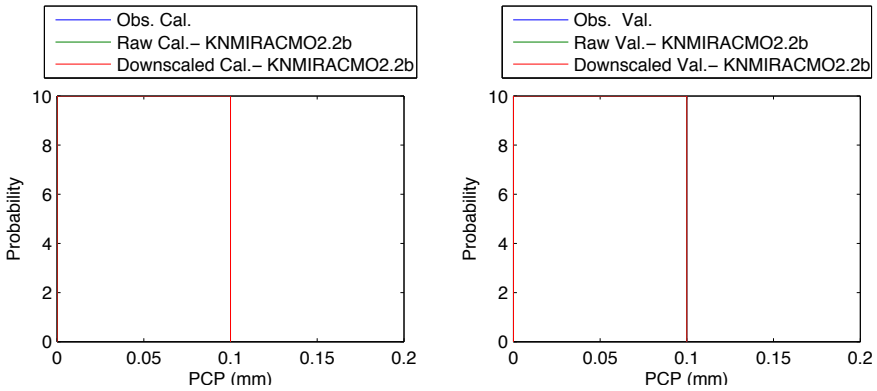

Figure 508 - Probability density of precipitation at Niamey airport with KNMIRACM 02.2b in January

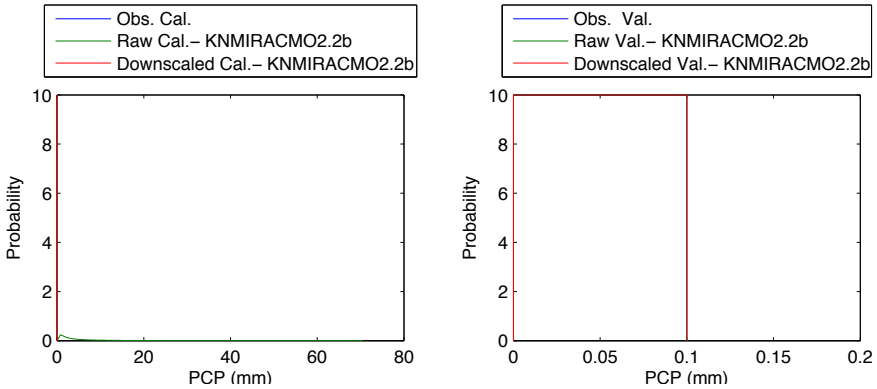

Figure 509 - Probability density of precipitation at Niamey airport with KNMIRACM 02.2b in February

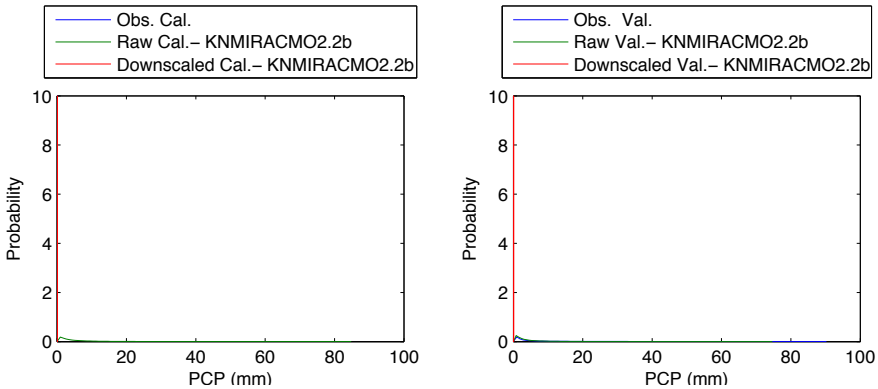

Figure 510 - Probability density of precipitation at Niamey airport with KNMIRACM 02.2b in March

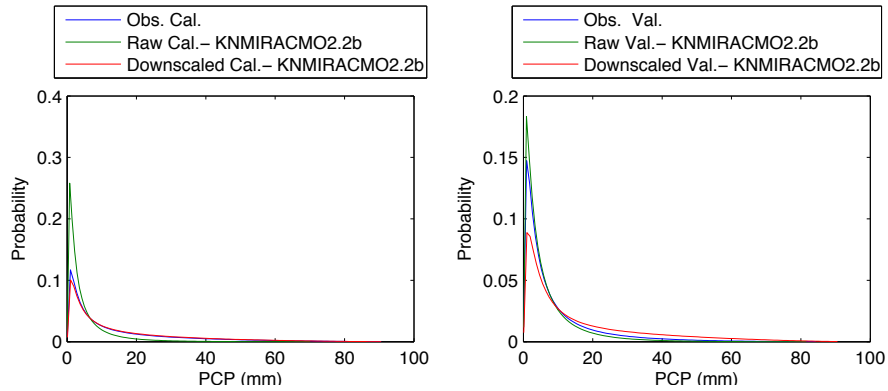

Figure 511 - Probability density of precipitation at Niamey airport with KNMIRACM 02.2b in April

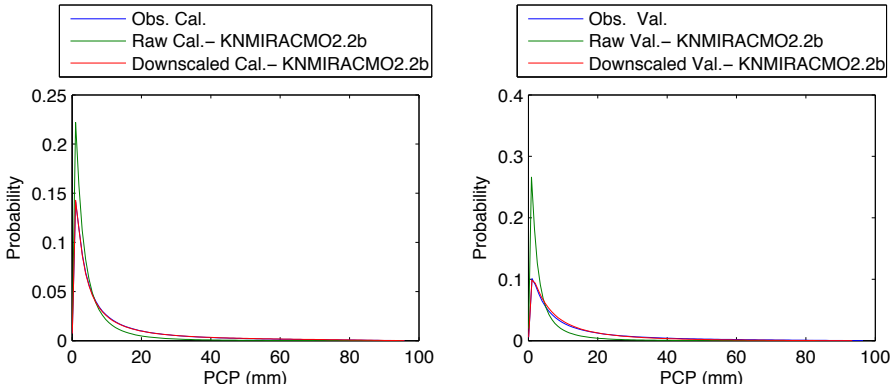

Figure 512 - Probability density of precipitation at Niamey airport with KNMIRACM 02.2b in May

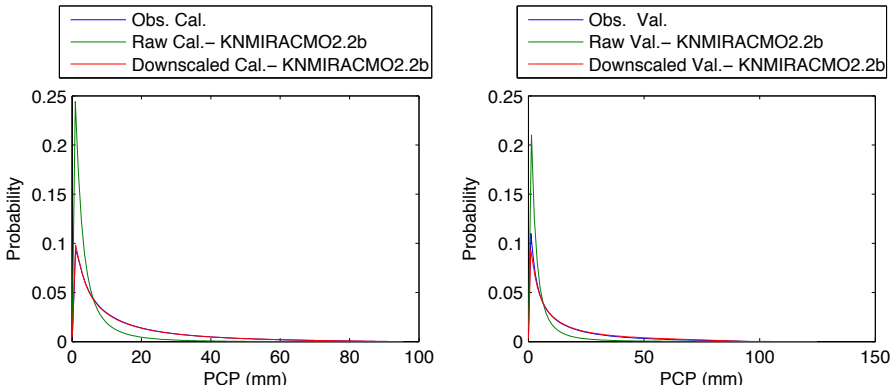

Figure 513 - Probability density of precipitation at Niamey airport with KNMIRACM 02.2b in June

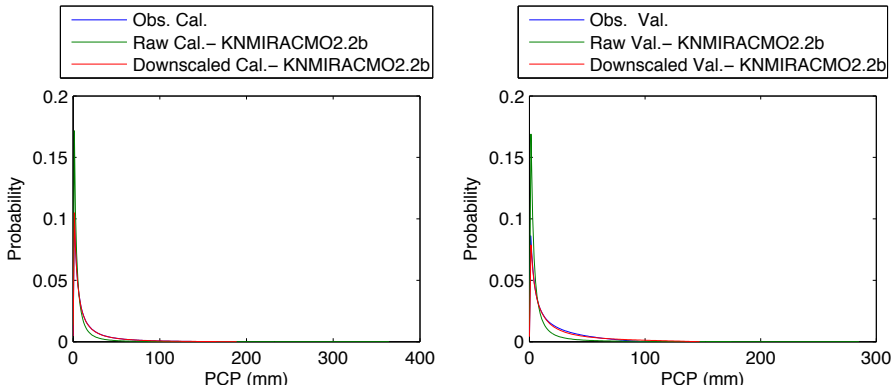

Figure 514 - Probability density of precipitation at Niamey airport with KNMIRACM 02.2b in July

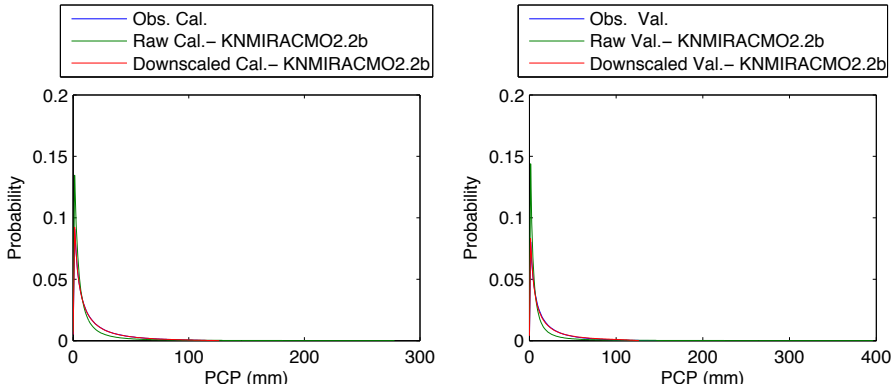

Figure 515 - Probability density of precipitation at Niamey airport with KNMIRACM 02.2b in August

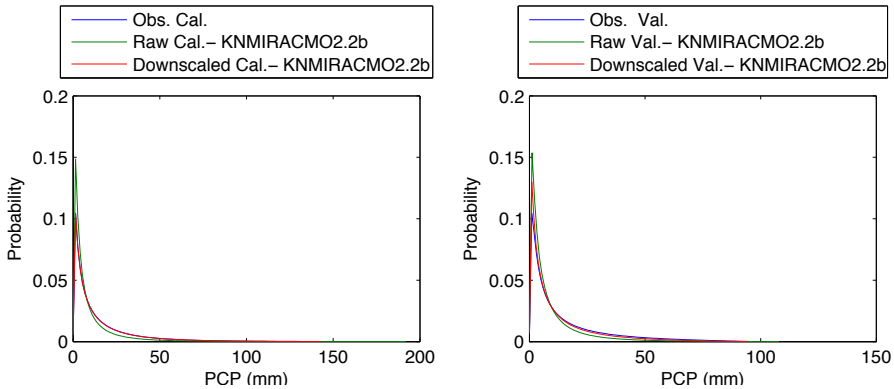

Figure 516 - Probability density of precipitation at Niamey airport with KNMIRACM 02.2b in September

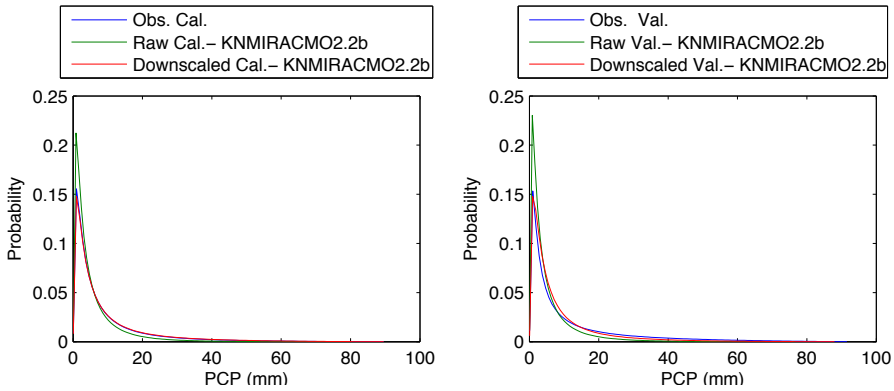

Figure 517 - Probability density of precipitation at Niamey airport with KNMIRACM 02.2b in October

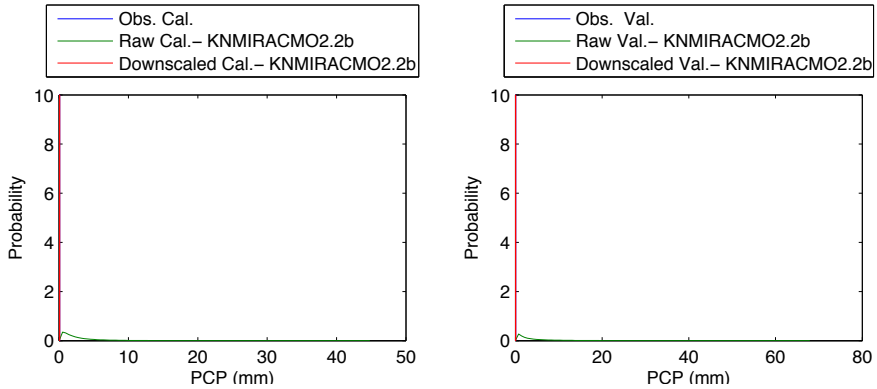

Figure 518 - Probability density of precipitation at Niamey airport with KNMIRACM 02.2b in November

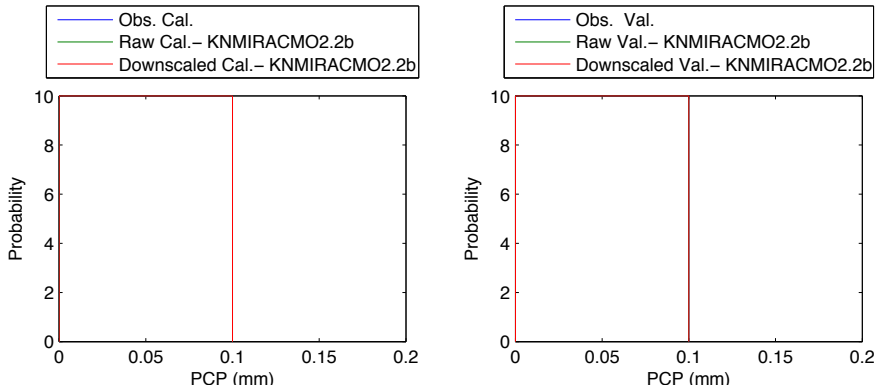

Figure 519 - Probability density of precipitation at Niamey airport with KNMIRACM 02.2b in December

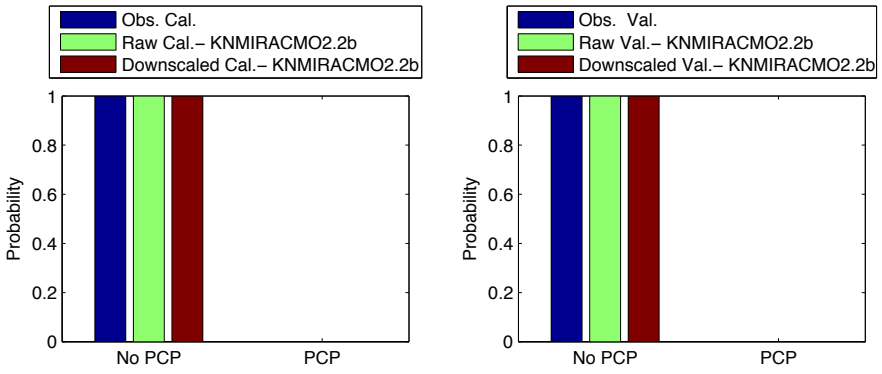

Figure 520 - Precipitation occurrence at Niamey airport with KNMIRACM 02.2b in January

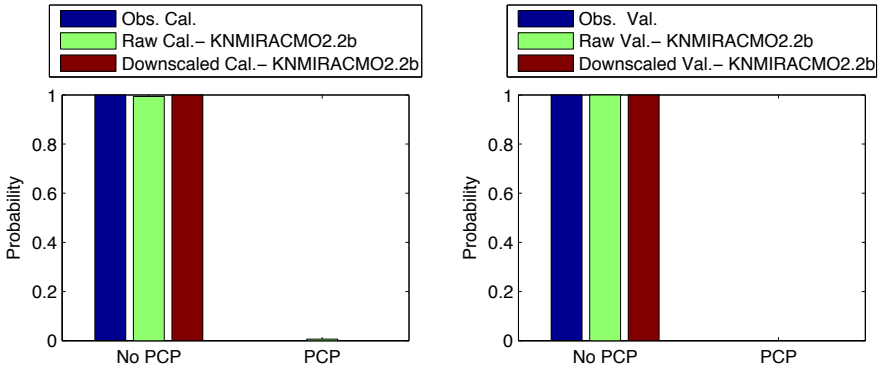

Figure 521 - Precipitation occurrence at Niamey airport with KNMIRACM 02.2b in February

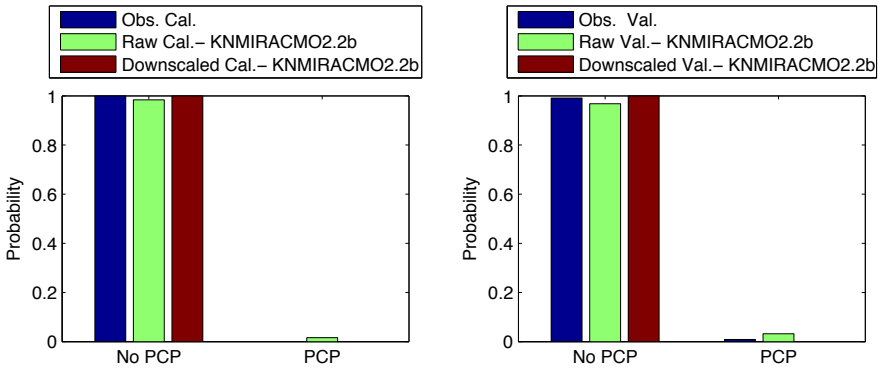

Figure 522 - Precipitation occurrence at Niamey airport with KNMIRACM 02.2b in March

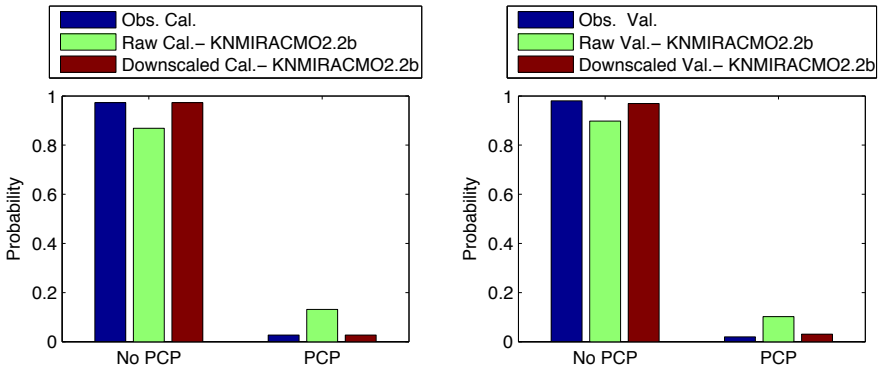

Figure 523 - Precipitation occurrence at Niamey airport with KNMIRACM 02.2b in April

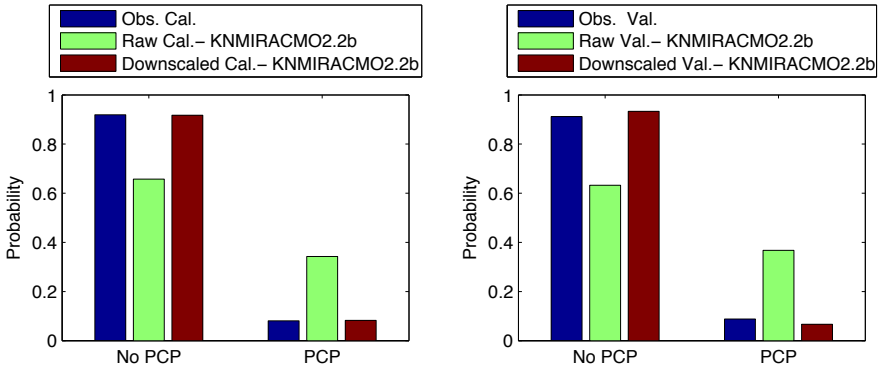

Figure 524 - Precipitation occurrence at Niamey airport with KNMIRACM 02.2b in May

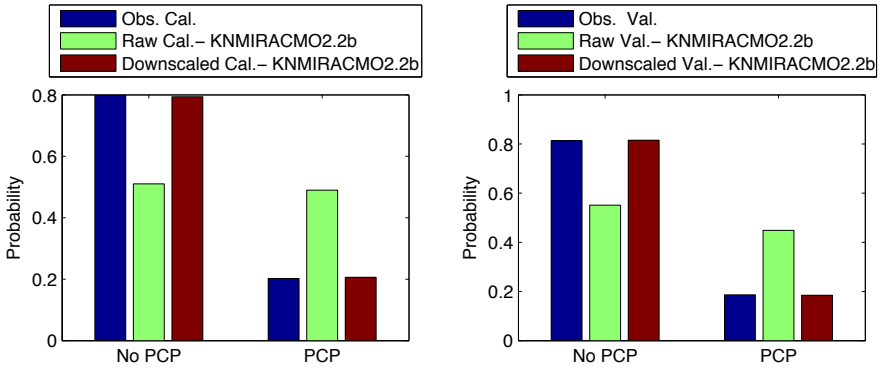

Figure 525 - Precipitation occurrence at Niamey airport with KNMIRACM 02.2b in June

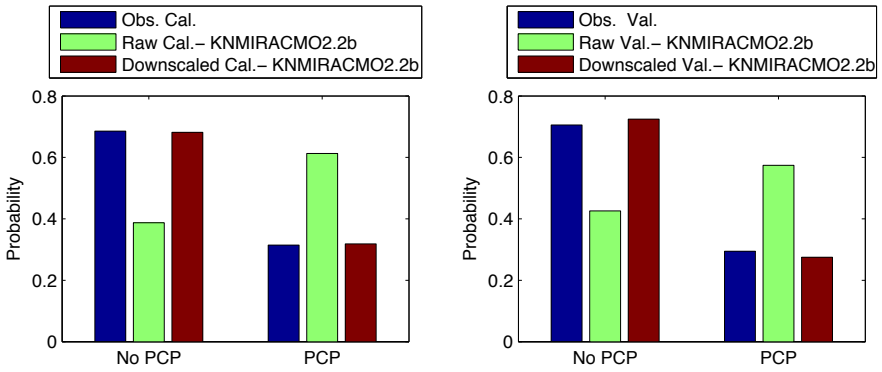

Figure 526 - Precipitation occurrence at Niamey airport with KNMIRACM 02.2b in July

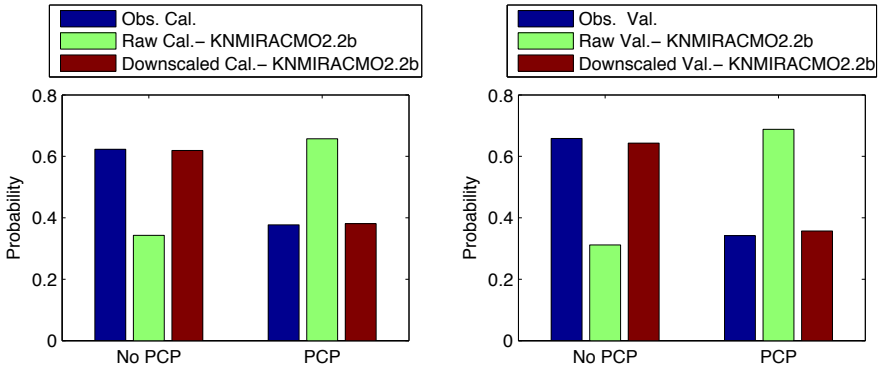

Figure 527 - Precipitation occurrence at Niamey airport with KNMIRACM 02.2b in August

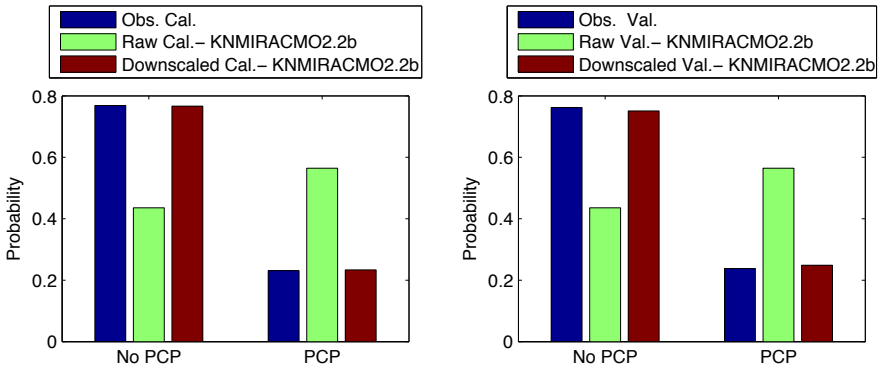

Figure 528 - Precipitation occurrence at Niamey airport with KNMIRACM 02.2b in September

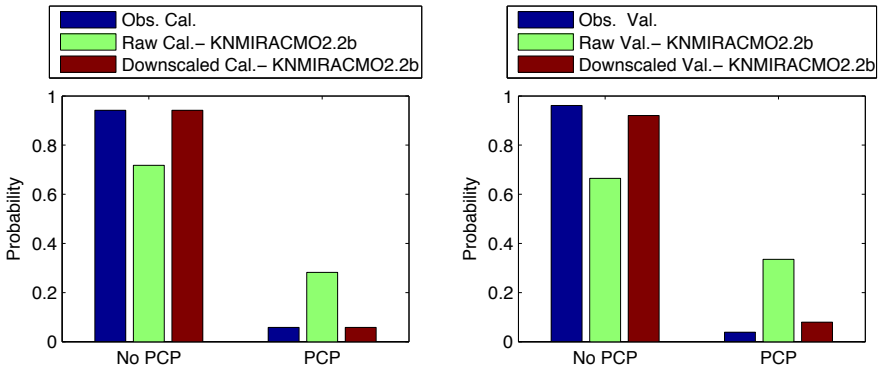

Figure 529 - Precipitation occurrence at Niamey airport with KNMIRACM 02.2b in October

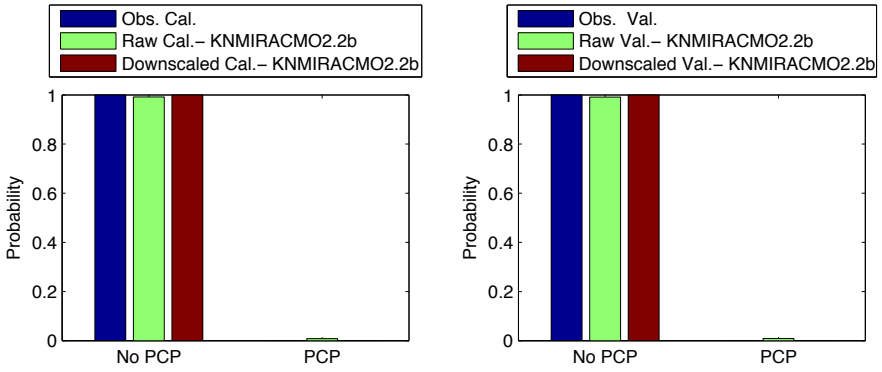

Figure 530 - Precipitation occurrence at Niamey airport with KNMIRACM 02.2b in November

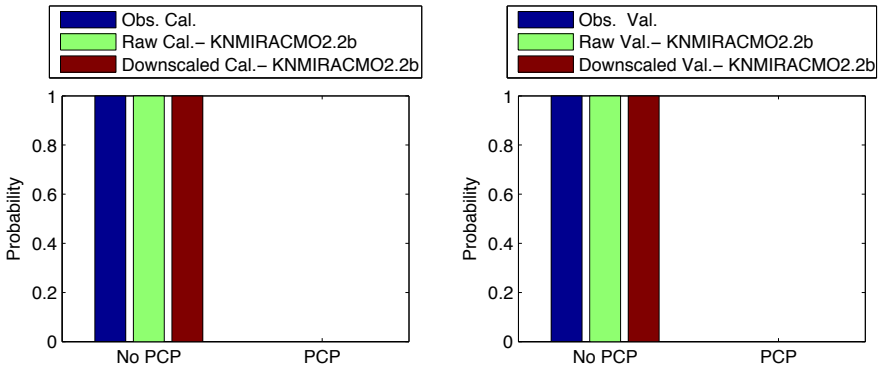

Figure 531 - Precipitation occurrence at Niamey airport with KNMIRACM 02.2b in December

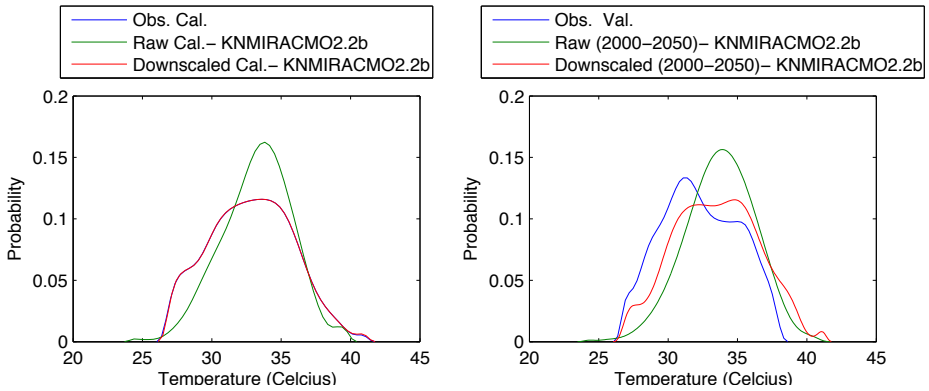

Figure 532 - Probability density for maximum temperature at Niamey airport with KNMIRACM 02.2b in January

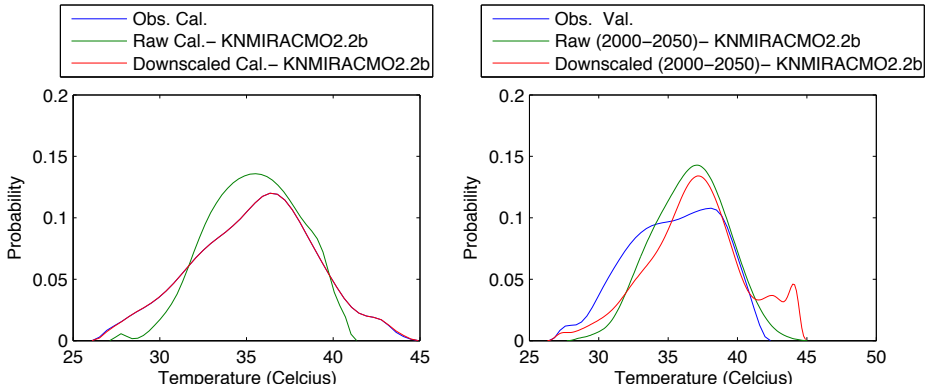

Figure 533 - Probability density for maximum temperature at Niamey airport with KNMIRACM 02.2b in February

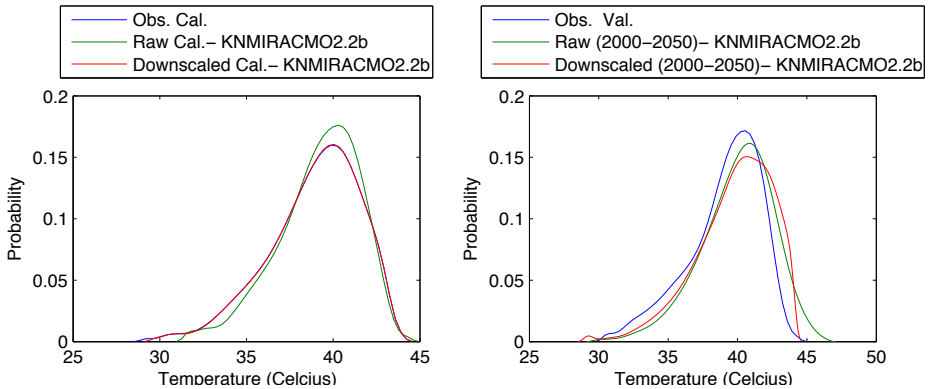

Figure 534 - Probability density for maximum temperature at Niamey airport with KNMIRACM 02.2b in March

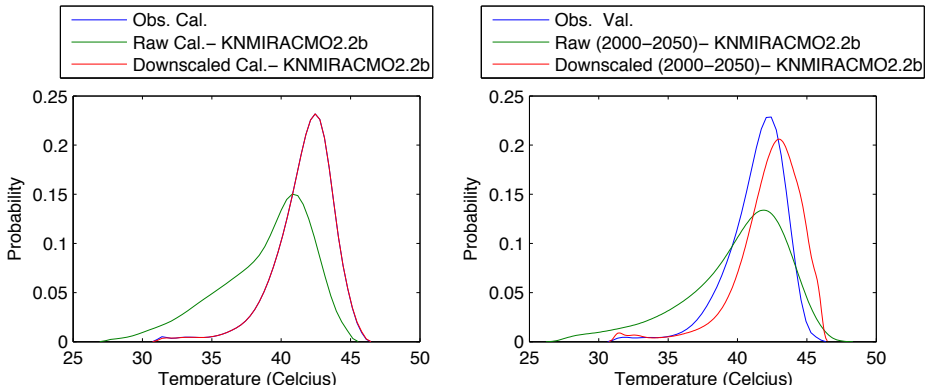

Figure 535 - Probability density for maximum temperature at Niamey airport with KNMIRACM 02.2b in April

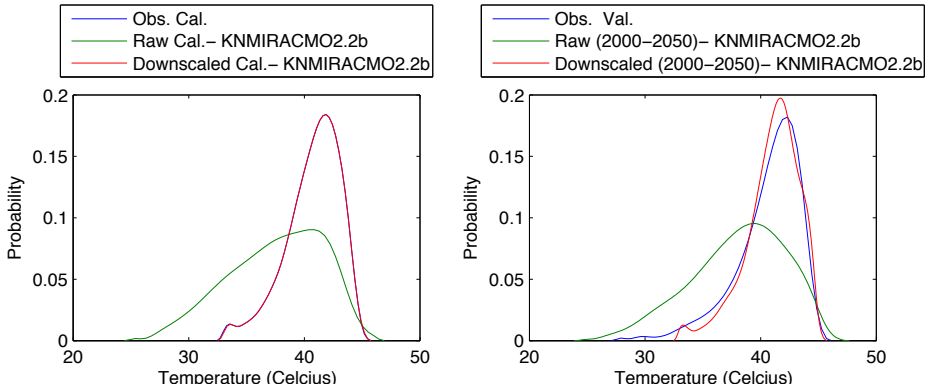

Figure 536 - Probability density for maximum temperature at Niamey airport with KNMIRACM 02.2b in May

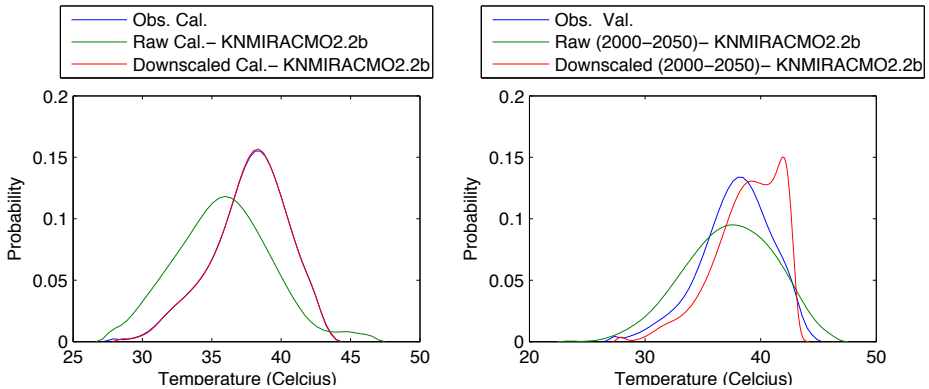

Figure 537 - Probability density for maximum temperature at Niamey airport with KNMIRACM 02.2b in June

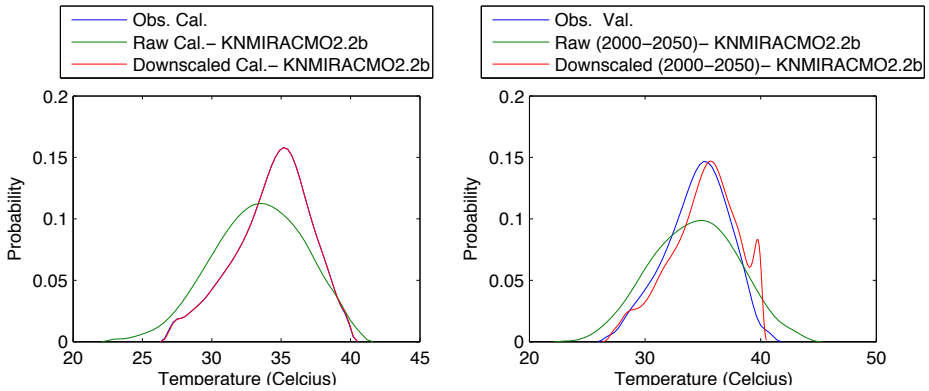

Figure 538 - Probability density for maximum temperature at Niamey airport with KNMIRACM 02.2b in July

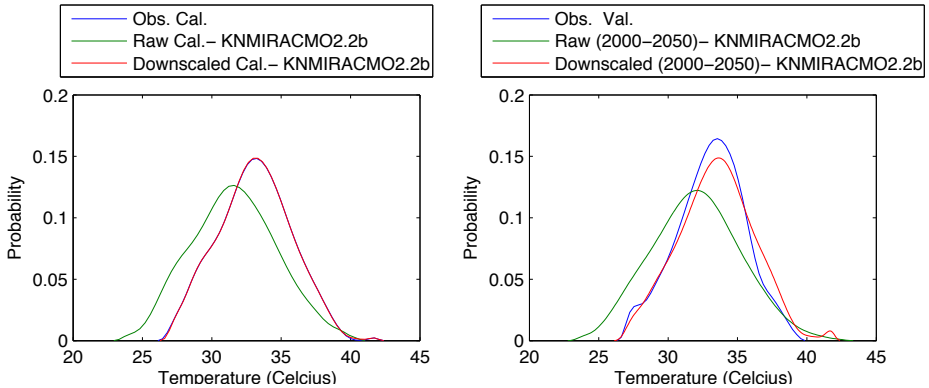

Figure 539 - Probability density for maximum temperature at Niamey airport with KNMIRACM 02.2b in August

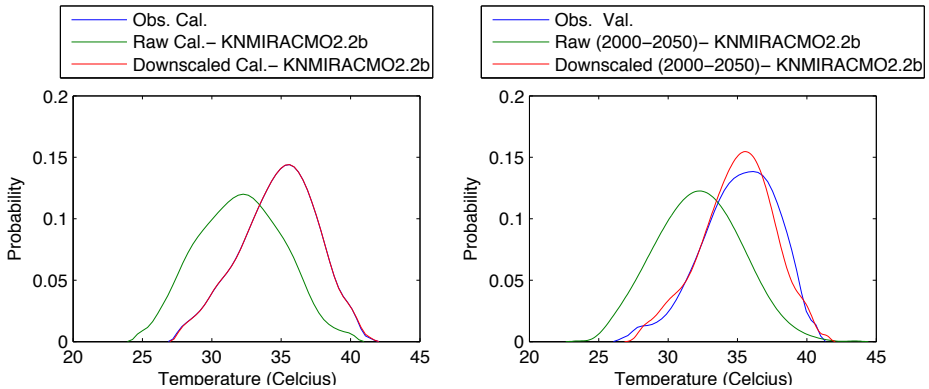

Figure 540 - Probability density for maximum temperature at Niamey airport with KNMIRACM 02.2b in September

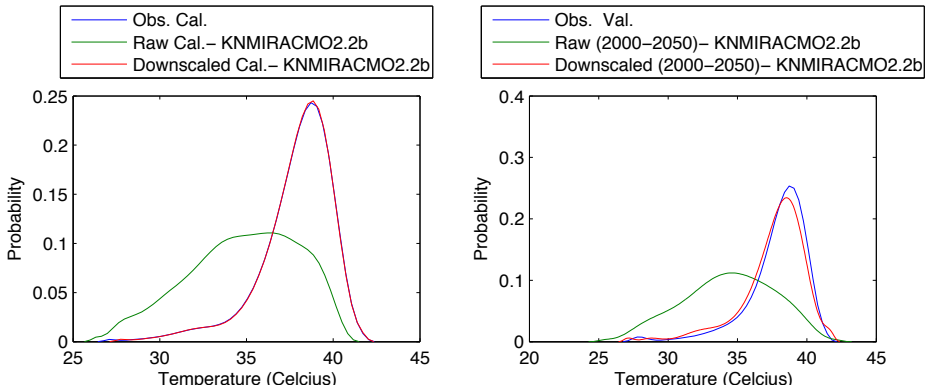

Figure 541 - Probability density for maximum temperature at Niamey airport with KNMIRACM 02.2b in October

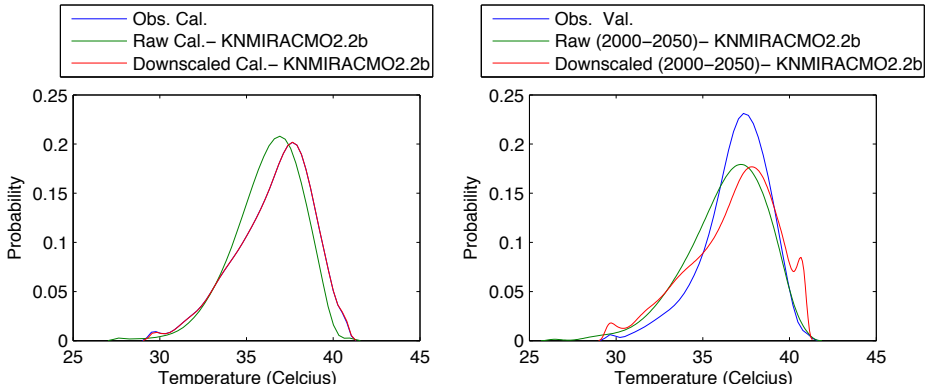

Figure 542 - Probability density for maximum temperature at Niamey airport with KNMIRACM 02.2b in November

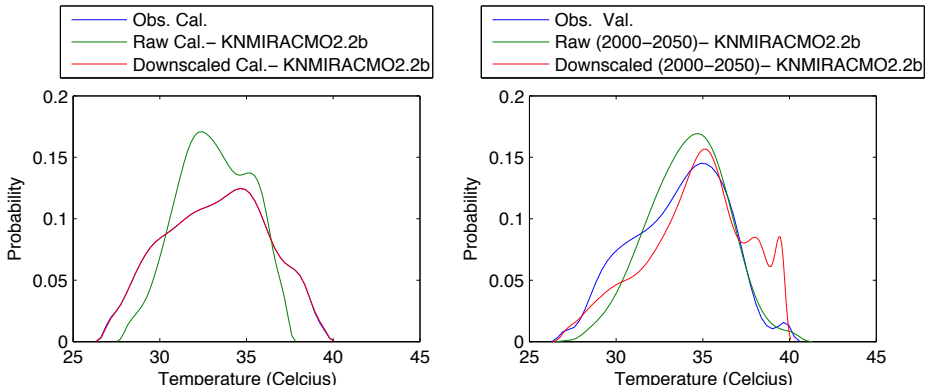

Figure 543 - Probability density for maximum temperature at Niamey airport with KNMIRACM 02.2b in December

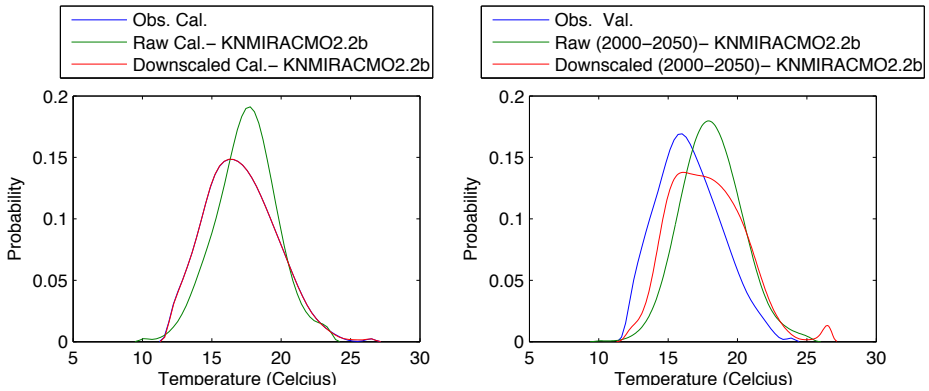

Figure 544 - Probability density for minimum temperature at Niamey airport with KNMIRACM 02.2b in January

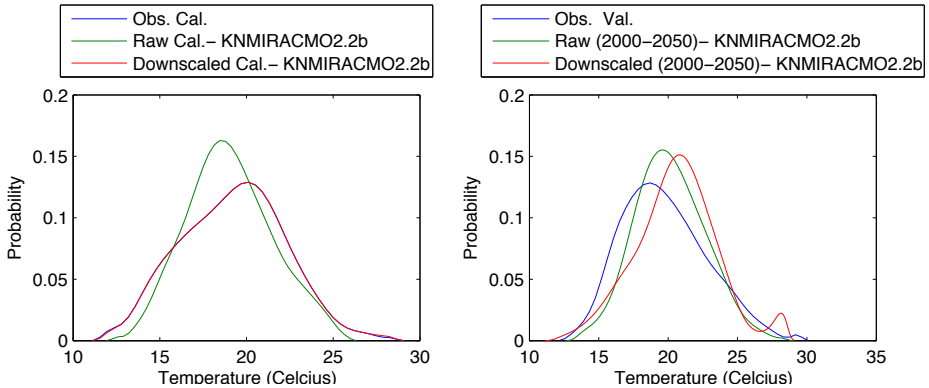

Figure 545 - Probability density for minimum temperature at Niamey airport with KNMIRACM 02.2b in February

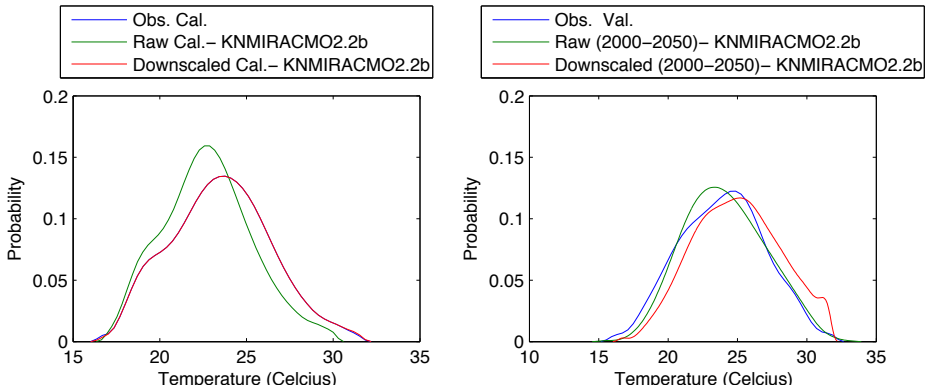

Figure 546 - Probability density for minimum temperature at Niamey airport with KNMIRACM 02.2b in March

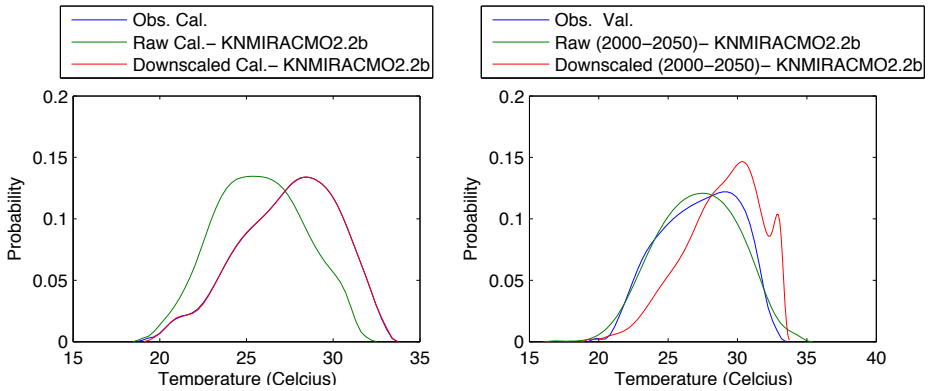

Figure 547 - Probability density for minimum temperature at Niamey airport with KNMIRACM 02.2b in April

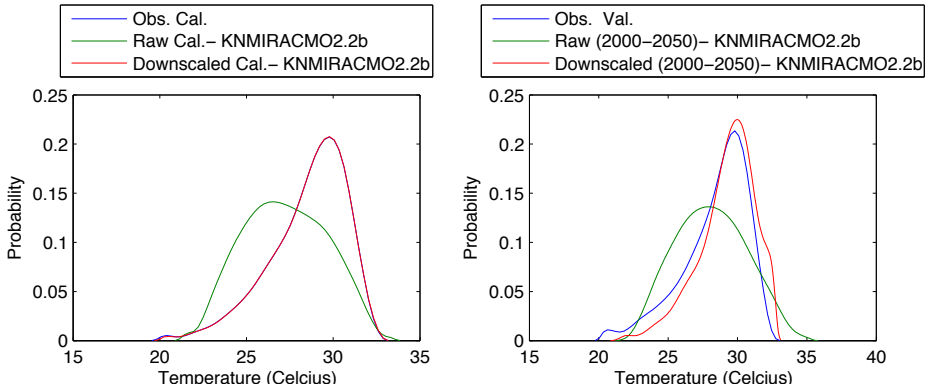

Figure 548 - Probability density for minimum temperature at Niamey airport with KNMIRACM 02.2b in May

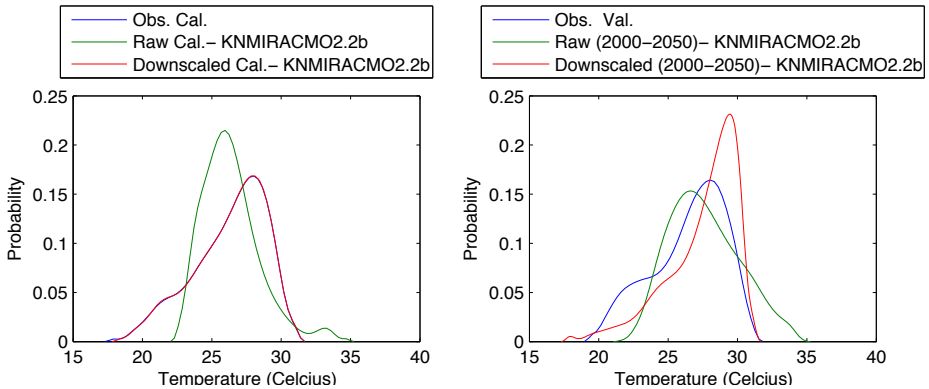

Figure 549 - Probability density for minimum temperature at Niamey airport with KNMIRACM 02.2b in June

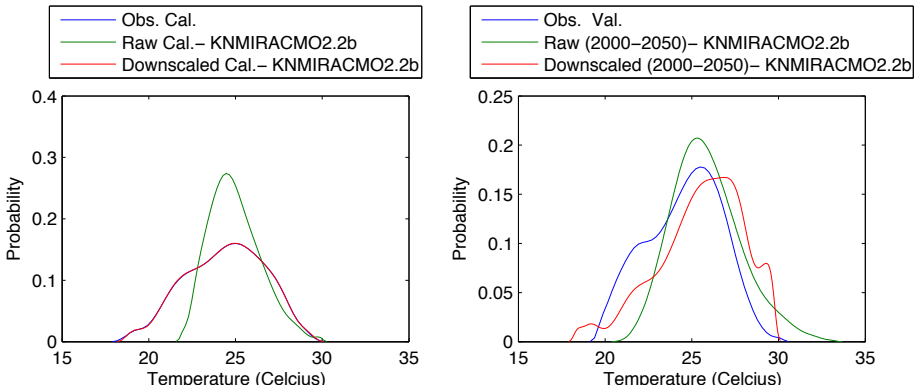

Figure 550 - Probability density for minimum temperature at Niamey airport with KNMIRACM 02.2b in July

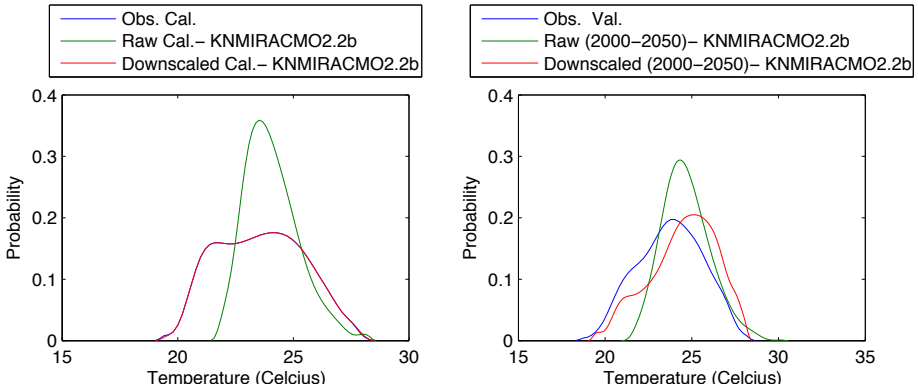

Figure 551 - Probability density for minimum temperature at Niamey airport with KNMIRACM 02.2b in August

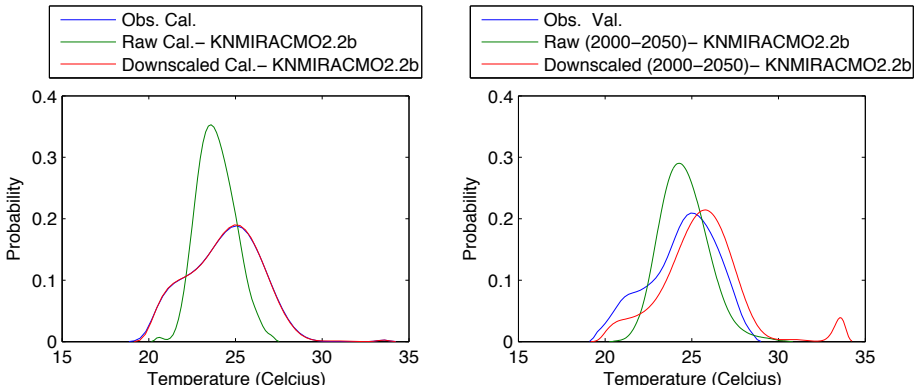

Figure 552 - Probability density for minimum temperature at Niamey airport with KNMIRACM 02.2b in September

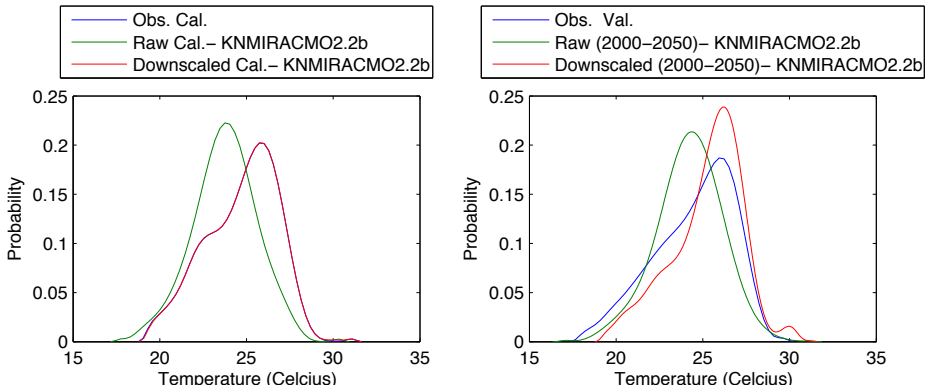

Figure 553 - Probability density for minimum temperature at Niamey airport with KNMIRACM 02.2b in October

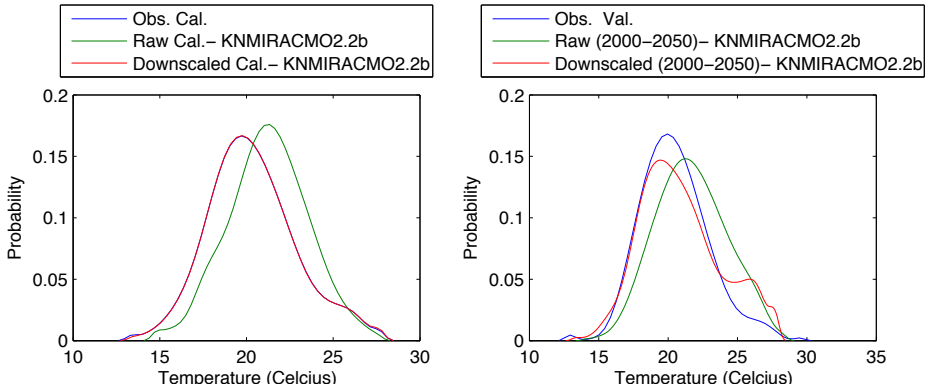

Figure 554 - Probability density for minimum temperature at Niamey airport with KNMIRACM 02.2b in November

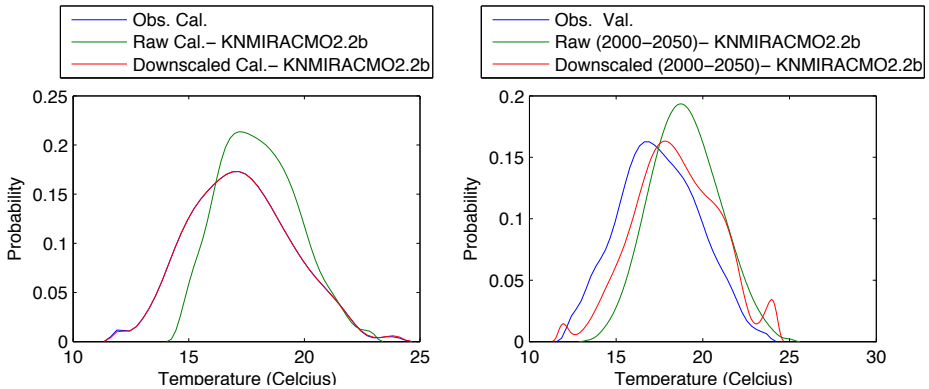

Figure 555 - Probability density for minimum temperature at Niamey airport with KNMIRACM 02.2b in December